

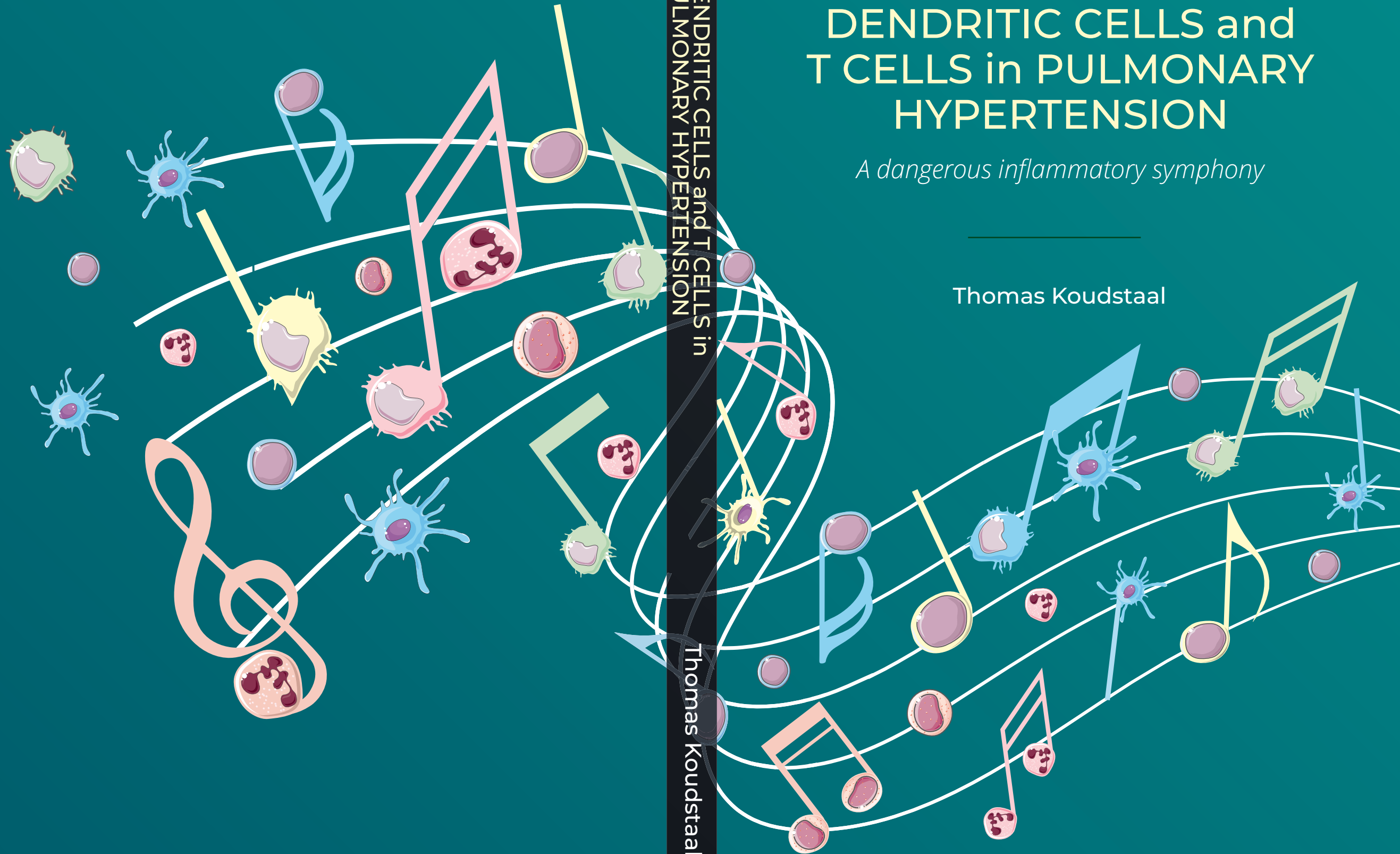
# DENDRITIC CELLS and T CELLS in PULMONARY HYPERTENSION

*A dangerous inflammatory symphony*

Thomas Koudstaal

DENDRITIC CELLS and T CELLS in  
PULMONARY HYPERTENSION

Thomas Koudstaal



Propositions belonging to the thesis

## **Dendritic cells and T cells in Pulmonary Hypertension.**

Thomas Koudstaal, Rotterdam, 02-11-2022

1. Constitutive activation of the NF- $\kappa$ B pathway in conventional dendritic cells results in experimental inflammatory-driven pulmonary hypertension in mice, independently of general immune activation or a mutation in the *Bmpr2* gene.  
(This thesis)
2. Elevated circulating plasma levels of the CXCL9 chemokine correlate with survival in chronic thromboembolic pulmonary hypertension (CTEPH) patients, and should therefore be further examined for clinical and therapeutical implications.  
(This thesis)
3. Peripheral blood analysis in CTEPH patients provides evidence for the involvement of the Th17-associated CCR6<sup>+</sup> T cell subset in disease pathogenesis and progression.  
(This thesis)
4. Idiopathic pulmonary arterial hypertension (IPAH) patients display a unique T cell phenotype characterized by reduced cytokine capacity which is different from CTD-PAH patients.  
(This thesis)
5. A multidisciplinary and fully outpatient pulmonary rehabilitation program is safe and efficacious in PAH and CTEPH patients.  
(This thesis)
6. Pulmonary hypertension is a global health affecting disease, and should immediately be added to the Global Burden of Diseases (GBD) list of 328 diseases.  
(Rich et al, The Lancet Respiratory Medicine, 2018)
7. A cohort of patients meeting diagnostic criteria for IPAH with a distinct, presumably smoking-related form of PH accompanied by a low diffusing capacity for carbon dioxide (DLCO), resemble patients with PH due to lung disease rather than classical IPAH.  
(Hoepfer et al, The Lancet, 2022)
8. Genetic and metabolic abnormalities are inextricably linked to dysregulated immunity and adverse remodeling in the pulmonary arteries.  
(Rabinovitch et al, Circulation Research, 2014)
9. Based on existing knowledge, around 25–30% of patients diagnosed with idiopathic PAH have an underlying Mendelian genetic cause for their condition and should be classified as heritable PAH (HPAH).  
(Morrell et al, European Respiratory Journal, 2019)
10. “I would describe having pulmonary hypertension as driving a car that cannot go faster than 10 miles/hour.”  
(Pulmonary arterial hypertension patient, during PH awareness month)
11. “No man ever steps in the same river twice, for it's not the same river and he's not the same man.”  
(Heraclitus of Ephesus, Greek philosopher, 540 B.C. – 480 B.C.)

# **Dendritic cells and T Cells in Pulmonary Hypertension**

A dangerous inflammatory symphony

Thomas Koudstaal

ISBN: 978-94-6458-562-9

Cover design and lay-out: Publiss | [www.publiss.nl](http://www.publiss.nl)

Print: Ridderprint | [www.ridderprint.nl](http://www.ridderprint.nl)

© Copyright 2022: Thomas Koudstaal, Hellevoetsluis, The Netherlands

All rights reserved. No part of this publication may be reproduced, stored in a retrieval system, or transmitted in any form or by any means, electronic, mechanical, by photocopying, recording, or otherwise, without the prior written permission of the author.

Financial support for the publication of this thesis was generously provided by:

- Peter and Adriana Foundation
- Erasmus University Rotterdam
- Reconcept
- Pulmonary medicine department Erasmus MC
- Ferrer S.A.
- ChipSoft

**Dendritic cells and T Cells in Pulmonary Hypertension**  
A dangerous inflammatory symphony

**Dendritische cellen en T cellen in pulmonale hypertensie**  
Een gevaarlijke inflammatoire symfonie

**Proefschrift**

ter verkrijging van de graad van doctor aan de  
Erasmus Universiteit Rotterdam  
op gezag van de  
rector magnificus

Prof. Dr. A.L. Bredenoord

en volgens besluit van het College voor Promoties.  
De openbare verdediging zal plaatsvinden op

Woensdag 2 november 2022 om 10:30 uur

door

**Thomas Koudstaal**  
geboren te Hellevoetsluis, Nederland.

**Erasmus University Rotterdam**

The logo of Erasmus University Rotterdam, featuring the word "Erasmus" in a stylized, cursive script.

## **Promotiecommissie**

Promotor: Prof. Dr. R.W. Hendriks

Overige leden: Prof. Dr. I.K.M. Reiss  
Prof. Dr. C. Guignabert  
Dr. B. Bartelds

Copromotor: Dr. K.A. Boomars

## TABLE OF CONTENTS

1.	Introduction	7
	<i>Part of this chapter was published in J Clin Med.</i> <b>J Clin Med. 2020 Feb 19;9(2).</b>	
2.	<i>DNGR1-Cre-mediated Deletion of Tnfrsf3/A20 in Conventional Dendritic Cells Induces Pulmonary Hypertension in Mice.</i>	33
	<b>Am J Respir Cell Mol Biol 2020 Nov; 63(5):665-680.</b>	
3.	<i>Central role of dendritic cells in human and murine pulmonary arterial hypertension.</i>	61
	<b>Int. J. Mol. Sci. 2021, 22(4), 1756.</b>	
4.	<i>Plasma markers in pulmonary hypertension subgroups correlate with patient survival.</i>	87
	<b>Respir Res. 2021 May 4;22(1):137.</b>	
5.	<i>Evidence for a role of CCR6+ T cells in chronic thromboembolic pulmonary hypertension patients.</i>	111
	<b>Front Immunol 2022 Apr 27;13:861450</b>	
6.	<i>Peripheral blood T-cells of patients with IPAH have a reduced cytokine-producing capacity.</i>	143
	<b>Int. J. Mol. Sci. 2022, 23(12), 6508.</b>	
7.	<i>The effects of a 10-week outpatient pulmonary rehabilitation programme on exercise performance, muscle strength, soluble biomarkers and quality of life in patients with pulmonary hypertension.</i>	167
	<b>J Cardiopulm Rehabil Prev. 2019 Oct 4.</b>	
8.	Discussion	181
	<b>References</b>	199
	<b>English Summary</b>	217
	<b>Nederlandse Samenvatting</b>	223
	<b>List of publications</b>	231
	<b>Acknowledgements</b>	235
	<b>About the author</b>	243
	<b>Portfolio</b>	247



# CHAPTER 1

## *Introduction*

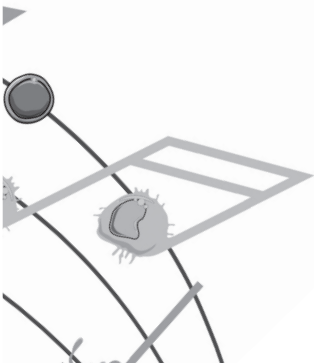
*Part of this chapter was published in J Clin Med.*

**T. Koudstaal**, K.A. Boomars\*, M. Kool\*

\*Contributed equally.

J Clin Med. 2020 Feb 19;9(2).

# 1



## 1.1 INTRODUCTION

Pulmonary hypertension (PH) is a devastating condition characterized by increased pulmonary vascular resistance and elevated pulmonary arterial pressure. The definition of PH has recently been updated and is currently defined as increased mean pulmonary arterial pressures (PAP) above 20 mmHg at rest (1). This enhanced pulmonary arterial pressure leads to elevated right ventricular (RV) hypertrophy, heart failure and ultimately, death (2). Structural remodeling of the vasculature, leading to diameter reduction, is linked to increased pulmonary vascular resistance and increased pulmonary pressure.

Based on the underlying causes of PH, the WHO classification system divides PH patients into 5 groups: (1) Pulmonary Arterial Hypertension (PAH), (2) PH due to left heart disease, (3) PH due to lung disease and hypoxia, (4) Chronic Thromboembolic PH (CTEPH), and (5) PH with unclear and/or multifactorial mechanisms (1) (**Figure 1**). A recent study in Ontario, Canada, showed an annual incidence of ~ 28.7 adult PH cases/100.000 population, subdivided into an estimated 13.8% group I PAH, 68.5% group II PH, 47% group III PH and 9% group IV CTEPH patients (3). Previous registry studies have shown an estimated prevalence of 10-52 PAH cases/1.000.000 population (4-9).

**WHO group I PAH**, which is defined as a condition with a mean PAP >20 mmHg, normal left atrium pressure and pulmonary vascular resistance  $\geq 3$  Wood units (1), consists of different subgroups based upon different underlying diseases or pathophysiological mechanisms. Heritable PAH (HPAH) includes patients with a family history or identified germline mutation. Such heritable susceptibility is conveyed not only through mutations in the bone morphogenetic protein receptor type II (*BMPR2*) gene, but also through newly identified mutations in novel causal genes (11). PAH can also be induced by specific drugs and toxins (12). Other causes of PAH are called APAH (Associated PAH); due to congenital heart disease (CHD), mainly comprising a ventricle septum defect, an atrial septum defect and patent ductus arteriosus; PAH due to liver disease (Porto-pulmonary PAH), PAH due to HIV and PAH due to schistosomiasis. PAH can also be associated with auto-immune diseases, specifically with systemic sclerosis (SSc, prevalence 10-15%), mixed connective tissue diseases (MCTD) and systemic lupus erythematosus (SLE). Two more separate identities in PAH WHO group 1 are pulmonary veno-occlusive disease (PVOD), which can be heritable (eukaryotic translation initiation factor 2a kinase *EIF2AK4* mutation), associated with autoimmune diseases or idiopathic, and persistent pulmonary hypertension of the newborn (PPHN). PPHN can be idiopathic or may be caused by several pulmonary diseases. In the largest group of PAH; idiopathic PAH (IPAH), no cause or associated disease is identified so far. Exercise intolerance is a key feature of PAH for which the underlying hemodynamic impairment is primarily responsible (13). In recent years, evidence for the beneficial effects of pulmonary rehabilitation (PR) therapy is increasing (14-16). The European Respiratory Society (ERS) and the European Society of Cardiology (ESC) guidelines for diagnosis and treatment of PH recommend supervised rehabilitation programs in expert centres for PAH patients in stable condition on optimized PH specific drug therapy (17). WHO group 4 patients (CTEPH) can be further differentiated into; operable (eligible for pulmonary endarterectomy (PEA) or balloon pulmonary angioplasty (BPA)) or inoperable CTEPH.

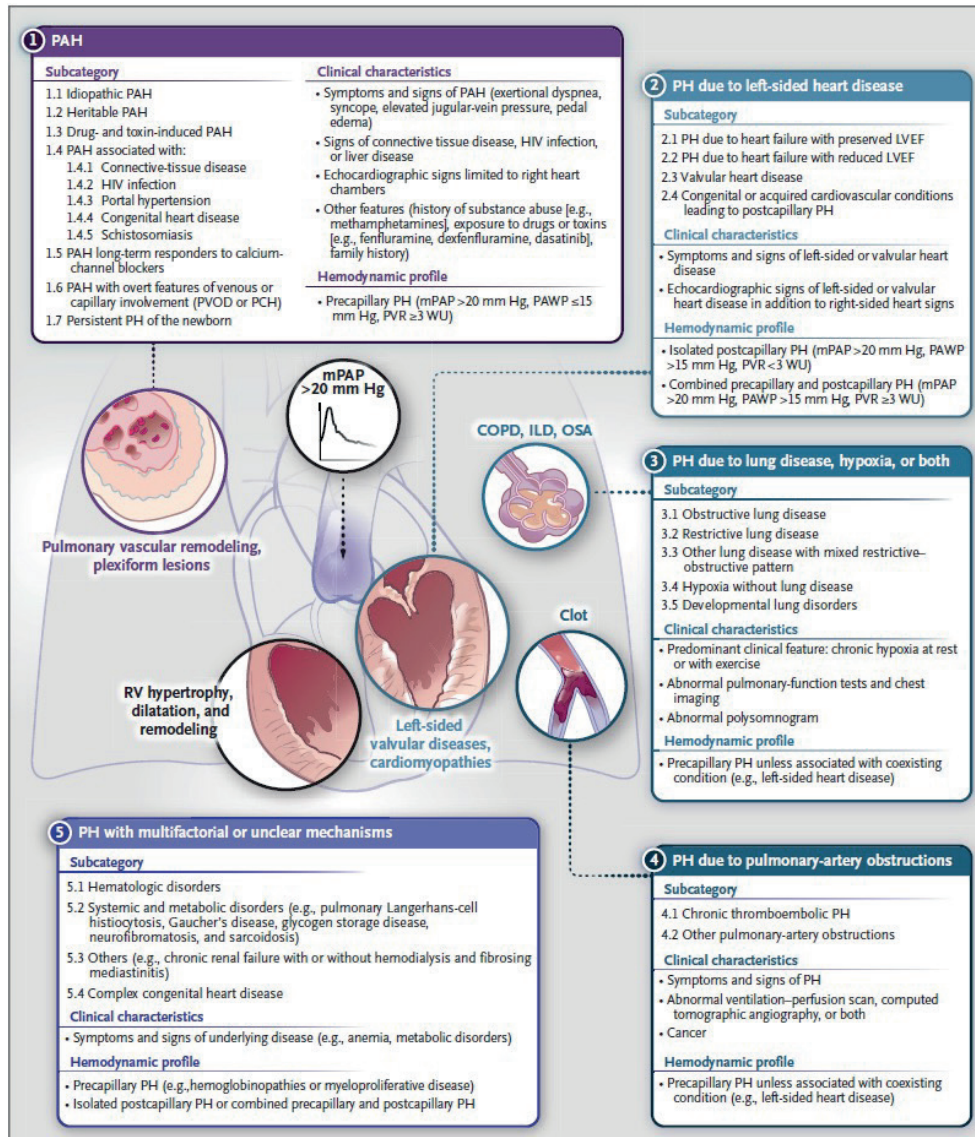


**Figure 1. Clinical Classification of Pulmonary Hypertension (PH).**

The PH classification based on the 2018 meeting of the World Symposium on Pulmonary Hypertension is shown, along with the clinical characteristics and hemodynamic profile of each group (1). COPD denotes chronic obstructive pulmonary disease, HIV human immunodeficiency virus, ILD interstitial lung disease, LVEF left ventricular ejection fraction, mPAP mean pulmonary arterial pressure, OSA obstructive sleep apnea, PAH pulmonary arterial hypertension, PAWP pulmonary arterial wedge pressure, PCH pulmonary capillary hemangiomatosis, PVOD pulmonary veno-occlusive disease, PVR pulmonary vascular resistance, RV right ventricular, and WU Wood units. *Adapted from Hassoun et al. 2021 (10).*

In **WHO group 2,3 and 5**; treatment of the underlying disease is the standard care. For PAH (group 1), treatment with PH specific drugs is indicated. Currently, three pathways are involved in treatment of PAH: (1) nitric oxide pathway treatment with phosphodiesterase type 5 (*PDE5*) inhibitors or a soluble guanylate cyclase (sGC) stimulator (2) Endothelin pathway treatment with endothelin receptor antagonists (ERA) and (3) the prostacyclin pathway treatment with prostacyclins directly or with a prostacyclin receptor stimulator (see **Figure 2**).

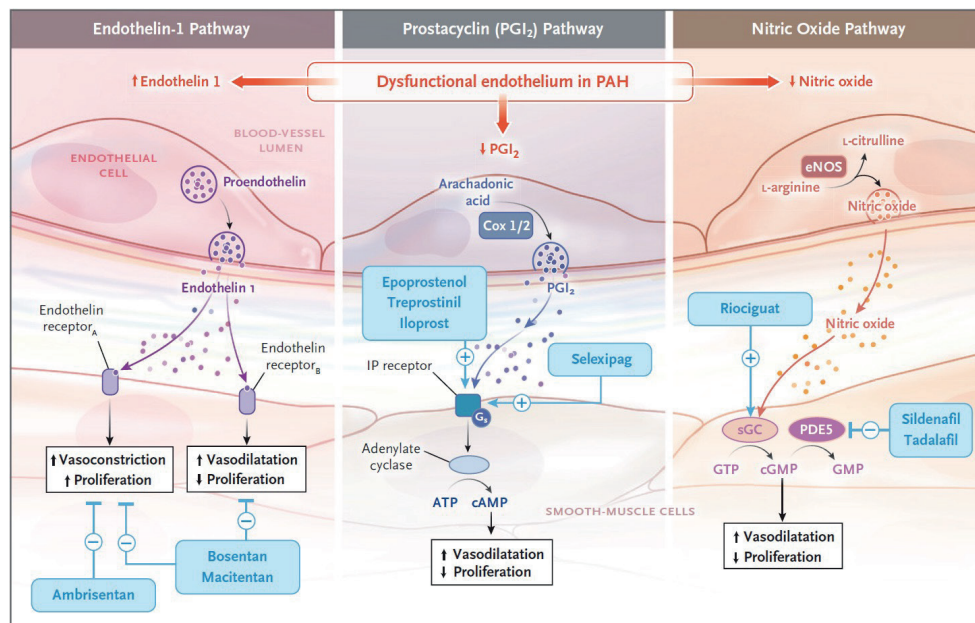


**Figure 2. Three Classic Pathways of Targeted Therapy for PAH.**

Current targeted therapy is aimed at correcting endothelial dysfunction (18) by inhibiting the endothelin pathway and enhancing the prostacyclin ( $\text{PGI}_2$ ) and NO pathways. Endothelin 1 ( $\text{ET}_1$ ), which is increased in PAH, can bind to either the endothelin A ( $\text{ET}_A$ ) receptor, causing vasoconstriction (of smooth-muscle cells) and cell proliferation, or the endothelin B ( $\text{ET}_B$ ) receptor, causing vasodilatation and antiproliferation. Thus, there are dual  $\text{ET}_A$ - $\text{ET}_B$  receptor antagonists (e.g., bosentan and macitentan) or selective  $\text{ET}_A$  receptor antagonists (e.g., ambrisentan), which leave the  $\text{ET}_B$  receptor functional. The expression and function of the  $\text{PGI}_2$  and NO pathways are decreased in PAH, resulting, respectively, in diminished cyclic adenosine monophosphate (cAMP) and cyclic guanosine monophosphate (cGMP), which are second messengers responsible for vasodilatation and antiproliferation. Agents that increase cAMP include  $\text{PGI}_2$  analogues given intravenously (e.g., epoprostenol and treprostinil), subcutaneously (e.g., treprostinil), by inhalation (e.g., iloprost and treprostinil), orally (treprostinil), or with the use of oral  $\text{PGI}_2$  receptor (IP) agonists (e.g., selexipag). Increased cGMP release can be achieved with inhaled NO (used essentially in the cardiac catheterization laboratory or intensive care unit), which stimulates soluble guanylate cyclase (sGC), or by inhibiting phosphodiesterase type 5 (PDE5, which degrades cGMP into GMP) with the use of oral PDE5 inhibitors (sildenafil or tadalafil). Direct sGC stimulators (e.g., oral riociguat) can increase the release of cGMP independently of NO release. These drugs have been approved by the Food and Drug Administration for patients with PAH who have an  $\text{mPAP} \geq 25$  mm Hg and a  $\text{PVR} \geq 3$  WU. Although they usually are associated with acceptable adverse-event profiles, these drugs have common side effects that are due essentially to their vasodilatory effects, including headache and light-headedness (particularly at the initiation of treatment), flushing and upper respiratory congestion, systemic hypotension (more frequent with systemically administered drugs but also common with certain drugs that need slower dose escalation, such as riociguat and selexipag), gastrointestinal symptoms (e.g., bloating, nausea or vomiting, and diarrhea), and rash ( $\text{PGI}_2$  analogues). These side effects usually diminish over time. AA denotes arachidonic acid, AC adenylate cyclase, Cox 1/2 cyclooxygenase 1/2, eNOS endothelial isoform of nitric oxide synthase, GS G-protein-coupled receptor, and GTP guanosine triphosphate. Adapted from Hassoun et al. 2021 (10).

These PAH-specific drugs focus predominantly on dilatation of the pulmonary arterial vasculature (19). **WHO Group 4 PH.** In inoperable CTEPH, PAH-specific drugs are also used to modulate the increased pulmonary vascular pressure (2). However, even with PAH-specific drug treatment, survival for PAH patients remains poor with a mean 5-year survival of 57-59% (20, 21) and 53-69% for inoperable CTEPH (21-23). Therefore, more insight into the pathogenesis of PAH and CTEPH is highly needed, so that new therapeutic strategies can be developed.

Especially in PAH, an increasing body of evidence shows that inflammation might play a role in its pathobiology (24). However, recent studies have demonstrated that also in CTEPH inflammatory cells may contribute to disease pathology (25, 26). The following overview aims to summarize the expanding knowledge on inflammatory cells in the pathogenesis of PH as well as the use of inflammatory biomarkers and immunomodulatory therapy in PAH and CTEPH.

## **Inflammation and immunity in PAH and CTEPH**

### ***Histopathology in PAH and CTEPH***

PAH and CTEPH is characterized by increased pulmonary arterial pressures as a result of vascular remodeling (**Figure 3**). Features of pulmonary vascular remodeling in PH are intima wall thickening and formation of obliterative concentric lesions in the endothelial and/or smooth muscle cell layers. In the media, which mainly consists of smooth muscle cells, an increase in thickness is also seen. Interestingly, the combined intima and media thickness correlated significantly to the PAP and the pulmonary vascular resistance (PVR) (27). Finally, increased adventitial thickness and remodeling were the most prominent findings in a series of 19 IPAH patient lung autopsies (28). However, this increased adventitial thickness was not confirmed in a recent study, which might be explained by methodological differences between these studies (27).

Besides increased intimal, medial and adventitial vascular thickness, another prominent feature in PAH patients is perivascular inflammation. A feature seen specifically in IPAH patients is the formation of plexiform lesions, which are typically defined as dynamic networks of vascular channels formed by monoclonal proliferation of endothelial cells (29). In CTEPH patients, histologic studies show neointimal, thrombotic, recanalized and atherosclerotic lesions in the pulmonary arterial vasculature. These chronic thrombotic lesions contain collagen, elastin, inflammatory cells, re-canalization vessels and calcification (30). Current concepts state that CTEPH is a dual vascular disorder with stenosis, webs and occlusions in large and medium-sizes PAs at the sites of previous pulmonary emboli. Furthermore, a secondary arteriopathy affecting small resistance vessels is visible in lung biopsies in CTEPH patients (31).

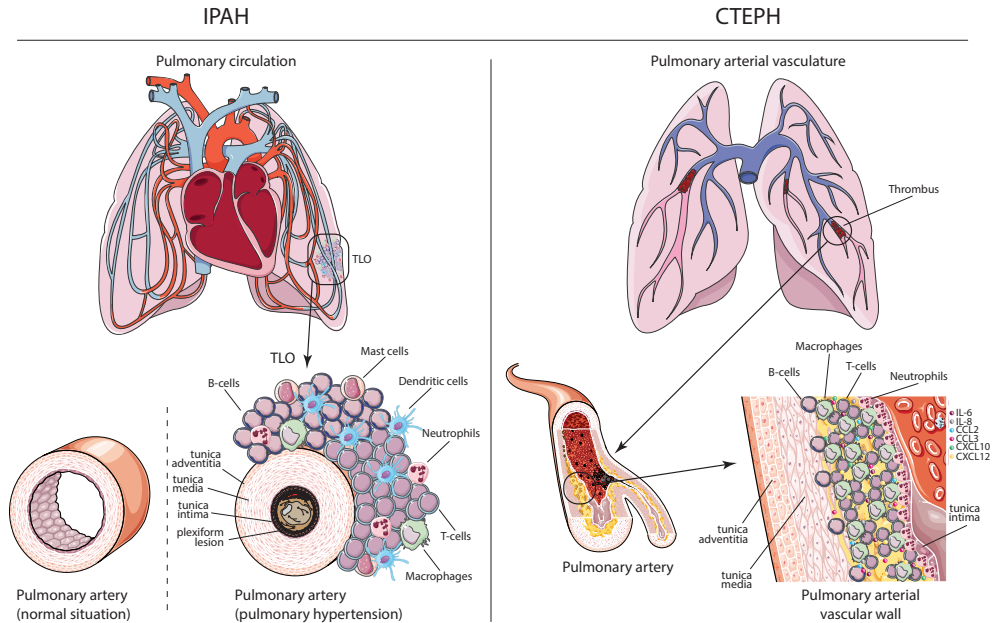


**Figure 3. Left:** Schematic overview of cells involved in tertiary lymphoid organs (TLOs) in idiopathic pulmonary arterial hypertension (IPAH) patients. In the pulmonary hypertension situation, endothelial hyperproliferation is visible in the tunica intima with plexiform lesion formation in the lumen of the artery. Furthermore, smooth muscle cell (SMC) hyperplasia is visible in the tunica media of the pulmonary artery. Surrounding the tunica adventitia, is a combination of B cells, T cells, mast cells, dendritic cells, neutrophils and macrophages. **Right:** Schematic overview of vascular remodeling and inflammation in thrombotic material in chronic thromboembolic pulmonary hypertension (CTEPH) patients. Between the (neo)intimal vascular wall and the tunica media, influx of inflammatory cells such as B cells, T cells, neutrophils and macrophages is visible. Moreover, enhanced presence of pro-inflammatory mediators such as Interleukin (IL)6, IL-8, chemokine (C-C motif) ligand 2 and 3 (CCL2 and CCL3), C-X-C motif chemokine 10 and 12 (CXCL10 and CXCL12) was found ((32)).

### ***Dysregulated immune responses in PAH and CTEPH***

Immune responses can be divided into innate and adaptive immunity. Innate immunity is our swift first-line defense against microorganisms and foreign pathogens, which is very broad and nonspecific. Innate immune responses are usually initiated and executed by macrophages, neutrophils, natural killer (NK) cells and dendritic cells (DCs). In parallel, adaptive immune responses are initiated, which allows for more specific responses executed by T and B lymphocytes. Next to their innate function, DCs initiate adaptive immune responses by migrating to lymphoid organs, mostly the tissue draining lymph nodes. There, they present parts of foreign pathogens on their cell surface through major histocompatibility complex (MHC) molecules to induce activation, differentiation and clonal expansion of antigen-specific T cells. Memory T cells and B cells can ensure lifelong immunity, allowing our body to rapidly and more vigorously respond to pathogens upon a second encounter. The adaptive response relies on the ability of T and B cells to distinguish self from non-self antigens. If this capacity is disturbed, the immune system may attack the body's own cells which can lead to autoimmune disease. Elements hereof can be found in both PAH and CTEPH. IPAH for instance is characterized by perivascular inflammation consisting of pulmonary lymphoid neogenesis with formation of tertiary lymphoid organs (TLOs), which contain specific T- and B-cell zones with on-site activation and production of antibodies (33). In addition to lymphocytes, these inflammatory lesions also contain DCs, macrophages

and mast cells (33, 34). Moreover, there is a positive correlation between the degree of pulmonary perivascular inflammation and vascular intimal/medial/adventitial thickness and mPAP, suggesting that inflammation could be involved in pulmonary vascular remodeling and PH development (35).

In CTEPH patients thrombotic and atherosclerotic lesions were found to contain activated B and T lymphocytes, macrophages, and neutrophils (36). In this study, topographic analyses revealed a transmural distribution of T cells, whereas B cells were low in number and mostly localized deep within the lesion, close to internal elastic lamina and native media. Although inflammatory cells are common in thrombotic material, the accumulation of inflammatory cells may be a sign of involvement in the pathology of non-resolution of thrombosis and atherosclerosis in CTEPH patients.

Below we discuss several different immune cells which are part of the innate or adaptive immune system and their possible role in the pathogenesis of PH.

## **Innate immunity**

### ***Macrophages***

Macrophages are first-line myeloid leucocytes observed in pulmonary lesions in PH patients (37, 38). Pulmonary macrophages can classically be divided into interstitial and alveolar macrophages, although recent single cell RNA sequencing and lineage tracing studies have defined multiple pulmonary macrophage subtypes in mice (39-41). In a hypoxia-driven PH mouse model, specifically interstitial macrophages – but not alveolar macrophages – were increased (42). They might be involved in PH development through their production of cytokines (43-45). Furthermore, macrophages present in lung perivascular spaces in PAH are derived from peripheral blood monocytes (46), likely indicating their recruitment and differentiation due to pulmonary inflammation. Through chemokines, such as chemokine (C-C motif) ligand 2 (CCL2) and chemokine (C-X3-C motif) ligand 1 (CX3CL1), monocytes are recruited to the site of inflammation and differentiate into inflammatory macrophages. In PH patients expression of chemokines such CCL1, CCL2, CCL5 and CX3CL1 was increased in circulatory monocytes, along with increased pulmonary levels of CC11, CCL2, CCL3, CLL3 and CX3CL1 (46). In CX3CR1 (receptor for CX3CL1) deficient mice, both pulmonary inflammation and vascular remodeling were reduced after exposure to hypoxia compared to control mice (46). Interestingly, in pulmonary vascular endothelial cells from PAH patients excessive expression of CCL2 was observed, which acts as a chemoattractant for circulating inflammatory cells and as a growth factor for pulmonary arterial smooth muscle cells (PASMCs). Moreover, PASMCs and perivascular macrophages from patients with PAH exhibited elevated CCR2 and CCR5 levels compared to controls (47, 48). Indeed, expression of CCR2 and CCL5-CCR5 was needed on both macrophages and PASMCs to initiate and amplify PASMC proliferation (48). When circulating monocytes differentiate into interstitial macrophages in hypoxia-induced PH in mice, they express thrombospondin-1 (TSP-1), leading to Rho kinase-mediated vasoconstriction through transforming growth factor beta (TGF- $\beta$ ) activation (49), thereby amplifying PH pathology. All these studies suggest a potentially crucial role for chemokine-mediated macrophage recruitment in the early pathogenesis of PH.

Macrophage recruitment and activation was also shown to play an important role in the pathogenesis of hypoxia-induced PH in the mouse and in Sugen/athymic rat models (50-52). A previous study has reported that hypoxia-inducible factor-1 $\alpha$  (HIF-1 $\alpha$ ) is expressed by pulmonary macrophages in PH patients, especially in plexiform lesions (53). When HIF-1 $\alpha$  was absent in mice, a significant reduction in right ventricular (RV) systolic pressure (RVSP) and RV hypertrophy was observed together

with less infiltration of macrophages in the lung and RV, indicating a direct effect of on-site macrophages in inducing PH (54). In IPAH patients, increased numbers of macrophages and monocytes were found in the lungs when compared to healthy controls (55). Another PH-inducing factor, resistin-like molecule- $\alpha$  (RELM $\alpha$ ) was increased in a hypoxia-induced mouse model for PH, and its human homologue resistin was also found to be upregulated in macrophage-like inflammatory cells in IPAH patients. In these patients, resistin-stimulated macrophages promoted apoptosis-resistant proliferation of PASMCs (56).

Macrophages may also play a role in other forms of PH, as increased presence of inflammatory macrophages was apparent in surgical pulmonary endarterectomy (PEA) material from CTEPH patients (36). Moreover, in serum from 8 CTEPH patients increased expression of macrophage inflammatory protein-1 $\alpha$  (CCL3) was detected, which can lead to the synthesis of inflammatory cytokines, vascular remodeling and recruitment of macrophages (32). Recently, the accumulating evidence for the role for macrophages in PH has been extensively reviewed by Florentin *et al* and Pullamsetti *et al* (57, 58). Taken together, macrophages play a pivotal role in the pathogenesis of PH, through production of inflammatory cytokines, initiation and proliferation of PASMCs and hypoxia factors.

### **Neutrophils**

Neutrophils are early responders and recruited to sites of acute inflammation, in response to chemokines produced by tissue-resident immune cells such as macrophages. Neutrophils are known phagocytes, capable of ingesting microorganisms or particles. Besides their phagocytic role, neutrophils are able to degranulate and release antimicrobial contents. In PAH patients, an increased neutrophil to lymphocyte ratio in peripheral blood samples positively correlates with the NYHA FC and a negative ratio can even predict event free survival (59, 60). In CTEPH patients the neutrophil to lymphocyte ratio could predict postoperative mortality and might be used as a noninvasive measuring tool for operative risk stratification (61). Currently, it is unclear if and how neutrophils contribute to PAH progression. In murine models, neutrophils accumulated at the site of inflammation/injury in the lungs of hypoxic PH and in monocrotaline (MCT)-induced PH rats (51, 62). Recent evidence suggests that neutrophilic production of myeloperoxidase (MPO), a catalyst for reactive oxygen species (ROS) formation, can cause disease progression (63). Plasma levels of MPO were found to be increased in PAH patients compared to healthy controls. Furthermore, hypoxia-exposed *Mpo*<sup>-/-</sup> mice showed a lower increase in RV pressure than wildtype mice (63), indicating a pathogenic role for neutrophils in PH through production of MPO and adverse pulmonary vascular function.

### **Mast cells**

Mast cells (MCs) are long lived tissue-resident immune cells known for their important role in the immune system by their release of histamine and production of inflammatory cytokines. MCs are also known for their role in angiogenesis through their production of vascular endothelial growth factor (VEGF) and MC proteases including chymase and tryptase (64-66). Accumulating evidence indicates a role for MCs in the pathophysiology of PH. MCs are present in inflammatory lesions in IPAH patients (34), even in the early perivascular cellular lesions in lungs of IPAH patients (67). Over the past years, a role for MCs has been shown in proof-of-principle experiments. In *Ws/Ws* rats, in which MCs are absent due to a mutation in mast cell growth factor receptor c-kit (68), features of experimental PH, such as RVSP, PVR, RV hypertrophy and vascular remodeling were largely attenuated after pulmonary arterial banding or MCT treatment (69). Also, when degranulation of MCs was inhibited by ketotifen,

development of PH was reduced in several experimental rat PH models (69-72). In a small clinical trial, 9 PAH patients were treated with the MC inhibitors cromolyn and fexofenadine. In these patients a decrease in VEGF levels and circulating proangiogenic myeloid cells was observed, together with an increase in exhaled nitric oxide (which is generally low in PAH), indicating this treatment might have a suppressive effect on MCs (73). Mechanistically, MC proteases are believed to play an important role in the process of PH development and severity. MC proteases such as chymase and tryptase, measured in lung tissue, correlate with the severity of PH and pulmonary vascular remodeling (66, 74-77). Moreover, excessive MC infiltration and degranulation was detected in lung tissue in MCT-rats and not in the RV, indicating a release of proteases such as tryptase which contribute to pulmonary vascular remodeling (78). Lastly, MCs are observed around distal pulmonary arteries, together with accumulated macrophages in MCT challenged rats, suggesting that MCs are involved in vascular remodeling in the lungs (78). In summary, MCs are involved in PH pathobiology, most likely through the release of proangiogenic factors and MC proteases.

### ***Natural killer cells***

Natural killer (NK) cells comprise an important part of the innate immune system as they provide rapid responses to virus-infected cells, but these cytotoxic cells are also known for regulating angiogenesis and vascular remodeling. Few studies have evaluated the possible contribution of NK cells in the pathogenesis of PAH and CTEPH. However, in both PAH patients and in rodent experimental PH models impaired NK cell numbers and cytotoxicity were found (79). Furthermore, in two independent genetic mouse models for NK cell dysfunction, involving deficiency for the NFIL3 transcription factor or the NK activating receptor NKp46, enhanced RV systolic pressures and RV hypertrophy were found. In both models, this experimental PH development was linked to increased interleukin-23 production, possibly due to NK cell or impairment, leading to increased production of IL-23 by pulmonary macrophages and other myeloid cell types (80). Interestingly, IL-23 is known for production of inflammatory cytokines such as IL-17A/F, IL-21, and IL-22 and for driving naïve T cells to a TH17 phenotype (81). Taken together, NK cell defects may contribute to PAH pathogenesis by aberrant regulation of pulmonary vascular remodeling, however further research is required to evaluate these findings.

## **Linking innate and adaptive immunity**

### ***Dendritic cells***

DCs are key modulators between tolerance and immunity and are known to function as a bridge between innate and adaptive immunity. The main function of DCs is to capture, process and present antigens to T cells. DCs can be activated either by microbial stimuli through pattern recognition receptors such as Toll-like receptors or by inflammatory cytokines, which leads to activation of the nuclear factor kappa-light-chain-enhancer of activated B cells (NF- $\kappa$ B) pathway. Next, DCs upregulate costimulatory molecules, produce various inflammatory cytokines such as interleukin (IL)-6 and IL-12, and together with antigen presentation, DCs promote T-cell activation, expansion and differentiation (82-84). This process must be tightly controlled, as continuous DC activation could lead to severe side-effects, such as presentation of self-antigens to T-cells, resulting in development of auto-immune diseases (83, 85). Rationally, DCs could also be involved in the pathophysiology of PAH (86).

In IPAH patients, DCs are increased in the lung, specifically accumulating around remodeled pulmonary arteries (87). However, in the parenchyma, mostly immature DCs are observed, shown by an increased number of dendritic cell-specific intercellular adhesion molecule-3 grabbing non-integrin (DC-SIGN)<sup>+</sup> DCs (87). DCs can be divided into four main subtypes: type 1 conventional DCs (cDC1s), which are efficient at cross-presentation (i.e., presentation of exogenous antigens in the context of MHC class I and elicit CD8<sup>+</sup> T-cell responses; type 2 cDCs (cDC2s), which are capable of inducing CD4<sup>+</sup> T-cell responses; plasmacytoid DCs (pDCs), which can produce large amounts of type I interferons to combat viral infections; and finally, monocyte-derived DCs (mo-DCs) that arise during inflammation and produce large amounts of chemokines, attracting T-cells to the site of inflammation (88).

Both the numbers of cDCs and pDCs were increased in total lung cell suspensions (either peripheral or perihilar samples) and larger pulmonary arteries of IPAH patients compared to controls (55). Confocal microscopy analyses showed that pDCs were predominantly localized in the alveolar space in proximity to blood vessels. In contrast, in peripheral blood cDC numbers were decreased in IPAH patients (89), and together with the increase in pulmonary cDCs, this suggests migration to the lungs. Currently, no data is available for different cDC subsets in the pathogenesis of PAH. Taken together, DCs are crucial in initiating adaptive immune responses and could be involved in the pathogenesis of PAH by antigen presentation and production of inflammatory cytokines.

## Adaptive immunity

### *T cells*

T cells are a vital part of the adaptive immune system. CD4<sup>+</sup> T cells or T-helper (Th)-cells, provide help by indirectly killing pathogens by supporting the activation of other cells of the immune system such as B cells. CD8<sup>+</sup> T cells are known as ‘cytotoxic T-cells’, which are able to directly kill pathogens through release of granzymes, which induce apoptosis, and the pore-forming protein perforin, which creates holes in target-cell membranes. Gamma delta ( $\gamma\delta$ ) T cells represent a small subset of T cells which are defined by expression of heterodimeric T-cell receptors (TCRs) composed of  $\gamma$  and  $\delta$  chains. An increased number of CD4<sup>+</sup>, CD8<sup>+</sup> T-cells and  $\gamma\delta$  T cells was found in close proximity to pulmonary arteries of IPAH lung biopsies using flow cytometry (55). These CD4<sup>+</sup> and CD8<sup>+</sup> T cells are present in the adventitial space around the pulmonary vessels in IPAH patients (34). In schistosomiasis-associated PAH and IPAH patients, increased peri-arterial CD4<sup>+</sup> T cells were found as well (90).

Th cells are known to play an important role in many inflammatory and autoimmune diseases (91). Th-cells can be roughly divided into Th1, Th2 and Th17 cells. Especially, Th17 cells are found in pulmonary TLOs of IPAH patients (33). Th17 cells are the main source of IL-17, IL-21, and IL-22. In remodeled PAs of IPAH patients, IL-21<sup>+</sup> cells are present (92). Th17 cell differentiate from naïve Th-cells in the presence of IL-1 $\beta$ , IL-6, and TGF- $\beta$  (93). In serum, both IL-1 $\beta$  and IL-6 are increased in IPAH patients compared to controls(94). In CTD-PAH, Th17 cells and Th17-related cytokines were increased compared to healthy controls (95). Work from our group has shown that the level of TNF Alpha Induced Protein 3 (Tnfaip3) expression in DCs controls T-cell differentiation, because Tnfaip3-deficient DCs promote Th17-cell differentiation through increased expression of IL-1 $\beta$ , IL-6 and IL-23 (85, 96). DC-specific deletion of the *Tnfaip3* gene also leads to increased NF- $\kappa$ B, creating a pro-inflammatory environment.

Follicular T-helper (Tfh) cells, expressing the CXCR5 chemokine receptor which contributes to their localization in B cell follicles, can support activated B cells under the influence of IL-21, IL-6, IL-12 and IL-27, leading to induction of humoral immune responses. In IPAH patients TLOs, an increase was found in IL-21<sup>+</sup> PD1<sup>+</sup> Tfh cells (33). In CTEPH patients, histological evaluation of PEA material showed accumulation of CD3<sup>+</sup> T cells in atherosclerotic and thrombotic lesions (36). Little is known about T-cell function differences in CTEPH and more research is needed to provide evidence for a possible pathogenic role for T cells in CTEPH pathogenesis. Taken together, T cells are increased in IPAH lungs and CTEPH PEA material. It appears that a dysregulated Th17-immune response is present in PAH, however more studies are needed to further elaborate this.

### ***B cells and humoral immune responses***

B cells are the effectors of the humoral immune response. Following antigen recognition by the B cell receptor they can present antigen, secrete cytokines, differentiate into memory B cells or to plasma cells that produce large amounts of antibodies. Upon activation B and T cells engage in a germinal center reaction, in which Tfh cells produce their canonical cytokine IL-21, which supports B cell survival, proliferation and differentiation. Moreover, activated T cells express CD40L, which interacts with its receptor CD40 on B cell to provide a co-stimulatory signal that is critical for B cell activation and germinal center formation. As mentioned above, lungs of PAH patients contain TLOs containing B cells, T cells and DCs. These highly organized structures contain high endothelial venules, enabling circulating lymphocytes to directly enter, and stromal cells including follicular dendritic cells that present antigens to B cells via Fc-receptors (97). Importantly, the presence of IL-21<sup>+</sup> Tfh cells, B cells that express activation-induced cytidine deaminase that is essential for immunoglobulin heavy chain class switch and antibody affinity maturation, and plasma cells provide evidence for local and ongoing antibody production (33). Next to the presence of TLOs in the lung, there is additional evidence supporting the notion that B-cell activation is dysregulated in IPAH and in connective tissue disease associated PAH (CTD-PAH) (98, 99). First, circulating plasma blasts are increased in IPAH patients (100). Second, autoantibodies are present in approximately 40% of patients with IPAH (101). These autoantibodies might be produced by plasma cells located within TLOs in IPAH lungs (33, 100), recognizing endothelial cell surface antigens (102). Anti-endothelial autoantibodies promote apoptosis of endothelium, which contributes to vascular remodeling (100). Furthermore, endothelial-specific IgA can promote cytokine production and upregulation of adhesion molecules by endothelial cells (100, 102-104). Anti-endothelial IgG antibodies activate endothelial cells to a pro-adhesive and pro-inflammatory state (105). In animal studies, injection of autoantibodies from CTD-PAH patients into healthy mice leads to more abundant vascular and airway smooth muscle cell numbers and inflammatory pulmonary vasculopathy (106). In MCT rats, high levels of plasma IgG were found that labeled lung vascular proteins. Also, transfer of autoantibodies into rats caused pulmonary vascular remodeling and pulmonary hypertension (107).

In CTEPH, little is known about circulating and thrombus-resident B-cells. A well-known risk factor for CTEPH is a splenectomy, and considering that the spleen is important for B cell maturation, there might be a role for pathogenic B-cells in the CTEPH pathogenesis. Currently studies are being performed using mass cytometry in PBMCs from CTEPH patients. Results from these studies are still in process.

In summary, autoantibodies are found in IPAH patients, specifically targeting endothelial cell surface antigens. B-cells and plasma cell formation prior to this could play a major role in the pathogenesis of PAH.

Table 1. Circulating cytokine/chemokine levels in patients with pulmonary arterial hypertension or chronic thromboembolic pulmonary hypertension.

Biomarker	PAH				CTEPH					
	Incident Patients	Prevalent Patients	Hemodynamic Correlation	Prognosis	Etiology	Ref.	Prevalent Patients	Hemodynamic Correlation	Prognosis	Ref.
IL-1 $\alpha$	↑(108)	↑	N/A	+	IPAH, HPAH	(108)				
IL-1 $\beta$	↑(108)	↑	-	+(108)	IPAH, HPAH, CHD-PAH	(94, 108)	↑(112)	-	-	(36, 110, 112)
IL-2	=	↑	-	-	PAH, HPAH	(94, 108)	↑	-	-	(112)
IL-4	=	↑	-	-	PAH, HPAH	(94, 108)	↑	-	-	(112)
IL-5	N/A	=	-	-	PAH, HPAH	(94)	=	-	-	(112)
IL-6	↑(108, 109, 113)	↑	+	+	IPAH, HPAH, CTD-PAH, CHD-PAH	(94, 108, 109, 113, 114)	↑(32, 111)	+	+(111, 112)	(32, 36, 109, 111, 112)
IL-8	=	↑	-	+(94)	IPAH, HPAH, CTD-PAH, CHD-PAH	(94, 108, 109, 113, 114)	↑(32, 111, 112)	-	+(111, 112)	(32, 109, 111, 112)
IL-10	=	↑	-	+(94)	IPAH, HPAH	(94, 108)	↑	-	+(111, 112)	(36, 111, 112)
IL-12	=	↑	-	+(94)	IPAH, HPAH	(94, 108)	=	-	-	(112)
IL-13	=	=	-	+(108)	IPAH, HPAH	(94, 108)	=	-	-	(112)
IFN- $\gamma$	=	=	-	-	IPAH, HPAH	(93, 107)	=	-	-	(112)
TNF- $\alpha$	↑(108, 109, 113)	↑	N/A	+(108)	IPAH, HPAH, CTD-PAH, CHD-PAH	(94, 108, 109, 113, 114)	=	-	+(110, 111)	(109-111)
MMP-9	↑	↑	+	+	PAH	(115)	↑	-	N/A	(36)
VEGF	=	↑	N/A	+(115)	IPAH, HPAH, CHD-PAH	(94, 108, 114, 115)	=	-	N/A	(36)
CCL-2	=	↑(48)	N/A	-	IPAH	(48, 108)	↑	-	N/A	(32, 36)

Biomarker	PAH				CTEPH					
	Incident Patients	Prevalent Patients	Hemodynamic Correlation	Prognosis	Etiology	Ref.	Prevalent Patients	Hemodynamic Correlation	Prognosis	Ref.
MIG	N/A	↑	-	N/A	IPAH	(32)	↑	-	N/A	(32)
CCL-3	=	=	-	N/A	IPAH	(32)	↑	+	N/A	(32, 36)
CXCL-10	N/A	↑	-	N/A	IPAH	(32)	↑	+	N/A	(32)
CCL-5	N/A	↑	-	N/A	IPAH, PAH	(32, 116)	↓	-	N/A	(32)
CX3CL-1	=	=	-	N/A	IPAH	(32)	=	-	N/A	(32)
CXCL-12	=	=	-	N/A	IPAH	(32)	=	-	N/A	(32)

Pulmonary arterial hypertension (PAH); idiopathic PAH (IPAH); hereditary PAH (HPAH); congenital heart disease-associated PAH (CHD-PAH); connective tissue disease-associated PAH (CTD-PAH); chronic thromboembolic pulmonary hypertension (CTEPH); no significant differences (=); positive correlation (+); no significant correlation (-); not assessed (N/A); interleukin (IL); interferon gamma (IFN- $\gamma$ ); tumor necrosis factor- $\alpha$  (TNF- $\alpha$ ); matrix metalloproteinase 9 (MMP-9); vascular endothelial growth factor (VEGF); chemokine (CCL) (C-C motif) ligand; monokine-induced by interferon- $\gamma$  (MIG); C-X-C motif chemokine (CXCL); C-X3-C motif ligand (CX3CL).

## Inflammatory diagnostic and prognostic biomarkers in PAH and CTEPH

Inflammatory biomarkers might be useful as diagnostic and prognostic tool in PAH and CTEPH (32, 36, 47, 94, 108-116), which are highlighted in **Table 1**. Inflammatory cytokines and chemokines can contribute directly to recruitment of immune cells, activation and proliferation of PSMCs, and endothelial dysfunction. Until now the most prominent cytokine appears to be IL-6, which has many links to PAH pathogenesis. In animal models, PH development has been seen after administration of recombinant IL-6 and also in IL-6 transgenic mice (117-119), whereas IL-6 knockout mice have shown resistance to hypoxia-induced PH development (120). In clinical studies, IL-6 has shown to correlate to survival and quality of life in IPAH patients (94, 121) and in predicting long-term response to PEA in CTEPH patients (112). In a recent study, cytokine clusters have been made in PAH patients using machine learning. The analyses showed that the immune phenotypes were not dependent on the subtypes within the WHO group 1 PAH classification (122), indicating that immune phenotypes may vary within the WHO group 1 subtypes. Furthermore, these findings might provide a framework to examine patient responses to emerging therapies targeting immunity in the future.

In tumor necrosis factor alpha (TNF- $\alpha$ )-overexpressing mice, spontaneous development of PH was observed (123). In a clinical study in CTEPH patients undergoing PEA, increased levels of TNF- $\alpha$ , IL-6 and IL-10 were found prior to surgery (111). IL-6 and IL-10 were shown to peak immediately after surgery, while TNF- $\alpha$  decreased significantly within the first 24 hours after PEA surgery (111).

In CTD-PAH, treatment-naïve patient baseline levels of *placental growth factor* (PIGF), sVEGFR-1, TNF- $\alpha$ , and VEGF-D were increased and could differentiate between healthy controls/IPAH and CTD-PAH. Moreover, after four months of PAH-targeted treatment, sVEGFR-1 levels were decreased, indicating that this growth factor is worthwhile to evaluate during therapies (113). In a study in 206 PAH patients, angiopoietin 1 (Ang-1), VEGF and matrix metalloproteinase 9 (MMP-9) levels have been associated with increased risk of death and hospitalization at 16-week follow-up after baseline (115). Many of the inflammatory biomarkers are still being investigated, because more pre-clinical, translational and clinical studies are needed to determine the clinical and prognostic value of these markers.

## Immunomodulatory therapy in PAH and CTEPH

Promising novel inflammatory therapeutic targets and ongoing clinical trials evaluating possible therapeutic drug compounds are highlighted in **Figure 4**. In addition, an overview of attenuation of experimental PH by targeting immunomodulatory pathways is given in **Supplementary Table 1**.

Based on the evidence described above, targeting immune and inflammatory pathways may be sufficient to treat and prevent progression of the disease. Previous studies have shown that in the inflammatory MCT-rat PH model, anti-inflammatory therapies such as dexamethasone, mycophenolate mofetil and nuclear factor of activated T cell (NFAT) inhibition with cyclosporine can prevent and reverse the PH phenotype (124-126). In SLE and MCTD-PAH patients, treatment with a combination of cyclophosphamide and glucocorticoids was possibly effective in lowering the PVR in patients with a less severe PH at baseline (127).

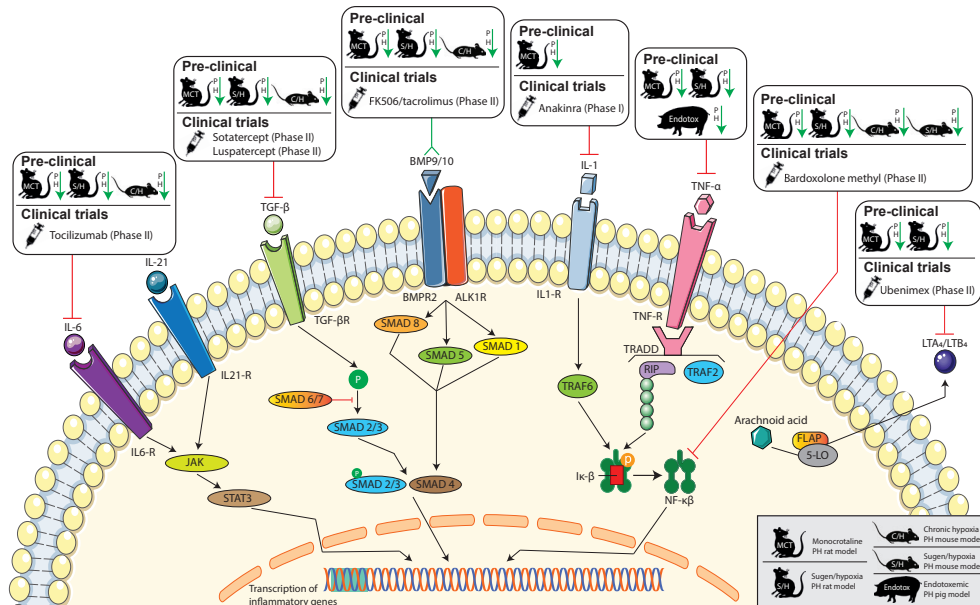


**Figure 4.** Schematic overview of (pre-)clinical targets for immunomodulatory therapy in pulmonary arterial hypertension (PAH) patients. Pre-clinical animal PH model signs are mentioned in the legend in the bottom right corner. IL, Interleukin; TGF- $\beta$ , transforming growth factor beta; BMP, bone morphogenetic protein; BMPR2, bone morphogenetic protein receptor type II; TNF- $\alpha$ , tumor necrosis factor- $\alpha$ ; NF- $\kappa\beta$ , nuclear factor kappa-light-chain-enhancer of activated B cells; LTA4/B4, Leukotriene A4/B4. JAK, janus kinases; STAT, signal transducer and activator of transcription proteins; SMAD, small Mothers Against Decapentaplegic; TRAF, TNF receptor associated factor; TRADD, Tumor necrosis factor receptor type 1-associated DEATH domain; RIP, receptor-interacting protein; NF- $\kappa\beta$ , nuclear factor kappa-light-chain-enhancer of activated B cells; IK- $\beta$ , inhibitor of  $\kappa\beta$ ; FLAP, 5-lipoxygenase activating protein; 5-LO, Arachidonate 5-lipoxygenase.

More targeted therapy such as anti-IL-1 treatment was shown to prevent the PH phenotype in MCT-PH rats (128). A current trial conducted by the Virginia Commonwealth University evaluating efficacy of treatment of PAH patients with Anakinra, an IL-1 receptor antagonist compound, will soon be finalized.

In recent studies, IL-6-specific antagonist treatment reversed experimental PH in MCT-PH and sugen/hypoxia (SU/Hx)-induced PH rat models (129). In hypoxia-induced PH in mice, an attenuating effect of blockade of IL-6 was also found (92). Preliminary results from a recent phase II clinical trial of anti-IL-6 therapy (Tocilizumab) in PAH patients showed no changes in WHO functional class, 6-minute walking test (6MWT), NT-proBNP and quality of life for the majority of PAH patients (130). However, an decrease in PVR >15% was seen in a small subgroup of CTD associated-PAH and in hereditary (H)PAH/IPAH patients (130). Possibly, this mild effect in IPAH patients could be due to the heterogeneous nature of IPAH patients, consisting of several subgroups, considering that ~40% of the IPAH patients have auto-antibodies (101).

In hypoxia-induced PH mice, increased expression levels were found for IL-17 and IL-21, signature genes for Th17 and Tfh cells, respectively (92). Whereas blockade of IL-17 showed no effects on the RVSP and the RV hypertrophy, IL-21-receptor knockout mice were resistant to hypoxia-induced PH (92). Increased expression of M2 macrophage markers and IL-21, which can polarize macrophages towards an M2 phenotype, was detected in the lungs of IPAH patients who underwent

lung transplantation. Together with the known prominent role of IL-21 in B-T cell interaction, these findings suggest that IL-21 is a potential target for treating PAH (92). In autoimmune experimental arthritis, a combination of IL-6/IL-21 blockade has shown synergistic beneficial effects associated with strongly reduced Th17 differentiation (131).

Anti-TNF- $\alpha$  therapy (Etanercept) has been demonstrated to attenuate the PH phenotype both in MCT-PH rats (132, 133) as well as in SU/Hx-induced PH rats (134). In endotoxemic pigs, anti-TNF- $\alpha$  therapy reversed the PAH phenotype (135). Currently, no (pre-)clinical trials are available to determine possible clinical effects of Etanercept in patients.

Increasing knowledge on loss-of-function mutations in the BMPR2 signaling pathway, have led to the initiation of studies evaluating possible novel therapeutic targets in this cascade. BMPR2, which is mainly expressed in vascular endothelial cells (136), is a member of the TGF- $\beta$  receptor family and many studies have shown an important role for BMPR2 in the pathogenesis of PAH. Upon binding to bone morphogenetic proteins (BMPs), BMPR2 initiates intracellular signaling that ultimately leads to the inhibition of proliferation of vascular smooth muscle tissue. In smooth muscle cells, BMP signaling can be directly inhibited by TGF- $\beta$  signaling and involved ligands are able to function as antagonists by competition for type II receptor binding (137). *BMPR2* loss-of-function mutations are a known cause for PAH development in patients and lead to more severe disease and increased risk of death when compared to PAH patients without a *BMPR2* mutation (138). In a recent study, BMP9 was shown to be a sensitive and specific biomarker of porto-pulmonary hypertension patients to predict transplant-free survival and the presence of PAH in liver disease (139). In human IPAH lungs and in hypoxia-induced PH in mice, reduced BMPR2 expression induced macrophage recruitment – involving enhanced production of the chemokine granulocyte macrophage colony-stimulating factor GM-CSF - and led to exacerbation of PAH features (140). In rodent models such as the MCT-rat, Su/Hx PH mouse model and in mice harboring a human *BMPR2* mutation knock-in allele, BMPR2 activation can prevent vascular remodeling and can attenuate the PAH phenotype with endothelial growth and proliferation (141-143). Currently, a therapeutic drug discovery company (MorphogenIX, Cambridge, UK) was founded for development of BMPs as a novel treatment in PAH.

Targeting TGF- $\beta$  signal pathways may also be an effective treatment in PAH, considering the upregulation of TGF- $\beta$  downstream of the loss of function in BMPR2, which has shown correlation to PH development (144, 145). In a recent study, treatment with immunoglobulin-Fc fusion protein of TGF- $\beta$  (TGFBR2-Fc), a selective TGF- $\beta$  inhibitor targeting THF-b 1/3, has shown attenuation of the PH phenotype in MCT-PH rats and SU/Hx-induced PH rats and mice (146). Currently, ligand traps such as Sotatercept and Luspatercept with high selectivity for members of the TGF- $\beta$  superfamily are being investigated in phase II trials (PULSAR trial), as they were successful before in phase I clinical trials. These ligand traps may rebalance BMPR2 signaling and restore vascular homeostasis.

Another potentially interesting compound in the BMPR2 pathway is calcineurin inhibitor FK506 (tacrolimus), which has been reported to increase expression and activity of BMPR2. In MCT-PH and SU/Hx-induced PH rats and hypoxia induced PH mice, FK506 was reported to reverse the severe PAH phenotype (147). In IPAH patients FK506 treatment reversed dysfunctional BMPR2 signaling in pulmonary artery endothelial cells (147). In a recent phase IIa trial, treatment of FK506 in 20 PAH patients showed increased expression of BMPR2, improvement of 6MWD and serological and echocardiographic parameters of heart failure in some patients, however these changes were not significant (148). Nonetheless, FK506 was generally well tolerated and this study supports the

initiation of a phase IIb efficacy trial. Important to note is that tacrolimus is also well known for other immunosuppressive effects such as T cell inhibition in the organ-transplant field, so the effects might not be exclusively limited to the BMP2 pathway.

NF- $\kappa$ B is a ubiquitous transcription factor that is known for regulation of many aspects of innate and adaptive immune functions. By inducing expression of various pro-inflammatory genes for cytokines and chemokines, NF- $\kappa$ B is an important regulator for cell survival, proliferation and mobility (149). Targeting NF- $\kappa$ B may therefore be an interesting novel therapeutic pathway for treatment of PAH. In MCT-PH rats, the NF- $\kappa$ B was found to be activated and an NF- $\kappa$ B-blocking treatment attenuated the PH phenotype (150-152). This ameliorating effect was also found in SU-Hx rats in which NF- $\kappa$ B targeting severely reduced lung vascular lumen obliteration (153). Furthermore, in MCT-treated transgenic mice overexpressing a cardiac-specific dominant-negative I $\kappa$ B $\alpha$  (inhibitory binding partner of NF- $\kappa$ B), inhibition of NF- $\kappa$ B prevented RVH (154). In PAH patients, NF- $\kappa$ B has been shown to be highly activated in pulmonary lymphocytes, macrophages, ECs and PASMCs (155).

Currently, several NF- $\kappa$ B inhibitory compounds are available for evaluation of treatment efficacy in PH patients. Bardoxolone methyl is a known inhibitor of NF- $\kappa$ B and shows effects in suppressing activation of pro-inflammatory mediators, enhancement of endothelial NO bioavailability, improvement of metabolic dysfunction, suppressing vascular proliferation and preventing maladaptive remodeling (156-158). Currently, bardoxolone methyl is being evaluated in a Phase 2 clinical trial in pulmonary hypertension patients (IPAH, CTD-PAH, WHO group III or group V PH).

Another promising compound is dimethyl fumarate (DMF), with potent anti-inflammatory effects through inhibition of NF- $\kappa$ B. DMF is an activating agent for the transcriptional regulator nuclear factor erythroid 2-related factor 2 (NRF2), which is known for key regulation of antioxidant genes (159). NRF2 function is linked to NF $\kappa$ B signaling with activation of NRF2 leading to inhibition of NF $\kappa$ B signaling and thereby inducing an anti-inflammatory response (160). In the chronic hypoxia and SU/Hx-induced PH mouse model, DMF has been reported to attenuate the PAH phenotype (161). Currently, no clinical trial for evaluation of clinical therapeutic value for DMF is being performed.

As previously described, accumulating evidence is beginning to show a pathological role for B cells and plasma cells in PH pathogenesis. Therefore, targeting CD20, which is a B-cell specific surface marker, could be a promising drug therapy to evaluate. In a case report, rituximab treatment significantly improved early onset PAH in a young patient suffering from SLE (162). However, a recent phase II trial for evaluating the effect of treatment of Rituximab in patients suffering from SSc-PAH did not reach statistical significance for its primary outcome measure of 6MWD (163).

Another interesting therapeutic target is Leukotriene B<sub>4</sub> (LTB<sub>4</sub>), a pro-inflammatory lipid mediator produced from arachidonic acid by consecutive activities of 5-lipoxygenase, 5-lipoxygenase-activating protein, and leukotriene A<sub>4</sub> hydrolase (164). In MCT-PH rats, LTB<sub>4</sub> receptor antagonist (ONO4057) has been reported to reduce RVH after MCT treatment, and prevented development of PH (165).

Nonspecific inhibition of Leukotriene A<sub>4</sub> through bestatin (ubenimex) reversed the PH phenotype in MCT-PH and SU/Hx-induced PH rats (52). Currently, a clinical phase II trial (LIBERTY trial) is evaluating the efficacy of bestatin treatment in 61 PAH patients. Preliminary results for the trial sponsor (Eiger Biopharmaceuticals, Palo Alto, CA, USA) however, show no significant treatment effect in comparison to placebo treatment.

## Summary

Taken together, there is mounting evidence that the immune system plays a pivotal role in the pathogenesis of PAH and CTEPH. Both PAH and CTEPH histology demonstrated extensive accumulation of immune cells. Further analyses in IPAH patient lungs and lung biopsy material from CTEPH patients provided compelling evidence for activation of the innate immune system. Pathological involvement of macrophages, MCs and neutrophils by production of inflammatory cytokines, recruitment of other immune cells and local inflammation and damage was demonstrated. In the lungs of IPAH patients increased numbers of DCs were observed, acting as a bridge between innate and the adaptive immune system by presentation of antigens to T cells. DCs contribute to increased production of cytokines and chemokines, attracting other inflammatory cells to the site of inflammation. Dysregulated Th17 immunity was found in PAH patients, creating a pro-inflammatory auto-immune environment. Moreover, IPAH patients displayed an increase of circulating autoantibodies specifically targeting endothelial cell surface antigens. Extensive biomarker research revealed that many inflammatory and immune markers correlate with hemodynamics and/or prognosis of PAH and CTEPH patients. However, further evaluation is required to investigate the applicability of these parameters in the clinical work-up of PAH and CTEPH patients. Currently, clinical trials are being performed to assess the value of promising inflammatory and immune targets defined in pre-clinical research in PAH. A combination of immunomodulatory therapies might be required besides current treatment based on vasodilatation alone, to establish an effective treatment and prevention of progression of this disease.

## 1.2 TOWARDS THE AIMS OF THIS THESIS

### Current Clinical Practice: more research is required

As outlined above, there is growing evidence that the immune system plays an important role in the pathogenesis of PAH and CTEPH. Although new immunomodulatory therapeutic strategies are under development, pulmonary hypertension remains a debilitating and devastating disease. Considering the poor survival despite current treatment options, there is a great need for more detailed insight into the etiology of this disease and development of prognostic tools such as inflammatory biomarkers. Therefore, the aim of this thesis is to further unravel the immune-related pathogenesis in PAH and CTEPH pathobiology. To this end, two major players in the pathogenesis of pulmonary hypertension were investigated: (I) activated dendritic cells in the pathogenesis of PAH and (II) T cells and inflammatory cytokines in PAH and CTEPH. In this research, we took advantage of two important tools (I) the *Tnfaip3*<sup>DNGRI-KO</sup> DC mouse model and (II) the Biopulse cohort of pulmonary hypertension patients. Both tools are described in detail below.

### An animal model to study the pathophysiological role of dendritic cells in pulmonary hypertension

As described above, several lines of evidence provide evidence for the involvement of DCs in the pathogenesis of PH. DCs are key modulators between tolerance and immunity and are known to function as a bridge between innate and adaptive immunity. Upon activation by different microbial stimuli and cytokines, DCs are able to present antigen to CD4<sup>+</sup> and CD8<sup>+</sup> T cells and are thereby capable of eliciting T helper cell and cytotoxic T cell responses, respectively. Since DC activation is a

critical step in immune modulation, their activation must be tightly controlled. Central to understanding DC activation is the NF- $\kappa$ B pathway (**Figure 5**).

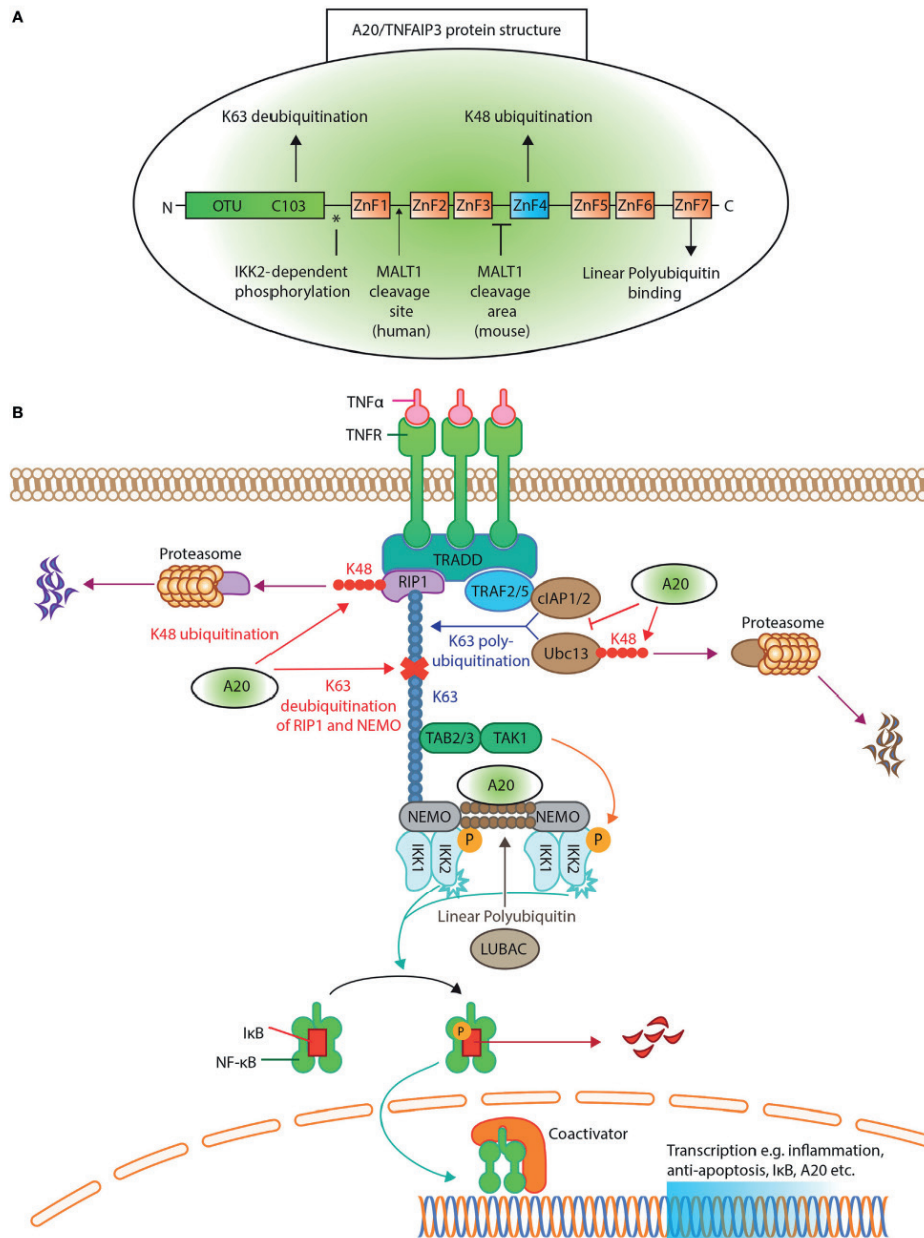


**Figure 5.** A20/tumor necrosis factor  $\alpha$ -induced protein 3 (TNFAIP3) protein structure and its function in the inhibition of tumor necrosis factor receptor (TNFR)-induced nuclear factor kappa-light-chain-enhancer of activated B cells (NF- $\kappa$ B) activation.

(A) The protein structure of A20/TNFAIP3. The N-terminus contains the ovarian tumor (OTU) domain, with the C103 cysteine site of K63 deubiquitination. The seven zinc fingers (ZnF) are illustrated, where ZnF4 has K48-ubiquitinating activity and ZnF7 can bind

linear polyubiquitin. The asterisk (\*) indicates the site of I $\kappa$ B kinase (IKK)2-dependent phosphorylation. An arrow indicates where mucosa associated lymphoid tissue translocation protein 1 (MALT1) cleaves human A20/TNFAIP3 (after Arginine 439), while for murine A20/TNFAIP3 it is only known that MALT1 cleaves A20/TNFAIP3 between ZnF3 and ZnF4. **(B)** TNFR activation of the NF- $\kappa$ B pathway. Ligand TNF $\alpha$  binds the TNFR receptor and allows binding of TNFR1-associated death domain protein (TRADD) to the TNFR. This recruits receptor-interacting serine/threonine-protein kinase 1 (RIP1) and TNFR-associated factor (TRAF)2 or TRAF5 to form the TNFR complex. RIP1 is K63 polyubiquitinated by E2-E3 ubiquitin-conjugating enzyme (Ubc)13 and cellular inhibitor of apoptosis protein (cIAP)1/2. The polyubiquitin acts as a scaffold for TAK1 binding protein (TAB)2/TAB3 and NF- $\kappa$ B essential modulator (NEMO) to recruit the transforming growth factor beta-activated kinase 1 (TAK1)-TAB 2/3 complex. TAK1 phosphorylates and activates the IKK, composed of IKK1( $\alpha$ ), IKK2( $\beta$ ), and NEMO. The linear ubiquitin chain assembly complex (LUBAC) was shown to generate linear polyubiquitin on NEMO (and also RIP1), recruiting and stabilizing another IKK-NEMO complex. IKK2, phosphorylates I $\kappa$ B, allowing I $\kappa$ B K48 polyubiquitination and consequently degrading by proteasomes, thereby releasing NF- $\kappa$ B to translocate to the nucleus. A20/TNFAIP3 acts in different levels of the pathway. A20/TNFAIP3 removes K63-linked polyubiquitin chains from RIP1 and NEMO, thereby disrupting downstream signals. In addition, A20/TNFAIP3 adds K48-linked polyubiquitin chains to RIP1 and Ubc13, thus targeting them for proteasomal destruction. Beyond (de) ubiquitinating mechanisms, A20/TNFAIP3 also destabilizes Ubc13 interaction with cIAP1/2, thereby preventing new K63-ubiquitinating activity. The ZnF7 of A20/TNFAIP3 binds linear ubiquitin, thereby accelerating the dissociation of LUBAC and IKK/NEMO, resulting in NF- $\kappa$ B termination. *Adapted from Das et al 2018 (166).*

Processes involved in regulation of DC activation are crucial to maintain a necessary balance between immunity and tolerance in response to different stimuli. Several studies have shown a crucial role for *TNFAIP3/A20* in controlling inflammatory disease *in vivo* (85, 167-169) (**Figure 5**). Polymorphisms in the *TNFAIP3* locus are significantly associated with several autoimmune conditions, as well as PH (170). Through conditional targeting of A20 in (subsets) of DCs in mice, much has been learned about A20 biology *in vivo*. This conditional targeting was achieved by using the site-specific cre-lox recombination technique, which has the capacity to carry out deletions, insertions, translocations and inversions at specific sites in the DNA of cells in a cell-type specific manner. DC-specific deletion of *Tnfaip3/A20* using the *Cd11c-cre* in mice (*Tnfaip3*<sup>CD11c-KO</sup> mice) resulted in constitutive activation of DCs. *Tnfaip3*<sup>CD11c-KO</sup> mice spontaneously developed a severe and complex autoimmune inflammatory phenotype with features that resembled inflammatory bowel disease (IBD) and spondyloarthritis (167) or systemic lupus erythematosus (SLE) (85).

However, it remains unclear what the contribution is of the individual DC subsets to the autoimmune or inflammatory phenotype in *Tnfaip3*<sup>CD11c-KO</sup> mice. As is depicted in **Figure 6**, DCs can be subdivided into various subsets, each of which have a specific function in the activation of CD4<sup>+</sup> or CD8<sup>+</sup> T cells and cytokine production. In previous work from our group, several mouse models with Cre-mediated targeting of different DC subsets have been investigated, each with its own specific phenotype (96, 171). These models were developed to evaluate helper (TH) subset differentiation, mechanisms of house dust mite-triggered asthma and signs of autoimmunity. In the CD11c-cre (targeting all DCs), TNFAIP3-deficient DCs induced HDM-specific TH17 cell differentiation through increased expression of the TH17-instructing cytokines IL-1 $\beta$ , IL-6, and IL-23, whereas HDM-specific TH2 cell differentiation was hampered by increased IL-12 and IL-6 production (96). Considering the increased numbers of cDCs in IPAH lungs (55), and regarding that uncontrolled type 1 cDCs (cDC1s) activation can potentially lead to severe side-effects, such as presentation of self-antigens to T-cells, we hypothesized that it would be very interesting to evaluate the role for cDCs in PAH pathogenesis. However, to date very few studies have addressed the possible mechanistic role of conventional DCs in development of PH. Here, we used DNDR1(*Clec9a*)-Cre-mediated (172) deletion of *Tnfaip3/A20* (*Tnfaip3*<sup>DNDR1-KO</sup> mice, **Figure 6**) to specifically target cDC1s in our studies. Since DNDR1 promoter-driven Cre expression resulted in very specific deletion of the *Tnfaip3* gene in cDC1 (resulting in ~95% LoxP recombination), this allowed for mechanistic studies on the role of cDC1.

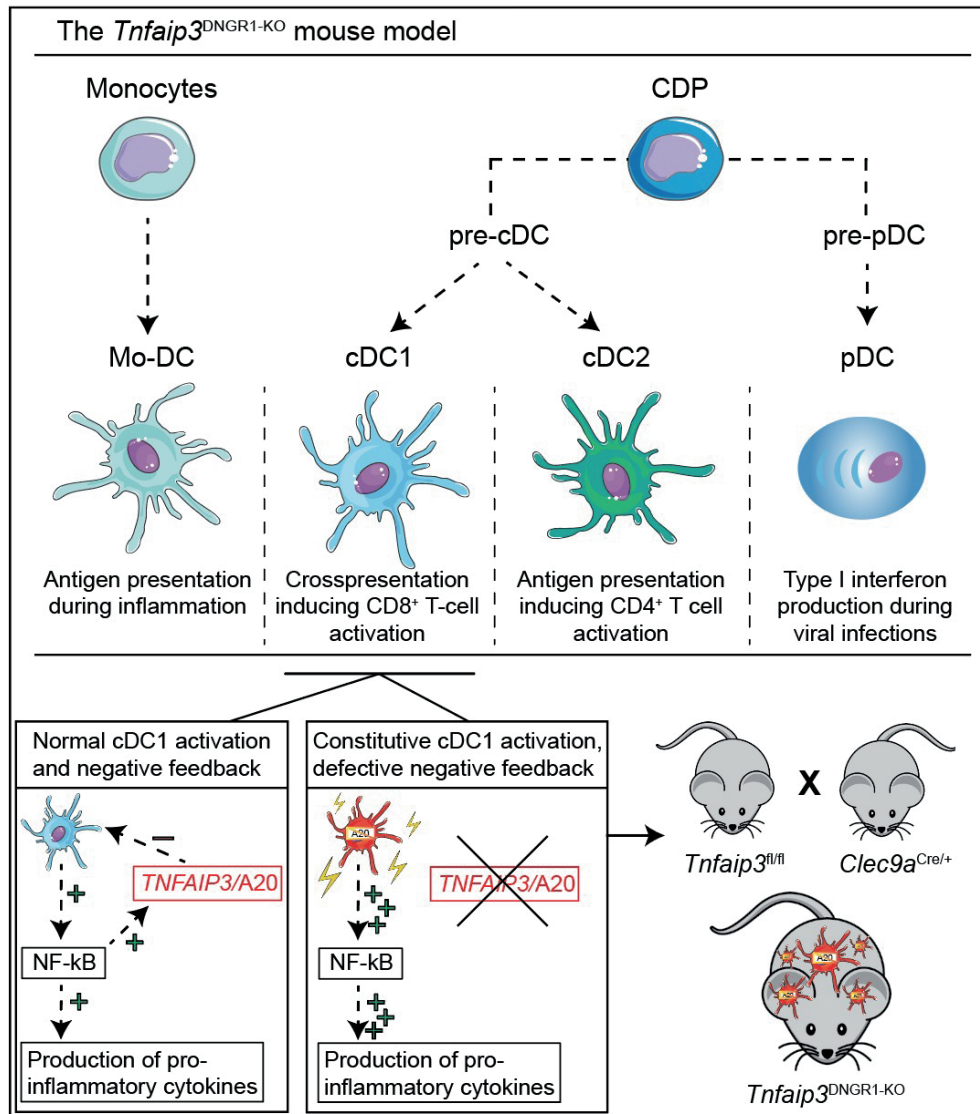


**Figure 6.** The *Tnfaip3*<sup>DNGR1-KO</sup> mouse model for PH studies.

**Upper part,** graphical display of the different DC subsets. CDP; common dendritic cell precursor cell. cDC; conventional dendritic cell; pDC; plasmacytoid dendritic cell. **Lower part,** graphical display of normal DC activation with negative feedback, and constitutive DC activation with defective negative feedback. In crosses of *Tnfaip3*<sup>fl/fl</sup> and *clec9a*<sup>Cre/+</sup> (~95% specific for cDC1s) mice, *Tnfaip3*<sup>DNGR1-KO</sup> mice are born with specific *TNFAIP3/A20* deletion in cDCs. *Tnfaip3*; TNF Alpha Induced Protein 3. *Clec9a*; C-Type Lectin Domain Containing 9A.

## The Biopulse PH patient cohort

The presenting symptoms of PH are nonspecific and therefore the diagnosis is often delayed by two years on average (173). However, an early diagnosis is crucial, because without treatment PH patients have a median survival of ~2.8 years and an estimated 5-year survival of ~34% (174). The definitive diagnosis can only be set after right heart catheterization. Nevertheless, to monitor the patients' clinical condition less invasive methods are preferred. Currently the six-minute walking test, NYHA classification and echocardiography, all diagnostic tests which have proven to correlate with disease severity and prognosis (175), are used to evaluate the clinical condition of the patient. However, these diagnostic tools have significant limitations and fail to identify early changes in cardiac function. Because of the frequent delay in diagnosis and limitations of current diagnostic tools, there is a great need to identify additional measures. Such new measures, e.g. inflammatory biomarkers, may be combined with existing tools to detect and monitor subtle molecular changes in the pulmonary vessels and the right ventricle that reflect and possibly prelude early deteriorations in cardiac function before they become clinically visible. Furthermore, as described above, increasing evidence indicates a pathophysiological role for immune cells such as DCs, T-cells and B-cells. To investigate the presence, activation and differentiation of these immune cells, and the presence of circulating inflammatory biomarkers such as cytokines, chemokines and vascular growth factors, the Biopulse study (Figure 7) was set up.

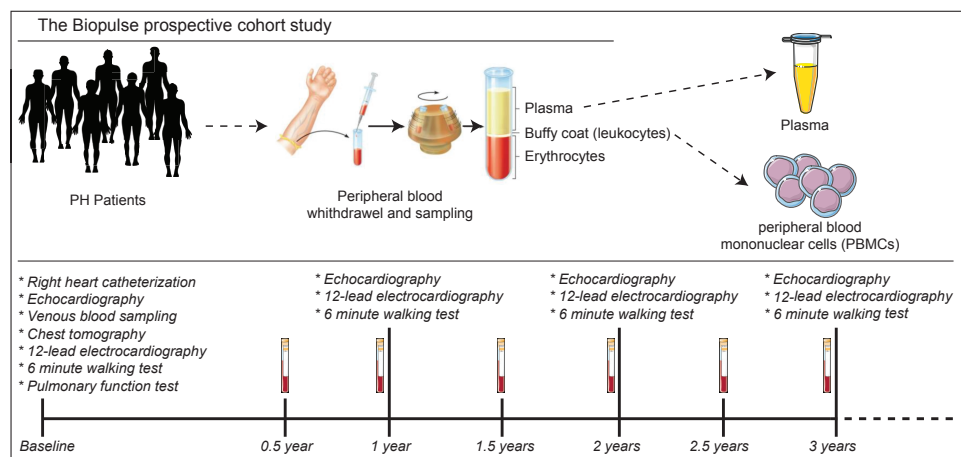


**Figure 7.** Overview of the Biopulse study.

The Biopulse study is a prospective observational cohort study, in which PH patients >18 years old with a mPAP  $\geq$  25mmHg were included at diagnosis. All patients were diagnosed according to the ERS/ECSC guidelines (2) and were subdivided according to the World Health Organization (WHO) classification (1, 2). At inclusion, all patients undergo physical examination by a pulmonary physician and a cardiologist, pulmonary function tests, VQ scan, chest computed tomography scan, 6-minute walking test, ultrasound of the abdomen, 12-lead electrocardiography (ECG), transthoracic echocardiography, venous blood sampling and right heart catheterization. Exclusion criteria were incomplete diagnostic work-up and therefore no confirmed PH diagnosis, not treatment-naïve, age <18 years, or not capable of understanding or signing informed consent. Consequently, venous blood samples are collected at every half year visit and patients undergo an annual extensive investigation including echocardiography, 12-lead electrocardiography and 6-minute walking test.

## General outline of the thesis

Accumulating evidence points to critical involvement of the immune system in PAH and CTEPH pathogenesis, leading to decreased survival and high burden of disease. However, there are still many questions unanswered, such as in which way the immune system is involved and which immune cells are the main players. Therefore, the aim of this thesis was to further unravel the immune-related pathogenesis in PAH and CTEPH.

Considering that cDCs are increased in the lungs of IPAH (87), in **chapter 2** our aim was to investigate whether constitutive activation of cDCs would result in PH development in mice. To this end, we utilized the *Tnfaip3*<sup>DNGR1-KO</sup> mouse model, with a Clec9a/DNGR1-Cre-mediated deletion of the *Tnfaip3* gene specifically in the cDC1 subset. In these studies, we found that *Tnfaip3*<sup>DNGR1-KO</sup> mice develop an experimental PH phenotype characterized by increased right ventricular (RV) systolic pressure (RVSP), RV hypertrophy (RVH), perivascular lymphocytic infiltration, and vascular remodeling.

The exact mechanism by which these *Tnfaip3*<sup>DNGR1-KO</sup> mice, described in **chapter 2**, develop PH symptoms and the importance of the altered activation status of DCs or other immune cells in this model is largely unknown. In **chapter 3**, we investigated the immunological landscape of the heart in *Tnfaip3*<sup>DNGR1-KO</sup> mice more closely. We also addressed the question whether additional immune activation in *Tnfaip3*<sup>DNGR1-KO</sup> mice would have effects on PH development by exposing the airways of these mice to TLR-ligands in vivo. Furthermore, our aim was to determine whether a vascular trigger would result in enhancement of the PH phenotype, which is also described in **chapter 3**. To this end, we crossed *Tnfaip3*<sup>DNGR1-KO</sup> mice with mice that harbor a mutation in the *Bmpr2* gene, which is associated with a susceptibility to develop PH (see above). Lastly, in this chapter we explored the relevance of our findings by determining DC and CD8<sup>+</sup> T cell co-localization in human IPAH lung tissue.

In PAH and CTEPH patients, increased levels of inflammatory cytokines and chemokines were observed in previous studies. However, limited data are available regarding the levels of cytokines and chemokines in treatment-naïve patients, particularly in CTEPH. Furthermore, little is known about possible changes in cytokine and chemokine levels during follow-up of these patients and about the correlation of inflammatory marker signatures with prognosis. Therefore, in **chapter 4** we studied circulating inflammatory markers in PAH and CTEPH patients at diagnosis and at 1-year follow-up in relation to clinical outcome parameters.

An increased presence of T cells and chemokines in surgical PEA material from CTEPH patients was demonstrated in previous studies. However, there is limited data available on the phenotype and classification of these T cells. Moreover, few data on T-cell activation, cytokine production and Th-subset division are available in treatment-naïve CTEPH patients. Therefore, our aim was to investigate more closely T cell activation, cytokine production and Th-subset division in CTEPH patients at diagnosis and after 1-year of follow up. The results of our analyses are described in **chapter 5**.

In PAH patients, numbers of CD4<sup>+</sup> T cells (especially Tregs) and CD8<sup>+</sup> T cells were found to be altered. To date, in depth classification and phenotypical characterization of these T cells is still lacking, particularly in treatment-naïve patients. In **chapter 6**, our aim was to investigate in more detail, T-cell activation, cytokine production and Th-subset distribution in PAH patients at diagnosis and after 1-year of PAH-specific treatment.

A common clinical feature of PAH patients is deterioration of physical condition and diminished quality of life, which obviously needs improvement. Accumulating evidence is showing beneficial effects of pulmonary rehabilitation (PR) therapy (14-16). In current literature, most studies have been

performed in an entirely clinical setting. Knowledge about safety and efficacy of a PR program in an exclusively outpatient setting is still lacking. Furthermore, little is known about soluble biomarkers levels and possible changes herein during PR therapy. Our aim was to design and study an achievable multidisciplinary outpatient PR program and to evaluate soluble biomarker levels during PR therapy, which is described in **chapter 7**.

Finally, in **chapter 8**, the findings in this thesis are integrated into a general discussion, providing an overview of the pathophysiological role for the immune system in pulmonary hypertension, as well as the prognostic value of immunological parameters for disease progression and PH-specific treatment. Furthermore, remaining research questions and suggestions for future research are defined.

### **Author Contributions**

Conceptualization, T.K. and M.K.; writing—original draft preparation, T.K.; writing—review and editing, M.K. and K.B.; visualization, T.K.; project administration, T.K.

### **Funding**

TK was supported by an unrestricted grant by Actelion pharmaceuticals.

### **Acknowledgments**

We would like to thank R.W. Hendriks and J.J.P. Collins for critically reading the manuscript and providing valuable feedback.

### **Conflicts of Interest**

All authors declare that there is no conflict of interest.

## SUPPLEMENTARY MATERIAL

Supplementary Table 1.

Target	Therapy	MCT-PH Rats	Sugen/hypoxia PH rats	Chronic/ hypoxia PH mice	Sugen/ hypoxia PH mice	Endotoxemic PH pigs	Ref
IL-1	Antagonist	X					(128)
IL-6	Antagonist	X	X	X			(92, 129)
TGF- $\beta$	Antagonist	X	X	X			(146)
BMPR2	Agonist	X	X	X			(141, 142, 145)
TNF- $\alpha$	Antagonist	X	X			X	(132-135)
NF- $\kappa\beta$	Antagonist	X	X	X	X		(150-153, 161)
LTA4/B4	Antagonist	X	X				(52, 165)

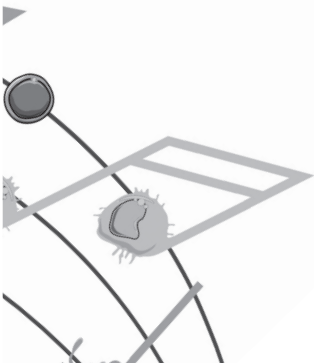


# CHAPTER 2

## *DNGR1-Cre-mediated Deletion of Tnfaip3/A20 in Conventional Dendritic Cells Induces Pulmonary Hypertension in Mice.*

**T. Koudstaal**, J.A.C. van Hulst, T. Das, S.F.H. Neys, D. Merkus, I.M. Bergen, M.A. de Raaf, HJ. Bogaard, L. Boon, G. van Loo, J.G.J.V. Aerts, K.A. Boomars, M. Kool\*, R.W. Hendriks\*  
\*Contributed equally.

Am J Respir Cell Mol Biol 2020 Nov; 63(5):665-680.



## ABSTRACT

### Background:

Chronic perivascular inflammation is a prominent feature in the lungs of idiopathic pulmonary arterial hypertension (IPAH). Although the proportions of conventional dendritic cells (cDCs) and plasmacytoid DCs are increased in IPAH lungs, it remains unknown whether activated cDCs play a pathogenic role. The *Tnfaip3* gene encodes the ubiquitin-binding protein A20, which is a negative regulator of NF- $\kappa$ B, critically involved in DC activation. Targeting of Tnfaip3/A20 in cDCs was achieved by *Clec9a* (DNGR1)-Cre-mediated excision of the *Tnfaip3* gene in *Tnfaip3*<sup>DNGR1-KO</sup> mice. Mice were evaluated for signs of pulmonary hypertension (PH) using right heart catheterization, echocardiography and measurement of the Fulton index. Inflammation was assessed by immunohistochemistry and flow cytometry. Pulmonary cDCs and mo-DCs from 31-week-old *Tnfaip3*<sup>DNGR1-KO</sup> mice showed modulated expression of cell surface activation markers compared to *Tnfaip3*<sup>DNGR1-WT</sup> mice. *Tnfaip3*<sup>DNGR1-KO</sup> mice developed elevated right ventricular (RV) systolic pressure and RV hypertrophy. The lungs of these mice displayed increased vascular remodeling and perivascular and peribronchial immune cell infiltration resembling tertiary lymphoid organs. Proportions of activated T cells and expression of IL-1 $\beta$ , IL-6 and IL-10 were enhanced in the lungs of *Tnfaip3*<sup>DNGR1-KO</sup> mice. Autoreactive IgA and IgG1 was detected in bronchoalveolar lavage and autoreactive IgA recognizing pulmonary endothelial antigens was present in the serum of *Tnfaip3*<sup>DNGR1-KO</sup> mice. All signs of PH were ameliorated in *Tnfaip3*<sup>DNGR1-KO</sup> mice by anti-IL-6 antibody treatment.

These results indicate that activation of the NF- $\kappa$ B pathway in DCs, through deletion of A20/*Tnfaip3*, leads to experimental PH with accompanied pulmonary inflammation in an IL-6-dependent fashion.

## INTRODUCTION

Pulmonary arterial hypertension (PAH) is a debilitating disease in which increased pulmonary vascular pressure leads to right ventricular (RV) hypertrophy, heart failure, and eventually death (2). An increasing body of evidence supports dysregulated immunity in the pathobiology of PAH (24, 176, 177). Idiopathic PAH (IPAH) patients showed enhanced expression of circulating inflammatory cytokines, such as interleukin-6 (IL-6), IL-8, IL-10 and IL-12p70, which was found to correlate with survival (94, 108). In IPAH patients, CD11c<sup>+</sup> dendritic cell (DC) numbers are enhanced in the lung, accumulating around remodeled pulmonary arteries (87). In the parenchyma, DCs present with an immature phenotype, indicated by an increased number of immature DC-SIGN<sup>+</sup> DCs (87). Both the numbers of conventional DCs (cDCs) and plasmacytoid DCs (pDCs) are augmented in total lung cell suspensions of IPAH patients compared to controls (55). In contrast, in peripheral blood, cDC numbers are decreased in IPAH patients (89), suggesting migration to the lungs. Finally, lungs of IPAH patients often display perivascular lymphocytic infiltration and formation of tertiary lymphoid organs (TLOs) in comparison with healthy controls (33). These TLOs consist of T cells, B-cells, mast-cells and DCs (33, 34).

DCs are crucial for the induction and maintenance of lung TLO formation during pulmonary infection in mice (178). DCs in TLOs often show an activated phenotype, suggesting that they exert one of their main functions at this site, i.e. antigen presentation and activation of T cells (179, 180). DCs can be divided into cDCs, monocyte-derived DCs (mo-DCs) and pDCs. cDCs can be subdivided into type 1 cDCs (cDC1s), which are efficient at presentation of exogenous self-antigens in major histocompatibility complex class I (MHC-I) and can induce CD8<sup>+</sup> T cell responses, and type 2 cDCs (cDC2s), which are capable of eliciting Th2 and Th17-cell responses. Upon inflammation, mo-DCs arise and are able to produce large amounts of chemokines, leading to attraction of T cells to the site of inflammation (88). Finally, pDCs are best known for producing large amounts of type I interferons during viral infections.

By exerting these functions, DCs play a pivotal role in the balance between immunity and tolerance. DC triggering by microbial products via Toll-like receptors or cytokines, leads to activation of the nuclear factor kappa-light-chain-enhancer of activated B cells (NF- $\kappa$ B) pathway. Upon translocation to the nucleus, NF- $\kappa$ B is responsible for the transcription of numerous pro-inflammatory and cell-survival genes. Following stimulation, DCs upregulate costimulatory molecules, produce various inflammatory cytokines such as IL-6 and drive T cell priming and effector differentiation (82-84). A breach of tolerance through inappropriate DC activation can lead to several autoimmune diseases (83). Especially cDCs are involved in the control of tolerance, which is less evident for pDCs and moDCs.

Since DC activation is a critical step in immune modulation, their activation must be tightly controlled. One of several mechanisms for this control involves the key regulatory ubiquitin-binding protein A20, encoded by the *TNFAIP3* gene. Several studies have shown a crucial role for *TNFAIP3/A20* in controlling inflammatory disease *in vivo* (85, 167-169). Polymorphisms in the *TNFAIP3* locus are significantly associated with several auto-immune conditions, including PH (170). Strikingly, a specific single nucleotide polymorphism (SNP) in the *TNFAIP3* locus has been associated with PAH development in systemic sclerosis (SSc) patients (181).

Currently, it has not been elucidated whether defects in DC subsets contribute to the pathogenesis of PAH. Considering that cDCs are increased in the lungs of IPAH, our aim was to investigate whether constitutive activation of cDCs in mice would result in the development of PH. To this end, we used the *Tnfaip3*<sup>DNGR1-KO</sup> mouse model with a *Clec9a*/DNGR1-Cre-mediated deletion of the *Tnfaip3* gene, which

specifically targets cDC1s, and to a lesser extent cDC2s and mo-DCs, but not pDCs (172). Previous work from our group indicated that in these mice the *Tnfaip3* gene was deleted in ~95% of the cDC1s, ~35% of the cDC2s and ~45% of the mo-DCs present in the liver, based on yellow fluorescent protein (YFP) expression as a tracer of DNGR1-Cre-driven gene deletion (169). At the age of ~30 weeks, these mice generally showed chronic liver inflammatory infiltrates surrounding the portal triads that was often associated with development of IgA auto-antibodies recognizing liver periportal antigens.

In the current study, we found that *Tnfaip3*<sup>DNGR1-KO</sup> mice developed experimental PH over time, characterized by increased RV systolic pressure, RV hypertrophy, extensive lymphocytic infiltration, vascular remodeling, and increased cytokine (IL-6) production in the lung. Blockade of IL-6 in *Tnfaip3*<sup>DNGR1-KO</sup> mice ameliorated the experimental PH phenotype to wildtype level, indicating a crucial role for IL-6 in DC-driven PH pathophysiology.

## MATERIAL & METHODS

### Mice

Male and female C57Bl/6 mice harbouring a conditional *Tnfaip3* allele flanked by LoxP sites (182) were crossed to a transgenic line expressing the Cre recombinase under the control of the promoter region of the C-type lectin domain family 9a (*Clec9a*) gene, which encodes the DC NK lectin group receptor 1 (DNGR1) (172), generating *Tnfaip3*<sup>fl/fl</sup>*x**Clec9a*<sup>+cre</sup> mice (*Tnfaip3*<sup>DNGR1-KO</sup> mice), as previously described (169). *Tnfaip3*<sup>fl/fl</sup>*x**Clec9a*<sup>+/+</sup> littermates (*Tnfaip3*<sup>DNGR1-WT</sup> mice) served as controls. All mice were sacrificed between 24-31 weeks of age.

To identify cells that have undergone DNGR1-Cre-mediated recombination, *Tnfaip3*<sup>+/+</sup>*x**Clec9a*<sup>+cre</sup> mice and *Tnfaip3*<sup>fl/fl</sup>*x**Clec9a*<sup>+cre</sup> mice were crossed to Rosa26-Stop<sup>fl/fl</sup>-yellow fluorescent protein (YFP) mice (183), yielding *Tnfaip3*<sup>DNGR1-ROSA-WT</sup> and *Tnfaip3*<sup>DNGR1-ROSA-KO</sup> mice, respectively. *Rag1*<sup>-/-</sup> mice (184) were on the C57Bl/6 background. Mice were housed under specific pathogen-free conditions and had *ad libitum* access to food and water. All experiments were approved by the animal ethical committee of the Erasmus MC, Rotterdam, The Netherlands.

### Echocardiographic measurements

Mice were anaesthetised using urethane which produced anaesthesia with spontaneous breathing. Subsequently, thorax hairs were removed by hair removal cream for optimal ultrasound imaging. Using a microscan transducer (VEVO2100, Visual Sonics), right ventricle wall thickness (RVWT), pulmonary arterial acceleration time (PAAT), stroke volume (SV) and cardiac output (CO) were measured as described (185).

### Flexivent airway lung function assessment

For evaluation of airway resistance (Rn), tissue damping (G) and elastance coefficient (H), mice underwent measurements on a small-animal ventilator (flexiVent, EMKA, SCIREQ Inc.) after placement of a tracheal canule after sedation through urethane. To prevent spontaneous breathing, mice received curare intraperitoneally (186).

### **Right heart catheterization**

In anesthetized mice, a tracheal cannula was placed for ventilation (miniVent type 845, Hugo Sachs Elektronik, Germany). Then a midline sternal incision was made, and the RV of the heart was punctured at the apex using a small gauge needle. A pressure catheter (Miller Inc.) was positioned in the RV of the heart for RV systolic pressure (RVSP) and RV end diastolic pressure (RVeDP) measurement (102). Pressures were recorded and analysed using WinDaq (DataQ instruments) and Matlab (the Mathworks).

### **Heart weight measurement and Fulton Index**

Following excision of the heart, the RV free wall was separated from the left ventricle (LV) and the septum (S). The RV and the LV+s were weighed separately (185).

### **Real-time quantitative RT-PCR in lungs and the heart**

For RT-PCR analysis, the post-caval lung lobe and the heart (after separation of RV and LV/S) were stored in  $-80^{\circ}\text{C}$  until processing of the material. Lung and heart tissue were homogenized using lysis buffer with 2-mercaptoethanol and  $\frac{1}{4}$ " ceramic spheres (MP biomedical, 6540-034) by shaking for 40 seconds (MP biomedical, Fastprep-24 5G). Subsequently, RNA was extracted using TRI reagent (Sigma, T9424) and cDNA synthesis was performed using a RevertAid H minus First Strand cDNA synthesis Kit (Thermoscientific, K1632). The cDNA was used for measuring IL-1  $\beta$ , IL-6, IL-10, TGF $\beta$ , FGF2, VEGF and HGF expression by RT-PCR in a 7300 Real time PCR system (Applied Biosystems). For control, a housekeeping gene was also measured as an internal control, to which the relative mRNA expression was determined. Primers used for RT-PCR are given in Supplementary Table 1.

### **Lung histology and pulmonary vascular remodeling assessment**

The left lung was either frozen in Tissue-TEK O.C.T. (VWR International, Darmstadt, Germany) solution and kept at  $-80^{\circ}\text{C}$  until further processing into cryosections or fixed with 4% paraformaldehyde (PFA) (Carl Roth, Karlsruhe, Germany) before paraffin embedding. For immunohistochemical stainings, six- $\mu\text{m}$ -thick cryo-sections were fixed in acetone. Antigen retrieval on paraffin sections were established using citrate buffer (Sigma Aldrich). five- $\mu\text{m}$ -thick paraffin-embedded lung sections were stained with hematoxylin and eosin or Elastica von Giessen (EVG).

To assess pulmonary vascular remodeling, cryosections were stained for  $\alpha$ -smooth muscle actin ( $\alpha$ SMA) and CD31. Using Adobe Photoshop, the ratio between  $\alpha$ SMA-positive and total pulmonary artery (PA) diameter was calculated. This was performed for a minimal of 5 arteries per mouse for small-sized PAs (20-50  $\mu\text{m}$ ).

To visualize immune cells, cryosections were stained for CD138, IgD, IgM, GL7, Ki67, IgA, CD3 and B220, using standard procedures. The primary antibodies and their dilutions, used for immunohistochemistry, are listed in Supplementary Table 2. Sections were incubated for 1 hour with the primary antibodies. After washing, slides were incubated for 30 minutes with secondary antibodies (Supplementary Table 3). On paraffin sections, which were stained for CD3, the anti-Rabbit ABC Peroxidase Kit was utilized (Vector Labs, Burlingame, CA, USA). Diaminobenzene (DAB) and Fast Blue Alkaline phosphatase substrates were used to retrieve specific staining.

## Cell suspension preparation

Bronchoalveolar lavage (BAL), mediastinal lymph node (MLN) and lungs were obtained and used for flow cytometry. BAL was centrifuged at 400g for 3 minutes, where after the supernatant was stored at -80°C for further analysis and the single cells were used for flow cytometry. MLN were homogenized through a 100- $\mu$ m cell strainer. Lung single-cell suspensions were obtained by digesting with Liberase™ (Roche, Basel, Switzerland) for 30 minutes at 37°C. After digestion, the lungs were homogenized using a 100- $\mu$ m cell strainer (Fischer Scientific). Finally, erythroid cells were lysed using osmotic lysis buffer.

## Flow cytometry procedures

Flow cytometry surface and intracellular staining procedures have been described previously (187). Monoclonal antibodies used for flow cytometric analyses are listed in Supplementary Table 3. For all experiments, dead cells were excluded using fixable AmCyan viability dye (eBioscience, San Diego, CA, USA). To measure cytokine production, cells were stimulated with 10 ng/mL PMA (Sigma-Aldrich, St. Louis, MI, USA) and 250 ng/mL ionomycin (Sigma-Aldrich) in the presence of GolgiStop (BD Biosciences, San Jose, CA, USA) for 4 hours at 37°C. Data were acquired using an LSR II flow cytometer (BD Biosciences) with FACS Diva™ software with a minimal of 100 cells per gate of interest and analyzed by FlowJo version 9 (Tree Star Inc software, Ashland, OR, USA).

## Ig levels

For quantification of total Ig levels in BAL fluid and serum, Nunc Microwell plates (Life technologies, Carlsbad, CA, USA) were coated with 1  $\mu$ g/ml goat-anti-mouse IgM, IgA or an IgG isotype (IgG1, IgG2a, IgG2b, IgG3) (Southern Biotech, Birmingham, AL, USA) overnight at 4°C. Wells were blocked with 10% Fetal calf serum (Capricorn Scientific, Ebsdorfergrund, Germany) in Phosphate-buffered saline (PBS) (Thermo Scientific, Waltham, MA, USA) for 1 hour. Standards, BAL and serum were diluted in PBS and incubated for 3 hours at room temperature. Depending on the isotype to be measured, anti-mouse biotin labeled IgM, IgA or IgG isotype (Southern Biotech) was incubated for 1 hour. Streptavidin-HRP (eBioscience) and Tetramethylbenzidine (TMB) substrate (eBioscience) was used to develop the Enzyme-Linked Immuno Sorbent Assay (ELISA) and optical density (OD) was measured at 450 nm on a Microplate Reader (Bio-Rad, Hercules, CA, USA) (169).

## Human epithelial type 2 cell (HEp-2) assessment of auto-reactive antibodies

For HEp-2 autoreactivity assessment, BAL fluid and serum samples (1/100 diluted in PBS) were incubated on Kallestad HEp-2 slides (Bio-Rad Laboratories, Hercules, CA, USA), followed by AF488 labelled donkey anti-mouse IgM antibodies (Invitrogen, Carlsbad, CA, USA) or anti-mouse IgG (Invitrogen). Analysis was performed on a Meta311 confocal microscope (Zeiss, Oberkochen, Germany).

## Autoreactivity assessment of antibodies

For detection of anti-cardiolipin antibodies, Nunc Microwell plates were coated with 10  $\mu$ g/ml cardiolipin from bovine heart (Sigma) in ethanol and left to dry overnight. For detection of anti-dsDNA antibodies, 20 $\mu$ g/ml dsDNA from calf thymus was coated overnight on pre-coated poly-l-lysine

microwells. Wells were blocked with 2% BSA/PBS for 2 hrs, after which serum (diluted in multiple series) was incubated for 2 hrs. Depending on the isotype, anti-mouse IgG biotin/streptavidin-HRP or anti-mouse IgA biotin/streptavidin-HRP were used to develop the ELISA. OD was measured at 450 nm on a Microplate Reader (169).

For serum autoreactive IgA binding to tissues, cryo-sectioned *Rag1*<sup>-/-</sup> mouse lungs were used. After 10 minutes acetone fixation (Sigma) and 10 minutes block with 10% normal goat serum (NGS), serum was differently diluted for WT (1:33) and KO (1:100) mice to compensate for differences in total serum IgA levels. Anti-mouse IgA biotin/streptavidin (BD) was used to stain bound IgA. Goat anti-Rat-AP (Sigma) was the secondary antibody used for 30 minutes after which New Fuchsin (Sigma) was used to detect specific binding (169).

### Anti-IL-6 antibody treatment

To evaluate the effects of neutralisation of IL-6 *in vivo*, mice were treated with anti-IL-6 antibodies. Starting at the age of 24 weeks, mice received 0.3 mg of anti-IL-6 mAb (clone 20F3) or isotype-matched control mAb, anti-β-Gal (clone GL113) intraperitoneally twice weekly for a total period of 8 weeks.

### Statistics

Statistical significance of data was calculated using a non-parametric Mann Whitney *U*-test or Bonferroni's Multiple Comparison Test ANOVA. P-values < 0.05 were considered significant. All analyses were performed using Prism (GraphPad Software, La Jolla, CA, USA). Data are presented as mean values, together with symbols for individual measurements.

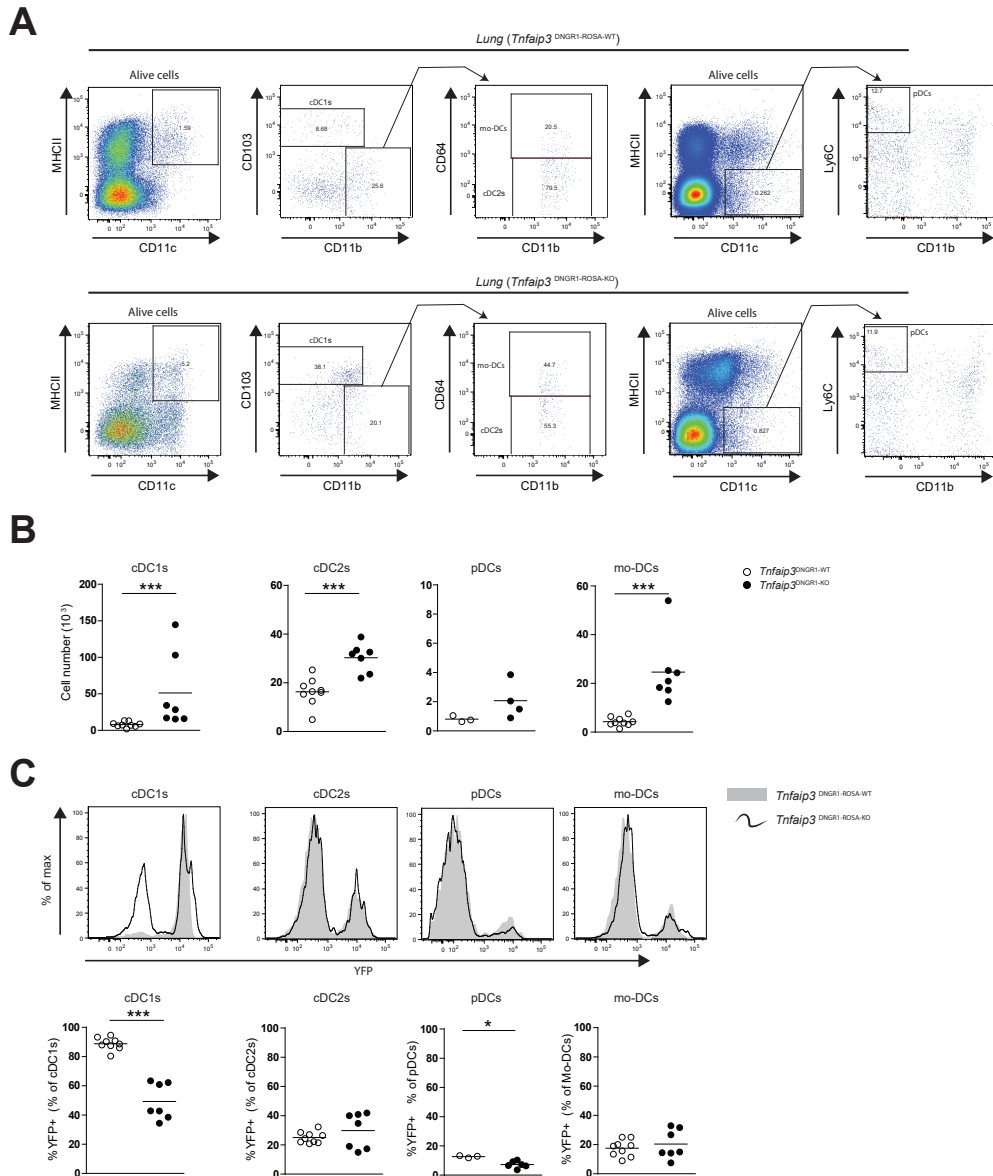
## RESULTS

### DNGR1-cre-mediated *Tnfaip3/A20* deletion induces an increase of cDC1s, cDC2s and mo-DCs in the lung.

To evaluate the effects of DNGR1-cre-mediated *Tnfaip3/A20* deletion in the lungs, *Tnfaip3*<sup>DNGR1-KO</sup> mice were investigated for pulmonary DC subset distribution and conditional deletion efficiency. In 31-week-old *Tnfaip3*<sup>DNGR1-KO</sup> mice, cDC1, cDC2 and mo-DC numbers were significantly increased compared to *Tnfaip3*<sup>DNGR1-WT</sup> mice (Figure 1A, B). To investigate the efficiency of DNGR1-cre-mediated deletion, YFP expression was evaluated in crosses with Rosa26-Stop<sup>fl/fl</sup>-YFP mice (172, 183). In line with our previous findings in liver DC populations (169, 172), ~90% of pulmonary cDC1s in *Tnfaip3*<sup>DNGR1-ROSA-WT</sup> mice were targeted by DNGR1-cre, which unexpectedly declined to ~50% in *Tnfaip3*<sup>DNGR1-ROSA-KO</sup> mice (Figure 1C). In cDC2s and mo-DCs, DNGR1-cre targeting efficiency was lower and not significantly different between *Tnfaip3*<sup>DNGR1-ROSA-WT</sup> and *Tnfaip3*<sup>DNGR1-ROSA-KO</sup> mice (~25% and ~20%, respectively) (Figure 1C). In pDCs YFP expression ~10% in *Tnfaip3*<sup>DNGR1-ROSA-WT</sup> and even lower in *Tnfaip3*<sup>DNGR1-ROSA-KO</sup> mice. Using fluorescence microscopy, we observed that YFP<sup>+</sup> cells specifically accumulated perivascularly and within pulmonary lymphocytic infiltrations in the lungs of *Tnfaip3*<sup>DNGR1-ROSA-KO</sup> mice. By contrast, only low numbers of YFP<sup>+</sup> cells were found in *Tnfaip3*<sup>DNGR1-ROSA-WT</sup> mice (Figure 1D).

CHAPTER 2

In summary, DNGR1-Cre-mediated targeting efficiency and subset-specific tracing in control mice was similar to earlier reports (169, 172). Strikingly, compared with *Tnfaip3*<sup>DNGR1-ROSA-WT</sup> mice, YFP-expression in cDC1s *Tnfaip3*<sup>DNGR1-KO</sup> mice dropped from ~90% to ~50%, suggesting a selective disadvantage of A20-deficient cDC1s. Furthermore, in *Tnfaip3*<sup>DNGR1-ROSA-KO</sup> mice, YFP<sup>+</sup> DCs were located near pulmonary vessels.



**D**

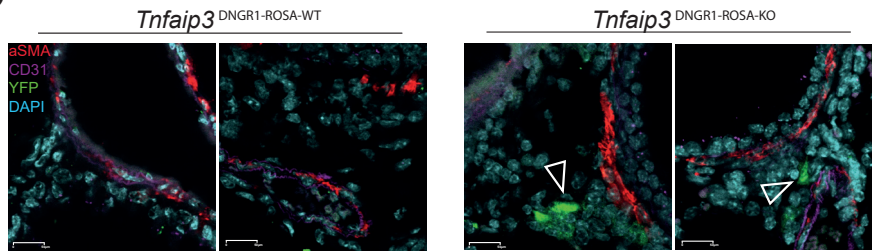


**Figure 1. DNGR1-cre-mediated *Tnfaip3/A20* deletion induces an increase of cDC1s, cDC2s and mo-DCs in the lung.** (A) Gating strategy for pulmonary dendritic cell (DC) subset evaluation; conventional type 1 (cDC1, CD11c<sup>+</sup>MHCII<sup>+</sup>CD103<sup>+</sup>) and type 2 (cDC2, CD11c<sup>+</sup>MHCII<sup>+</sup>CD11b<sup>+</sup>, CD64<sup>+</sup>) DCs, monocyte derived DCs (mo-DCs, CD11c<sup>+</sup>MHCII<sup>+</sup>CD11b<sup>+</sup>CD64<sup>+</sup>) and plasmacytoid DCs (pDCs, CD11c<sup>+</sup>Ly6C<sup>+</sup>CD11b<sup>+</sup>CD64<sup>+</sup>). (B) Absolute cell numbers for pulmonary cDC1s, cDC2s, pDCs and mo-DCs in the indicated mouse strains: *Tnfaip3*<sup>+/+</sup>xClec9a<sup>+/cre</sup>xRosa26-Stop<sup>fl/fl</sup>-YFP (*Tnfaip3*<sup>DNGR1-ROSA-WT</sup> mice) and *Tnfaip3*<sup>fl/fl</sup>xClec9a<sup>+/cre</sup>xRosa26-Stop<sup>fl/fl</sup>-YFP mice (*Tnfaip3*<sup>DNGR1-ROSA-KO</sup> mice). (C) YFP expression of lung cDC1s, cDC2s, pDCs and mo-DCs by flow cytometry, shown as histograms (top) and quantification as proportions of YFP<sup>+</sup> cells (bottom). (D) Confocal microscopy evaluation for YFP<sup>+</sup> cells co-stained with DAPI, CD31 and a smooth muscle actin (aSMA) in pulmonary vascular histology slides in 31-week-old *Tnfaip3*<sup>DNGR1-KO</sup> mice. Representative examples are shown (top) and results are presented as symbols for individual mice, together with means of 3-4 mice per group (bottom). Mice were evaluated at 31 weeks of age. Experiments shown are representative of 2 or more independent experiments. \**P* < 0.05, \*\**P* < 0.01, \*\*\**P* < 0.001.

### DNGR1-cre-mediated *Tnfaip3/A20* deletion induces both cell-intrinsic and cell-extrinsic effects.

Next, we investigated whether deletion of the *Tnfaip3* gene affected surface expression of typical DC activation markers. No significant differences between *Tnfaip3*<sup>DNGR1-KO</sup> mice and WT mice were observed for MHCII expression on any of the three DC subsets (Figure 2A). However, MHCII expression was enhanced in YFP<sup>+</sup> cDC1s and YFP<sup>+</sup> mo-DCs in *Tnfaip3*<sup>DNGR1-KO</sup> mice in comparison to their wildtype counterparts (Figure 2B). Because MHCII expression was also significantly increased in YFP<sup>+</sup> pulmonary cDC1s in *Tnfaip3*<sup>DNGR1-KO</sup> mice, compared to WT mice, we conclude that MHCII expression was regulated in cDC1s by *Tnfaip3/A20* in a cell non-intrinsic fashion. For mo-DCs upregulation of MHCII expression appeared to be cell-intrinsically regulated, because YFP<sup>+</sup> pulmonary mo-DCs and WT DCs showed a similar MHCII surface expression level.

In the YFP<sup>-</sup> and YFP<sup>+</sup> fractions for cDC1s, cDC2s and mo-DCs, MHCII expression appeared to be slightly decreased when compared to wildtype (data not shown). However, this analysis is complicated by the usage of the MHCII expression level to gate the individual DC subsets, as shown in Figure 1A. In accordance with previous reports (169, 171), CD86 expression was decreased cDC1s in *Tnfaip3*<sup>DNGR1-KO</sup> mice compared to WT, both in YFP<sup>+</sup> and YFP<sup>-</sup> cDC1s. CD40 expression was generally low on all three DC subsets, although increased for YFP<sup>+</sup> cDC1s, cDC2s and mo-DCs in *Tnfaip3*<sup>DNGR1-KO</sup> mice compared to WT cDC1s. Considering CD40 expression was not increased in YFP<sup>-</sup> cDC1s, cDC2s and mo-DCs, we conclude that the increase of CD40 expression in the three subsets of *Tnfaip3*<sup>DNGR1-KO</sup> mice is regulated in a cell-intrinsic manner. Compared to WT mice, in *Tnfaip3*<sup>DNGR1-KO</sup> mice PDL1 expression was significantly increased in pulmonary cDC1s, cDC2s and mo-DCs (Figure 2A), both in the YFP<sup>-</sup> and the YFP<sup>+</sup> fractions (Figure 2B). Such a cell non-intrinsic regulation of PDL1 expression on DCs would parallel our previous finding in the context of *Tnfaip3/A20*-deficient DCs (171), that PD-L1 expression on DCs can be induced by high levels of IFN $\gamma$ .

In summary, upon DNGR1-cre-mediated *Tnfaip3* deletion, cell surface expression of activation markers on cDC1, cDC2 and mo-DC populations was regulated by both cell-intrinsic and cell-extrinsic mechanisms.

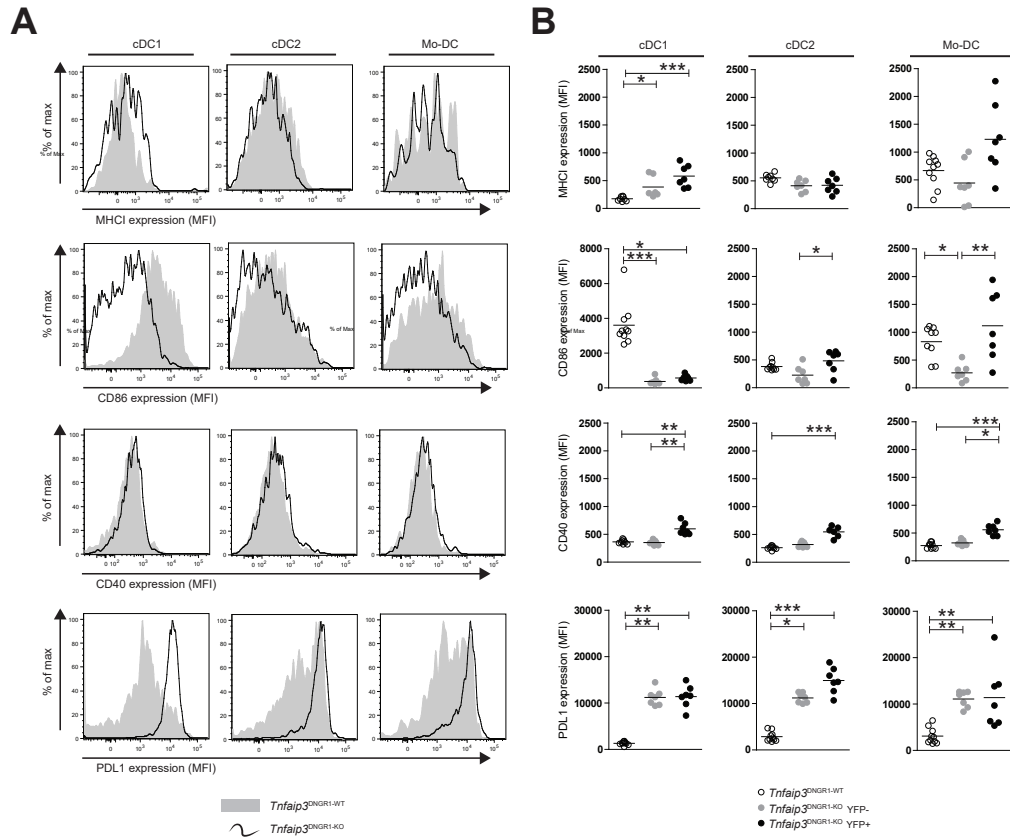


**Figure 2.** DNGR1-cre-mediated *Tnfaip3*/A20 deletion induces both cell-intrinsic and cell-extrinsic effects.

Activation status of pulmonary DC subsets was analyzed by flow cytometry. **(A)** Expression of MHC1, CD86, CD40 and PDL1 was quantified in gated cDC1s, cDC2s, pDCs and mo-DCs in lungs of the indicated mice and is shown as histogram overlays. **(B)** Cell-intrinsic versus cell-extrinsic effects of *Tnfaip3*/A20 deletion in DCs on the expression levels (MFI = median fluorescence intensity) of MHC1, CD86, CD40 and PDL1, as revealed by a separate analysis of YFP<sup>-</sup> and YFP<sup>+</sup> DC subsets. Results are presented as mean values of 3 to 4 mice per group and representative of 2 or more independent experiments. \* $P < 0.05$ , \*\* $P < 0.01$ , \*\*\* $P < 0.001$ .

### Lungs of *Tnfaip3*<sup>DNGR1-KO</sup> mice show increased perivascular lymphocytic infiltrates, consisting of activated T and B-cells.

To investigate whether pulmonary homeostasis is changed by *Tnfaip3*/A20-deficient DCs, we evaluated lungs of *Tnfaip3*<sup>DNGR1-KO</sup> mice by histological analysis at 31 weeks of age. In the small pulmonary arteries of *Tnfaip3*<sup>DNGR1-KO</sup> mice, we observed increased perivascular inflammatory infiltration and the presence of CD11c positive cells (Figure 3A). Furthermore, RT-PCR experiments and flow cytometric analysis was performed in heart tissue of *Tnfaip3*<sup>DNGR1-KO</sup> mice, showing increased *Itgax*

(encoding CD11c) expression and increased proportions of DCs, both in the left and right ventricle of the heart (Supplementary Figure 1).

Since lymphocytic infiltrations in the lungs of PAH patients contain increased numbers of T and B cells (33), we explored the inflammatory landscape in the lungs of *Tnfaip3*<sup>DNGR1-KO</sup> mice. The peribronchial infiltrates consisted of distinct T cell (CD3<sup>+</sup>) and B-cell (B220<sup>+</sup>) zones (Figure 3B). A staining for the plasma cell marker CD138 and IgA indicated the presence of IgA-producing plasma cells in both peribronchially and perivascularly infiltrated areas in the lungs of *Tnfaip3*<sup>DNGR1-KO</sup> mice, while being absent in *Tnfaip3*<sup>DNGR1-WT</sup> mice. Of note, CD138 staining was also observed in bronchial epithelial cells (Figure 3B), paralleling reported findings (188). Evaluation of lymphocytic infiltrates also showed specific IgD<sup>+</sup> zones and proliferating cells (Ki67<sup>+</sup>) (Figure 3B).

Next, we used flow cytometry to quantify T and B cells and to investigate their phenotype in the lungs. The numbers of CD4<sup>+</sup> T helper (Th)-cells were increased in *Tnfaip3*<sup>DNGR1-KO</sup> mice compared to *Tnfaip3*<sup>DNGR1-WT</sup> mice, although this increase did not reach significance. The proportions of activated/memory (CD44<sup>high</sup>) and proliferating CD44<sup>+</sup>Ki67<sup>+</sup> Th-cells were significantly higher in *Tnfaip3*<sup>DNGR1-KO</sup> mice than in *Tnfaip3*<sup>DNGR1-WT</sup> mice (Figure 3C). Regulatory T cells (Tregs) were unaltered in cell number, but an augmented proportion of CD44<sup>high</sup> activated/memory Tregs was observed in *Tnfaip3*<sup>DNGR1-KO</sup> mice, compared to *Tnfaip3*<sup>DNGR1-WT</sup> mice (Figure 3D). The total numbers of CD8<sup>+</sup> T cells were not significantly increased in the lungs of *Tnfaip3*<sup>DNGR1-KO</sup> mice compared to *Tnfaip3*<sup>DNGR1-WT</sup> mice, but the proportions of CD44<sup>high</sup> activated/memory and proliferating CD44<sup>+</sup>/Ki67<sup>+</sup> CD8<sup>+</sup> T cells were significantly higher in *Tnfaip3*<sup>DNGR1-KO</sup> mice (Figure 3E).

The presence of specific T and B-cell zones in the lung, as detected by histology, was indicative for the formation of TLO-like structures. Therefore, lungs were investigated for follicular Th cells (Tfh) and B cell subsets. The frequency of Tfh cells, defined as CXCR5<sup>+</sup>/PD1<sup>+</sup>, within the fraction of total CD4<sup>+</sup> T cells was increased in *Tnfaip3*<sup>DNGR1-KO</sup> mice compared to *Tnfaip3*<sup>DNGR1-WT</sup> mice (Figure 3F). Although the number of total B cells did not differ between the two genotypes, the proportions of germinal center (GC) (CD95<sup>+</sup>/GL7<sup>+</sup>) B cells and CD138<sup>+</sup> plasma cells were increased in lungs of *Tnfaip3*<sup>DNGR1-KO</sup> mice compared to *Tnfaip3*<sup>DNGR1-WT</sup> mice (Figure 3G, H).

Since recruitment of macrophages also plays an important role in pulmonary vascular remodeling (52, 189), an F4/80 staining was performed, showing the perivascular presence of macrophages in *Tnfaip3*<sup>DNGR1-KO</sup> mice (Supplementary Figure 2).

From these findings we conclude that the pulmonary inflammatory infiltrates in *Tnfaip3*<sup>DNGR1-KO</sup> mice contained dendritic cells, macrophages as well as lymphocytes present in TLO-like structures. CD4<sup>+</sup> and CD8<sup>+</sup> T cells showed enhanced activation and proliferation, and GC B cells and plasma cells were present. In summary, these data indicate that T and B cells were most likely chronically activated in inflammatory lesions in the lungs of *Tnfaip3*<sup>DNGR1-KO</sup> mice.

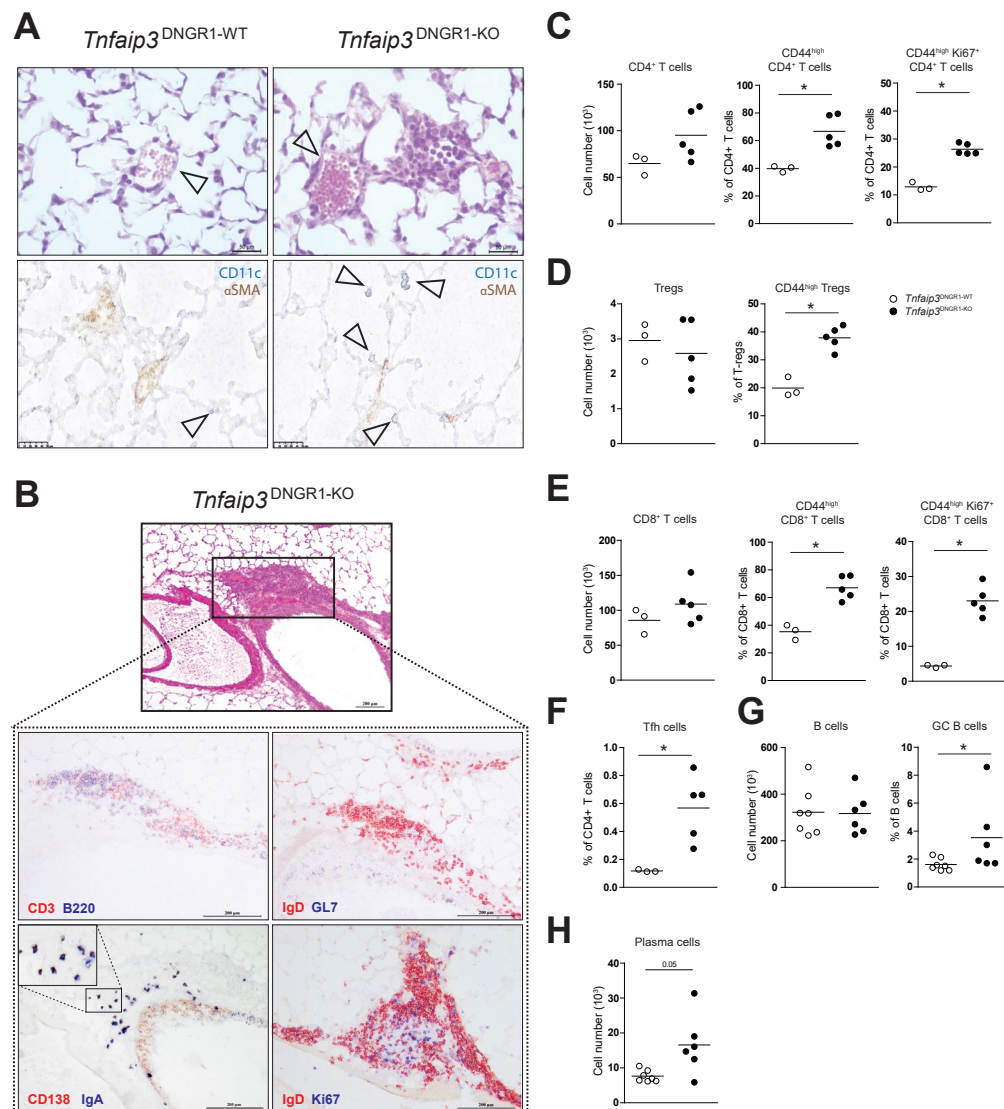


**Figure 3. Lymphocytic infiltrates in the lungs of *Tnfaip3*<sup>DNGR1-KO</sup> mice consist of activated T and B cells.**

(A) Hematoxylin and eosin (H&E) staining and immunohistochemistry staining for CD11c combined with aSMA was performed on tissue sections of lungs of 31-week-old *Tnfaip3*<sup>DNGR1</sup> mice. (B) T cell (CD3, red) and B cell (B220, blue) staining on pulmonary cryosections. IgD (red) and GL7 (blue) staining for GC B-cells. CD138 (red) and IgA (blue) staining for plasma cells. IgD (red) and Ki67 (blue). (C-E) Flow cytometric quantification of the indicated subsets of (C) CD4<sup>+</sup> T cells, (D) Tregs and (E) CD8<sup>+</sup> T cells. (F) Flow cytometry analysis for follicular T helper cells (PD-1<sup>+</sup>CXCR5<sup>+</sup>CD4<sup>+</sup>T cells), (G) total B cells and GC B cells (GL7<sup>+</sup>CD95<sup>+</sup>CD19<sup>+</sup>) and (H) plasma cells (CD138<sup>+</sup>B220<sup>+</sup>). \**P* < 0.05, \*\**P* < 0.01, \*\*\**P* < 0.001. Results are presented as mean values with symbols for individual mice (5 to 8 per group), representative of 2 or more independent experiments.

### **DNGR1-cre-mediated *Tnfaip3/A20* deletion leads to a PH phenotype in *Tnfaip3*<sup>DNGR1-KO</sup> mice.**

Considering the pulmonary perivascular infiltration, we investigated possible vascular remodeling in *Tnfaip3*<sup>DNGR1-KO</sup> mice. Pulmonary vascular remodeling with increased lymphocytic infiltration and vascular muscular wall thickening was observed in the small (20-50  $\mu$ m) arteries of the lungs of *Tnfaip3*<sup>DNGR1-KO</sup> mice, compared to *Tnfaip3*<sup>DNGR1-WT</sup> mice at 24 and 31 weeks of age (Figure 4A, B). Quantification of the muscularization of the small pulmonary arteries by staining for  $\alpha$ SMA showed that this was significantly enhanced in 31-week-old *Tnfaip3*<sup>DNGR1-KO</sup> mice (Figure 4B, C).

Because arteries in *Tnfaip3*<sup>DNGR1-KO</sup> mice showed vascular remodeling, we evaluated these mice for signs of PH at the age of 24 and 31 weeks. No significant differences in RV systolic pressure (RVSP) or RV end diastolic pressure (RVeDP) were found between 24-week-old *Tnfaip3*<sup>DNGR1-KO</sup> and *Tnfaip3*<sup>DNGR1-WT</sup> mice. Strikingly, at the age of 31 weeks, both RVSP and RVeDP were significantly elevated in *Tnfaip3*<sup>DNGR1-KO</sup> mice (Figure 4D). Echocardiographic evaluation showed a decreased pulmonary arterial acceleration time (PAAT) and increased RV wall thickness (RVWT) in 31-week-old *Tnfaip3*<sup>DNGR1-KO</sup> mice compared to *Tnfaip3*<sup>DNGR1-WT</sup> mice (Figure 4E). To investigate cardiac remodeling due to elevated RVSP, right ventricular hypertrophy (RVH) was explored by determining the Fulton index. Both in 24- and 31-week-old mice, an augmentation in the Fulton index was observed in *Tnfaip3*<sup>DNGR1-KO</sup> mice compared to *Tnfaip3*<sup>DNGR1-WT</sup> mice. The elevated Fulton index indicative for RVH in *Tnfaip3*<sup>DNGR1-KO</sup> mice was due to increased RV weight and not to a decreased LV+s weight (Figure 4F). The PAAT determined by echocardiography showed a significant inverse correlation with RVSP (Figure 4G). No correlations were found between a higher grade of vascular remodeling and more pronounced PH in our mice (data not shown). The PH phenotype was likely not induced by obstructive airway pathology or hypoxia, as no differences were seen in lung function nor pulmonary hypoxia factor expression (*Hif1a*, *Bnip3* and *Slc2a1* mRNA) between *Tnfaip3*<sup>DNGR1-KO</sup> mice and *Tnfaip3*<sup>DNGR1-WT</sup> mice (Supplementary Figure 3 and data not shown).

Known mediators involved in vascular remodeling are TGF $\beta$ , VEGFA and HGF. TGF $\beta$  mRNA expression was significantly increased in lungs (at 31 weeks), RV (at 31 weeks) and LV+s (both at 24 and at 31 weeks) from *Tnfaip3*<sup>DNGR1-KO</sup> mice, compared to control mice (Figure 4H). Although the lungs of 31-week-old *Tnfaip3*<sup>DNGR1-KO</sup> mice did not show increased *Vegf* expression, it was increased in RV and LV+s. *Hgf* transcription was specifically increased in the RV of *Tnfaip3*<sup>DNGR1-KO</sup> mice compared to *Tnfaip3*<sup>DNGR1-WT</sup> at 31 weeks (Figure 4H). An  $\alpha$ SMA staining on heart tissue of 31-week-old *Tnfaip3*<sup>DNGR1-KO</sup> showed no differences between vascular endothelial cells of *Tnfaip3*<sup>DNGR1-KO</sup> and wildtype mice (data not shown).

Taken together, these data show that 31-week-old *Tnfaip3*<sup>DNGR1-KO</sup> mice developed experimental PH with RVH and increased pulmonary and RV/LV-expression of vascular remodeling/growth factors.

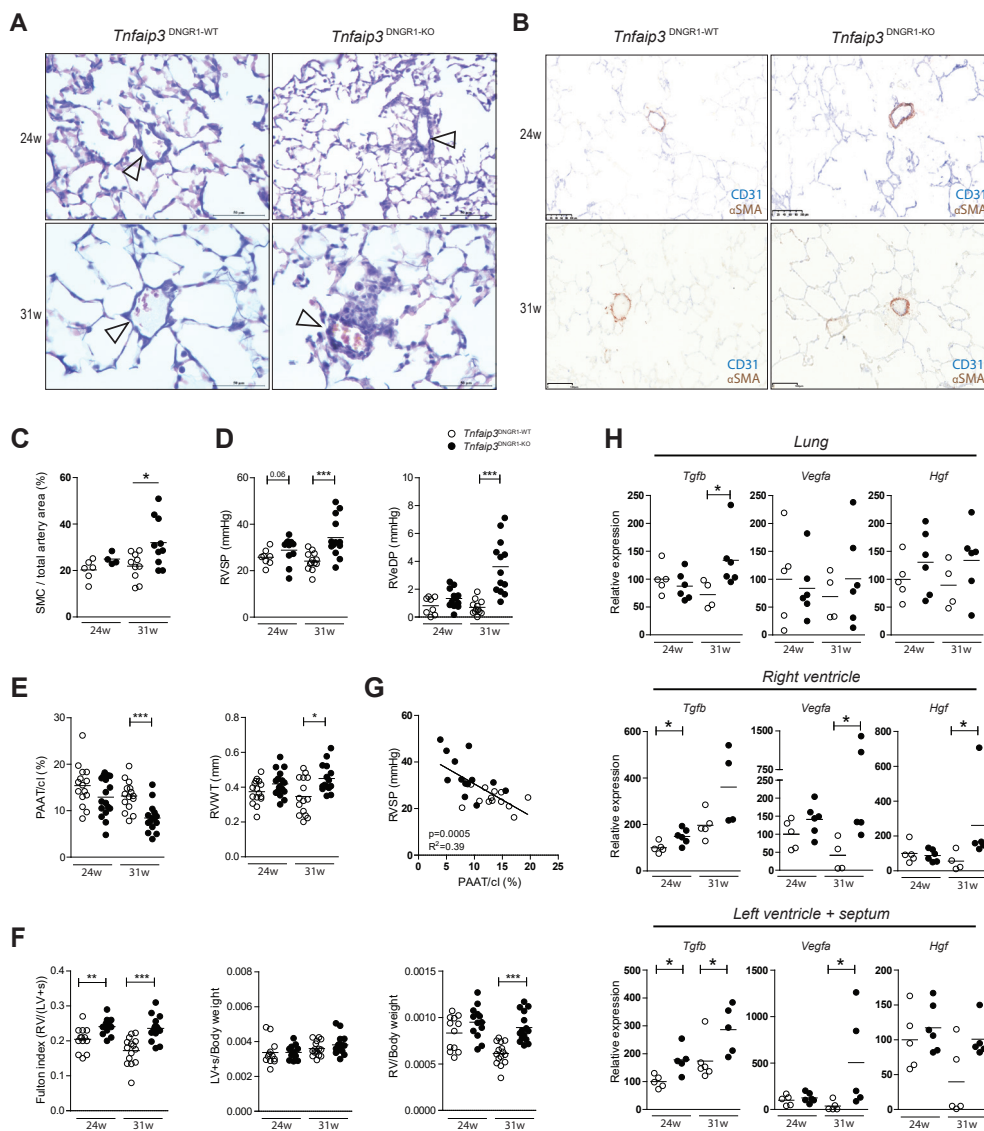


**Figure 4. DNCR1-cre specific *Tnfaip3*/A20 deletion leads to a pulmonary hypertension phenotype in *Tnfaip3*<sup>DNCR1-KO</sup> mice.** (A) Elastin von Giessen (EvG) stained lung histology of *Tnfaip3*<sup>DNCR1-WT</sup> and *Tnfaip3*<sup>DNCR1-KO</sup> mice for representative sections for small pulmonary arteries (PAs) (20–50  $\mu$ m). Scale bars are 50  $\mu$ m. Arrows indicate PAs. (B) Using immunohistochemistry staining for CD31 and  $\alpha$ SMA (a smooth muscle actin) in the lung, vascular muscular wall thickness was evaluated (scale bars are 100  $\mu$ m) and (C) quantified. (D) Right Ventricular Systolic Pressure (RVSP) and Right Ventricular end-diastolic Pressure (RVEDP), as determined using right heart catheterization, in the indicated mice. (E) Echocardiographic measurements in the indicated mice for pulmonary arterial acceleration time (PAAT) and right ventricular wall thickness (RVWT). (F) Right Ventricular hypertrophy assessed using the Fulton index (right ventricle (RV)/ Left ventricle + septum (LV+s)), as well as separate LV+s and RV measurements for the indicated mice. (G) Correlation of RVSP and PAAT in both *Tnfaip3*<sup>DNCR1-WT</sup> and *Tnfaip3*<sup>DNCR1-KO</sup> mice at 31 weeks of age. (H) Relative mRNA expression of vascular remodeling factors in the indicated tissues of 31-week-old *Tnfaip3*<sup>DNCR1-KO</sup> mice. Expression in 24-week-old *Tnfaip3*<sup>DNCR1-WT</sup> mice was set to 100%. TGF $\beta$  = transforming growth factor- $\beta$ ; VEGFa = vascular endothelial growth factor-a; HGF = hepatocyte growth factor. Results are presented as symbols for individual mice, together with mean values of 7 to 15 mice per group and representative of 3 or more independent experiments. \* $P < 0.05$ , \*\* $P < 0.01$ , \*\*\* $P < 0.001$ .

### ***Tnfaip3*<sup>DNGR1-KO</sup> mice have auto-antibodies, including IgA recognizing pulmonary vasculature.**

We previously reported increased levels of total IgG1 and IgA, but no other isotypes, in serum of *Tnfaip3*<sup>DNGR1-KO</sup> mice compared to control mice (169). When we determined Ig levels in BAL fluid, we observed increased total IgG1 and IgA in *Tnfaip3*<sup>DNGR1-KO</sup> mice compared to *Tnfaip3*<sup>DNGR1-WT</sup> mice (Figure 5A). To evaluate the presence of auto-antibodies, we screened HEP-2 cells and found staining with IgG present in the serum – but not in BAL fluid – in three out of six *Tnfaip3*<sup>DNGR1-KO</sup> mice (Figure 5B). These HEP-2 IgG staining patterns were nuclear speckled and anti-mitochondrial (190). In contrast, none of the four WT control sera were positive.

Previously, we have shown that both anti-dsDNA IgG1 and anti-cardiolipin IgG1 concentrations were significantly enhanced in the serum of *Tnfaip3*<sup>DNGR1-KO</sup> mice compared to WT controls, as measured at an age of 31 weeks (169). Because anti-dsDNA and anti-cardiolipin Igs can be found in autoimmune diseases associated with PAH (191), we also investigated whether *Tnfaip3*<sup>DNGR1-KO</sup> mice showed antibodies with these specificities in BAL fluid. The levels of dsDNA- and cardiolipin-specific autoantibodies – both IgG1 and IgA – were significantly increased in *Tnfaip3*<sup>DNGR1-KO</sup> mice compared to WT controls (Figure 5C).

We next investigated whether autoantibodies would recognize pulmonary antigens and stained lung sections of *Rag1*<sup>-/-</sup> mice with serum of *Tnfaip3*<sup>DNGR1-KO</sup> and *Tnfaip3*<sup>DNGR1-WT</sup> mice. In *Rag1*<sup>-/-</sup> mice, endogenous Igs are absent, facilitating the detection of binding of serum autoantibodies in tissues. IgA, but not IgG, in the serum of *Tnfaip3*<sup>DNGR1-KO</sup> mice specifically recognized antigens present in pulmonary endothelial cells (Figure 5D).

Summarizing, in *Tnfaip3*<sup>DNGR1-KO</sup> mice levels of total IgA and IgG1 and auto-antibodies recognizing dsDNA and cardiolipin levels were elevated in serum and BAL fluid. In these mice, circulating IgA contained specific reactivity towards the pulmonary vasculature.

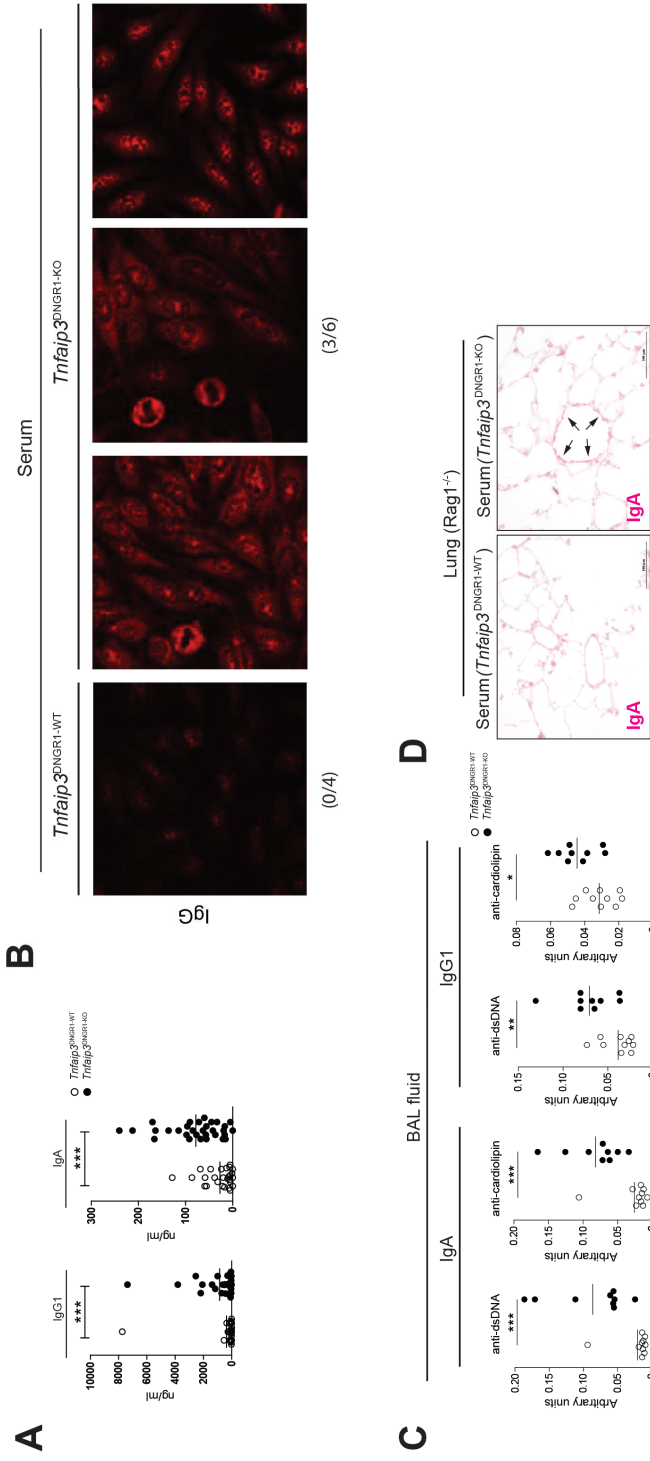


**Figure 5. *Tnfaiip3<sup>DNNGRI-KO</sup>* mice show IgG and IgA autoantibodies in BAL fluid and serum.**

(A) Quantification of bronchial alveolar lavage (BAL) fluid immunoglobulins (IgG1 and IgA) in *Tnfaiip3<sup>DNNGRI-WT/KO</sup>* mice. Results are presented as symbols for individual mice, together with mean values of 30-32 mice per group (B) Immunofluorescence assessment of autoreactive IgG immunoglobulins from 31-week-old mice of the indicated genotype using HEP-2 cells. (C) Quantification of autoreactive IgG1 and IgA for dsDNA and cardioliplin in serum from 31-week-old mice using ELISA. Results are presented as symbols for individual mice, together with mean values of 9-10 mice per group (D) Immunohistochemical evaluation for the presence of autoreactive IgA in *Tnfaiip3<sup>DNNGRI-WT</sup>* and *Tnfaiip3<sup>DNNGRI-KO</sup>* mouse serum, using lung tissue from *Rag1<sup>-/-</sup>* mice. Scale bars in panel 5D are 100 μm. \* $P < 0.05$ , \*\* $P < 0.01$ , \*\*\* $P < 0.001$ .

### ***Tnfaip3*<sup>DNGRI-KO</sup> mice show increased IL-1 $\beta$ , IL-6 and IL-10 expression in the lungs and heart.**

In IPAH patients, the increased presence of inflammatory cytokines in serum negatively correlated with patient survival (94). Especially IL-1 $\beta$ , IL-6 and IL-10 serum levels were increased in IPAH patients versus healthy controls. Therefore, we investigated cytokine expression in the lungs and hearts of *Tnfaip3*<sup>DNGRI-KO</sup> mice. Increased pulmonary *Il1b*, *Il6* and *Il10* mRNA expression was observed in 31-week-old *Tnfaip3*<sup>DNGRI-KO</sup> mice compared to *Tnfaip3*<sup>DNGRI-WT</sup> mice (Figure 6A). In contrast, only *Il1b* – but not *Il6* or *Il10* - mRNA expression was significantly increased in the RV of *Tnfaip3*<sup>DNGRI-KO</sup> mice; no significant differences were observed for the three cytokines examined in LV+s (Figure 6B).

We next evaluated whether increased proportions of inflammatory cytokine-producing CD4<sup>+</sup> and CD8<sup>+</sup> T cells were present in the lungs of *Tnfaip3*<sup>DNGRI-KO</sup> mice. Strikingly, IL-10 and IFN $\gamma$ -producing CD4<sup>+</sup> and CD8<sup>+</sup> T cells were significantly increased in *Tnfaip3*<sup>DNGRI-KO</sup> mice compared to *Tnfaip3*<sup>DNGRI-WT</sup> mice (Figure 6C, D). Furthermore, the CD4<sup>+</sup> T cell population in the lungs of *Tnfaip3*<sup>DNGRI-KO</sup> mice contained increased proportions of IL-17A-producing cells (Figure 6C). No differences in the frequencies of tumor necrosis factor alpha (TNF $\alpha$ )-producing CD4<sup>+</sup> or CD8<sup>+</sup> T cells were found between *Tnfaip3*<sup>DNGRI-KO</sup> mice and wildtype control mice.

Taken together, lungs of *Tnfaip3*<sup>DNGRI-KO</sup> mice had increased mRNA expression of IL-6 and IL-10, accompanied by increased proportions of IL-10<sup>+</sup> and IFN $\gamma$ <sup>+</sup> CD4<sup>+</sup> and CD8<sup>+</sup> T cells and increased proportions of IL-17A<sup>+</sup> CD4<sup>+</sup> T cells.

### **Anti-IL-6 treatment ameliorates the pulmonary hypertension phenotype in *Tnfaip3*<sup>DNGRI-KO</sup> mice.**

Because IL-6 is thought to have a prominent role in PAH pathology (94, 129) and given the increased expression of *Il6* in the lungs of *Tnfaip3*<sup>DNGRI-KO</sup> mice, we investigated whether neutralisation of IL-6 could ameliorate the PH phenotype. To this end, *Tnfaip3*<sup>DNGRI-WT</sup> and *Tnfaip3*<sup>DNGRI-KO</sup> mice received either IL-6-neutralizing antibodies or an isotype control antibody intraperitoneally twice per week starting at the age of 24 weeks. Mice were investigated for signs of development of PH at week 31 (Figure 7A).

As expected, an increased RVSP/RVedP, a trend towards a decreased PAAT, and a significantly increased Fulton index were found in isotype-treated *Tnfaip3*<sup>DNGRI-KO</sup> compared to *Tnfaip3*<sup>DNGRI-WT</sup> mice. No differences between isotype and anti-IL-6-treated *Tnfaip3*<sup>DNGRI-WT</sup> mice were detected. However, in *Tnfaip3*<sup>DNGRI-KO</sup> mice, anti-IL-6 treatment prevented the increase in RVSP/RVedP compared to isotype-treated *Tnfaip3*<sup>DNGRI-KO</sup> mice (Figure 7B). Echocardiographic analysis showed, albeit not significant, normalisation of the PAAT following anti-IL-6 treatment in *Tnfaip3*<sup>DNGRI-KO</sup> mice, when compared to isotype-treated *Tnfaip3*<sup>DNGRI-KO</sup> mice (Figure 7C). Furthermore, the enhanced Fulton index observed in control-treated *Tnfaip3*<sup>DNGRI-KO</sup> mice was diminished after anti-IL-6 treatment in *Tnfaip3*<sup>DNGRI-KO</sup> mice, reaching values similar to *Tnfaip3*<sup>DNGRI-WT</sup> mice (Figure 7D).

Pulmonary lymphocytic infiltration was unaffected by IL-6 blockade in *Tnfaip3*<sup>DNGRI-KO</sup> mice (Figure 7E). The small to medium-sized pulmonary arteries of isotype-control *Tnfaip3*<sup>DNGRI-KO</sup> mice exhibited significantly increased muscularization compared to *Tnfaip3*<sup>DNGRI-WT</sup> mice (Figure 7E, quantified in Figure 7F). Following anti-IL-6 treatment the increase in muscularization was only moderate (Figure 7E, F).

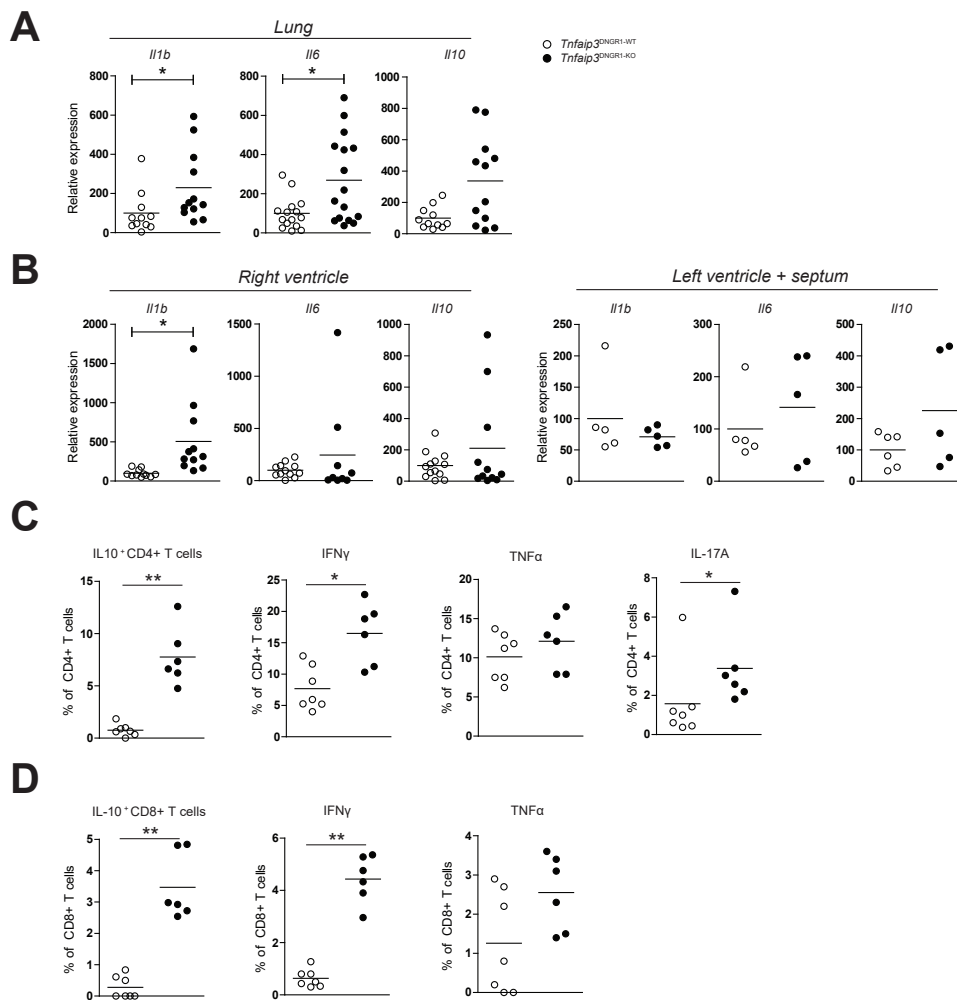


**Figure 6.** *Tnfaip3<sup>DNGRI-KO</sup>* mice show increased IL1 $\beta$ , IL6 and IL10 mRNA expression in the lungs and heart.

(A-B) Expression of IL-1 $\beta$  (*Il1b*), IL-6 (*Il6*) and IL-10 (*Il10*) mRNA in lung (A) and in the indicated parts of the heart (B). (C-D) Intracellular flow cytometry analysis of the indicated cytokines. Data are shown as proportions of cytokine positive CD4<sup>+</sup> T cells (C) or CD8<sup>+</sup> T cells (D). Results are presented as symbols for individual mice, together with mean values of 15 vs 16 (A-B) and 7 vs 6 (C-D) mice per group. \* $P < 0.05$ , \*\* $P < 0.01$ , \*\*\* $P < 0.001$ .

Anti-IL-6 treatment did not affect the numbers of total CD4<sup>+</sup> or CD8<sup>+</sup> T cells, nor the proportions of actively cycling CD44<sup>+</sup>Ki67<sup>+</sup> CD4<sup>+</sup> or CD8<sup>+</sup> T cells (Supplementary Figure 4). Only the proportions of IL-17<sup>+</sup>CD4<sup>+</sup> T cells, which were increased in isotype-treated *Tnfaip3<sup>DNGRI-KO</sup>* mice, were significantly decreased after anti-IL-6 treatment (Figure 7G). Anti-IL-6 therapy did not influence the amount of IgA and IgG1 in BAL fluid in *Tnfaip3<sup>DNGRI-KO</sup>* mice (data not shown).

In conclusion, these data showed amelioration of the experimental PH phenotype in *Tnfaip3<sup>DNGRI-KO</sup>* mice upon IL-6 neutralisation, indicating a crucial role for an active IL-6 pathway in the pathophysiology of PH in *Tnfaip3<sup>DNGRI-KO</sup>* mice.

DNGR1-Cre-mediated Deletion of *Tnfaip3/A20* in Conventional Dendritic Cells Induces Pulmonary Hypertension in Mice

2

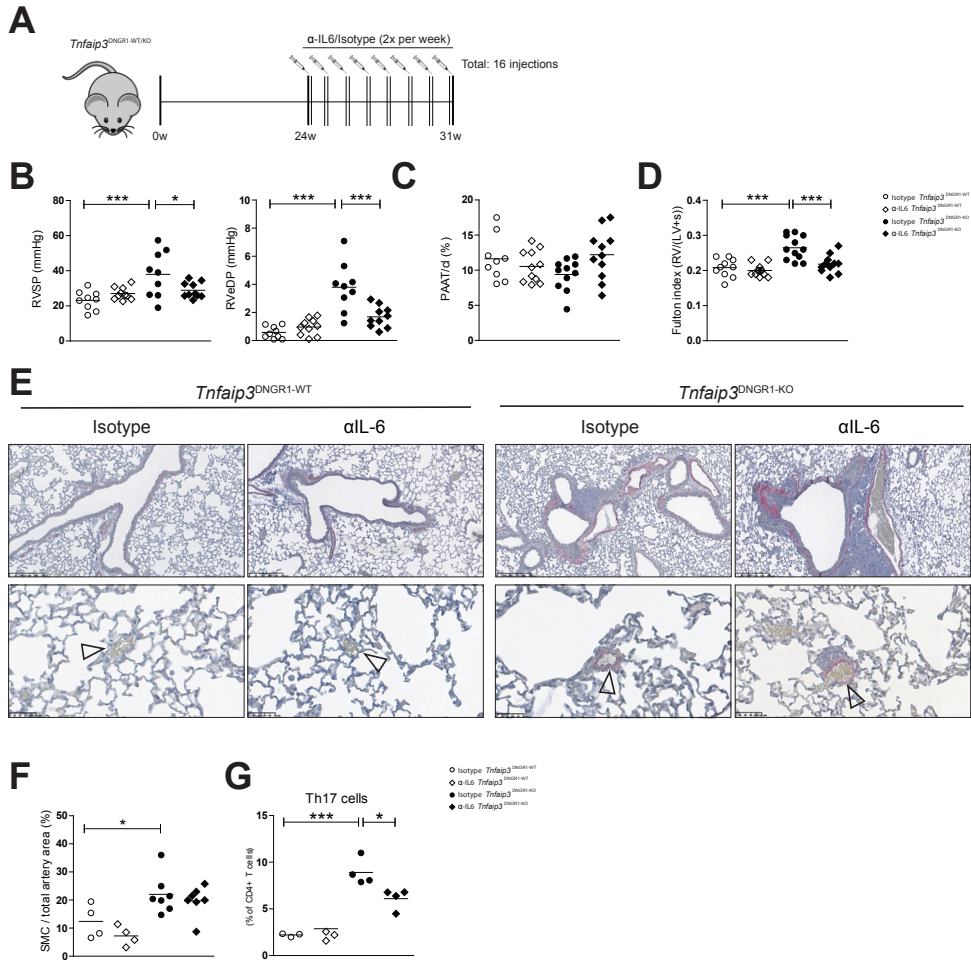


**Figure 7. Anti-IL-6 treatment ameliorates the pulmonary hypertension phenotype in *Tnfaip3*<sup>DNGR1-KO</sup> mice.** (A) Experimental setup for anti-IL6 antibody treatment and isotype treatment in 31-week-old *Tnfaip3*<sup>DNGR1-KO</sup> mice and wildtype mice. (B) Right heart catheterization measurements for Right Ventricular Systolic Pressure (RVSP) and Right Ventricular end-diastolic Pressure (RVEDP) values in the indicated mouse groups. (C) Echocardiographic measurements for Pulmonary arterial acceleration time (PAAT) values in the indicated mouse groups. (D) Right Ventricular Hypertrophy assessment using the Fulton Index (right ventricle (RV)/ Left ventricle + septum (LV+s)) in the indicated mouse groups. (E) a smooth muscle actin (aSMA) stained lung histology of *Tnfaip3*<sup>DNGR1-WT</sup> and *Tnfaip3*<sup>DNGR1-KO</sup> mice for representative sections of large and small pulmonary arteries. (F) SMC (= smooth muscle cells) per total artery area, as determined by quantification of vascular muscular wall thickness using CD31 and aSMA immunohistochemistry. (G) Proportions of Th17 cells as a percentage of CD4<sup>+</sup> T cells. \* $P < 0.05$ , \*\*\* $P < 0.001$ . Results are presented as symbols for individual mice, together with mean values of 9-10 (B-D) and 4-7 (F-G) mice per group and are representative of 2 independent experiments.

## DISCUSSION

Increasing evidence suggests a prominent role for an activated immune system in the pathophysiology of PAH and experimental PH models (94, 117, 192-194). While it is known that in IPAH lungs, TLO formation and increased DC numbers are often present (33, 34), our study investigated the role of DCs in the pathophysiology of PAH in more detail in a mouse model.

In this study, we investigated *Tnfaip3*<sup>DNGR1-KO</sup> mice, in which the *Tnfaip3/A20* gene – a negative regulator of the NFκB pathway – was deleted mainly in cDC1s using the *Clec9a*(DNGR1)-Cre transgene. These mice developed a PH phenotype, as indicated by increased RVSP, RVH, perivascular lymphocytic infiltration, and vascular remodeling. In comparison to established PH models, such as the monocrotaline rat model, our model seems less pronounced in vascular remodeling. Nevertheless, striking parallels exist, as in monocrotaline-exposed rats the mean number of arterial DCs was found to be increased during development of vasculopathy (87). In this model, arterial DC accumulation precedes pulmonary arterial thickening and hemodynamic alteration and is constantly present in remodeled vessels, indicating that DC influx is not merely a consequence of increased pulmonary arterial pressure.

Upon evaluation of known PH-inducing factors in *Tnfaip3*<sup>DNGR1-KO</sup> mice, we concluded that the experimental PH phenotype was not likely to be induced by obstructive airway pathology or hypoxia. In particular, no differences were seen in lung function nor in pulmonary expression of hypoxia factors including *Hif1a*, *Bnip3* and *Slc2a1*, between *Tnfaip3*<sup>DNGR1-KO</sup> mice and *Tnfaip3*<sup>DNGR1-WT</sup> mice (Supplementary Figure 3 and data not shown). Furthermore, in previous work performed by our group (169), inflammatory auto-immune hepatic injury was found in *Tnfaip3*<sup>DNGR1-KO</sup> mice. Considering that no signs of porto-pulmonary hypertension (PoPH) were observed, PoPH seems unlikely to be the causal factor for the experimental PH phenotype in *Tnfaip3*<sup>DNGR1-KO</sup> mice. Neither did we find any signs of LV involvement or signs of LV failure resembling WHO PH group 2.

Most likely, pulmonary inflammation occurs concomitantly with vascular remodelling, both of which appear to be present at 24 weeks of age. Analysis at 24 weeks showed a trend towards increased RVSP. Also, a trend of arterial remodeling was noticed in 24-week-old *Tnfaip3*<sup>DNGR1-KO</sup> mice (Figure 4C). These findings suggest that 24-week-old mice are in transition to develop PH, with a near-significant RVSP increase, a significantly increased Fulton Index and a trend of vascular remodeling. Additionally, EvG stainings of the hearts of 24-week-old *Tnfaip3*<sup>DNGR1-KO</sup> and WT mice showed right ventricular hypertrophy and no differences in collages deposition or cardiomyocyte shape and size (T.K., unpublished findings).

However, the severity of the PH phenotype is variable in *Tnfaip3*<sup>DNGR1-KO</sup> mice, with RVSP values ranging from mild/no PH to severe PH. At 31 weeks, ~50% of the mice have developed PH with increased RVSP, increased Fulton index and vascular remodeling. Variability of the *Tnfaip3/A20* gene deletion efficiency across different DC subsets and cell-extrinsic effects of the targeted deletion might partly be an explanation as to why not all mice develop experimental PH.

DNGR1-cre specific deletion of *Tnfaip3* led to increased numbers of pulmonary cDC1s, cDC2s, and mo-DCs. Specifically, cDCs harbored an altered activation status, e.g. enhanced MHCI, CD40 and PDL1 expression, which was regulated by both cell-intrinsic and cell-extrinsic effects. The increase in PDL1 is most likely caused by cell-extrinsic factors, for which IFNγ is a likely candidate as the proportion of IFNγ-producing T cells is augmented in *Tnfaip3*<sup>DNGR1-KO</sup> mice (Figure 6). Possibly, this increased expression of PDL1 might be a feedback mechanism, induced by the increased production of IFNγ or IL-12 (171).

Currently, the exact mechanism by which experimental PH develops in *Tnfaip3*<sup>DNGR1-KO</sup> mice is unclear. Although cDC1s were mainly affected by DNGR1-mediated ablation, cDC1s, cDC2s and mo-DCs showed an increase in cell number. This might partially be due to targeting of a minor fraction of cDC2s and mo-DCs (172). These findings make it difficult to determine which DC subset is exactly contributing to the PH phenotype. Moreover, the direct and indirect effects of activated DCs on other immune cells, such as T cells and B cells, and pulmonary vasculature remain to be characterized in detail. Importantly however, our results do show that this experimental PH model is likely to be IL-6 dependent and that activation of the NF- $\kappa$ B pathway in DCs is sufficient to induce experimental PH in mice. Previous research has shown that *Tnfaip3*-deficient DCs are able to produce a variety of inflammatory cytokines such as IL-6 (96). Although we did not study whether vascular remodeling is a direct effect of *Tnfaip3*-deficient cDCs, the presence of YFP-expressing DCs around blood vessels suggests a direct interaction. Possibly, *Tnfaip3*-deficient DCs may contribute to vascular remodelling either by production of cytokines and growth factors, and/or by attraction of other immune cells.

The translatability of our findings in the *Tnfaip3*<sup>DNGR1-KO</sup> mice to human PAH remains to be investigated. Nevertheless, the findings of (I) increased numbers of DCs in remodelled pulmonary vessels of IPAH patients (87) and (II) of a specific SNP in the *TNFAIP3* locus that is associated with PAH development in SSc patients may support a pathological role of activated DCs in human PH. It is currently unknown whether the reported increased presence of DCs in IPAH patient lungs is causal or a circumstantial effect.

DCs excel at antigen-presentation to T cells, leading to T cell activation and differentiation (82-85). The level of *Tnfaip3* expression in DCs has been shown to control T cell differentiation, as *Tnfaip3*-deficient DCs promote Th17-cell differentiation through increased expression of IL-1 $\beta$ , IL-6 and IL-23 (85, 96). In *Tnfaip3*<sup>DNGR1-KO</sup> mice a modest increase in Th17 cells was observed, which was lower after anti-IL-6 treatment. Also, increased proportions of IFN $\gamma$ -producing Th1 cells and IL-10-producing Th cells were found in *Tnfaip3*<sup>DNGR1-KO</sup> mice. These findings may support involvement of both Th17 cells and Th1 cells in IPAH and PAH pathology (195, 196).

Conventional DC1s are especially equipped to promote CD8<sup>+</sup> T cell activation (197). In support of cDC1 activation in *Tnfaip3*<sup>DNGR1-KO</sup> mice, the number of CD8<sup>+</sup> T cells, their proliferative capacity, and the proportion of IFN $\gamma$  and IL-10-producing cells was higher in lungs of *Tnfaip3*<sup>DNGR1-KO</sup> mice compared to control mice. Strikingly, also in IPAH patients a dramatic increase in pulmonary CD8<sup>+</sup> T cells has been observed, specifically located in the adventitia of pulmonary vessels (34, 198). These results are suggestive of a role for both Th1 and Th17 cells as well as activated CD8<sup>+</sup> T cells in the pathogenesis of PAH, though direct causality has not been shown yet.

The presence of TLOs is a hallmark characteristic for chronic immune activation with a specific role for GC formation where B cells are activated and can become antibody-producing plasma cells. In IPAH lungs, TLOs are present near the vasculature, and harbor Tfh cells, activated B cells, and antibody-producing plasma cells (33).

In *Tnfaip3*<sup>DNGR1-KO</sup> mice, inflammatory lesions with separated T and B cell zones were observed in the lung as well. The observed increase in GC B cells, Tfh cells, and plasma cells suggests that these inflammatory lesions are active TLOs in *Tnfaip3*<sup>DNGR1-KO</sup> mice. It is conceivable that activation of these cells led to the enhanced total IgG1 and IgA levels found in serum (169) and BAL fluid in *Tnfaip3*<sup>DNGR1-KO</sup> mice. Specifically, autoreactive IgA recognizing lung vasculature was found in serum – but not in BAL fluid – of *Tnfaip3*<sup>DNGR1-KO</sup> mice. Autoreactive IgA might be secreted by lung plasma

cells, and rapidly bound to the lung vasculature, whereby residual IgA concentrations were too small to be detected. Moreover, IgA staining was less pronounced in the smaller vasculature. Approximately 40% of IPAH patients are known to have auto-antibodies (101, 102) which may specifically target endothelial cell surface antigens (103).

In the *Tnfaip3*<sup>DNGRI-KO</sup> mouse model, it is unclear whether T and B cells are mobilized from bone marrow/lymphatic tissue to the lungs or whether they are already stationary pulmonary resident cells. Future experiments are required to provide further insight in these possible mechanisms.

In PAH patients, several cytokines are enhanced in the peripheral blood and correlate with survival (94). Several lines of evidence support a prominent role for IL-6, as (I) serum IL-6 concentrations correlate with survival (94), (II) IL-6-overexpressing transgenic mice spontaneously develop a PH phenotype (117), and (III) IL-6 receptor (IL-6R) expression and signalling is crucial for PAH development and progression (129). In *Tnfaip3*<sup>DNGRI-KO</sup> mice, we observed a higher mRNA expression of the pro- and anti-inflammatory cytokines IL-1 $\beta$ , IL-6 and IL-10, both in lungs and hearts (Figure 6). However, DCs, B cells and macrophages are known producers of these inflammatory cytokines. In previous work by our group (96), *Tnfaip3*-deficient DCs have been shown to promote Th17-cell differentiation through increased expression of IL-1 $\beta$ , IL-6 and IL-23. Possibly, DCs are one of the main contributors to the increased mRNA expression of IL-1 $\beta$ , IL-6 and IL-10. Strikingly, membrane-bound IL-6 expression on DCs is required for the differentiation and priming of pathogenic Th17 cells (199). Our data also showed enhanced proportions of Th17 cells in *Tnfaip3*<sup>DNGRI-KO</sup> mice, which were reduced upon blockade of IL-6. Neutralization of IL-6 in *Tnfaip3*<sup>DNGRI-KO</sup> mice ameliorated the experimental PH phenotype, providing evidence that IL-6 is a major contributor to PH development in these mice. Possibly, anti-IL-6 treatment of KO mice may attenuate the pulmonary vascular remodeling through a different mode of action, including through reduction of PA-SMC survival (129).

In summary, *Tnfaip3*<sup>DNGRI-KO</sup> mice develop an experimental PH phenotype characterized by increased RVSP, RVH, perivascular lymphocytic infiltration, and vascular remodeling. To our knowledge, this is the first study that shows that that activation of the NF- $\kappa$ B pathway in DCs is sufficient for the development of experimental PH in an IL-6 dependent fashion.

### Acknowledgements

We would like to thank Prof. Caetano Reis e Sousa for providing critical mouse strains. We would also like to thank the animal caretakers in our animal experimental facility. Also, we would like to express our gratitude to Odilia Corneth and Jasper Rip for their help in staining and analysing the B-cells and plasma cells in *Tnfaip3*<sup>DNGRI-KO</sup> mice.

### Conflict of interest

The authors declare no conflict of interest.

### Grants supporting this work:

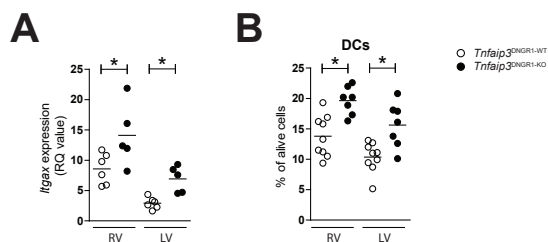
MK was supported by the Dutch Heart Foundation (2016T052). TK was supported by an unrestricted grant by Actelion pharmaceuticals and the Pulmonary hypertension patient association.

DM was supported by the Netherlands Cardiovascular Research Initiative; the Dutch Heart Foundation, the Dutch Federation of University Medical Centers, the Netherlands Organization for Health Research and Development and the Royal Netherlands Academy of Science (CVON (2012-08), Phaedra). HJB

DNGRI-Cre-mediated Deletion of Tnfaip3/A20 in Conventional Dendritic Cells Induces Pulmonary Hypertension in Mice

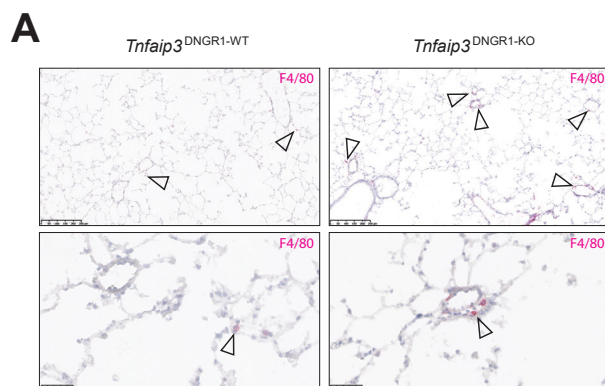
was supported by the Netherlands CardioVascular Research Initiative: The Dutch Heart Foundation, Dutch Federation of University Medical Centres, the Netherlands Organisation for Health Research and Development, and the Royal Netherlands Academy of Sciences (CVON-2012-08 PHAEDRA, CVON-2018-29 PHAEDRA-IMPACT and CVON-2017-10 Dolphin-Genesis).

## SUPPLEMENTARY MATERIAL



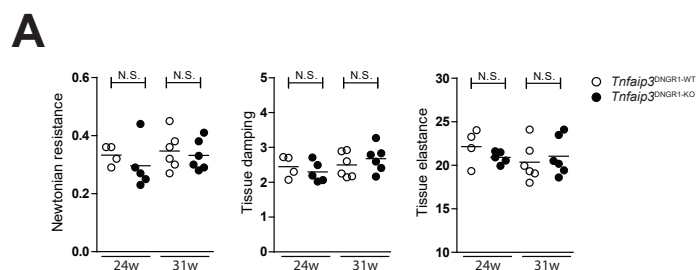
**Supplementary figure 1. RT-PCR and flow cytometry analysis in hearts of 31w *Tnfaip3*<sup>DN</sup> mice show increased *itgax* (encoding CD11c) expression and increased proportions of DCs, both in right and left ventricle.**

(A) RT-PCR values for *itgax* (encoding CD11c) expression in 31w old *Tnfaip3*<sup>DN</sup> and *Tnfaip3*<sup>WT</sup> mice, data shown in RQ values. (B) Flow cytometry analysis in 31w old *Tnfaip3*<sup>DN</sup> and *Tnfaip3*<sup>WT</sup> mice of right and left ventricle dendritic cell proportions. Results are presented as symbols for individual mice, together with mean values of 6 to 8 mice per group. \* $P < 0.05$ , \*\* $P < 0.01$ , \*\*\* $P < 0.001$ .



**Supplementary figure 2. F4/80 staining for pulmonary macrophages shows perivascular presence of macrophages in *Tnfaip3*<sup>DN</sup> mice.**

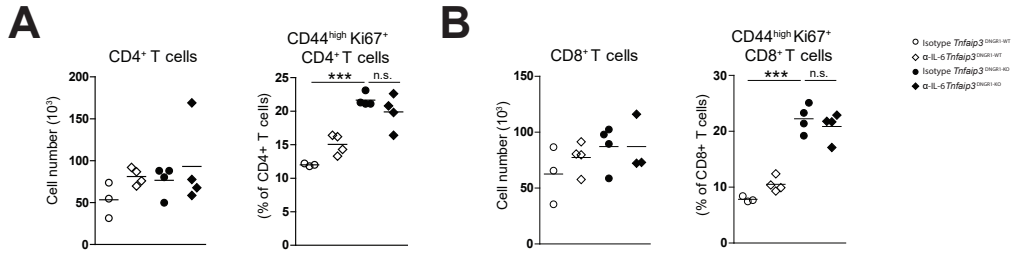
(A) Using immunohistochemistry staining for F4/80 in the lung, the presence of pulmonary macrophages was evaluated (scale bars are 250  $\mu\text{m}$  for the upper panels and 50  $\mu\text{m}$  for the lower panels).



**Supplementary figure 3. Lung function assessment shows no differences in lung tissue resistance, damping or elastance.**

(A) Evaluation of lung function through flexivent analysis in 24w and 31w old *Tnfaip3*<sup>DN</sup> and *Tnfaip3*<sup>WT</sup> mice compared to wildtype for Newtonian resistance, tissue damping and tissue elastance. Results are presented as symbols for individual mice, together with mean values of 5 to 6 mice per group. N.S. = not significant.

DNGRI-Cre-mediated Deletion of *Tnfaip3/A20* in Conventional Dendritic Cells Induces Pulmonary Hypertension in Mice



**Supplementary figure 4. Similar CD4+ and CD8+ T cell numbers in the lungs of anti-IL-6 treated and untreated *Tnfaip3*<sup>DNGRI-KO</sup> mice and *Tnfaip3*<sup>DNGRI-WT</sup> mice.**

(A-B) Evaluation of absolute cell numbers and proportions of CD44<sup>+</sup>Ki67<sup>+</sup> cells for CD4<sup>+</sup> (A) and CD8<sup>+</sup> T cells (B) in anti-IL-6 treated and untreated *Tnfaip3*<sup>DNGRI-KO</sup> mice and *Tnfaip3*<sup>DNGRI-WT</sup> mice. Results are presented as symbols for individual mice, together with mean values of 4 mice per group. \**P* < 0.05, \*\**P* < 0.01, \*\*\**P* < 0.001.

**Supplementary table 1: Primers for RT-PCR.**

Primer	Sequence
IL-6 FW	CCTAGTGC GTTATGCCTAAGCA
IL-6 RV	TCGTAGAGAACAACATAAGTCAGATACCT
IL-10 FW	GGTTGCCAAGCCTTATCGGA
IL-10 RV	ACCTGCTCCACTGCCTTGCT
IL-1b FW	AGTTGACGGACCCCAAAG
IL-1b RV	TTTGAAGCTGGATGCTCTCAT
TGF-β FW	TGACGTCACCTGGAGTTGTACGG
TGF-β RV	GGTTCATGTCATGGATGGTGC
FGF2 FW	TGACTTGATCCCTCCCAGT
FGF2-RV	AAGAATCTGTCCCGCTAGGC
VEGF-a FW	GCACATAGAGAGAATGAGCTTCC
VEGF-a RV	CTCCGCTCTGAACAAGGCT
VEGF-b FW	CAGAGTATGCCTGGTGGGTC
VEGF-b RV	CCCTGTGGCTATGTAAGGTC
HGF FW	ACCATGTTCAAGGACGGAGT
HGF RV	AATGCCCTTACCACCACTG

**Supplementary table 2: Primary antibodies used for immunohistochemical staining.**

Reactivity	Conjugate	Dilution	Isotype	Clone	Reference	Company
$\alpha$ -smooth muscle actin	PE	1/100	Mouse IgG2a, K	IA4	IC1420P	R&D systems
B220	FITC	1/150	Rat IgG2a, K	RA3-6B2	11-0452-82	eBioscience
CD3e	PE	1/150	Hamster IgG1	145-2C11	12-0031-85	eBioscience
CD4	EF450	1/200	Rat IgG2b, K	GK1.5	11-0041-85	eBioscience
CD11c	FITC	1/100	Hamster IgG	N418	11-0114-82	eBioscience
CD31	FITC	1/80	Rat IgG2a, K	390	14-0311-82	eBioscience
CD138	PE	1/100	Rat IgG2a, K	281-2	553714	BD
IgA	FITC	1/100	Rat IgG1, K	C10-3	559354	BD
IgA	Biotin	1/100	Rat IgG	C10-1	556978	BD
IgD	PE	1/50	Rat IgG2a, K	11-26c	12-5993-82	eBioscience
IgG	Biotin	1/100	Goat IgG	Polyclonal	1030-08	Southern Biotech
GL-7	FITC	1/50	Rat IgM, K	GL7	553666	BD
Ki67	FITC	1/100	Rat IgG2a, K	SolA15	11-5698-82	eBioscience

**Supplementary table 3: Secondary antibodies used for immunohistochemical staining.**

Reactivity	Host	Conjugate	Dilution	Reference	Company
FITC	Goat	AP	1/50	600-105-096	Rockland
FITC	Goat	PO	1/50	600-103-096	Rockland
Goat	Rabbit	AP	1/100	A4187	Sigma Aldrich
Hamster	Goat	AP	1/50	127-055-099	Jackson
PE	Goat	PO	1/50	600-103-387	Rockland
Rat	Goat	AP	1/50	A8438	Sigma Aldrich
Rat	Goat	AP	1/100	112-055-167	Jackson

**Supplementary table 4: Antibodies used for Flow cytometry.**

<b>Antibody</b>	<b>Conjugate</b>	<b>Clone</b>	<b>Company</b>
CD24	PE	M1/69	BD
CD11c	PE-Texas Red	N418	Invitrogen
CD86	PE-Cy7	GL1	BD
CD64	APC	X54-5/7.1	BD
MHC II	Alexa Fluor 700	M5/114.15.3	eBioscience
CD103	Brilliant Violet 421	2E7	eBioscience
Ly6C	Brilliant Violet 605	AL-21	BD
PD-L1	Brilliant Violet 711	MIH5	BD
CD11b	Biotin	M1/70	BD
IL-6	PE	MP5-20F3	BD
IL-10	PerCP-CY5.5	JES5-16E3	eBioscience
MHCI	Biotin	AF6-88.5	BD
B220	Alexa Fluor 700	RA3-6B2	eBioscience
CD19	APC-Cy7	1D3	BD
CD138	Brilliant Violet 605	281-2	BD
FOXP3	FITC	FJK-16s	eBioscience
RORyt	PE	Q31-378	BD
CD3	PE-Texas Red	CF594	BD
CD44	PerCP-CY5.5	IM7	eBioscience
CD8	PE-Cy7	53-6.7	eBioscience
Ki67	Alexa Fluor 700	SolA15	eBioscience
CD25	Brilliant Violet 605	PC61	Biolegend
CD4	Brilliant Violet 711	RM4-5	BD
Granzyme B	PE-Cy7	NGZB	eBioscience
IL17A	Alexa Fluor 700	TC11-18H10.1	BD
CD3	APC-Cy7	17A2	eBioscience
CD8	Biotin	53-6.7	BD
Streptavidin	Brilliant Violet 786		BD
Streptavidin	Brilliant Violet 421		BD
IFN- $\gamma$	Brilliant Violet 650	XMG1.2	BD
PD-1	Brilliant Violet 421	J43	BD
CXCR5	Brilliant Violet 650	2G8	BD



# CHAPTER 3

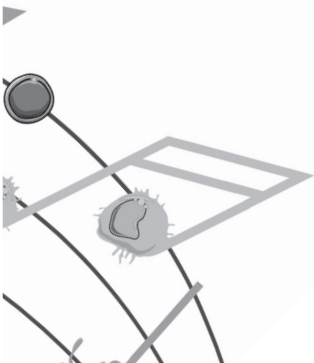
## *Central role of dendritic cells in human and murine pulmonary arterial hypertension.*

D. van Uden, **T. Koudstaal**, J.A.C. van Hulst, I.M. Bergen,  
C. Gootjes, N.W. Morrell, J.H. von der Thüsen, T.P.P. van den Bosch,  
M.R. Ghigna, F. Perros, D. Montani, M. Kool, K.A. Boomars\*,  
R.W. Hendriks\*

\*Contributed equally.

Int. J. Mol. Sci. 2021, 22(4), 1756.

3



## ABSTRACT

The pathogenesis of idiopathic pulmonary arterial hypertension (IPAH) is not fully understood, but evidence is accumulating that immune dysfunction plays a significant role. We previously reported that 31-week-old *Tnfaip3<sup>DNGRI-KO</sup>* mice develop PH symptoms. These mice harbor a targeted deletion of the TNF $\alpha$ -induced protein-3 (*Tnfaip3*) gene, encoding the NF- $\kappa$ B regulatory protein A20, specifically in type I conventional dendritic cells (cDC1s). Here, we studied the involvement of DCs in PH in more detail. We found various immune cells, including DCs, in the hearts of *Tnfaip3<sup>DNGRI-KO</sup>* mice, particularly in the right ventricle (RV). Secondly, in young *Tnfaip3<sup>DNGRI-KO</sup>* mice innate immune activation through airway exposure to Toll-like receptor ligands *in vivo* did not result in elevated RV pressures, although we did observe RV enlargement. Thirdly, PAH symptoms in *Tnfaip3<sup>DNGRI-KO</sup>* mice were not enhanced by concomitant mutation of bone morphogenetic protein receptor type 2 (*Bmpr2*), which is the most affected gene in PAH patients. Finally, in human IPAH lung tissue we found co-localization of DCs and CD8<sup>+</sup> T cells, representing the main cell type activated by cDC1s. Taken together, these findings support a unique role of cDC1s in PAH pathogenesis, independent of general immune activation or a mutation in the *Bmpr2* gene.

## INTRODUCTION

Pulmonary arterial hypertension (PAH) is characterized by structural remodeling of the arterial vasculature of the lung with a mean pulmonary arterial pressure (PAP) at rest of  $\geq 20$  mmHg, a mean capillary wedge pressure of  $\leq 15$  mmHg and a pulmonary vascular resistance of  $\geq 3$  Wood Units (1). This high pulmonary pressure causes hypertrophy of the right ventricle (RV), which can lead to heart failure and eventually death. Individuals with PAH are classified into world health organization (WHO) subgroups based on etiology and predisposing factors, such as genetic mutations classifying heritable PAH (HPAH) or systemic autoimmunity classifying connective tissue disease PAH (CTD-PAH). PAH patients with no known predisposing factor are classified as idiopathic PAH (IPAH) (1).

The major mutation found in HPAH patients is in the bone morphogenetic protein receptor type 2 (*BMPR2*) gene, causing loss-of-function or reduced receptor signaling (reviewed in (200)). *BMPR2*, which belongs to the transforming growth factor- $\beta$  (TGF $\beta$ ) receptor family, is expressed by various cell types including vascular pulmonary endothelial cells and pulmonary artery smooth muscle cells (PASMCs) and is crucial in vascular homeostasis (201). Reduced *BMPR2* signaling is associated with endothelial dysfunction and is not solely present in HPAH patients but also in 14-35% of PAH patients, so-called sporadic cases without a known family history (202, 203). In the absence of a *BMPR2* gene mutation, reduced *BMPR2* signaling can be induced by numerous causes, including aberrant activity of the immune system (reviewed in (204)). Conversely, not all patients with a *BMPR2* mutation develop PAH, indicating that additional factors are needed to cause disease.

Several lines of evidence support the critical involvement of the immune system in PAH pathogenesis. Firstly, blood expression profiling and transcriptomic studies in patients and in a rat model showed an enrichment of toll-like receptor (TLR) signaling (205-207). PASMCs and dendritic cells (DCs) of the immune system use these TLRs to sense pathogens (208, 209). Specific TLR activation on PASMCs leads to the production of chemokines, such as the X-X-C-motif chemokine ligand 8 (CXCL8 or interleukin (IL)-8) and CXCL10 (IP-10), and endothelin-1, which may participate in PAH pathogenesis (208). Infections with viruses such as HIV, human herpes virus 8 and hepatitis B and C are associated with PAH development (210). Host defense to bacteria is also thought to contribute to disease by autoantigen-related molecular mimicry (211). Nevertheless, only a minor proportion of infected individuals develop PAH. Secondly, serum levels of particular pro-inflammatory cytokines, including IL-6, IL-8, IL-10 and IL-12p70, are elevated in PAH patients and correlate with survival (94). Unsupervised analysis of blood proteomic profiles showed that PAH patients have distinct immune phenotypes comprising multiple cytokines, chemokines and growth factors, which are independent of WHO subgroups and correlate with clinical risk (94, 122). Thirdly, lung biopsies from IPAH patients often contain accumulations of lymphoid cells that form tertiary lymphoid organs (TLOs) (33), in which DCs are present and crucial for TLO maintenance (178, 212).

DCs form the bridge between the innate and adaptive immune system. They take up antigens and - after processing - present these to T cells, thereby inducing an adaptive immune response. Several DC subsets exist under steady state conditions, including (i) plasmacytoid DC (pDC) which are known for their interferon production; (ii) type 1 conventional DCs (cDC1s) that excel in cross-presentation of antigens, and (iii) type 2 cDCs (cDC2s) which are known for CD4+ T cell induction (209). Under inflammatory conditions, monocytes often differentiate to monocyte-derived-DCs (mo-DCs). Most of the DC subsets have been implicated in the pathobiology of IPAH and CTD-PAH (reviewed in (86)). Importantly, not only the abundance of DCs is different between PAH patients and healthy individuals,

but also their activation status (55, 89, 195). Further support for the involvement of DCs comes from the *Tnfaip3<sup>DNGRI-KO</sup>* mouse model in which the TNFa-induced protein-3 (*Tnfaip3*) gene encoding the A20 protein, a negative regulator of the nuclear factor-kappa B (NF- $\kappa$ B) signaling pathway, is deleted in DCs using the Cre-LoxP system (213). In this model, the *Tnfaip3* gene is mainly targeted in cDC1s, whereby Cre expression is driven by the DNGR1 promoter. *Tnfaip3<sup>DNGRI-KO</sup>* mice spontaneously develop PH over time and show lymphocytic infiltration and vascular remodeling (213).

The exact mechanism by which *Tnfaip3<sup>DNGRI-KO</sup>* mice develop PH symptoms and the importance of the altered activation status of DCs or other immune cells in this model, is not known. In this study we investigated the immunological landscape of the heart in *Tnfaip3<sup>DNGRI-KO</sup>* mice more closely. Since signs of PH are absent in young *Tnfaip3<sup>DNGRI-KO</sup>* mice, we wondered whether additional triggers might be required to induce the PH phenotype. Therefore, we investigated the effects of immune activation on PH development by airway exposure to TLR ligands *in vivo*. By crossing *Tnfaip3<sup>DNGRI-KO</sup>* mice to *Bmpr2<sup>+R899X</sup>* mice, we determined whether a vascular trigger would result in enhancement of the PH phenotype. Finally, we explored the relevance of our findings by determining DCs and CD8+ T cell co-localization in human IPAH lung tissue.

## MATERIALS AND METHODS

### Mice

*Tnfaip3<sup>DNGRI-KO</sup>* mice (*Clec9a<sup>+Cre</sup>* X *Tnfaip3<sup>fl/fl</sup>*) have been described previously (172, 213). *Tnfaip3<sup>DNGRI-WT</sup>* mice (*Clec9a<sup>+non-cre</sup>* X *Tnfaip3<sup>fl/fl</sup>*) littermates served as WT controls. Mice were sacrificed and analyzed at 14-16 weeks. *Tnfaip3<sup>DNGRI-KO</sup>* mice were crossed with *Bmpr2<sup>+R899X</sup>* mice, which have a premature stop codon in the *Bmpr2* gene leading to reduced BMPR2 expression (143). In the experiments four groups of mice were analyzed: WT, single *Bmpr2<sup>+R899X</sup>* mice, single *Tnfaip3<sup>DNGRI-KO</sup>* and *Bmpr2<sup>+R899X</sup>* X *Tnfaip3<sup>DNGRI-KO</sup>* mice. Mice were sacrificed and analyzed when 31 weeks old. Mice were bred and housed at the Erasmus MC under SPF conditions. Experiments were approved by the animal ethical committee of the Erasmus MC, Rotterdam, The Netherlands.

### Exposure of TLR ligand in *Tnfaip3<sup>DNGRI-KO</sup>* mice

For exposure to TLR ligands, 11-13-week-old *Tnfaip3<sup>DNGRI-KO</sup>* and *Tnfaip3<sup>DNGRI-WT</sup>* mice were anesthetized using 2.5% isoflurane and subsequently administered intra-tracheally (i.t.) either 10-25  $\mu$ g CpG (ODN 1668, Invitrogen), 40-100  $\mu$ g Poly I:C (Invivogen), 10  $\mu$ g LPS (Sigma) or 0.9% sodium chloride (NaCl) at day 0 and day 7. Mice were weighted daily and sacrificed at day 14 for analysis.

### Right heart catheterization and Fulton index

To determine RV pressures mice were weighted and anesthetized by an intraperitoneal (i.p.) injection with urethane (2 mg/g, given according to weight of the mice). Urethane was used since this anesthetic has a minimal effect on the cardiovascular and respiratory system. After placing a tracheal canula (miniVent type 845, Hugo Sachs Elektronik) the RV pressure was measured using a pressure catheter (Miller Inc.), as described previously (213). WinDaq (DataQ instruments) and matlab (the mathworks) were used to record and analyze pressures. After excision of the heart, RV and left ventricle

(LV) + septum (S) were separated and weighted separately (213). Fulton index was calculated by dividing the weight of the RV by the weight of LV+S.

### RNA extraction Real-time quantitative RT-PCR

Heart tissue (after separation of RV and LV/S) of *Tnfrap3<sup>DNGRI-WT/KO</sup>* mice was stored in -80°C until processing of the material. Heart tissue was homogenized using lysis buffer with 2-mercaptoethanol and ¼” ceramic spheres (MP biomedical, 6540-034) by shaking for 40 seconds (MP biomedical, Fastprep-24 5G). Subsequently, RNA was extracted using TRI reagent (Sigma, T9424) and cDNA synthesis was performed using a RevertAid H minus First Strand cDNA synthesis Kit (Thermoscientific, K1632). The cDNA was used to measure expression of CD11c, BATF3, CD4 and CD8, as well as the Glyceraldehyde-3-phosphate dehydrogenase (GAPDH) housekeeping gene by RT-PCR in a 7300 Real time PCR system (Applied Biosystems). Primer sequences are given in Supplementary Table 1.

### Histology of lung and heart tissues

Five-µm-thick paraffin-embedded mouse lung sections were stained with hematoxylin and eosin (H&E). Sections were stained for alpha smooth muscle actin (a-SMA) using mouse anti-human a-SMA-PE (R&D system) and goat anti-PE-alkaline phosphatase (Rockland) as primary and secondary antibody, respectively. Antibodies used for immunohistochemical staining are listed in Supplementary Table 2. Prior to a-SMA staining, an antigen retrieval was done by incubating slides in citrate buffer (PH 6.0, Sigma C9999-1000MC) at 78°C for 10 minutes. Elastic Van Gieson (EvG) staining (Elastic Stain kit (HT25), Sigma-Aldrich) was performed, using standard procedures. To determine co-localization of CD11c with either CD3+ or CD8+ T cells, lung slides were first stained with hamster anti-mouse CD11c PE (clone N418, ThermoFisher scientific) and rat anti-mouse CD3 APC-ef780 (clone 17A2, ThermoFisher) or rat anti-mouse CD8 Fitc (clone 53-6.7, BD). Next, slides were stained by secondary antibodies goat anti-PE-alkaline phosphatase (Rockland) and goat anti-rat PE (Sigma).

Mouse hearts were either directly separated after section and embedded for whole mount analyses of the RV or fixed in total with 4% paraformaldehyde (PFA) (Carl Roth, Karlsruhe, Germany) before paraffin embedding. Five-µm-thick paraffin-embedded heart sections were stained with EVG. For the evaluation of DCs in the heart, whole mount RVs were analysed. Directly after separation of the left ventricle/septum, the RV was pinned and fixed overnight using fresh 4% PFA/PBS. The next day, the RVs were washed and incubated with the primary antibody specific for MHCII and GFP (antibody details in Supplementary Table 2). After 24 hours, the RVs were washed and incubated with the secondary antibody. Finally, the RVs were embedded and analysed using a meta311 confocal microscope.

For immunohistochemical analysis of human lung tissue, we performed a 4-plex chromogenic multiplex by automated IHC using the Ventana Benchmark Discovery ULTRA (Ventana Medical Systems Inc.). Slides of 4 µm thick formalin-fixed paraffin-embedded (FFPE) sections were stained for CD8, CD68, a-SMA and CD206. All antibodies are listed in Supplementary Table 2. In brief, following deparaffinization and heat-induced antigen retrieval with CC1 (#950-224, Ventana) for 32 minutes, anti-CD8 was incubated for 32 minutes at 37°C followed by omnimap anti-rabbit HRP (#760-4311, Ventana) and detection with chromomap DAB (#760-159, Ventana). An antibody denaturation step was performed with CC2 (#950-123, Ventana) at 100°C for 20 minutes. Secondly, incubation with anti-CD68 was performed for 16 minutes at 37°C, followed by omnimap anti-mouse HRP (#760-4310, Ventana)

and detection with discovery purple (#760-229, Ventana) for 32 minutes. An antibody denaturation step was performed with CC2 at 100°C for 20 minutes. Thirdly, anti- $\alpha$ -SMA was incubated for 32 minutes at 37°C, followed by omnimap anti-mouse HRP (#760-4310, Ventana) and detection with Discovery green (#760-271, Ventana) for respectively 32 and 16 minutes. An antibody denaturation step was performed with CC2 at 100°C for 20 minutes. Lastly, sections were incubated with anti-CD206 for 32 minutes at 37°C followed by mouse-NP (#760-4816, Ventana) for 24 minutes at 37°C and subsequently anti-NP-AP (#760-4827, Ventana) for 16 minutes and detection with discovery Yellow (#760-239, Ventana) for 44 minutes. Incubation was followed by hematoxylin II counter stain for 4 minutes and then a blue coloring reagent for 4 minutes according to the manufactures instructions (Ventana).

### Flow cytometry

To obtain single-cell suspensions, lungs and heart tissues were digested using DNase and Liberase at 37°C for 30 minutes. After digestion, lungs and heart were homogenized through a 100- $\mu$ m cell strainer (BD Bioscience, San Jose, CA, USA) and red blood cells were lysed using an osmotic lysis buffer. Flow cytometry extracellular and intracellular staining procedures have been described previously (96). Dead cells were excluded using Fixable viability dye Live/Dead eF506 (eBioscience). Monoclonal antibodies used are listed in Supplementary Table 3. Data was acquired using a LSR II flow cytometer (Beckton Dickinson) with FACS software (Beckton Dickinson). Data analysis was done using FlowJo version 10 (Tree Star Inc software, Ashland, OR, USA).

### Statistic analysis

For comparisons between *Tnfaip3*<sup>DNGRI-WT</sup> and *Tnfaip3*<sup>DNGRI-KO</sup> mice or between TLR stimulation and NaCl stimulation a Mann-Whitney U test was used. For comparisons between multiple groups (WT, *Tnfaip3*<sup>DNGRI-KO</sup>, *BMPR2*<sup>+/R899X</sup> and *Tnfaip3*<sup>DNGRI-KO</sup> *X* *BMPR2*<sup>+/R899X</sup> mice) a Kruskal Wallis test was used, in combination with a Dunn's multiple comparison test comparing either mouse group to the WT mouse group or comparing all groups. P-values of < 0.05 were considered statistically significant. Statistical analysis was performed using Prism 8 (GraphPad Software).

## RESULTS

### Increased myocardial infiltration of dendritic cells in the RV of *Tnfaip3*<sup>DNGRI-KO</sup> mice

*Tnfaip3*<sup>DNGRI-KO</sup> mice show increased RV pressures, RV hypertrophy and increased numbers of pulmonary DCs (213). Strikingly, in contrast to wild-type (WT) control mice, we found high number of DCs that were YFP<sup>+</sup>, indicating *Tnfaip3* gene deletion, in the RV of *Tnfaip3*<sup>DNGRI-KO</sup> mice from 14 weeks of age onwards (Figure 1a). Flow cytometric analysis showed an increase of the proportions of DCs in the RV and of T cells in both RV and left ventricle (LV) of *Tnfaip3*<sup>DNGRI-KO</sup> mice, compared with WT control mice (Figure 1b). The increase in the proportions of DCs and T cells was supported by RT-PCR analysis for the expression of the DC markers CD11c and basic leucine zipper transcriptional factor ATF-like 3 (BATF3), and the T cell subset markers CD4 and CD8, respectively (Figure 3c). An Elastin von Giessen (EvG) staining for collagen and vascular intima wall thickening on heart tissue showed

signs of lymphocytic infiltration and RV hypertrophy in 24-week-old *Tnfaip3*<sup>DNGRI-KO</sup> mice without evidence for myocardial vascular remodeling, when compared to WT mice (Figure 1d).

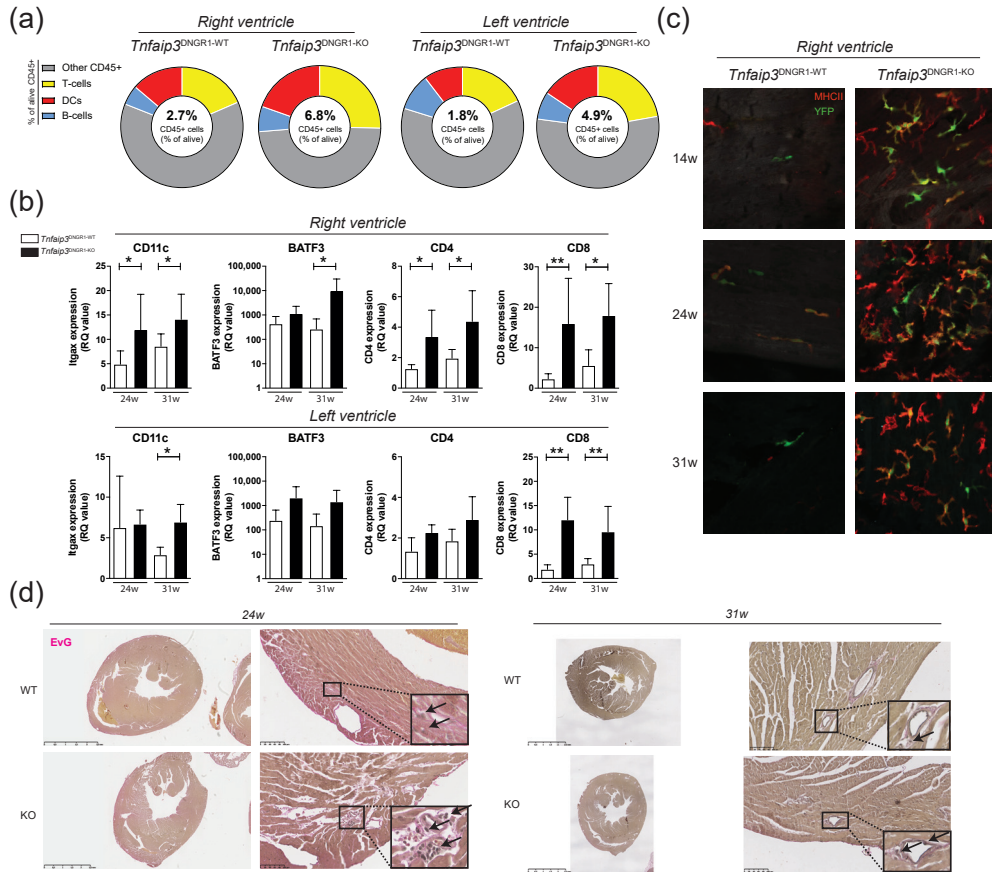


**Figure 1. Increased myocardial infiltration of DCs in the RV of *Tnfaip3*<sup>DNGRI-KO</sup> mice.** (a) Whole mount analysis of right ventricle staining for YFP (green) and MHCII (red) in age 14-, 24- or 31-week-old *Tnfaip3*<sup>DNGRI-KO</sup> mice; (b) Flow cytometry analysis for lymphoid fraction (SSC<sup>low</sup>, alive, CD45<sup>+</sup>), DCs (CD3<sup>-</sup>/CD19<sup>-</sup>, MHC-II+CD11c<sup>+</sup>), T cells (CD3<sup>+</sup>) and B cells (CD19<sup>+</sup>) in separately measured right- and left ventricle cell suspensions from hearts of *Tnfaip3*<sup>DNGRI-WT/KO</sup> mice; (c) mRNA expression (relative to the glyceraldehyde-3-phosphate dehydrogenase (GAPDH) housekeeping gene) of DC markers CD11c and BATF3 and the T cell subset markers CD4 and CD8 in 24- and 31-week-old *Tnfaip3*<sup>DNGRI-KO</sup> and WT control mice. Results are presented as mean values + standard deviations of 4-6 mice per group. \**P* < 0.05, \*\**P* < 0.01; (d) Elastin von Giessen (EvG) stained whole heart section histology of *Tnfaip3*<sup>DNGRI-WT</sup> and *Tnfaip3*<sup>DNGRI-KO</sup> mice for representative sections. Arrows indicate myocardial vasculature.

### TLR4 activation leads to RV enlargement but not to increased RV pressures in *Tnfaip3<sup>DNGRI-KO</sup>* mice

The first signs of immune cell involvement in the *Tnfaip3<sup>DNGRI-KO</sup>* mice were already present at 14 weeks of age when the right ventricular systolic pressure (RVSP) was not yet elevated (Figure 1a). Since bacteria and viruses may be inducers of PAH (210, 211), we wondered if an additional inflammatory trigger such as exposure to TLR ligands, would result in development of PH at younger age. Therefore, 11-13-week-old *Tnfaip3<sup>DNGRI-KO</sup>* were intratracheally (i.t.) challenged with TLR4 ligand lipopolysaccharide (LPS), TLR3 ligand polyinosinic-polycytidylic acid (Poly I:C) or TLR9 ligand CpG, which was repeated after 7 days (Figure 2a). Two weeks after the last exposure, mice were analyzed for RV pressures, RV enlargement and immune cell involvement. In these experiments, LPS-treated or saline (NaCl)-treated WT mice were included as controls.

Administration of LPS or Poly I:C, but not CpG, induced weight loss in *Tnfaip3<sup>DNGRI-KO</sup>* mice (Supplementary Figure 1). This was also seen following LPS administration in WT mice. Exposure of *Tnfaip3<sup>DNGRI-KO</sup>* mice to TLR ligands did not result in increased RV pressures, compared to saline-treated *Tnfaip3<sup>DNGRI-KO</sup>* or WT mice that were administered saline or LPS (Figure 2b). However, in LPS-exposed *Tnfaip3<sup>DNGRI-KO</sup>* mice, the RV was larger than in *Tnfaip3<sup>DNGRI-KO</sup>* mice treated with saline, Poly I:C or CpG, or in LPS- or saline-treated WT mice (Figure 2c). As shown by EvG staining (Supplementary Figure 2), mid-sized pulmonary vessels of LPS-exposed *Tnfaip3<sup>DNGRI-KO</sup>* and WT mice were thickened compared to saline-treated WT mice. Moreover, LPS exposure in *Tnfaip3<sup>DNGRI-KO</sup>* led to inflammatory infiltrates around the vessels. Thus, LPS exposure alone was not sufficient to cause elevation of the Fulton index, but in combination with the altered immune system in *Tnfaip3<sup>DNGRI-KO</sup>* mice, this was sufficient.

The induction of immune activation by LPS in *Tnfaip3<sup>DNGRI-KO</sup>* and WT mice was confirmed by the observation of increased proportions of interstitial macrophages (IM) in the lung (214) (Figure 2d; see for gating: Supplementary Figure 3a). In these analyses, we found that the total population of monocytes/macrophages, which have also been implicated in PH pathogenesis (215), was decreased in saline- or LPS-exposed *Tnfaip3<sup>DNGRI-KO</sup>* mice compared to WT control mice (Figure 2d).

The frequency of pulmonary cDCs or the cDC1/cDC2 ratio in *Tnfaip3<sup>DNGRI-KO</sup>* and WT mice did not significantly change after LPS exposure (Figure 2e,f; see for gating: Supplementary Figure 3b). Consistent with our reported findings in 31-week-old mice (213), we found altered expression of the cell surface markers CD86, CD40 and PD-L1 on cDCs in 14–17-week-old *Tnfaip3<sup>DNGRI-KO</sup>* mice, compared to WT mice (Figure 2g). LPS exposure increased CD40 and reduced PD-L1 expression but did not affect CD86 expression on cDC1s in the lungs of *Tnfaip3<sup>DNGRI-KO</sup>* mice. These changes in activation marker expression following LPS exposure were not seen in cDC2s in *Tnfaip3<sup>DNGRI-KO</sup>* mice, nor in either subset in WT mice (Figure 2g). LPS exposure did not induce changes in the numbers of T or B cells in the lungs of *Tnfaip3<sup>DNGRI-KO</sup>* or WT mice (data not shown).

In summary, TLR stimulation - mimicking bacterial or viral infection - did not lead to increased RV pressures and therefore did not appear to enhance the PH phenotype in young *Tnfaip3<sup>DNGRI-KO</sup>* mice. However, LPS exposure in *Tnfaip3<sup>DNGRI-KO</sup>* mice was associated with RV enlargement and an altered surface phenotype of cDC1s but not cDC2s in the lung.

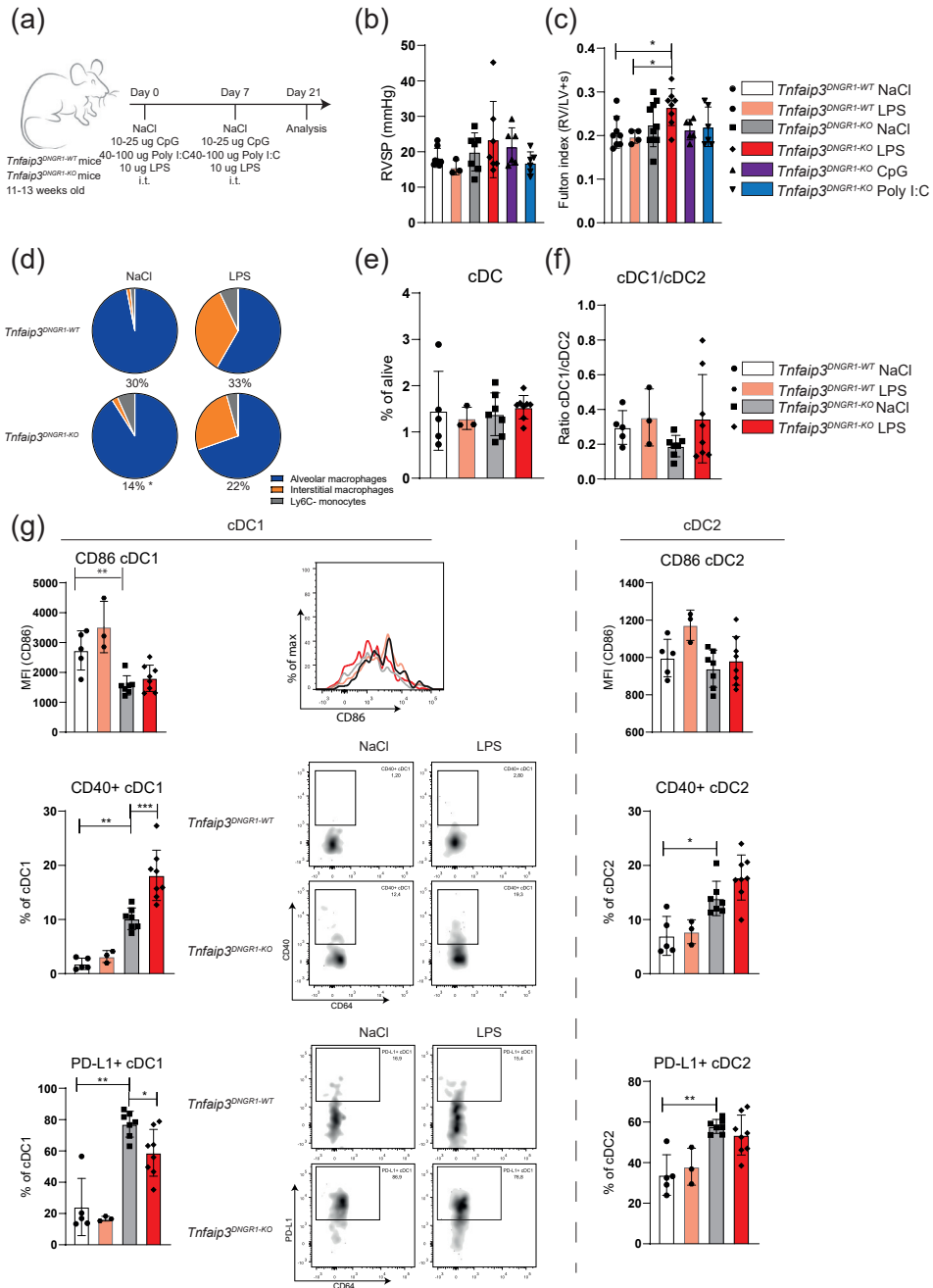


**Figure 2.** TLR4 activation leads to RV enlargement and cDC1 phenotype changes in *Tnfaip3*<sup>DN</sup> mice. (a) Scheme of intra-tracheal (i.t.) administration of CpG, LPS and Poly I:C in WT and *Tnfaip3*<sup>DN</sup> mice on day 0 and 7 and analysis on day 21; (b) Right ventricular systolic pressure (RVSP) in TLR-exposed WT and *Tnfaip3*<sup>DN</sup> mice, determined by right heart catheterization; (c) Enlargement of RV measured by Fulton index (right ventricle/ left ventricle + septum); (d) Assessment

of the indicated cell types in LPS-exposed WT and *Tnfaip3*<sup>DNGRI-KO</sup> mice. Proportion of the CD64<sup>+</sup>GR1<sup>+</sup> macrophage/monocyte population from total alive cells is indicated below the pie charts. (e-f) Quantification of total DCs (e) and the cDC1/cDC2 subset ratio (f) in the lungs of the indicated mice, as determined by flow cytometry; (g) Quantification of surface CD86, CD40 and PDL-1 expression on cDC1s (left) and cDC2s (right) in the indicated mouse groups. Flow cytometry analyses are shown as histogram overlays of CD86 expression (top), as dot plots with CD64/CD40 profiles (middle) and dot plots with CD64/PDL-1 profiles (bottom) of gated cDC1s. Results are presented as mean values  $\pm$  standard deviation of 3-10 mice (b,c) or 3-6 (e-g) mice per group. MFI= median fluorescence intensity. \**P* < 0.05, \*\**P* < 0.01, \*\*\* *P* < 0.001.

## The PH phenotype of *Tnfaip3*<sup>DNGRI-KO</sup> mice is not enhanced by concomitant *Bmpr2* mutation

Next, we wondered if involving structural cells would result in enhancement of the PH phenotype in *Tnfaip3*<sup>DNGRI-KO</sup> mice. To this end, we employed *Bmpr2*<sup>+/*R899X*</sup> mice, harboring a heterozygous knock-in allele of the R899X mutation as is seen in HPAH patients, which results in a premature stop codon (143, 216). These mice develop spontaneous PH by the age of 6 months, likely due to defective *Bmpr2* expression in pulmonary endothelial cells (143).

The *Tnfaip3*<sup>DNGRI-KO</sup> mice were crossed with *Bmpr2*<sup>+/*R899X*</sup> mice and analyzed at 31 weeks. Compared to WT mice, RV pressure was significantly increased in *Tnfaip3*<sup>DNGRI-KO</sup> mice, but not in *Bmpr2*<sup>+/*R899X*</sup> or *Tnfaip3*<sup>DNGRI-KO</sup> X *Bmpr2*<sup>+/*R899X*</sup> mice (Figure 3a). In all three mutant mouse groups the Fulton index was significantly higher than in WT mice (Figure 3a). A hematoxylin and eosin (H&E) staining showed that both *Tnfaip3*<sup>DNGRI-KO</sup> and *Tnfaip3*<sup>DNGRI-KO</sup> X *Bmpr2*<sup>+/*R899X*</sup> mice had signs of inflammatory infiltrates, which were not seen in WT and *Bmpr2*<sup>+/*R899X*</sup> mice (Supplementary Figure 4). Also, thickening of the small and mid-sized pulmonary vessels was evident in all three mutant mouse groups (shown by EvG and a smooth muscle actin (α-SMA) staining in Supplementary Figure 4). However, the RV pressures were only increased in *Tnfaip3*<sup>DNGRI-KO</sup> mice (Figure 3a).

We subsequently investigated whether the *Bmpr2*<sup>+/*R899X*</sup> genotype affected immune cells in the lung. The frequencies of total cDCs and the cDC1 subset were similar across the different mouse groups (Figure 3b and data not shown). Surface CD86 expression on cDC1s was specifically reduced in *Tnfaip3*<sup>DNGRI-KO</sup> mice, irrespective of the *Bmpr2* genotype (Figure 3b). In all three mutant mouse groups, the CD64<sup>+</sup>GR1<sup>+</sup> macrophage/monocyte populations were unaltered (Figure 3c). The proportions of T cells in the lung were significantly increased in *Tnfaip3*<sup>DNGRI-KO</sup> mice, irrespective of the *Bmpr2* genotype (Figure 3d). Hereby, the proportions of CD4<sup>+</sup> and CD8<sup>+</sup> T cells were similar in the four mouse groups (data not shown). The proportions of CD44<sup>+</sup>CD62L<sup>-</sup> memory cells within the CD8<sup>+</sup> T cell population were increased in *Tnfaip3*<sup>DNGRI-KO</sup> mice, irrespective of the *Bmpr2* genotype (Figure 3e). Finally, the frequency of pulmonary B cells was slightly lower in *Tnfaip3*<sup>DNGRI-KO</sup> mice, irrespective of the *Bmpr2* genotype, compared to WT or *Bmpr2*<sup>+/*R899X*</sup> mice (Figure 3f).

Overall, *Tnfaip3*<sup>DNGRI-KO</sup> X *Bmpr2*<sup>+/*R899X*</sup> mice did not show increased RV pressure and immunologically paralleled the *Tnfaip3*<sup>DNGRI-KO</sup> mice. From these findings we conclude that *Tnfaip3*<sup>DNGRI-KO</sup> cDC1 cells have a unique and dominant ability to induce PH symptoms, which is not modulated or enhanced by aberrant pulmonary endothelial cells in *Bmpr2*<sup>+/*R899X*</sup> mice.

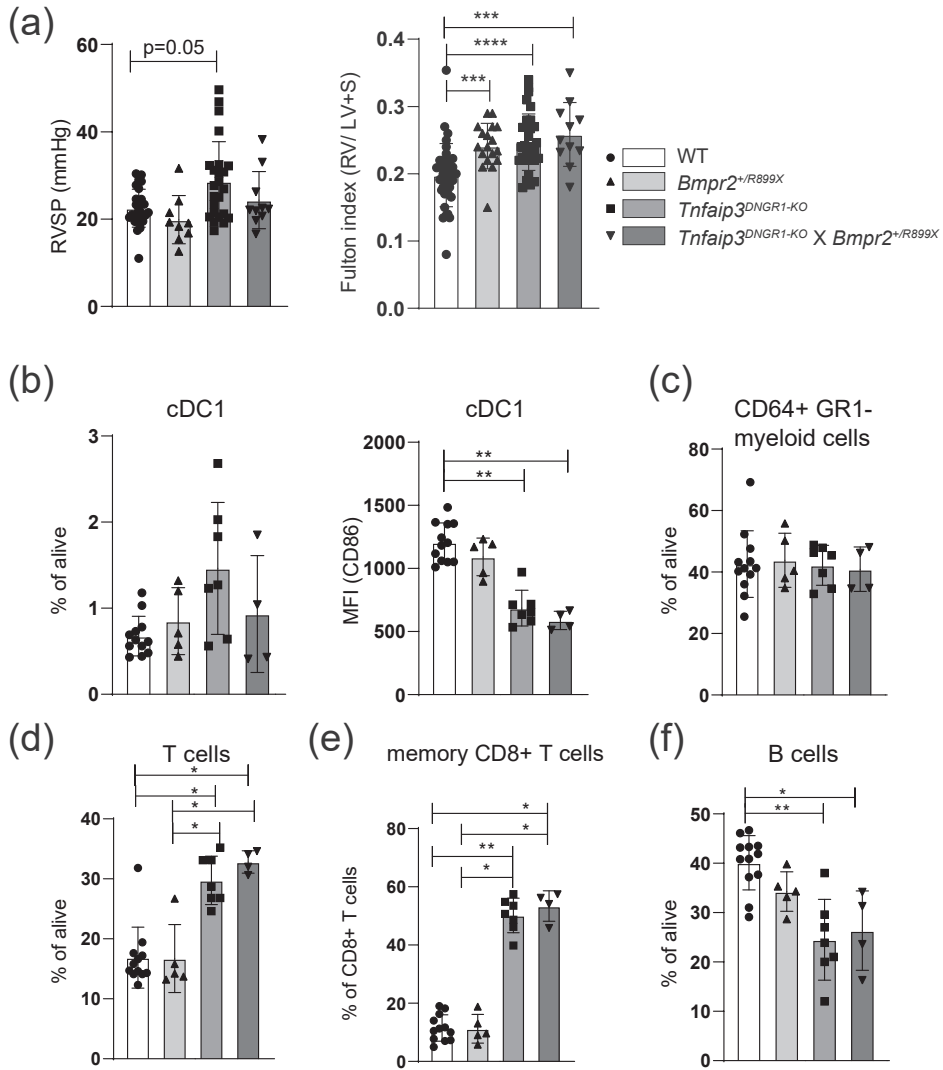


**Figure 3. Concomitant *Bmpr2* mutation does not alter the PH phenotype in *Tnfaip3*<sup>DNGR1-KO</sup> mice.** (a) Right ventricular systolic pressure (RVSP), determined by right heart catheterization and enlargement of RV measured by Fulton index (right ventricle/ left ventricle + septum) of the indicated mouse groups; (b) Quantification of lung cDC1 frequencies and CD86 expression (MFI = median fluorescence intensity) by flow cytometry; (c-f) Quantification of CD64+GR1- monocyte/macrophage population, T cells (c), Memory CD8+ T cells (e) or of B cells (b) determined by flow cytometry in the indicated mouse groups. Results are presented as mean + standard deviation (SD) values of 10-31 mice (a) or 4-12 mice (b-e) per group. \**P* < 0.05, \*\**P* < 0.01, \*\*\**P* < 0.001, \*\*\*\**P* < 0.0001.

## DCs and CD8<sup>+</sup> T cells co-localization around blood vessels in lungs of IPAH patients

The cDC1 subset excels in cross presentation and is known for its ability to activate CD8<sup>+</sup> T cells (209). Since cDC1s seem to have a unique and dominant ability to induce a PH phenotype, we determined the presence of DCs and CD8<sup>+</sup> T cells in both *Tnfaip3<sup>DNGRI-KO</sup>* mice and human IPAH lung tissue by immunohistochemistry.

Identification of DCs and T cells by CD11c and CD3 expression, respectively, showed the presence of these two cell types in the lung parenchyma as well as around vessels in 31-week-old WT and *Tnfaip3<sup>DNGRI-KO</sup>* mice (Figure 4a,b). Most DCs and T cells were located around blood vessels and were increased in numbers in *Tnfaip3<sup>DNGRI-KO</sup>* mice, as compared to WT mice (Figure 4a compared to b). In the lungs of *Tnfaip3<sup>DNGRI-KO</sup>* mice DCs often were in close proximity to CD3<sup>+</sup> T cells. A fraction of these T cells were CD8<sup>+</sup> T cells, as shown by staining for CD8 (Figure 4c).

To determine co-localization of DCs with CD8<sup>+</sup> T cells in the lungs of IPAH patients, we studied the presence of these cells by chromogenic multiplex in paraffin-embedded lung tissue of six IPAH patients. DCs express several mannose receptors such as CD209 and CD206, therefore we used the mannose receptor CD206 to identify DCs (209). Since macrophages also express CD206 we co-stained for CD68, which is only expressed by macrophages to distinguish DCs (CD68-CD206<sup>+</sup>) from macrophages (CD68+CD206<sup>+</sup>). The multiplex staining further included staining for CD8 and for  $\alpha$ -SMA to identify blood vessel structures. In healthy lung tissue the number of immune cells is generally limited, whereby immune cell infiltrates mostly consist of macrophages and the numbers of DCs and CD8 cells are limited (Figure 5a). Occasionally, we found CD8<sup>+</sup> T cells close to CD68-CD206<sup>+</sup> DCs (Shown for a control lung in Figure 5b).

In IPAH lungs remodeling of pulmonary vessels and the presence of plexiform lesions was evident from the prominent staining with  $\alpha$ -SMA (Figure 5c,e). In the lungs of all six IPAH patients analyzed macrophages were present, although in two patients the numbers were high, forming dense macrophage infiltrates (data not shown). DCs were abundantly detectable as CD68-CD206<sup>+</sup> cells in lung tissue of all six IPAH patients, although their presence in the parenchyma and around arterioles varied between patients. Figure 5 shows two representative patients, one patient with limited remodeling (panel c) and one patient with more severe remodeling (panel e). Close proximity of DCs and CD8<sup>+</sup> T cells, indicative for DC-CD8<sup>+</sup> T cell interaction, was mostly observed near affected, partly occluded vessels, but less frequently near fully occluded vessels (Figure 5c,e; shown in higher magnification in Figure 5d,f). Macrophages (CD206+CD68<sup>+</sup>) were particularly present near fully occluded vessels. Notably, in IPAH lungs with extensive remodeling and immune cell infiltration, co-localization of DCs and CD8<sup>+</sup> T cells was most prominent. IPAH patient 2 had more remodeling and showed more DC and CD8 interaction than IPAH patient 1, in which remodeling of the vessels was less severe.

In conclusion, these findings demonstrate close proximity of DCs and CD8<sup>+</sup> T cells around vessels and in parenchyma in lungs of *Tnfaip3<sup>DNGRI-KO</sup>* mice and IPAH patients, supporting the relevance of cDC1s in PAH pathology.

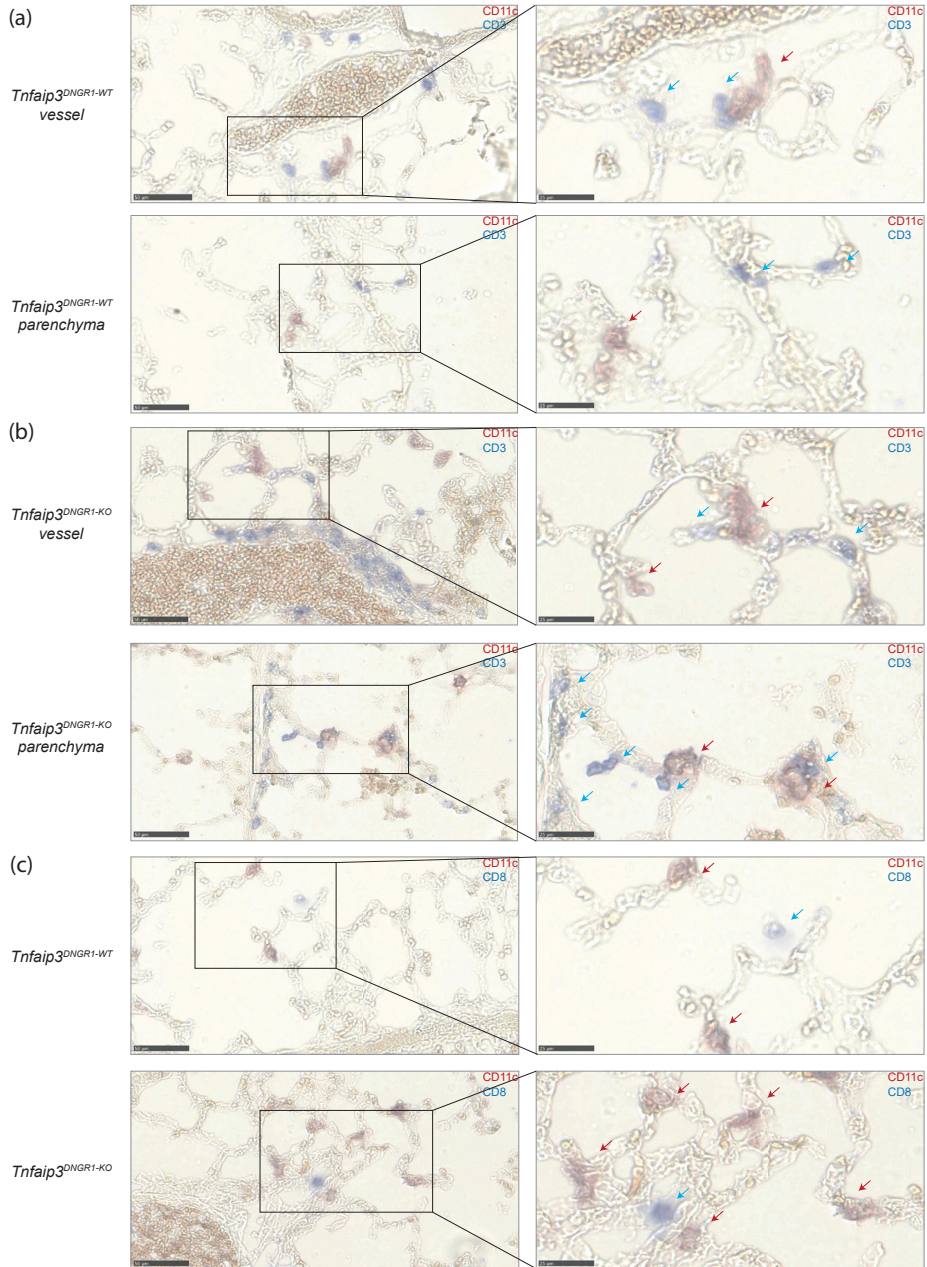


**Figure 4.** DCs and T cells are more often in close proximity around vessels and in parenchyma in *Tnfaip3<sup>DNDR1-KO</sup>* mice. (a) DC (CD11c, red) and T cell (CD3, blue) staining on lung cryosections of 31-week-old WT mice of which an area around a vessel (*left*) and parenchyma (*right*) of the same mouse is depicted. Magnification of selected areas (*bottom*); (b) DC (CD11c, red) and T cell (CD3, blue) staining on lung cryosections of 31-week-old *Tnfaip3<sup>DNDR1-KO</sup>* mice of which an area around a vessel (*left*) and parenchyma (*right*) of the same mouse is depicted. Magnification of selected areas (*bottom*); (c) DC (CD11c, red) and CD8+ T cells (CD8, blue) of WT (*left*) and *Tnfaip3<sup>DNDR1-KO</sup>* (*right*) mice around a vessel. Magnification of selected area (*bottom*). Data shown are representative for 4-6 mice per group. Arrows in top panels indicate DCs and arrows in lower panels indicate T cells and DCs.

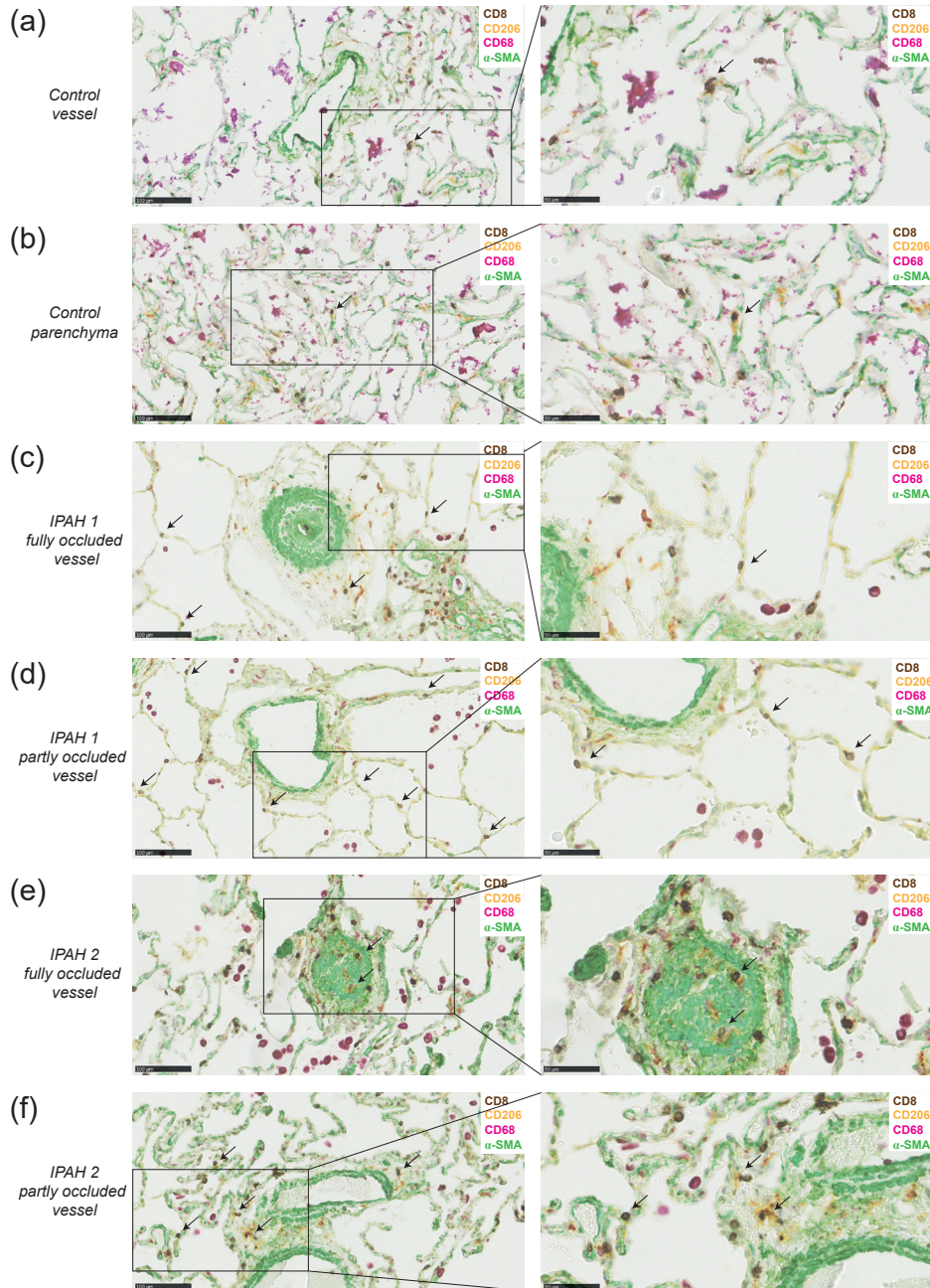


**Figure 5.** DCs are in close proximity to CD8+ T cells around vessels and in parenchyma in lungs of IPAH patients. (a) 4-plex chromogenic multiplex staining of DCs (CD206+, yellow), macrophages (CD68+, purple with or without CD206), T cells (CD8, DAP) and α-SMA (green) around a vessel (*left*) or in parenchyma (*right*) in the same healthy tissue from a patient who was diagnosed for adenocarcinoma; (b) Magnification of areas indicated in panel a; (c-e) Determination of DCs (CD206+CD68-), CD8+ T cells (CD8+), macrophages (CD68+) and vessels (α-SMA) around a fully occluded vessel (*left*) or partly occluded vessel (*right*)

of the same IPAH patient with moderate remodeling (c) or of a IPAH patient with extensive remodeling and immune cell infiltration (e); (d-f) Magnification of areas indicated in panel c or e. Data shown are representative for 6 IPAH patients. Arrows indicate DC and CD8 co-localization.

## DISCUSSION

We have previously shown that targeted deletion of the *Tnfaip3* gene, encoding the NFκB regulator A20, specifically in type I conventional dendritic cells (cDC1s) is sufficient to induce PAH symptoms in mice. In this study, we investigated the importance of the altered activation status of DCs in the development of PH.

We show that the heart, predominantly the RV, of *Tnfaip3<sup>DNGRI-KO</sup>* mice is infiltrated with MHCII+CD11c+ DCs, CD19+ B cells and CD3+ T cells. Exposing 11-13-week-old *Tnfaip3<sup>DNGRI-KO</sup>* mice to an additional TLR trigger did not lead to increased RV pressures and thereby a full PH phenotype. However, LPS exposure did induce enlargement of the RV and an altered activation of specifically cDC1s. We also found that adding a vascular trigger by reducing BMPR2 expression in older *Tnfaip3<sup>DNGRI-KO</sup>* mice did not result in an enhanced PH phenotype. As in our *Tnfaip3<sup>DNGRI-KO</sup>* mouse model the DNGRI-cre-driven deletion mostly targets the cDC1s, our findings indicate a key role of these cells in PAH development, which cannot be modulated by additional innate immune activation or defective BMPR2 function in structural cells. cDC1s excel in cross presentation and thereby predominately interact with CD8+ T cells. DCs and T cells were mostly present near the small-to-mid-sized pulmonary vessels in *Tnfaip3<sup>DNGRI-KO</sup>* and WT mice. Importantly, this was confirmed by the presence of DCs in close proximity to CD8+ T cells mostly around affected, but not fully occluded, pulmonary vessels in the lungs of IPAH patients.

We demonstrate that immune cells are not only present in the lungs of *Tnfaip3<sup>DNGRI-KO</sup>* mice (213), but also in the heart and especially in the RV. Using flow cytometry, we found higher frequencies of lymphocytes in the RV than in the LV of the hearts from both *Tnfaip3<sup>DNGRI-KO</sup>* and WT mice. Histological analysis of DCs in the RV showed more pronounced differences between WT and *Tnfaip3<sup>DNGRI-KO</sup>* mice than was seen by flow cytometry. An explanation might be that large local differences within RV regions exist between two mouse groups, which may be obscured in an analysis of whole RV cell suspensions, as is done in flow cytometry. The RV is the ventricle that is enlarged in PAH and immune cells may be crucial in its remodeling and enlargement. However, it cannot be excluded that the influx of immune cells is a bystander effect, next to a primary process in the heart. Although the current knowledge on the presence of immune cells in the hearts of PAH patients is limited (reviewed in (217)), it has been shown that immune cells are increased in the hearts of SSc-PAH and IPAH patients compared to controls (218). In SSc-PAH patients, immune cells were predominantly increased in the RV, but DCs were not specifically analyzed (218).

In our *Tnfaip3<sup>DNGRI-KO</sup>* mice, a large part of the cardiac low SSC lymphoid fraction consisted of DCs. Moreover, we found that DCs were present in the RV before pressures in the RV were elevated. To our knowledge, this is the first study that shows increased presence of myocardial DCs in an inflammatory-driven murine model for PH. Further studies are necessary to investigate if this increased presence of myocardial DCs is also found in the heart of PAH patients.

A large proportion of the CD45+ hematopoietic cells appeared to be neither T-cells, B-cells nor DCs, but might be macrophages or monocytes, since these cells comprise a large population in the heart, both in health and disease (reviewed in (219, 220)). Macrophages are implicated in PAH (55,

215), possibly by inflammasome-dependent secretion of pro-inflammatory cytokines such as IL-1 $\beta$  and IL-18 (221, 222), which are increased in serum of PAH patients (94). Interestingly, it has been found in mice that A20-deficient macrophages show spontaneous inflammasome activity and IL-1 $\beta$  secretion (223, 224). It is therefore conceivable that in *Tnfaip3*<sup>DNGRI-KO</sup> mice cDC1s also exhibit increased inflammasome activity and IL-1 $\beta$  secretion and that A20-deficient cDC1s might therefore parallel pathogenic macrophages in PAH. However, it is also attractive to speculate that increased inflammasome-dependent IL-1 $\beta$  secretion stimulates potent cytotoxic T cell responses by CD8+ T cells, as was very recently reported in the context of anti-tumor immunity (225). Further experiments are required to investigate the role of inflammasome activation in DC-T cell interaction in inflamed lymph nodes as well as in local myocardial inflammation in *Tnfaip3*<sup>DNGRI-KO</sup> mice.

31-week-old *Tnfaip3*<sup>DNGRI-KO</sup> mice show signs of PH, but PH is absent in young *Tnfaip3*<sup>DNGRI-KO</sup> mice. We wondered whether additional triggers would lead to increased RV pressures in young *Tnfaip3*<sup>DNGRI-KO</sup> mice. It is believed that in order to develop PAH a second trigger might be needed. For example, a viral infection alone is unlikely to cause PAH, since only one in 200 AIDS patients and only 10% of Hepatitis C patients show signs of PAH (210). Therefore, we exposed 11-13-week-old *Tnfaip3*<sup>DNGRI-KO</sup> mice to TLR3, TLR4 and TLR9 triggers, but none of these led to increased RV pressures. These findings indicate that the alterations in the A20-deficient DCs are already sufficient to induce increased pressures over time and cannot be further enhanced by TLR triggering. Even though there was no increase in pressure, TLR4 triggering by LPS resulted in RV enlargement and even two weeks after the last triggering, had effects on the activation of cDC1s only in the *Tnfaip3*<sup>DNGRI-KO</sup> mice. The *in vivo* exposure to LPS increased CD40 expression and reduced PD-L1 expression on cDC1s in the lungs of *Tnfaip3*<sup>DNGRI-KO</sup> mice. In *in vitro* experiments it has been demonstrated that activation of DCs by LPS can prime DCs for subsequent signals from T cells (226). The observed increase in CD40 expression and decrease in PD-L1 expression on cDC1s may indicate an increased CD8+ T cell priming capacity of the cDC1. This effect was not observed in cDC1s of WT mice, suggesting that their activation status during LPS exposure was unaltered.

Reduced *Bmpr2* signaling as an additional trigger in an inflammatory-based 31-week-old *Tnfaip3*<sup>DNGRI-KO</sup> mouse model did not result in an enhanced PH phenotype. This might be related to the mild PH phenotype seen in *Bmpr2*<sup>+ /R899X</sup> mice (143). *Bmpr2*<sup>+ /R899X</sup> mice do show an increased RV pressures at 6 months of age, but do not have an increased fulton index, indicating that there is no RV enlargement. In our hands however, the *Bmpr2*<sup>+ /R899X</sup> mouse model did not display detectable increased RV pressures but did show remodeling of the pulmonary arteries and a higher fulton index compared to WT controls. We did not find evidence for an additional effect of reduced *Bmpr2* signaling on the immune system. The *Bmpr2*<sup>+ /R899X</sup> mice showed no apparent changes in DCs, T cells or B cells. It was quite unexpected that there were no signs of altered immunity in the *Bmpr2*<sup>+ /R899X</sup> mice, since it is known that *Bmpr2* deficiency leads to the recruitment of lymphocytes, macrophages and neutrophils to the vessels (204). Because there is a genotype-phenotype relationship regarding *Bmpr2* mutations (216), it might be that this is also the case for immune involvement. Therefore, we cannot exclude that a more severe *BMPR2*-deficient PH mouse model may display changes in the immune system and may enhance the PH symptoms in *Tnfaip3*<sup>DNGRI-KO</sup> mice.

In our immunohistochemical analyses, the lungs of *Tnfaip3*<sup>DNGRI-KO</sup> mice showed more CD3+ T cells and DCs than WT mice, mostly around vessels. These DCs and T cells might contribute to vessel remodeling, which is the major hallmark of PAH pathology. In WT and *Tnfaip3*<sup>DNGRI-KO</sup> mice only a minor fraction of the T cells in the lung appeared to be CD8+ T cells. This was in contrast to the lungs

of IPAH patients in which both CD8+ T cells and DCs were abundantly present, even though we noticed heterogeneity among the IPAH patients. It is known that DCs expressing mannose receptors (CD209) are increased in lung tissue of IPAH patients, compared to control tissues (55). The presence of DCs around pulmonary vessels has been shown before (33), but it remained unknown whether at this location they would also interact with T cells. We found that in lung tissue of IPAH patients many DCs localized adjacent to CD8+ T cells. Interestingly, this co-localization was particularly observed near affected, not fully occluded vessels, but to a lesser extent near fully occluded and remodeled vessels. This might be explained by the role of DCs and CD8+ T cells in the process of inflammation and remodeling, which may be less present in fully occluded vessels (33). Since DCs that interact with CD8+ T cells are mainly cDC1s, the DCs adjacent to CD8+ T cells in the IPAH lungs are most likely cDC1s. However, additional markers such as IRF8 are needed to determine if these cells are indeed cDC1s.

Taken together, our findings in *Tnfaip3<sup>DNGRI-KO</sup>* mice support a unique role of cDC1s in PAH pathogenesis, independent of general immune activation or a mutation in the *Bmpr2* gene. This unique role includes the engagement of CD8+ T cells, given the observed co-localization of DCs and CD8+ T cells around vessels in the lungs of aged *Tnfaip3<sup>DNGRI-KO</sup>* mice with PH symptoms and in the lungs of IPAH patient. Deeper knowledge about the functional role of DC subsets in the activation of T cells in PAH improves our understanding of PAH pathobiology and is expected to contribute to the identification of candidate therapeutical targets.

#### Author Contributions

Conceptualization, methodology and designing experiments, D.U., T.K., M.K., K.B., R.H.; Performing and analyzing experiments, D.U., T.K., J.H., I.B., C.G., J.T., T.B.; Providing critical mouse strains, G.L., N.M., M.T.; Providing FFPE IPAH lung tissue, M.G., F.P., D.M.; Writing-reviewing and editing, D.U., T.K., K.B., R.H. All authors have read and agreed to the published version of the manuscript.

#### Funding

This research was funded by Dutch Heart Foundation, grant number 2016T052 (DU). T.K. was supported by an unrestricted grant by Actelion Pharmaceuticals and the Pulmonary hypertension Patients Association.

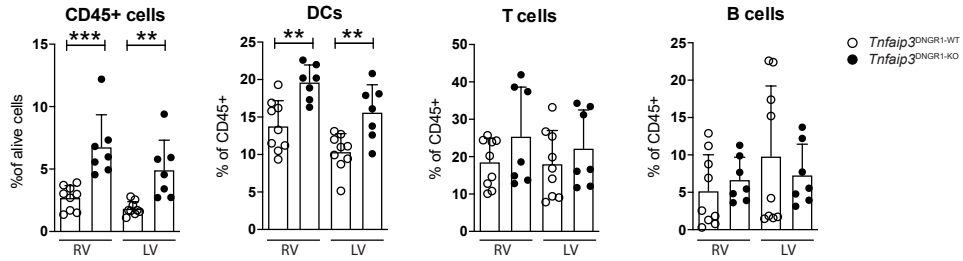
#### Acknowledgments

We thank prof. Caetano Reis e Sousa for providing critical mouse strains, dr. Daphne Merkus for providing the millar for measuring the RV pressure and Madelief Vink for assistance during experiments. Finally, we thank the Erasmus Mc Animal Facility (EDC) staff for their assistance during the project.

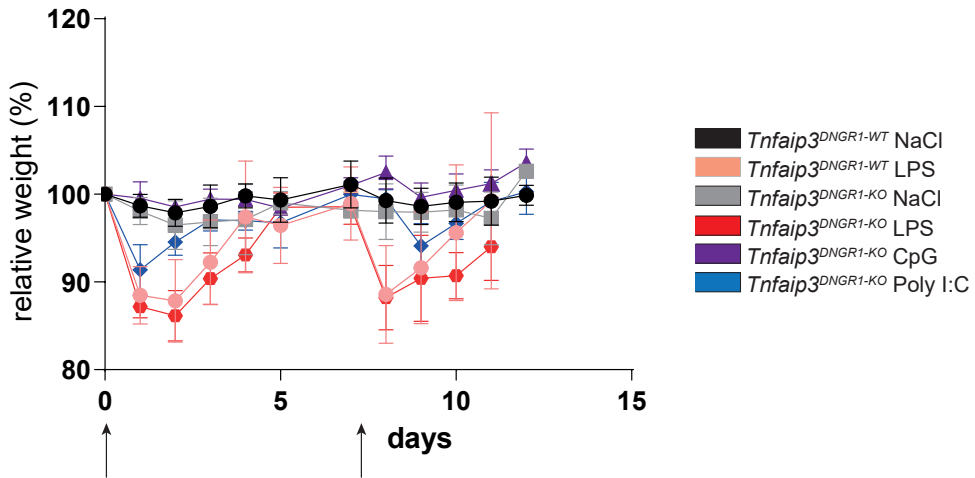
## Abbreviations

AM	Alveolar macrophages
BATF3	Basic leucine zipper transcriptional factor ATF-like 3
BMPR2	Bone morphogenetic protein receptor type 2
cDC1s	Type 1 conventional DCs
cDC2s	Type 2 conventional DCs
CTD-PAH	Connective tissue disease PAH
CXCL8	X-X-C-motif chemokine ligand 8
DCs	Dendritic cells
EvG	Elastic von Gieson
H&E	Hematoxylin and eosin
HPAH	Heritable PAH
i.p.	Intraperitoneal
i.t.	Intratracheally
IL	Interleukin
IM	Interstitial macrophages
IPAH	Idiopathic PAH
LPS	Lipopolysaccharide
LV	Left ventricle
Mo-DC	Monocyte-derived-DC
NaCl	Sodium chloride
NF- $\kappa$ B	Nuclear factor-kappa B
PAH	Pulmonary arterial hypertension
PAP	Pulmonary arterial pressure
PASMCs	Pulmonary artery smooth muscle cells
pDC	Plasmacytoid DC
PFA	paraformaldehyde
Poly I:C	Polyinosinic-polycytidylic acid high molecular weight
RV	Right ventricle
RVSP	Right ventricular systolic pressure
S	Septum
TGF $\beta$	Transforming growth factor- $\beta$
TLOs	Tertiary lymphoid organs
TLR	Toll like receptor
<i>Tnfrif3</i>	TNF $\alpha$ -induced protein-3
WHO	World health organization
WT	Wild type
$\alpha$ -SMA	Alpha smooth muscle actin

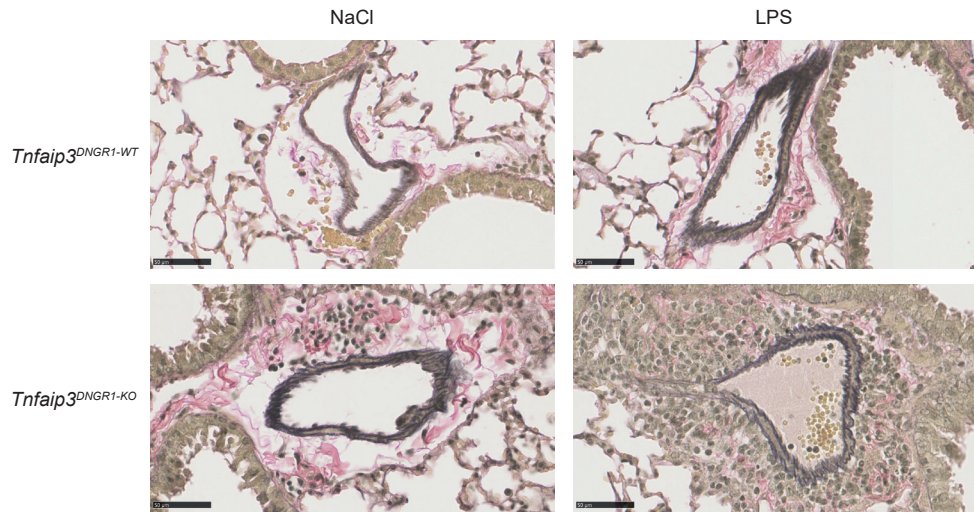
## SUPPLEMENTARY MATERIAL



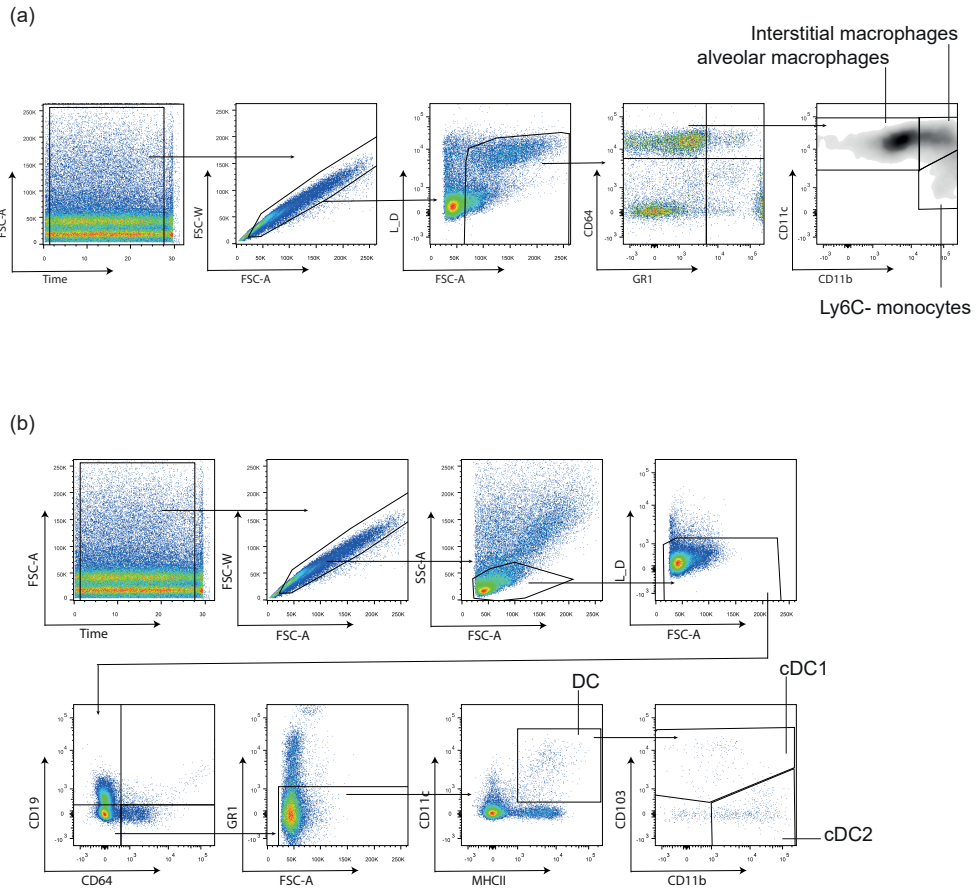
**Supplementary Figure S1.** Flow cytometry analysis in hearts of 31-week-old *Tnfaip3DNGR1-KO* mice shows increased proportions of CD45+ cells and DCs, both in right and left ventricle. Flow cytometry analysis for CD45+ cells (alive, CD45+), DCs (CD3-/CD19-, MHC-II+CD11c+), T cells (CD3+) and B cells (CD19+) in separately measured right ventricle (RV) and left ventricle (LV) cell suspensions from hearts of *Tnfaip3DNGR1-WT/KO* mice. Results are presented as mean values + standard deviation of 7-9 mice per group. \* $P < 0.05$ , \*\* $P < 0.01$ , \*\*\* $P < 0.001$ .



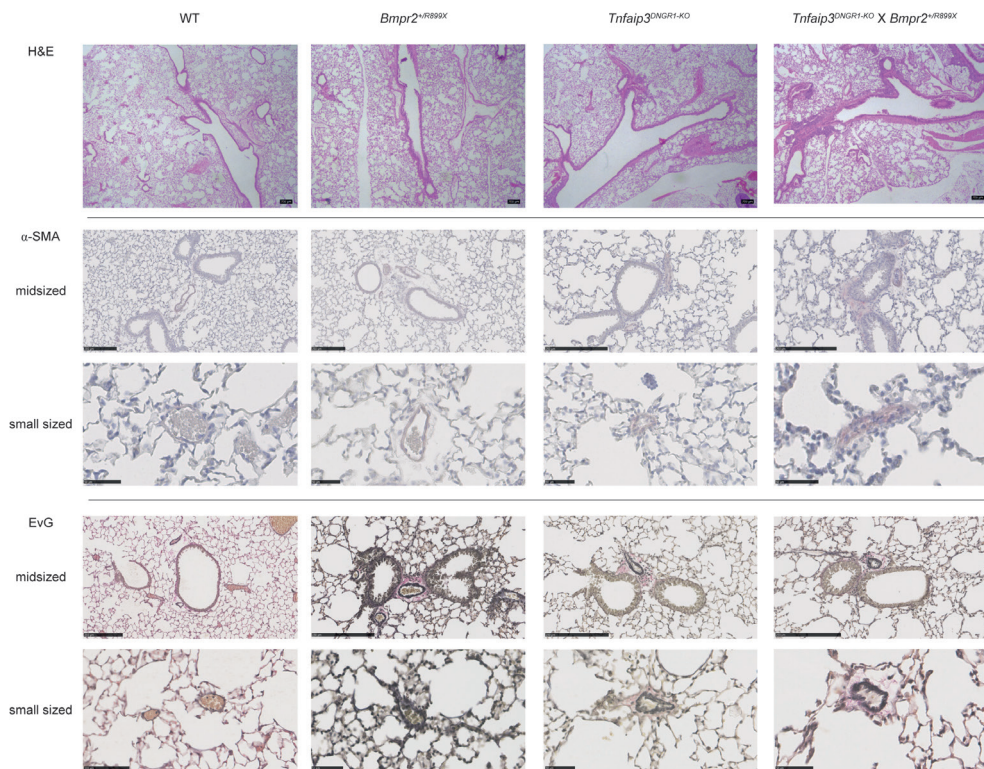
**Supplementary Figure S2.** Weight curve of TLR-exposed WT and *Tnfaip3DNGR1-KO* mice. Weight curve of WT and *Tnfaip3DNGR1-KO* mice, exposed to TLR4 ligand lipopolysaccharide (LPS), TLR3 ligand polyinosinic-polycytidylic acid (Poly I:C) or TLR9 ligand CpG. Arrows indicate moments of i.p. TLR exposure. For each mouse the weight at day 0 was set to 100%. Data are shown as mean values + standard deviations from 5-10 mice per group.



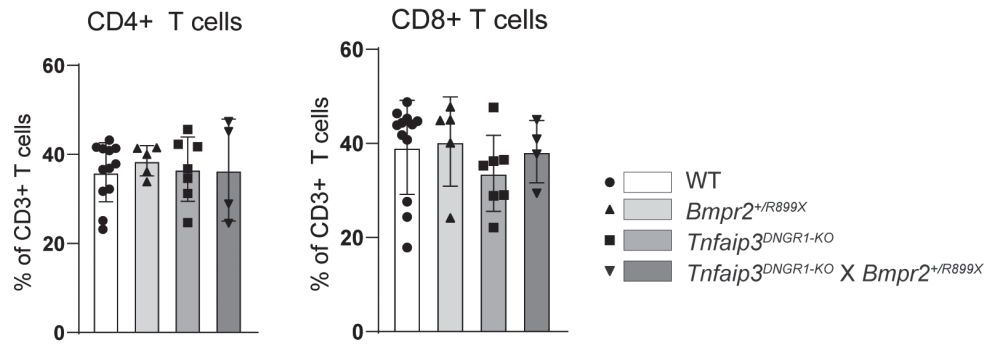
**Supplementary Figure S3.** LPS-exposure in WT and *Tnfaip3DNGR1-KO* mice leads to thickening of vessels. Elastin van Gieson (EvG) staining in lung tissue of saline- and LPS-exposed WT and *Tnfaip3DNGR1-KO* mice showing thickening of mid-sized vessels. Data shown are representative for 4-6 mice per group.



**Supplementary Figure S4.** Gating strategy for lung myeloid cell populations. (a) Flow cytometric gating of lung macrophages and Ly6C- monocytes; (b) flow cytometric gating strategy of cDC subsets in the lung.



**Supplementary Figure S5.** Remodeling of small and mid-sized vessels in *Tnfaip3*<sup>DNGRI-KO</sup>, *Bmpr2*<sup>+R899X</sup> and *Tnfaip3*<sup>DNGRI-KO</sup> X *Bmpr2*<sup>+R899X</sup>. Hematoxylin and eosin (H&E), smooth muscle acting staining ( $\alpha$ -SMA) and Elastin van Gieson (EvG) staining in lung tissue of WT, *Bmpr2*<sup>+R899X</sup>, *Tnfaip3*<sup>DNGRI-KO</sup> and *Bmpr2*<sup>+R899X</sup> X *Tnfaip3*<sup>DNGRI-KO</sup> mice. Data shown are representative for 6-8 mice per group.



**Supplementary Figure S6.** Proportions of CD4+ T cells and CD8+ T cells are similar between WT, *Tnfaip3DNGR1-KO*, *Bmpr2*<sup>+/*R899X*</sup> and *Tnfaip3DNGR1-KO* X *Bmpr2*<sup>+/*R899X*</sup> mice. Quantification of CD4+ T cells and CD8+ T cells (as proportions of total CD3+ T cells) in the lungs of the indicated mouse groups, determined by flow cytometry. Results are presented as mean + standard deviation of 4 – 12 mice per group.

**Supplementary Table 1.** RT-PCR primers.

<b>Primer</b>	<b>Sequence</b>
CD11c FW	GGCTGCAAGCATCATTTCGTT
CD11c RW	AGCCTTCCCTGGTTCCATA
BATF3 FW	CTTGTGTCAGCTTCGGTCAG
BATF3 RW	GTGTGCAAACCAAGGTTCAG
CD4 FW	CCAGCTGTCTGCTTGGATCA
CD4 RW	GCCCTCTCGTAAACTGTGCT
CD8 FW	GTTCCAGTTTCGGGGTCCAT
CD8 RW	CACCAGTCAGTGAGGGTTC
RQ GAPDH FW	TTCACCACCATGGAGAAGGC
RQ GAPDH RW	GGCATGGACTGTGGTCATGA

**Supplementary Table 2.** Monoclonal antibodies used for histology.

<b>Antibody</b>	<b>Type</b>	<b>Clone</b>	<b>Company</b>
$\alpha$ -SMA-PE	Mouse anti-human	IA4	R&D
CD11c PE	Hamster anti-mouse	N418	ThermoFisher scientific
CD3 APC-ef780	Rat anti-mouse	17A2	ThermoFisher scientific
CD8 Fite	Rat anti-mouse	53-6.7	BD
CD8	Rabbit anti-human	SP57	Ventana
CD68	Mouse anti-human	KP1	Ventana
CD206	Mouse anti-human	685645	R&D
$\alpha$ -Sma	Mouse anti-human	IA4	Ventana
MHCII-bio	Rat anti-mouse	MRC OX-6	Abcam
GFP	Rabbit anti-GFP	polyclonal	Abcam

**Supplementary Table 3.** Monoclonal antibodies used for flow cytometry.

<b>Antibody</b>	<b>Conjugate</b>	<b>Clone</b>	<b>Company</b>
CD40	PE	1C10	eBioscience
CD11c	PE-TXR	N418	Invitrogen
CD11b	PercCP-Cy5.5	M1/70	BD
GR1	PE-Cy7	RB6.8C5	eBioscience
CD64	AF647	X54-5/7.1	BD
MHCII	AF700	M5/114.15.3	eBioscience
CD19	APC-Cy7	1D3	BD
CD103	eF450	2E7	eBioscience
CD86	BV650	FUN1	BD
PD-L1	BV711	MIH5	BD
CD8	Fitc	53-6.7	eBioscience
CD19	PerCP-Cy5	eBio1D3	eBioscience
CD3	APC-Cy7	17A2	eBioscience
KI-67	FITC	SolA15	eBioscience
CD25	PercP-Cy5.5	PC61	BD
CD8	Pe-Cy7	53-6.7	eBioscience
CD62L	APC	MEL-14	eBioscience
FOXP3	AF700	FJK-16s	eBioscience
CD3	BV421	145-2c11	BD
CD44	BV650	IM7	BD
CD4	BV711	RM4-5	BD
MHCII	Biotine	M5/114.15.2	eBioscience
Streptavidin	BV786		BD
CD45	PerCP-Cy5.5	30-F11	eBioscience
CD19	APC	1D3	BD

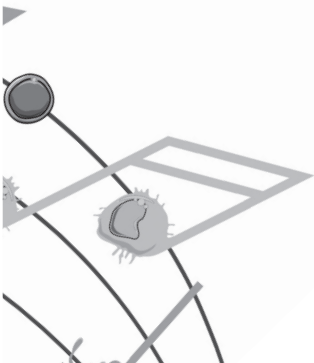


# CHAPTER 4

*Plasma markers in pulmonary hypertension subgroups correlate with patient survival.*

**T. Koudstaal**, D. van Uden, J.A.C. van Hulst, P. Heukels, I.M. Bergen, L.W. Geenen, V.J.M. Baggen, A.E. van den Bosch, L.M. van den Toorn, P.P. Chandoesing, M. Kool, E. Boersma, R.W. Hendriks, K.A. Boomars

Respir Res. 2021 May 4;22(1):137.



## ABSTRACT

### Background

Recent studies have provided evidence for an important contribution of the immune system in the pathophysiology of pulmonary arterial hypertension (PAH) and chronic thromboembolic pulmonary hypertension (CTEPH). In this report, we investigated whether the inflammatory profile of pulmonary hypertension patients changes over time and correlates with patient WHO subgroups or survival.

### Methods

50 PAH patients (16 idiopathic (I)PAH, 24 Connective Tissue Disease (CTD)-PAH and 10 Congenital Heart Disease (CHD)-PAH), 37 CTEPH patients and 18 healthy controls (HCs) were included in the study. Plasma inflammatory markers at baseline and after 1-year follow-up were measured using ELISAs. Subsequently, correlations with hemodynamic parameters and survival were explored and data sets were subjected to unbiased multivariate analyses.

### Results

At diagnosis, we found that plasma levels of interleukin-6 (IL-6) and the chemokines (C-X3-C) motif ligand CXCL9 and CXCL13 in CTD-PAH patients were significantly increased, compared with HCs. In idiopathic PAH patients the levels of tumor growth factor- $\beta$  (TGF $\beta$ ), IL-10 and CXCL9 were elevated, compared with HCs. The increased CXCL9 and IL-8 concentrations in CTEPH patients correlated significantly with decreased survival, suggesting that CXCL9 and IL-8 may be prognostic markers. After one year of treatment, IL-10, CXCL13 and TGF $\beta$  levels changed significantly in the PAH subgroups and CTEPH patients. Unbiased multivariate analysis revealed clustering of PH patients based on inflammatory mediators and clinical parameters, but did not separate the WHO subgroups. Importantly, these multivariate analyses separated patients with <3 years and >3 years survival, in particular when inflammatory mediators were combined with clinical parameters.

### Discussion

Our study revealed elevated plasma levels of inflammatory mediators in different PAH subgroups and CTEPH at baseline and at 1-year follow-up, whereby CXCL9 and IL-8 may prove to be prognostic markers for CTEPH patients. While this study is exploratory and hypothesis generating, our data indicate an important role for IL-8 and CXCL9 in CHD and CTEPH patients considering the increased levels serum and the observed correlation with survival.

### Conclusion

In conclusion, our studies identified an inflammatory signature that clustered PH patients into WHO classification-independent subgroups that correlated with patient survival.

## INTRODUCTION

Pulmonary hypertension (PH) is a debilitating disease characterized by structural remodeling of the arterial vasculature of the lung leading to increased vascular resistance and increased pulmonary arterial pressures, right ventricular (RV) hypertrophy, heart failure and ultimately, death (2). In pulmonary arterial hypertension (PAH) patients, endothelial cell proliferation along with concurrent neoangiogenesis, when exuberant, results in the formation of glomeruloid structures in pulmonary arterioles known as the plexiform lesions (18, 38, 176, 227). PH is a heterogeneous disease, subdivided into five subgroups according to the WHO ERS/ESC classification (2). Currently, PH-specific drugs are used to treat patients with PAH (WHO subgroup 1 PH) and inoperable chronic thromboembolic pulmonary hypertension (CTEPH) (WHO subgroup 4 PH), in contrast to WHO groups 2, 3 and 5, in which only the underlying diseases can be treated (2). However, even with PH-specific treatment strategies, survival remains poor with a mean 5-year survival of ~60% for PAH (20, 21) and CTEPH patients (21-23).

Over the years, accumulating evidence points to a pathological role for the immune system in PAH and CTEPH (24, 86, 215). Lungs of idiopathic PAH (IPAH) patients (belonging to WHO subgroup 1 PH) display an increased inflammatory mark consisting of T and B lymphocytes, mast cells, dendritic cells and macrophages (33, 87). Furthermore, activation of B lymphocytes and circulating auto-antibodies were found in PAH patients (100-102). Thrombotic lesions in CTEPH patients contain activated T and B lymphocytes, macrophages and neutrophils and patients display elevated levels of circulating cytokines and chemokines (32, 36). These inflammatory mediators can contribute directly to recruitment of immune cells, activation and proliferation of pulmonary arterial smooth muscle cells, and endothelial dysfunction. A very recent unbiased whole-blood transcriptome analysis in PAH patients and healthy controls (HCs) (228) identified a signature of 507 PAH-associated genes, in which T cell signaling, phosphoinositide 3-kinase (PI3K) signaling in B lymphocytes and interleukin-6 (IL-6) signaling were among the top canonical pathways.

In cross-sectional studies of PAH patients, increased IL-6, IL-8 and IL-10 in serum correlated with reduced survival and quality of life (94, 121). Increased levels of circulating pro-inflammatory cytokines were also found in CHD-PAH and CTD-PAH (109, 113, 114). In an unsupervised analysis of blood cytokine profiles of PAH patients, different immune phenotypes were distinguished with different clinical risk profiles, independent of WHO PH subgroups (122). Accumulating evidence supports a major role for IL-6, considering that IL-6 receptor (IL-6R) expression and signalling is crucial for PAH development and progression (129) and that circulating IL-6 associates with specific clinical phenotypes and outcomes in various PAH subgroups (229). Increased transforming growth factor (TGF) $\beta$  receptor signalling and decreased Bone morphogenetic protein receptor type II (BMPRII) signalling were shown to contribute to PAH pathogenesis (230).

Serum of PAH patients contains increased levels of the CXCL9 chemokine, which is involved in the differentiation of IFN $\gamma$ -producing T-helper 1 (Th1) cells expressing its receptor CXCR3 (122, 231). Likewise, in PAH and CTEPH serum samples and lung tissue an increase was found of CXCL13 (232), which is implicated in the organization of B cells in follicles and germinal centers because its receptor is expressed on B cells and follicular T-helper cells. Levels of *vascular endothelial growth factor* (VEGF) are increased in PAH patients during treatment and are associated with risk of death and hospitalization at 16-week follow-up (115).

Nevertheless, many questions remain unanswered. Currently, limited data are available on the levels of cytokines or chemokines in treatment-naïve patients, particularly in CTEPH, on changes in cytokine and chemokine levels during follow-up and on the possible correlation of inflammatory marker signatures with prognosis. Therefore, our aim was to study circulating inflammatory markers in PAH and CTEPH patients at diagnosis and at 1-year follow up. To the best of our knowledge, our study is the first to investigate different subgroups of PAH and CTEPH patients together. We performed unsupervised clustering of inflammatory profiles and correlated these to transplant-free survival.

## MATERIALS AND METHODS

### Patients and study design

This prospective observational cohort study was conducted between May 2012 and July 2019. PH patients >18 years old with a mean pulmonary arterial pressure (mPAP)  $\geq$  25mmHg, a wedge pressure  $\leq$ 15 mmHg and a PVR  $\geq$  3WU measured by right heart catheterization were invited to take part in the study at diagnosis and a large majority agreed (1). PAH and CTEPH patients were diagnosed according to the ERS/ECSC guidelines (2). Patients were subdivided according to the World Health Organization (WHO) classification in 16 idiopathic PAH (IPAH), 24 connective tissue disease-associated PH (CTD-PAH), 10 congenital heart disease-associated PH (CHD-PAH) and 37 CTEPH (Table 1) (1, 2).

Similar to prior work from our group (233), exclusion criteria were incomplete diagnostic work-up and therefore no confirmed PH diagnosis, not treatment-naïve, age <18 years, or not capable of understanding or signing informed consent. The study protocol was approved by the medical ethical committee. A written informed consent was provided by all patients. This study was performed conform the principles outlined in the Declaration of Helsinki.

**Table 1. Demographic and patient characteristics.**

	<b>IPAH (n= 16)</b>	<b>CTD-PAH (n= 24)</b>	<b>CHD-PAH (n= 10)</b>	<b>CTEPH (n=37)</b>	<b>HC (n=18)</b>	<b>p Value</b>
<b>Baseline clinical characteristics</b>						
Gender, female (%)	12 (75%)	21 (88%)	4 (40%)	20 (54%)	9 (50%)	
Age, y	54.3 $\pm$ 17.2	63.6 $\pm$ 11.8	41.0 $\pm$ 17.7	61.4 $\pm$ 14.2	31.6 $\pm$ 9.9	<0.0001
BMI, kg/m <sup>2</sup>	27.7 $\pm$ 8.0	27.1 $\pm$ 4.4	23.7 $\pm$ 4.8	28.8 $\pm$ 6.0		0.16
NYHA class 3-4, n (%)	12 (75%)	15 (63%)	3 (30%)	17 (46%)		
6MWT, m	350 $\pm$ 135	333 $\pm$ 122	426 $\pm$ 173	379 $\pm$ 129		0.35
NT-pro BNP, pmol/L	317 $\pm$ 467	519 $\pm$ 1037	65 $\pm$ 88	127 $\pm$ 199		0.07
<b>Underlying CTD</b>						
SSc, n (%)		20/24 (83%)				
SLE, n (%)		4/24 (17%)				
<b>Baseline right heart catheterization</b>						
mPAP, mmHg	58.9 $\pm$ 16.5	41.5 $\pm$ 12.5	43.11 $\pm$ 14.9	40.1 $\pm$ 12.6		0.0001
mRAP, mmHg	11.9 $\pm$ 6.7	10.4 $\pm$ 6.0	10.8 $\pm$ 6.2	9.6 $\pm$ 7.1		0.72

	<b>IPAH</b> <b>(n= 16)</b>	<b>CTD-PAH</b> <b>(n= 24)</b>	<b>CHD-PAH</b> <b>(n= 10)</b>	<b>CTEPH</b> <b>(n=37)</b>	<b>HC</b> <b>(n=18)</b>	<b>p Value</b>
Capillary wedge pressure, mmHg	9.2 ±4.2	12.9 ±8.1	14.5 ±6.6	12.3 ±4.5		0.21
PVR, wood units	10.6 ±3.9	6.0 ±3.5	4.3 ±2.9	5.3 ±3.4		0.0002
<b>PH-Medication</b>						
At baseline, n (%)	0/16 (0%)	0/24 (0%)	0/10 (0%)	0/37 (0%)		
At 1 year follow up						
No PH-medication	0/13 (0%)	0/11 (0%)	2/6 (33%) <sup>3</sup>	3/19 (16%) <sup>5</sup>		
Mono therapy, n (%)	1/13 (8%) <sup>1</sup>	1/11 (9%) <sup>2</sup>	1/6 (17%) <sup>4</sup>	11/19 (58%)		
Duo therapy, n (%)	6/13 (46%)	9/11 (82%)	3/6 (50%)	5/19 (26%)		
Triple therapy, n (%)	6/13 (46%)	1/11 (9%)	0/6 (0%)	0/19 (0%)		
<b>Immunomodulatory drugs</b>						
At baseline, n (%)	0/16 (0%)	3/24 (13%)	0/10 (0%)	0/37 (0%)		
At 1 year follow up, n (%)	0/13 (0%)	3/11 (27%)	0/6 (0%)	0/19 (0%)		
<b>Survival</b>						
Death/lung transplant <3 years	2 (12.5%)	8 (33.3%)	0 (0%)	6 (16.2%)		
Death/lung transplant >3 years	2 (12.5%)	0 (0%)	3 (30%)	2 (5.4%)		

Data given as 'mean, ±SD', unless otherwise indicated.

**Abbreviations:** BMI, body mass index; CTEPH, chronic thromboembolic pulmonary hypertension; PAH, pulmonary arterial hypertension; IPAH, idiopathic pulmonary arterial hypertension; CHD, congenital heart disease; CTD, connective tissue disease; 6MWT, 6-minute walk test; NT-pro BNP, The N-terminal prohormone of brain natriuretic peptide; SSc, systemic sclerosis; SLE, systemic lupus erythematosus; mPAP, mean pulmonary arterial pressure; mRAP, mean right atrium pressure; PVR, pulmonary vascular resistance; RV, right ventricle; RA, right atrium; RVSP, right ventricular systolic pressure.

<sup>1</sup>: This IPAH patient was on ERA monotherapy, due to severe side-effects on PDE5 therapy.

<sup>2</sup>: This CTD-PAH patient was on PDE5 monotherapy due to severe side-effects on ERA therapy

<sup>3</sup>: These CHD-PAH patients were not started on PAH-medication immediately, since in one patient a possible effect of a surgical correction was awaited, and the other patient was started on medication after one-year since she had persistent PAH

<sup>4</sup>: This CHD-PAH patient was on PDE5 monotherapy since the PAH was mild.

<sup>5</sup>: these CTEPH patients were not started on PH-medication since they underwent a pulmonary endarterectomy.

## Clinical data collection

Clinical data were collected during the inpatient screening visit for analysis of PH (233). All patients underwent physical examination by a cardiologist and a pulmonary physician, 6-minute walking test, spirometry, VQ scan, chest computed tomography scan, 12-lead electrocardiography (ECG), echocardiography, venous blood sampling and right heart catheterization. Patient characteristics and vital signs were collected, including age, sex, height, weight, systemic blood pressure, heart rate and peripheral oxygen saturation. The New York Heart Association (NYHA) functional class was used to grade the severity of functional limitations by the presence of signs and symptoms of heart failure. During right heart catheterization, a Swan-Ganz catheter was inserted in the internal jugular vein. A standardized protocol for the work-up of PH was used to obtain hemodynamic measurements

and thermodilution or Fick's principle was used to measure cardiac output (2). If the obtained capillary wedge pressure was ambiguous, a fluid challenge was performed to distinguish pre-capillary PH from PH due to left heart disease. Data were collected and stored in PAHTool (version 4.3.5947.29411, Inovoltus, Santa Maria da Feira, Portugal), an online electronic case report form.

### **Clinical follow-up and definition of endpoints**

Patients were treated according to the ERS/ESC guidelines (2) and prospectively followed-up by half-yearly scheduled visits to the outpatient clinic. CTEPH patients were assessed for eligibility for either a pulmonary endarterectomy or a balloon pulmonary angioplasty. In our CTEPH cohort, 7 patients underwent a pulmonary endarterectomy treatment in the period following after the baseline blood sampling. Patients who underwent one of the above procedures were not censored afterwards. The primary composite endpoint was defined as all-cause mortality or lung transplantation. Patients were continuously included in our study, with a mean follow-up duration of 39.5 months.

### **Inflammatory cytokine and chemokine assessment**

At baseline and at every half-yearly follow-up visit (up to 10-year follow-up), peripheral venous blood samples were collected and processed within 2 hours by Ficoll separation and divided into plasma and peripheral blood mononuclear cells (PBMCs) fractions. Plasma samples were subsequently stored at -80 degrees.

The concentrations of inflammatory markers (VEGF-A, TGF $\beta$ , CXCL-9, CXCL-13, IL-1 $\beta$ , IL-6, IL-8, IL-10) in plasma were determined in duplicate by ELISA (R&D systems Europe, Abingdon, UK) (**Supplementary Table 1**). Streptavidin-HRP (eBioscience) and tetramethylbenzidine (TMB) substrates (eBioscience) were used to develop the ELISA. Optical densities were measured at 450 nm using a Microplate Reader (Bio-Rad, Hercules, CA, USA).

### **Statistical analysis, principal component analysis and multiple factor analysis**

Statistical evaluation of baseline cytokine and chemokine measurements in IPAH, CTD-PAH, CHD-PAH and CTEPH patients was performed using a Kruskal Wallis test. Next, we compared multiple groups using Dunn's multiple comparison test, leading to separate P values for each comparison between two subgroups. Paired baseline and 1-year follow-up cytokine data were analyzed using a Wilcoxon signed rank test. The Kaplan-Meier method was applied to estimate the cumulative primary endpoint-free survival (based on all-cause mortality or lung transplantation) function. All statistical tests were two-sided and p-values <0.05 were considered statistically significant. Statistical analyses were performed using Prism (GraphPad Software, La Jolla, CA, USA) or SPSS version 24.

Principal component analysis (PCA) and multiple factor analysis (MFA) were performed using R and RStudio, and the packages FactoMineR and Factoextra (234). Missing data were imputed using the R package MissMDA (235). Missing variables were imputed using the R package. Only imputed variables with a small area of variability and thereby high credibility in the multiple imputation method were used for analysis. Prior to PCA and MFA analysis ELISA data were log<sub>10</sub> transformed to better fit a normal distribution and were scaled. Contribution of the variables to the PCs was determined in percentages by (squared cosine of the variable\*100) / (total squared cosine of the principal component).

The number of dimensions to be interpreted were determined by the R package FactoInvestigate. Dimensions with an inertia higher than the inertia obtained by a random distribution, therefore providing the best representation of the data variability, were considered. Patients were labelled by  $\geq 3$ -year survival or deceased/transplanted  $< 3$  years after diagnosis to determine clustering of individuals on the first and second PCs.

The variability explained by the PCA was tested for statistical significance by inertia of the first two dimensions using the R package FactoInvestigate. Separation of HC, PAH and CTEPH patients was tested using a 1way ANOVA test with a Kruskal Wallis test combined with a Dunn's multiple comparison test of Dim1 and/or Dim2 coordinates in Prism. Statistical evaluation of separation between  $\geq 3$ -year survival or deceased/transplanted  $< 3$  years after diagnosis in PCAs and MFAs was tested using a Mann-Whitney U test of Dim1 coordinates of alive versus deceased/transplanted individuals in Prism.

## RESULTS

### Analysis of inflammatory mediators in treatment-naïve PAH and CTEPH patients at diagnosis

Fifty PAH patients (16 IPAH, 24 CTD-PAH and 10 CHD-PAH), 37 CTEPH patients and 18 healthy controls (HC) were included (Table 1). Plasma from patients at diagnosis and HCs were analyzed for the cytokines IL-1 $\beta$ , IL-6, IL-8, IL-10 and TGF $\beta$ , the chemokines CXCL9 and CXCL13 and VEGF (Figure 1). Compared with HCs, plasma levels of IL-6 and IL-10 were significantly elevated in CTD-PAH and IPAH patients, respectively. TGF $\beta$  was significantly increased in both IPAH and CHD-PAH patients. The CXCL9 chemokine was elevated in IPAH, CTD-PAH and CTEPH patients, whereas CXCL-13 was only increased in CTD-PAH patients, when compared with HCs. No significant differences between HCs and any of the four patient groups were observed for IL-1 $\beta$ , IL-8 and VEGF.

In summary, at diagnosis we found significantly increased plasma levels of IL-10, TGF $\beta$ , and CXCL9 in IPAH patients, of IL-6, CXCL9 and CXCL13 in CTD-PAH patients, and of CXCL9 in CTEPH patients.

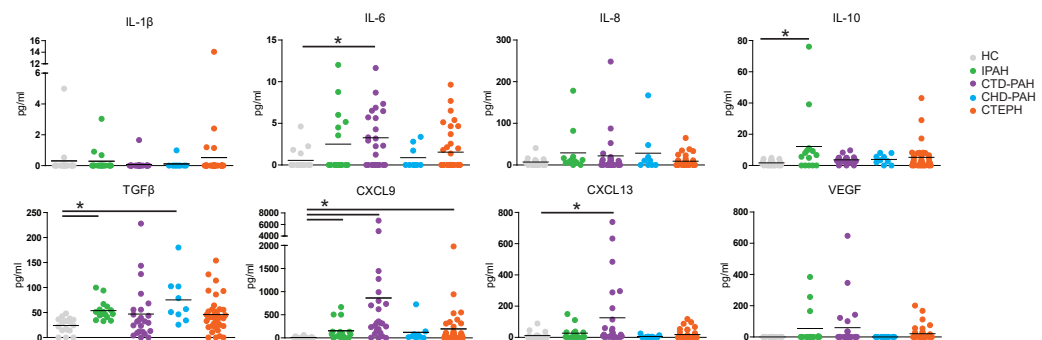


**Figure 1. Inflammatory markers in plasma of treatment-naïve PAH and CTEPH patients at diagnosis.**

The indicated inflammatory markers were measured in plasma samples from 50 PAH patients (16 IPAH, 24 CTD-PAH and 10 CHD-PAH), 37 CTEPH patients at diagnosis and 18 healthy controls (HC) by ELISA. Data are shown as symbols for individual patients or HCs; horizontal bars represent mean values. Statistical analysis was performed using a Kruskal-Wallis test combined with a Dunn's multiple comparison test. \* =  $p < 0.05$ .

## Correlation of inflammatory mediators at diagnosis with hemodynamic parameters and survival

We did not find significant relations between plasma levels of inflammatory mediators at baseline and hemodynamic parameters including pulmonary arterial pressure (mPAP), mean right atrial pressure (mRAP), pulmonary vascular resistance (PVR) and N-terminal pro B-type natriuretic peptide (NT-pro BNP), consistent with reported findings in a cross-sectional study (94) (data not shown).

Next, we explored potential correlations between inflammatory markers and patient survival by Kaplan-Meier analyses, whereby for each patient group two subgroups were defined with above or below median values for the inflammatory marker. At the time of censoring (mean follow-up duration of 39.5 months), 22 out of 87 patients had died without undergoing lung transplantation and two patients had received a lung transplantation. When we analyzed survival (all-cause mortality and/or lung transplantation), significant differences were found for IL-8 and CXCL9. CHD-PAH and CTEPH patients with high levels of IL-8 at baseline showed a significantly reduced survival compared with IL-8<sup>low</sup> patients ( $p=0.013$  and  $p=0.016$ , respectively; **Figure 2A**). Similar results were obtained when we compared CXCL9<sup>high</sup> and CXCL9<sup>low</sup> patients, whereby significance was reached for CTEPH but not for CHD-PAH patients ( $p=0.011$  and  $0.083$ , respectively) (**Figure 2B**). In IPAH and CTD-PAH patients, no significant differences were found (**Suppl. Fig. 1**). A similar analysis for time to clinical worsening (TTCW), defined as >15% decline in 6mwt, admission to the hospital for PH related complications, or the need for increase of PH specific medication or the start of increase of diuretics) only revealed a significant difference for CXCL9 in CTEPH patients (data not shown).

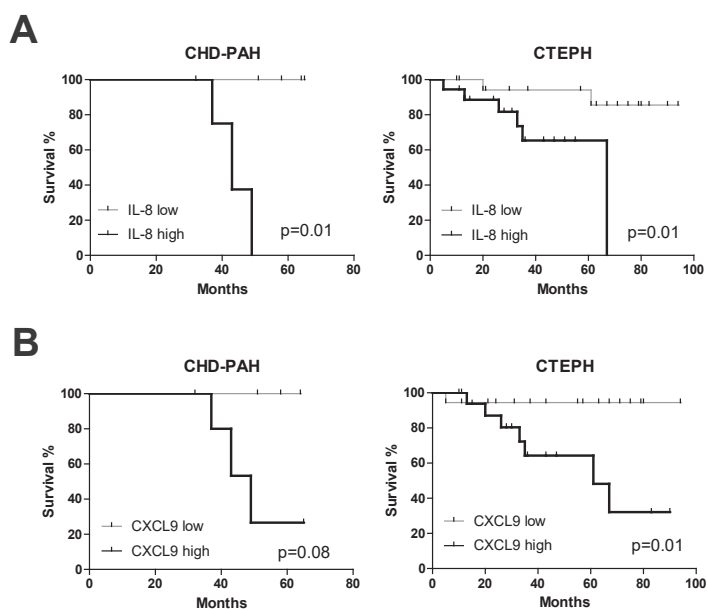


**Figure 2. Effects of IL-8 and CXCL9 plasma levels on patient survival.**

Kaplan-Meier survival analyses for (A) IL-8-high/low subgroups and (B) CXCL9-high/low of the indicated WHO PH patient subgroups. Statistical analysis was performed using a log-rank (Mantel-Cox) test and a Gehan-Breslow-Wilcoxon test. *P* values are shown for the (Mantel-Cox) test.

### Comparison of inflammatory mediators at diagnosis and at 1-year follow-up

To follow circulating inflammatory mediators over time, plasma levels were measured at 1-year follow-up in 31 PAH patients (13 IPAH, 11 CTD-PAH and 6 CHD-PAH) and 19 CTEPH patients and compared to their baseline values. For IL-1b, IL-6, IL-8, CXCL-9 and VEGF, no significant changes were found for any of the four patient groups (shown for IL-1b and IL-6 in **Suppl. Fig. 2**). Strikingly, a significant increase in IL-10 and TGFβ at 1-year follow-up compared to baseline was observed in CTD-PAH patients (**Figure 3A,B**). CTEPH patients showed a significant decrease in TGFβ levels. CXCL-13 was significantly decreased after 1-year follow-up in IPAH patients only (**Figure 3C**).

Only CXCL9 after 1-year follow up showed a significant correlation with survival in CTEPH patients (**Figure 3D**). For the other inflammatory markers or the delta values (difference between 1-year follow-up and baseline values) no significant changes were observed (data not shown).

Taken together, these results show that although in PH patients plasma levels of IL-1b, IL-6, IL-8, CXCL-9 and VEGF were dynamic, we did not observe a significant increase or decrease in any of the patient groups. By contrast IL-10, CXCL13 and TGFb showed disease group-specific changes at 1-year follow-up compared with baseline.

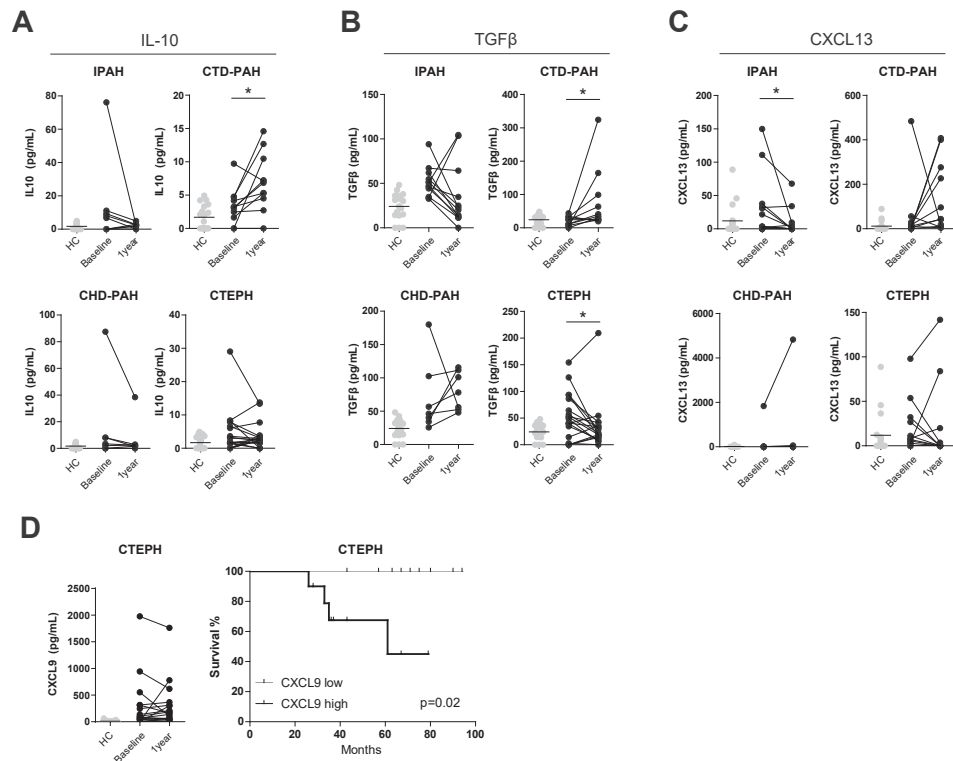


**Figure 3. Inflammatory markers in plasma of PAH and CTEPH patients at diagnosis and 1-year follow up.** (A-C) Paired plasma concentrations for interleukin IL-10 (A), TGFβ (B) and CXCL9 (C) measured by ELISA, for a subset of patients from the indicated WHO PH subgroups, at diagnosis and at 1-year follow-up, compared with HCs. Data are shown as symbols for individual patients or HCs. (D) Paired plasma cytokine measurements by ELISA for CXCL9 at diagnosis and at 1-year follow-up for

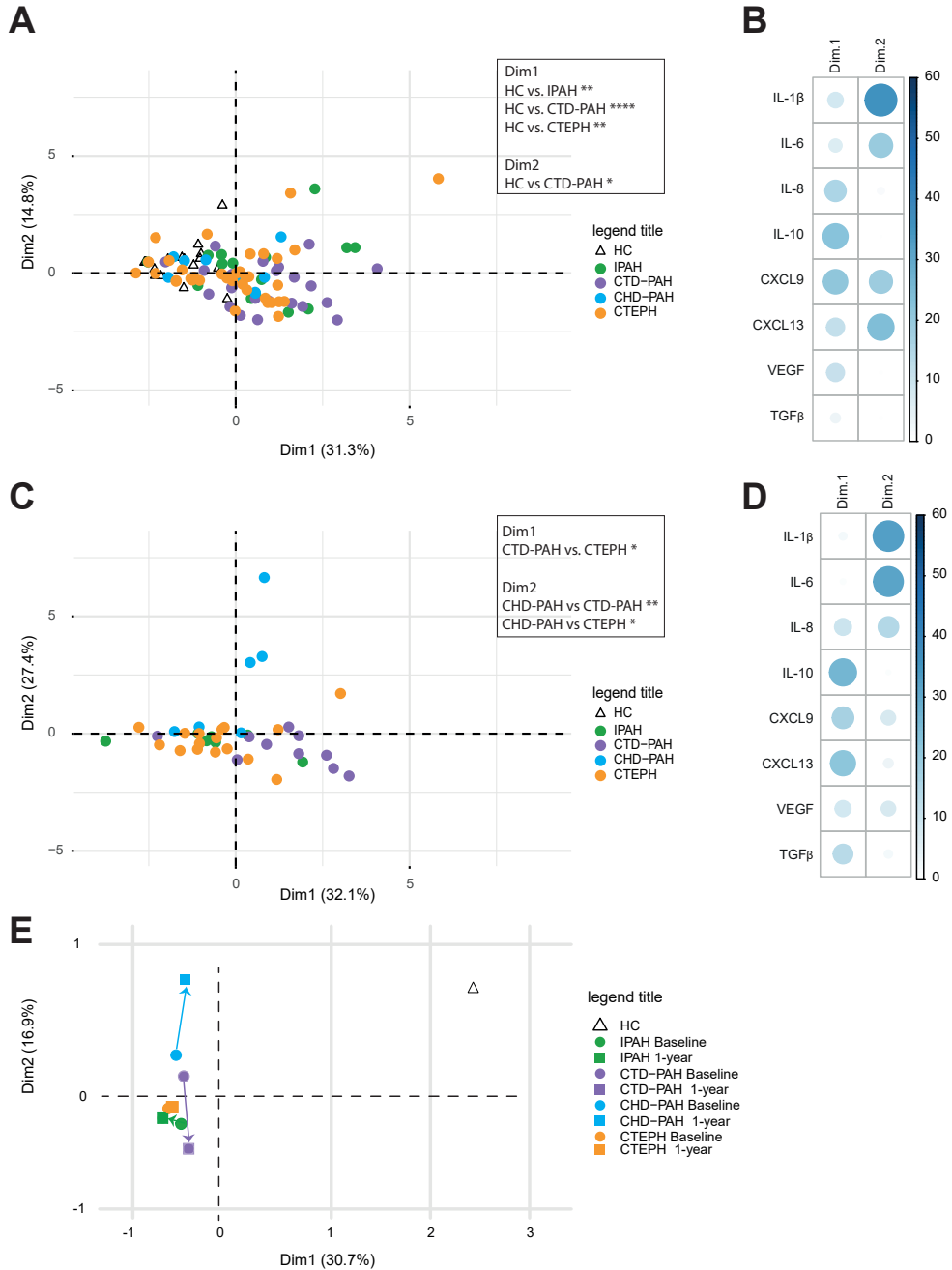
CTEPH patients and Kaplan Meyer survival analyses, starting at 12 months follow up, for CXCL9-high/low subgroups of CTEPH patients at 1-year follow up. Data are shown as symbols for individual patients or HCs; horizontal bars represent mean values; connecting lines between baseline and 1 year follow up samples indicate paired same-patient samples. Statistical analysis was performed using a Wilcoxon signed-rank test for the ELISA measurements and for the survival analysis a log-rank (Mantel-Cox) test and a Gehan-Breslow-Wilcoxon test was performed. \* =  $p < 0.05$ .

## Principal component analyses of inflammatory markers in WHO PH subgroups

To obtain a more comprehensive overview of the inflammatory marker profiles across the four patient groups and HCs, we performed principal component analyses (PCA), which reduced the dimensionality of the data set. The PCA of the eight inflammatory markers showed a non-random distribution over Dim1 and Dim2, which was not due to gender or age, and did not separate the WHO PH subgroups classified on the basis of etiology and predisposing factors (2) (**Figure 4A and data not shown**). For each WHO PH subgroup the individual patients were quite scattered over the PCA plot, whereby Dim1 revealed a modest but significant separation of HCs from IPAH, CTD-PAH and CTEPH patients (**Figure 4A**). No significance difference was found between HCs and CHD-PAH patients, consistent with our finding that CHD-PAH patients had a plasma inflammatory profile that was similar to that of HCs (**Figure 1**) except for TGF $\beta$ , which did not substantially contribute to Dim1 or Dim2 (**Figure 4B**). Whereas the impact of IL-8, IL-10 and CXCL9 was dominant in Dim1, IL-1 $\beta$ , IL-6 and the two chemokines dominated Dim2 (**Figure 4B**).

Furthermore, we performed a PCA on 1-year follow up cytokine levels. The inflammatory profile of CTD-PAH patients was separated from CTEPH patients by Dim1, to which particularly IL-10, CXCL9 and CXCL13 levels contributed (**Figure 4C,D**). Dim2 separated CHD-PAH patients from CTD-PAH and CTEPH, whereby IL-1 $\beta$  and IL-6 showed a major contribution.

To compare baseline and 1-year follow up samples for each WHO PH subgroup, we performed a PCA that included HCs and those patients for which baseline and 1-year follow up measurements were available (**Suppl. Figure 3A, B**). This PCA revealed that HCs were clearly separated from all PH subgroups, which clustered together. Subsequently, we determined and plotted the average Dim1 and Dim2 coordinates of the HCs and the two time points for each WHO PH subgroup (**Figure 4E**). This analysis revealed that for IPAH and CTEPH the differences between baseline and 1-year follow-up were limited. In contrast, CTD-PAH and CHD-PAH patients showed clear changes over time for Dim2, to which IL-1 $\beta$  contributed most (**Suppl. Figure 3A**), but in opposite directions. We did not find evidence for a normalization of the inflammatory markers towards the HC profile.



4

**Figure 4. Principal component analysis of inflammatory markers in plasma of PAH and CTEPH patients.**

(A-D) Unsupervised principal component analysis (PCA) of inflammatory markers, measured by ELISA, in plasma of healthy controls (HC) and the indicated WHO PH patient subgroups at diagnosis (A,B) and at 1-year follow-up (C,D). PCAs were on log10-transformed and scaled concentrations values; each symbol point represents an individual patient or HC sample (A,C). Representation of the contribution in percentages of the variables on the first (Dim.1) and second (Dim.2) principal component at

diagnosis (B) and at 1-year follow-up (D). The blue color range indicates the contribution to the principal components. (E) PCA plot of average coordinates of Dim1 and Dim2 for the indicated WHO PH patient subgroups. Arrows between the dots represent the PC change from diagnosis to 1-year follow up. Statistical analysis was performed by a one-way ANOVA (Kruskal-Wallis test) combined with a Dunn's multiple comparison test. \* =  $p < 0.05$ , \*\* =  $p < 0.01$ .

## Inflammatory profile and clinical parameters correlate with PH patient survival

We aimed to explore whether the inflammatory profiles would correlate with survival, independent of WHO subgroup classification. We first performed a PCA without including HCs. The obtained pattern was quite similar to the one that did include HCs, both regarding the weak separation between CHD-PAH and the other three PH subgroups (**Figure 5A**; compare with **Figure 4A**) and the inflammatory mediators that contributed most to Dim1 and Dim2 (**Suppl. Figure 4A**; compare with **Figure 4B**). To link inflammatory profiles to survival, patients were divided into two subgroups defined by  $>3$  years survival after diagnosis or  $<3$  years survival or lung transplant within 3 years after diagnosis. These two survival subgroups were significantly separated in the PCA based on Dim1 ( $p = 0.0083$ ; **Figure 5A,D**) in which the impact of IL-8, IL-10 and CXCL9 was dominant (**Suppl. Figure 4A**).

In parallel, a PCA was performed using four clinical parameters including mPAP, mRAP, PVR and NT-proBNP, resulting in significant separation of IPAH versus CTD-PAH and CTEPH, and a significant clustering of survival subgroups in Dim1, which was dominated by mPAP and PVR ( $p = 0.00014$ ; **Figure 5B, D**; **Suppl. Figure 4B**). Finally, a multiple factor analysis (MFA) was performed using both clinical and inflammatory parameters, which resulted in a significant separation of IPAH and CTEPH patients in Dim1 and of IPAH and CTD-PAH patients in Dim2 (**Figure 5C**). Importantly, the combination of parameters yielded the best separation of the two survival groups in Dim1 ( $p = 0.000037$ ) with a large impact of mPAP, PVR, CXCL9 and CXCL13 (**Figure 5C,D**).

Since CTEPH patients have a better prognosis than PAH patients (21-23), we additionally performed the PCA and MFA analyses with PAH patients only. Again, the two survival groups were separated in Dim1, which reached significance in the PCA for inflammatory markers ( $p = 0.0098$ ) and in the MFA for the combination of clinical and inflammatory markers ( $p = 0.017$ ) (**Suppl. Figure 5A**; **Figure 5E**). Hereby, the dominant mediators in Dim1 were similar to those in the analyses above that did include CTEPH patients (**Suppl. Figure 4C**). In the combined MFA CXCL9, mRAP and NT pro BNP had the largest contribution to Dim1 (**Figure 5E**).

In the PCA and MFA analyses of either PAH and CTEPH patients combined or in PAH patients alone, Dim2 was not able to significantly separate survival groups (**Suppl. Figure 5D,E**).

Taken together, these findings show that multivariate data analysis using a combination of inflammatory markers and clinical parameters most robustly clustered PH patients into WHO classification-independent subgroups that significantly correlated with patient survival.

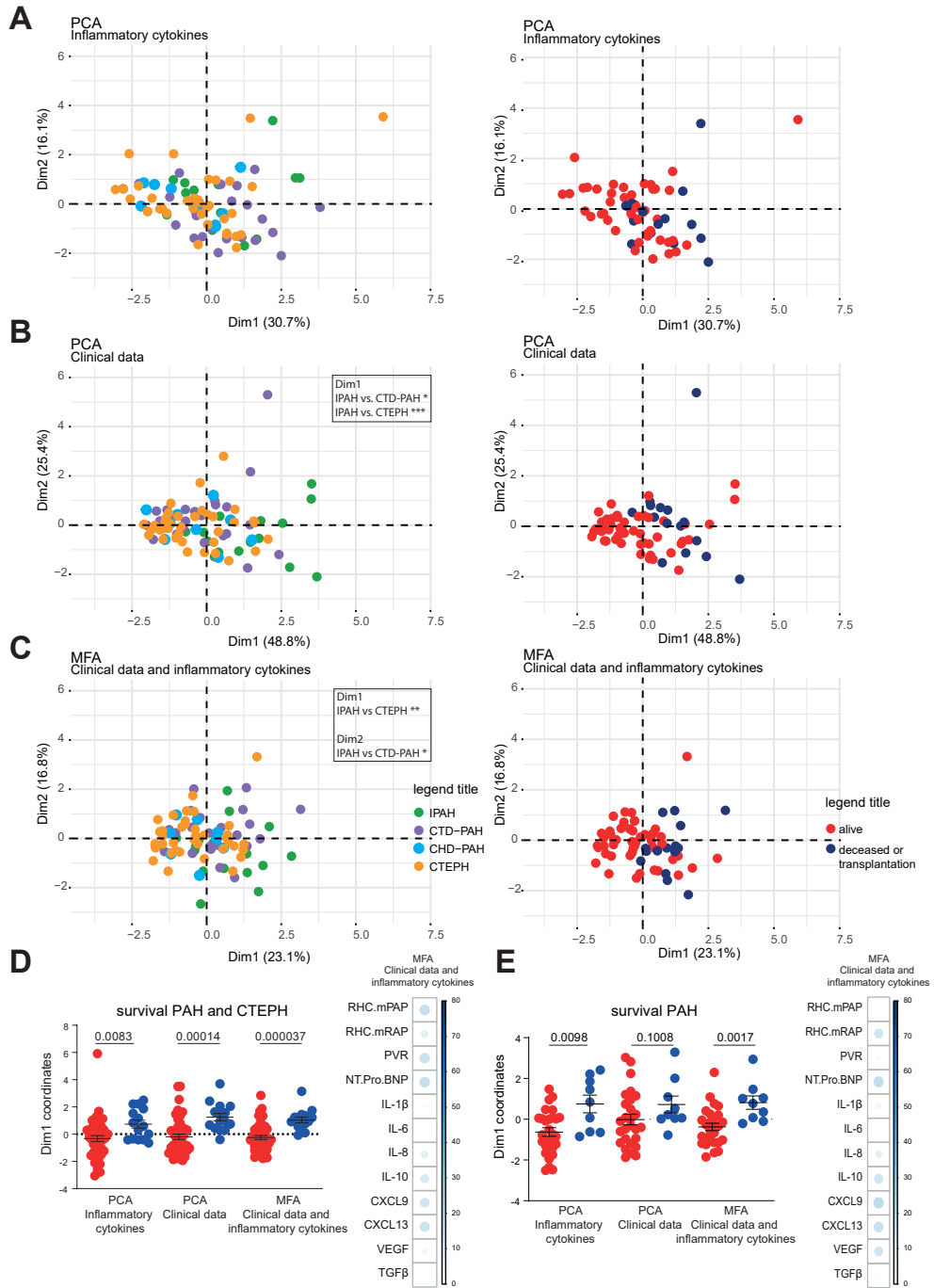


**Figure 5. PAH and CTEPH patients cluster based on survival in multivariate analyses.** (A,B) Unsupervised principal component analysis (PCA) of inflammatory markers measured by ELISA in plasma (A) and of clinical parameters (B), showing the indicated WHO PH patient subgroups (*left*) or subgroups of survival of >3 years (alive) or <3 years (deceased/transplantation) (*right*). (C) Multiple factor analysis (MFA) combining clinical data and log10 transformed and scaled

plasma inflammatory marker concentrations, showing the indicated patient subgroups (*left*) or survival of >3 years (alive) or <3 years (deceased/transplantation) (*right*). (D,E)

Dim1 coordinate values showing the separation between survival of >3 years (alive) or <3 years (deceased/transplantation) for the indicated PCAs and MFAs of PAH and CTEPH patients (D) or PAH patients alone (E) and contribution of the variables for Dim1 to the MFA. Statistical analysis was performed by a *one-way* ANOVA (Kruskal-Wallis test) combined with a Dunn's multiple comparison test. \* =  $p < 0.05$ , \*\* =  $p < 0.01$ , \*\*\* =  $p < 0.001$ . Separation between survival groups was evaluated using a Mann-Whitney U test on principal component 1 coordinates of alive versus deceased/transplantation. P values are indicated.

## DISCUSSION

We investigated inflammatory markers at different time-points in PAH and CTEPH patients, performed unsupervised clustering by PCA and correlated inflammatory profiles to transplant-free survival. We found significantly increased plasma levels of IL-10, TGF $\beta$ , and CXCL9 in IPAH patients, of IL-6, CXCL9 and CXCL13 in CTD-PAH patients, and of CXCL9 in CTEPH patients at diagnosis. Our analyses revealed lower levels of several circulating cytokines in our IPAH patients at diagnosis compared to previous reports of cross-sectional data (94, 108). Possibly, this is indicative for existing heterogeneity between patients, different pathophysiological changes over time during disease progression or therapeutic effects due to PAH-specific therapy.

In CTD-PAH patients IL-10 and TGF $\beta$  levels increased significantly compared to baseline levels after one year of therapy. Likewise, CXCL13 levels in IPAH patients decreased significantly compared to baseline levels. Our multivariate analyses suggested that the inflammatory profile changes over time: in CHD-PAH patients Dim2 shifted in the direction of the HC, whereas in CTD-PAH patients Dim2 shifted away from HCs. This may be linked to therapy or due to the natural course of pathophysiology in these patients. In this context, it is of note that there is growing evidence for anti-inflammatory and anti-aggregation activity of the phosphodiesterase type 5 inhibitor sildenafil (236). Nevertheless, we did not find correlations between changes in cytokine or chemokine levels over time and patient survival, indicating that these changes are most probably not prognostic for disease outcome.

In CTEPH patients, high levels of CXCL9 and IL-8 at baseline correlated with decreased survival. CXCL9 is a known regulator of immune cell migration, differentiation and activation and is required for optimal Th1 cell differentiation and IFN $\gamma$  production by T cells *in vivo* (231). The receptor for CXCL9 is CXCR3, which is a marker for Th1 cells and IFN $\gamma$ -producing Th17 cells, also known as Th17.1 cells (237). Previous research has shown that PAH patients display Th17 cell immune polarization (195). Possibly, by endovascular triggers in CTEPH, CXCL9 is upregulated for the recruitment of cytotoxic lymphocytes, natural killer cells and macrophages. Moreover, CXCL9 is known to be involved in activation of immune cells in response to IFN $\gamma$ . CXCL9 may prove to be a biomarker reflecting pathological involvement of the immune system in CTEPH patients.

Similar to CXCL9, also IL-8, a known chemokine produced by macrophages and other cell types such as epithelial cells, showed a negative correlation with survival in CTEPH patients. In contrast to CXCL9, which is a natural inhibitor of angiogenesis, IL-8 is a pro-angiogenic factor also known as a chemoattractant for immune cells to the site of endovascular damage. Previous studies have shown increased levels of IL-8 in CTEPH patients on treatment (32, 111, 112). To the best of our knowledge, our study is the first to show that – although high levels of IL-8 at baseline correlate with decreased survival in these patients - IL-8 was not increased in all CTEPH patients analyzed at baseline.

In accordance to previous studies, we found increased levels of IL-6 in a majority of CTD-PAH patients at baseline, as well as in a subgroup of IPAH patients. In contrast to earlier cross-sectional

studies in IPAH patients (94), we did not find a correlation of IL-6 with survival in any of the PAH subgroups or CTEPH patients. This might be indicative for the pathological role of IL-6 during disease progression, it might however also be a secondary or a bystander effect. In our data, we did not find a correlation between changes over time for IL-6 and survival. Furthermore, IL-6 did not display a major role in the distinction between <3 and >3-year survival of PAH patients in our multivariate analyses. Currently, a clinical trial with anti-IL6 treatment in PAH patients is ongoing to further elaborate the possible pathological role for IL-6 (238).

Except for TGF $\beta$ , our cohort of CHD-patients displayed no significant increases in circulating cytokines. In apparent contrast, a previous study identified a minor increase of endothelin-1, IL-1 $\beta$ , IL-6, IL-8, tumor necrosis factor  $\alpha$  and VEGF, but a significant correlation with lung function was not observed (114). Our PCA or MFA did not separate CHD-PAH patients and HCs, supporting the notion that inflammation does not play a significant role in the pathogenesis of PH in CHD-patients.

However, in the PCA a clear distinction between HCs and PAH or CTEPH patients was observed, together with an immunological overlap between the different PAH subgroups. A subgroup of IPAH patients shared immunological features with CTD-PAH patients. Considering that in ~40% of IPAH patients specific vascular autoantibodies were found (100-102), it is conceivable that this IPAH subgroup has a more autoimmune phenotype. Our MFA of inflammatory markers and clinical data revealed significant differences between IPAH and CTEPH (dim 1) and between IPAH and CTD-PAH (dim 2), but not between IPAH and CHD-PAH, indicating differential involvement of the immune system in disease pathology of PAH subgroups.

A key finding in our multivariate analyses was that combined profiling using both inflammatory and clinical parameters provided the most significant distinction for patient survival. We could exclude the relatively good prognosis for CTEPH as a dominant factor in this survival analysis, because our sub-analysis that included only PAH patients showed a comparable significant distinction of the <3 and >3-year survival groups. Interestingly, in this sub-analysis of the three PAH patient groups, clinical data alone did not provide a significant distinction in survival. Rather, levels of cytokines and particularly of the chemokines CXCL9 and CXCL13 appeared to be major determining factors in survival. Previously, it has been shown that CXCL9 and several CC-family chemokines important for chemotaxis of myeloid cells play a central role in distinguishing clusters of PAH immune phenotypes with different clinical risks (122). The finding that CXCL13 is one of the markers that could be linked to survival in our PCA/MFA analysis (Figure 5D) may support a critical role of B cell recruitment and organization in follicles and germinal centers in PAH. This would be consistent with the identification of bronchus-associated lymphoid structures (33) as well as circulating auto-antibodies in PAH patients (100-102). Nevertheless, it has been reported that on its own serum CXCL13 only showed a weak association with markers of disease severity (232).

There are some limitations to our study. Firstly, while this study is exploratory and hypothesis generating, our data indicate an important role for IL-8 and CXCL9 in CHD-PAH and CTEPH patients considering the increased levels serum and the observed correlation with survival. Due to the prospective design of our study, not all patients reached a follow-up duration of >3 years; this may have led to limited survival events. Furthermore, a survival bias may have occurred, because only patients who survived for >1 year were included in our paired 1-year follow-up measurements. Lastly, while our CTEPH cohort consisted of 37 patients, our PAH cohort was rather limited in size when stratified into the different PAH subgroups. Nevertheless, for many inflammatory markers we were able to detect significant differences between individual PAH subgroups and healthy controls.

In summary, we found significantly increased plasma levels of various cytokines in three PAH subgroups and CTEPH patients. Particularly when inflammatory mediators were combined with clinical parameters, PCA and MFA multivariate analyses clustered PAH and CTEPH patients into WHO classification-independent subgroups that correlated with patient survival.

## LIST OF ABBREVIATIONS

PH - Pulmonary hypertension  
PAH - pulmonary arterial hypertension  
IPAH - idiopathic PAH  
CTEPH - chronic thromboembolic pulmonary hypertension  
CTD-PAH - Connective Tissue Disease PAH  
CHD-PAH - Congenital Heart Disease PAH  
HC - healthy controls  
RV - right ventricular  
mRAP - mean right atrial pressure  
PVR - pulmonary vascular resistance  
mPAP - mean pulmonary arterial pressure  
NT-pro BNP - N-terminal pro B-type natriuretic peptide  
IL - interleukin  
PI3K - phosphoinositide 3-kinase  
TGF $\beta$  - transforming growth factor  
BMPR2 – Bone morphogenetic protein receptor type II  
Th - T-helper  
CXCL – chemokine (C-X3-C) motif ligand  
*VEGF* - *vascular endothelial growth factor*  
NYHA - New York Heart Association  
PBMCs - peripheral blood mononuclear cells  
PCA - Principal component analysis  
MFA - multiple factor analysis

## DECLARATIONS

### **Ethic approval and consent to participate**

The study protocol was approved by the medical ethical committee (MEC-2011-392). A written informed consent was provided by all patients. This study was performed conform the principles outlined in the Declaration of Helsinki.

### **Consent for publication**

All authors have read and approved the manuscript.

### **Availability of data and materials**

All data is available if required.

### **Competing interests**

The authors declare no conflict of interest.

### **Funding**

This research project was supported by an unrestricting grant by Actelion pharmaceuticals, by the Dutch Heart Foundation (grant number 2016T052) and an unrestricting grant by Ferrer pharmaceuticals.

### **Author contributions**

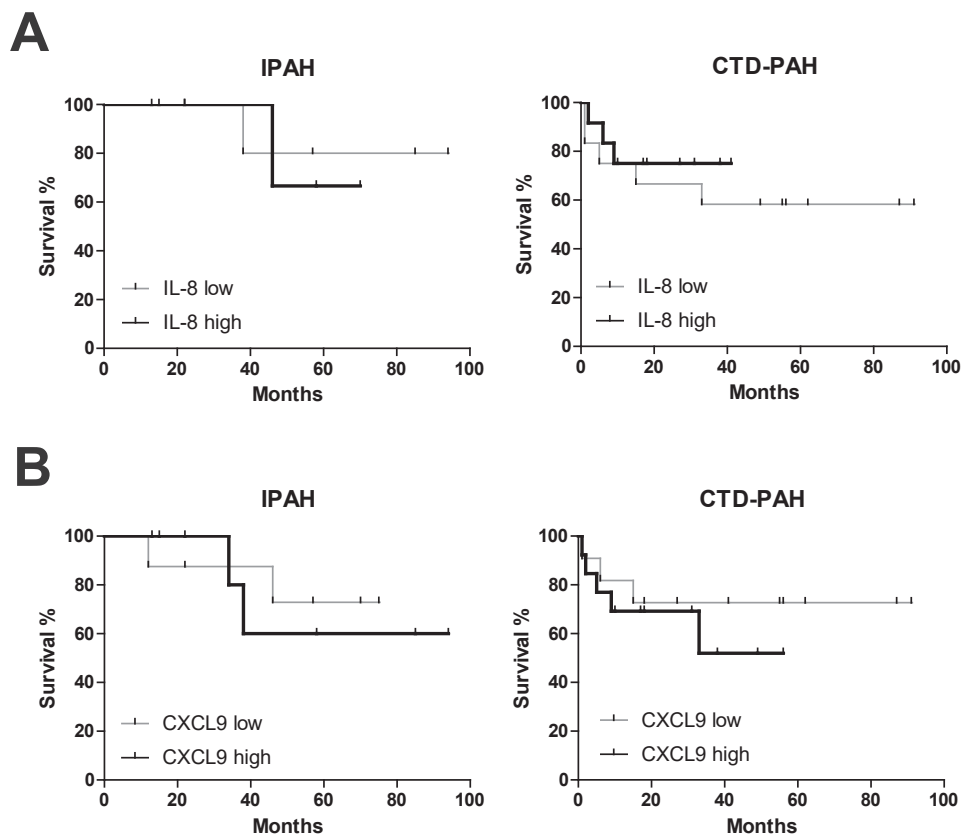
TK and KB designed the experiments. TK, KB, JvH, IB, MK, RWH and PH performed experiments and analyzed/interpreted data. DvU provided PCA and MFA analyses for this project. EB provided valuable feedback for statistics in our manuscript. KB, LG, VB, AB, LT, PC included patients for our study and provided valuable feedback for the manuscript. TK, KB, DvU and RWH wrote the manuscript. All authors read and approved the final manuscript.

### **Acknowledgements**

The authors would like to thank our specialized PH nurses Miriam de Groot and Corine Kolpa at the Erasmus University Medical Centre for their contribution to this study. The authors would also like to thank Martijn Kauling, cardiologist, for his contribution to this study. Also, the authors thank Menno van Nimwegen and Madelief Vink, for their help in processing the peripheral blood samples at our research department.

## SUPPLEMENTARY MATERIAL

## Supplementary figures

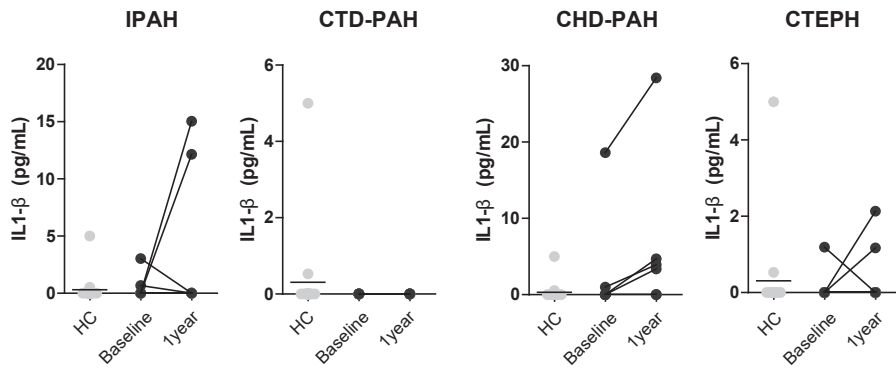


**Supplementary Figure 1. Effects of CXCL9 and IL-8 plasma levels on patient survival.**

Kaplan-Meier survival analyses for (A) IL-8-high/low subgroups and (B) CXCL9-high/low of the indicated WHO PH patient subgroups. Statistical analysis was performed using a log-rank (Mantel-Cox) test and a Gehan-Breslow-Wilcoxon test. *P* values are shown.

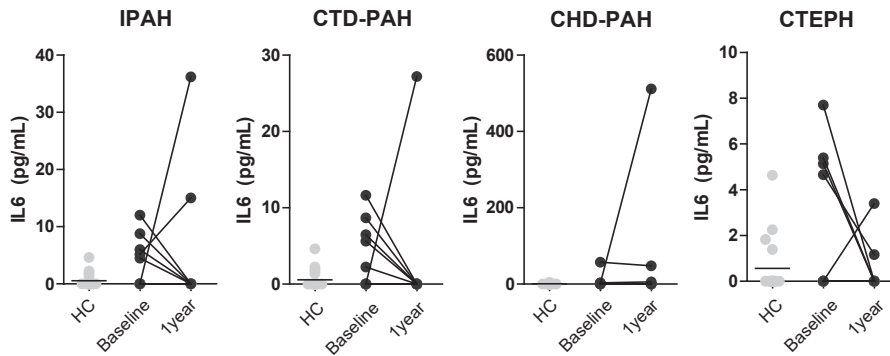
**A**

IL-1 $\beta$



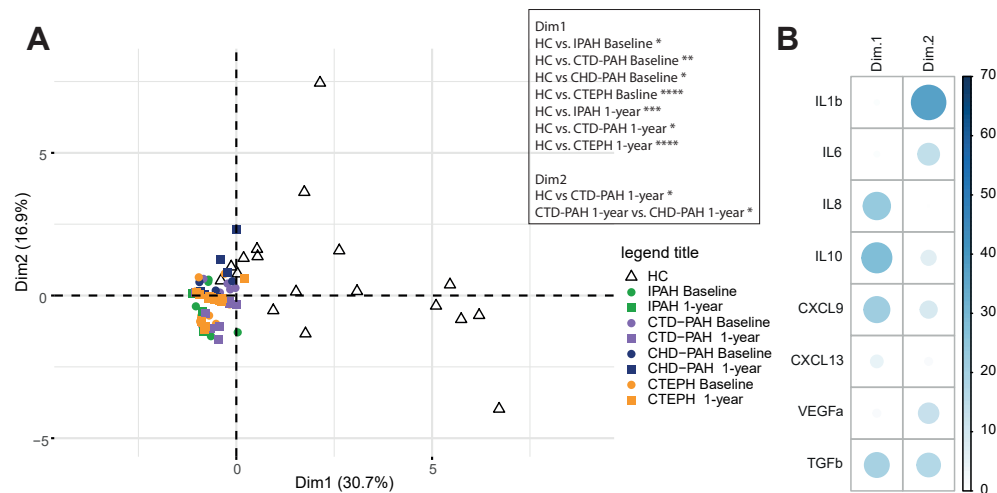
**B**

IL-6



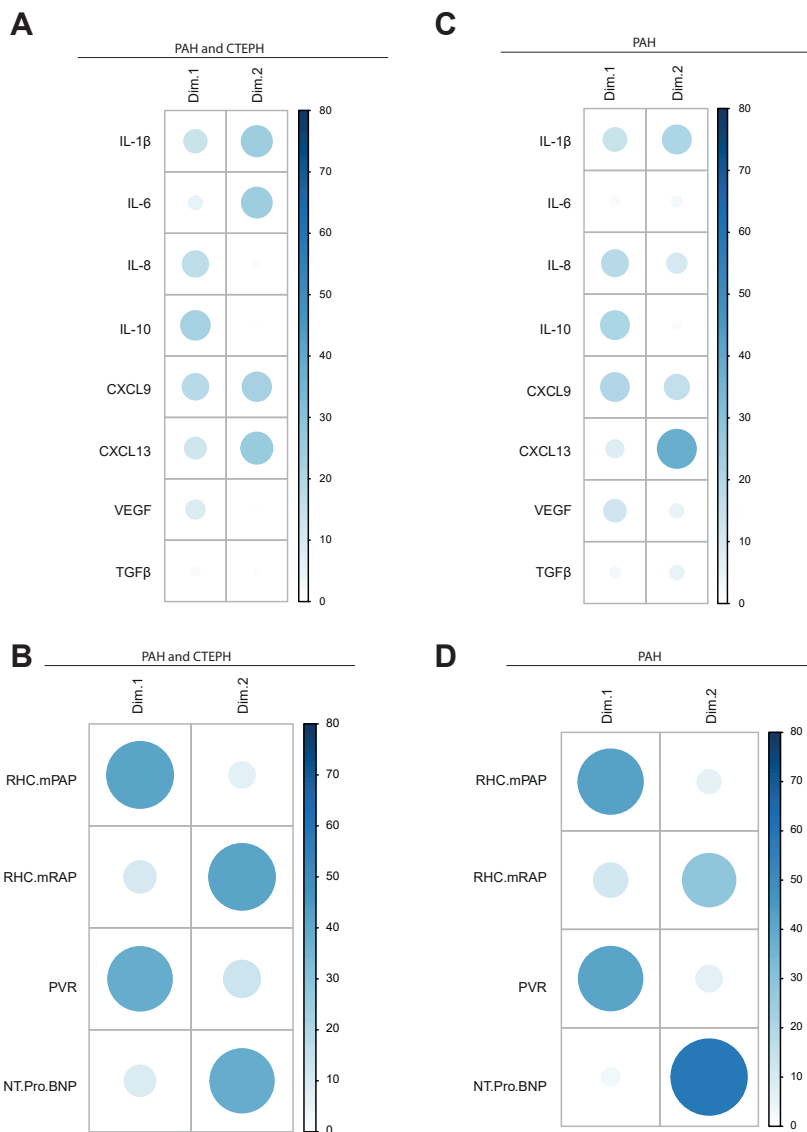
**Supplementary Figure 2. Plasma concentrations of IL-1 $\beta$  and IL-6 inflammatory markers in plasma of PAH and CTEPH patients at diagnosis and 1-year follow up.**

(A-B) Paired plasma cytokine measurements by ELISA for interleukin IL-1 $\beta$  (A) and IL-6 (B) at diagnosis and at 1-year follow up for a subset of patients from the indicated WHO patient subgroups, compared with HCs. Data are shown as symbols for individual patients and HCs. Statistical analysis was performed using a Wilcoxon signed-rank test. No significant differences were found.

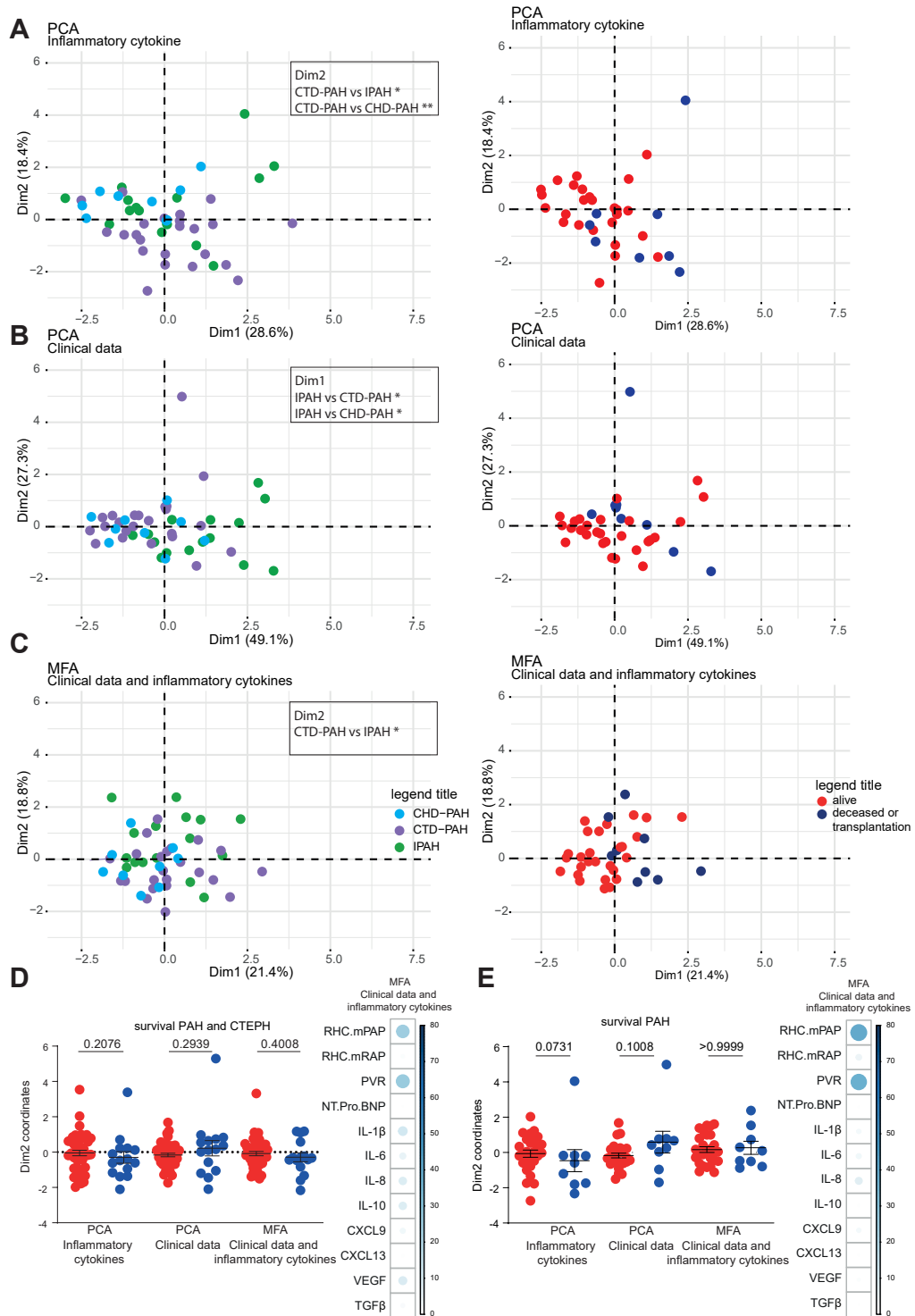


**Supplementary figure 3. Inflammatory marker concentration of PH patients at diagnosis and at 1-year follow up are not separated by principal component analysis.**

(A) Unsupervised principal component analysis (PCA) of inflammatory markers, measured by ELISA, in plasma of healthy controls and the indicated WHO PH patient subgroups at diagnosis and at 1-year follow-up. PCAs were on log10-transformed and scaled concentrations values; each symbol point represents an individual patient or HC sample. (B) Representation of the contribution in percentages of the variables on the first (Dim.1) and second (Dim.2) principal component of inflammatory markers. The blue color range indicates the contribution to the principal components. Statistical analysis was performed by a one-way ANOVA (Kruskal-Wallis test) combined with a Dunn's multiple comparison test. \* =  $p < 0.05$ , \*\* =  $p < 0.01$ .



**Supplementary figure 4. Contribution of inflammatory markers and clinical parameters to multivariate analyses.** (A-D) Representation of the contribution in percentages of the variables on the first (Dim.1) and second (Dim.2) principal component of baseline inflammatory markers of PAH and CTEPH patients (A), clinical parameters of PAH and CTEPH (B), baseline inflammatory markers of solely PAH patients (C) or clinical parameters of solely PAH patients to unsupervised principal component analyses. The blue color range indicates the contribution to the principal components.

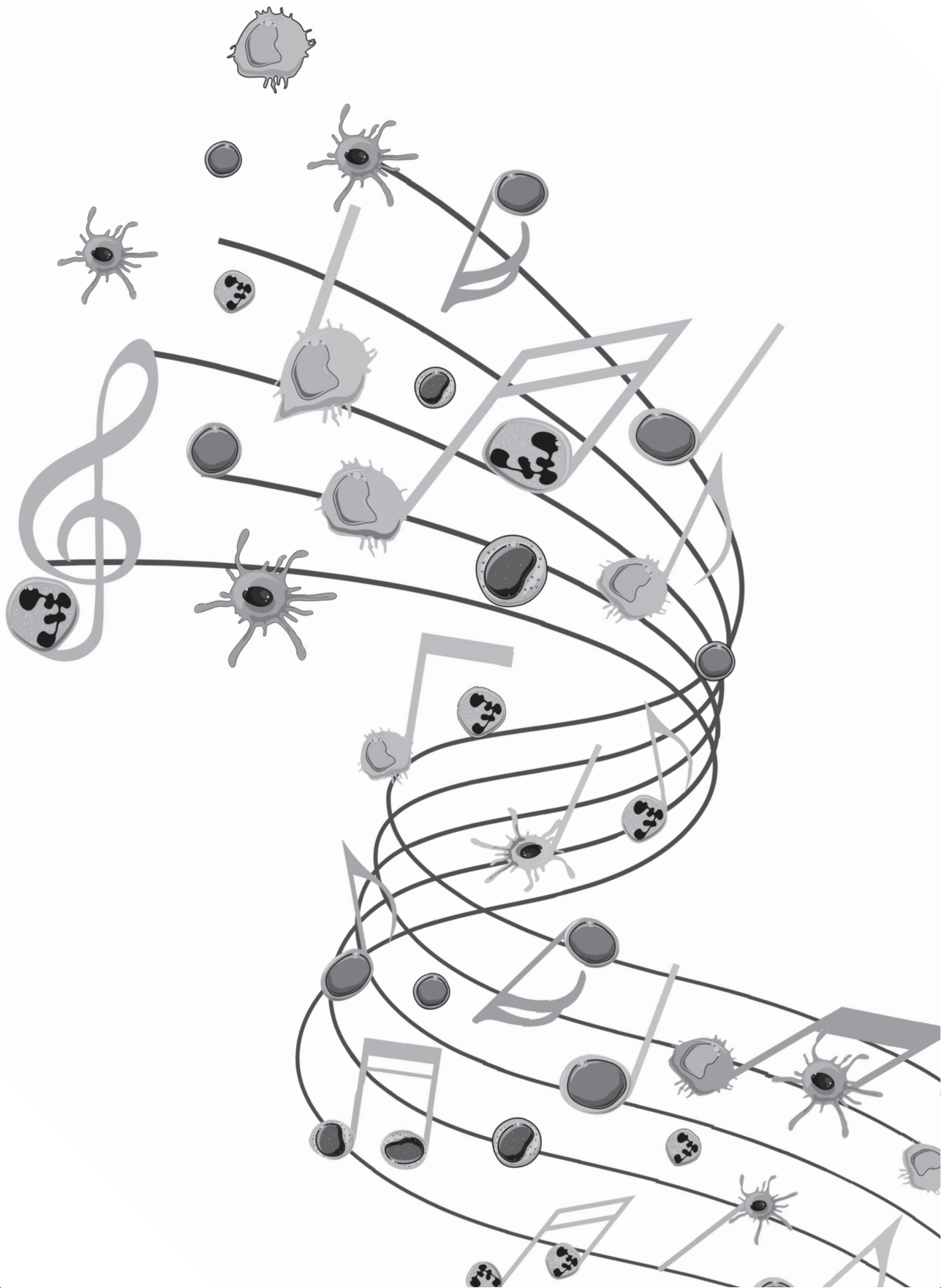


**Supplementary figure 5. Combination of inflammatory markers and clinical parameters leads to the best separation of survival in PAH patients.**

(A,B) Clustering in PAH patients by unsupervised principal component analysis (PCA) of inflammatory markers measured by ELISA in plasma (A) and of clinical parameters (B), showing the indicated PAH patient subgroups (*left*) or subgroups of survival of >3 years (alive) or <3 years (deceased/transplantation) (*right*). (C) Multiple factor analysis (MFA) combining clinical data and log10 transformed and scaled plasma inflammatory marker concentrations of PAH patients, showing the indicated patient subgroups (*left*) or survival of >3 years (alive) or <3 years (deceased/transplantation) (*right*). (D,E) Dim2 coordinate values of patients with survival of >3 years (alive) or <3 years (deceased/transplantation) for the indicated PCAs and MFAs of PAH and CTEPH patients (D) or PAH patients alone (E) and contribution of the variables for Dim2 to the MFA. Statistical analysis between PAH groups was performed by a *one-way ANOVA (Kruskal-Wallis test) combined with a Dunn's multiple comparison test*. \* =  $p < 0.05$ , \*\* =  $p < 0.01$ , \*\*\* =  $p < 0.001$ . Separation between survival groups was evaluated using a Mann-Whitney U test on principal component 1 coordinates of alive versus deceased/transplantation. P values are indicated.

**Supplementary Table 1. Antibody kits used for ELISA.**

<b>Cytokine/Chemokine</b>	<b>ELISA-kit (Company)</b>
IL1- $\beta$	R&D duoset ELISA kit human IL-1 $\beta$ (Catalog Numbers: DY201)
IL-6	R&D duoset ELISA kit human IL-6 (Catalog Numbers: DY206)
IL-8	R&D duoset ELISA kit human IL-8 (Catalog Numbers: DY208)
IL-10	R&D duoset ELISA kit human IL-10 (Catalog Numbers: DY217B)
CXCL9	R&D duoset ELISA kit human CXCL9 (Catalog Numbers: DY392)
CXCL13	R&D duoset ELISA kit human CXCL13 (Catalog Numbers: DY801)
VEGFa	R&D duoset ELISA kit human VEGFa (Catalog Numbers: DY293B)
TGF $\beta$	R&D duoset ELISA kit human TGF $\beta$ (Catalog Numbers: DY240)



# CHAPTER 5

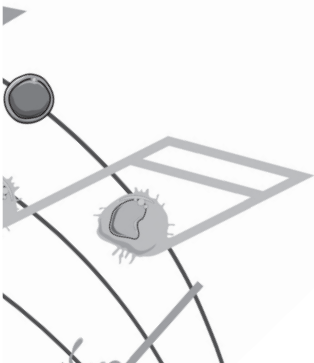
*Evidence for a role of CCR6<sup>+</sup>  
T cells in chronic thromboembolic  
pulmonary hypertension patients.*

D. van Uden, **T. Koudstaal**, J.A.C. van Hulst, T.P.P. van den Bosch,  
M. Vink, I.M. Bergen, K. Lila, A.E. van den Bosch, P. Bresser, M.  
Kool, J.H. von der Thüsen, R.W. Hendriks\*, K.A. Boomars\*

\*Contributed equally.

Front Immunol 2022 Apr 27;13:861450

# 5



## ABSTRACT

### Introduction

Previous studies have shown an increase of T cells and chemokines in vascular lesions of patients with chronic thromboembolic pulmonary hypertension (CTEPH). However, detailed characterization of these T cells is still lacking, nor have treatment effects been evaluated.

### Methods

We included 41 treatment-naive CTEPH patients at diagnosis, 22 patients at 1-year follow-up, and 17 healthy controls (HCs). Peripheral blood T cells were characterized by flow cytometry for subset distribution, cytokine expression and activation marker profile. We used multiplex immunofluorescence to identify CCR6<sup>+</sup> T cells in endarterectomy tissue from 25 patients.

### Results

At diagnosis, proportions of CCR6<sup>+</sup> CD4<sup>+</sup> T cells were increased in CTEPH patients compared with HCs. Patients displayed a significantly reduced production capacity of several cytokines including TNF $\alpha$ , IFN $\gamma$ , GM-CSF and IL-4 in CD4<sup>+</sup> T cells, and TNF $\alpha$  and IFN $\gamma$  in CD8<sup>+</sup> T cells. CD4<sup>+</sup> and CD8<sup>+</sup> T cells showed increased expression of the immune checkpoint protein CTLA4. Multivariate analysis separated CTEPH patients from HCs, based on CCR6 and CTLA4 expression. At 1-year follow-up, proportions of CCR6<sup>+</sup>CD4<sup>+</sup> T cells were further increased, IFN $\gamma$  and IL-17 production capacity of CD4<sup>+</sup> T cells was restored. In nearly all vascular lesions we found substantial numbers of CCR6<sup>+</sup> T cells.

### Conclusion

The observed increase of CCR6<sup>+</sup> T cells and modulation of the IFN $\gamma$  and IL-17 production capacity of circulating CD4<sup>+</sup> T cells at diagnosis and 1-year follow-up – together with the presence of CCR6<sup>+</sup> T cells in vascular lesions - support the involvement of the Th17-associated CCR6<sup>+</sup> T cell subset in CTEPH.

## INTRODUCTION

Chronic thromboembolic pulmonary hypertension (CTEPH) is a debilitating disease occurring as a rare complication following acute pulmonary embolism (239). The combination of occlusion of proximal pulmonary arteries by thrombotic material and secondary microvasculopathy of small vessels (<500nm) leads to increased pulmonary vascular resistance (PVR) and progressive right heart failure. Based on the localization and characterization of the thrombotic lesions in the pulmonary vasculature, therapy may consist of pulmonary endarterectomy (PEA) surgery, balloon pulmonary angioplasty (BPA) intervention, and/or pulmonary hypertension (PH)-specific drug therapy. In most cases, CTEPH patients are operable and eligible for PEA intervention, leading to very good long-term survival in expert centers (240-242). By contrast, when CTEPH patients display mainly peripheral localization of the thrombotic lesions or have considerable co-morbidities, they become inoperable. In that case survival remains poor with a mean 5-year survival of 53-69%, even when treated with specific PAH medication (21, 22). Therefore, more insight into the pathogenesis of CTEPH is urgently needed and would fuel the development of new therapeutic strategies.

Thrombotic lesions of CTEPH patients contain various immune cells, particularly myeloid cells including macrophages and neutrophils (36, 243-245). Myeloid cells are attracted towards the lesions by various chemokines that were found to be increased in plasma or thrombotic lesions of CTEPH patients (32, 36, 243, 246). Circulating neutrophils display an activated state and neutrophil extracellular trap formation has been implicated in CTEPH pathogenesis (247, 248).

By contrast, knowledge on the role of adaptive immunity in CTEPH is limited (25, 215, 249). T cells expressing the co-inhibitory marker CD200 are increased in the circulation of CTEPH patients. T cells are abundantly present in vascular lesions, as shown by histological analysis and single-cell RNA analysis on endarterectomy tissue (36, 250, 251). CCL2, produced by many cell types, can also regulate migration of T cells and natural killer cells (252). Myeloid cells in thrombotic lesions can interact with T lymphocytes, which in turn may enhance myeloid cell activity through cytokine production. Inflammatory mediators, such as interleukin (IL)-6, IL-8, IL-10 and tumor necrosis factor- $\alpha$  (TNF $\alpha$ ), are increased in serum or plasma of CTEPH patients (32, 36, 111, 246, 253-255). This increase might either promote T cell activation or may be a reflection thereof. Moreover, chemokine CXCL3, which is important for T helper 1 (Th1) cells expressing its receptor CXCR3, is increased in serum and lung tissue (232). The importance of these inflammatory mediators is illustrated by our earlier findings that increased plasma levels of CXCL9 and IL-8 correlated with decreased survival in CTEPH patients (254) and point to involvement of the adaptive immune system.

CD4<sup>+</sup> T cells can be divided into different functional subsets (237). Th1 (CCR6<sup>-</sup>CXCR3<sup>+</sup>CCR4<sup>+</sup>) cells are induced by IL-12 and secrete interferon  $\gamma$  (IFN $\gamma$ ) to defend against intracellular pathogens. Th2 cells (CCR6<sup>-</sup>CXCR3<sup>-</sup>CCR4<sup>+</sup>) produce IL-4, IL-5 and IL-13 and are involved in defense against helminths. Th17 cells (CCR6<sup>+</sup>) are induced by IL-1 $\beta$ , IL-6 and transforming growth factor  $\beta$  (TGF $\beta$ ) and secrete IL-17. They protect against extracellular pathogens, but are also involved in the pathophysiology of autoimmune diseases (256). In parallel, CCR6<sup>+</sup>CD8<sup>+</sup> T cells, known as Tc17 cells, are found in patients with different inflammatory diseases (257, 258). They migrate to similar sites as Th17 cells, attracted by CCL20, and produce IL-17, IFN $\gamma$  and TNF $\alpha$ . The increase of TNF $\alpha$  and IL-6 in serum of CTEPH patients, suggests a role for CCR6<sup>+</sup> T cells in disease pathogenesis (32, 111, 246, 255).

In this report, we used flow cytometry to investigate subset division, cytokine production and activation status of circulating T cells from a well-defined, treatment-naïve cohort of CTEPH patients.

We also investigated how treatment affected this T cell profile and we characterized T cells present in pulmonary vascular lesions.

## METHODS

### Subjects and study design

Our prospective observational cohort of CTEPH patients has been previously reported (254). Forty-one CTEPH patients were diagnosed according to the ERS/ECSC guidelines (Table 1) (2). Similar to prior work from our group, exclusion criteria were incomplete diagnostic work-up and therefore no confirmed PH diagnosis, not treatment-naive, age <18 years, or not capable of understanding or signing informed consent (233). Additionally, 17 HCs (41% female, mean age 55.3±12.5), were included with the following exclusion criteria: autoimmune disease, active infectious disease, use of immunomodulatory drugs, history of cardiopulmonary disease. At 1-year follow-up patients visited the outpatient clinic and did not have any active infection. The study protocol was approved by the Erasmus MC medical ethical committee (MEC-2011-392). Written informed consent was provided by all patients and controls. The study was performed conform the principles outlined in the declaration of Helsinki.

**Table 1. Baseline demographic and patient characteristics.**

	<b>CTEPH Baseline (n=41)</b>	<b>CTEPH Follow-up (n=22)</b>
<b>Baseline clinical characteristics</b>		
Gender, female (%)	20 (49%)	12 (55%)
Age, y	62.0 ±13.3 <sup>1</sup>	64.6 ±11.1
BMI, kg/m <sup>2</sup>	29.7 ±6.3	29.4 ±6.7
NYHA class 3-4, n (%)	19 (46%)	10 (45%)
6MWT, m	378 ±140	335 ±135
NT-pro BNP, pmol/L	115 ±184	136 ±213
<b>Baseline right heart catheterization</b>		
mPAP, mmHg	39.1 ±12.7	38.7 ±13.8
mRAP, mmHg	9.4 ±6.7	8.9 ±4.8
Capillary wedge pressure, mmHg	12.3 ±4.3	11.9 ±5.2
PVR, wood units	4.8 ±2.8	5.2 ±2.7
<b>Thrombotic lesion localization</b>		
Central vasculature	16 (39%)	8 (36%)
Mid vasculature	15 (37%)	6 (28%)
Peripheral vasculature	10 (24%)	8 (36%)

	<b>CTEPH Baseline (n=41)</b>	<b>CTEPH Follow-up (n=22)</b>
<b>Intervention received (at t= 1-year follow-up)</b>		
PEA		9 (22%)
PEA (technically operable, yet no surgery performed)		7 (17%)
BPA (within 1-year follow-up)		5 (12%)
BPA (after 1-year follow-up)		6 (15%)
No intervention, only PH-medication		14 (34%)
<b>PH-Medication</b>		
At baseline, n (%)	0/41 (0%)	
At 1-year follow-up		
No PH-medication <sup>2</sup>		3/22 (14%)
Mono therapy, n (%)		10/22 (45%)
Duo therapy, n (%)		9/22 (41%)
Triple therapy, n (%)		0/22 (0%)
<b>Immunomodulatory drugs</b>		
At baseline, n (%)	0/41 (0%)	
At 1-year follow-up, n (%)		0/22 (0%)

<sup>1</sup> Data given as mean values  $\pm$ SD, unless otherwise indicated.

<sup>2</sup> These CTEPH patients were not on PH-medication due to being technically operable for pulmonary endarterectomy.

**Abbreviations:** BMI, body mass index; CTEPH, chronic thromboembolic pulmonary hypertension; 6MWT, 6-minute walk test; NT-pro BNP, The N-terminal prohormone of brain natriuretic peptide; mPAP, mean pulmonary arterial pressure; mRAP, mean right atrium pressure; PVR, pulmonary vascular resistance; PEA, pulmonary endarterectomy; BPA, Balloon pulmonary angioplasty.

## Clinical Data Collection, Follow-up, and Definition of Endpoints

Hemodynamic and clinical data at diagnosis were collected during the inpatient cardiopulmonary screening visit for analysis of PH (233, 254). Data were collected and stored in PAHTool (version 4.3.5947.29411, Inovoltus), an online electronic case report form. Patients were treated according to the ERS/ESC guidelines (2) and prospectively followed-up by half-yearly scheduled visits to the outpatient clinic. All patients were assessed for eligibility for either a PEA or BPA (Table 1). The mean follow-up duration was 51.0 months. Survival was defined as all-cause mortality. In our cohort, 7 out of 41 patients died within the follow-up period.

## Flow cytometry and histology of vascular lesions

Peripheral blood mononuclear cells were stained for intra- and extracellular markers, using flow cytometry procedures essentially as described previously (259), using the antibodies given in Supplementary Table 1. Cell fractions were directly stained for chemokine receptors and extracellular markers for 60 minutes at 4°C. After fixation and permeabilization steps, cells were intracellularly

stained for FoxP3 and CTLA4. For the measurement of cytokines, PBMCs were incubated for 4 hours at 37°C in RPMI Medium 1640 + GlutaMAX-I (Gibco) supplemented with 5% fetal bovine serum (Gibco), 10 ng/ml phorbol 12-myristate 13-acetate (Sigma-Aldrich), 250 ng/ml ionomycin (Sigma-Aldrich) and Golgistop (BD Bioscience), after which cells were stained as previously described (260). Non-specific labelling was prevented by blocking Fc receptors using human TruStain FcX (Biolegend) and dead cells were excluded with Fixable Viability Dye Live/Dead eF506 (eBioscience). Data was acquired using a FACSymphony A5 flow cytometer (Beckton Dickinson) and analyzed using FlowJo version 10 (Tree Star Inc software).

Hematoxylin and eosin (H&E) staining and multiplex immunofluorescence were performed as described previously (261). For immunohistochemical analysis of human lung tissue, we performed a 5-plex immunofluorescent multiplex by automated IHC using the Ventana Benchmark Discovery ULTRA (Ventana Medical Systems Inc.). Formalin fixed paraffin embedded (FFPE)-tissue of lung vascular lesions of CTEPH patients were handled and used according to the guidelines of the declaration of Helsinki. This study was conducted in accordance with the guidelines of the Biomedical Scientific Societies (Dutch Federa code of conduct 2011) for the use of anonymized residual tissue obtained during regular treatment.

Slides of 4 µm thick FFPE sections were stained for CD3, CD4, CD8, FOXP3 and CCR6 (Supplementary Table 2). In brief, following deparaffinization and heat-induced antigen retrieval with CC1 (#950-224, Ventana) for 32 min, anti-CD3 was incubated for 32 min at 37 °C followed by omnimap anti-rabbit HRP (#760-4311, Ventana) and detection with R6G (#760-244, Ventana). An antibody denaturation step was performed with CC2 (#950-123, Ventana) at 100 °C for 20 min. Secondly, incubation with anti-FOXP3 was performed for 60 min at 37 °C, followed by universal HQ kit (#760-275, Ventana) and detection with DCC (#760-240, Ventana) for 8 min. An antibody denaturation step was performed with CC2 at 100 °C for 20 min. Thirdly, anti-CD4 was incubated for 32 min at 37 °C, followed by omnimap anti-rabbit HRP (#760-4311, Ventana) and detection with Red610 (#760-245, Ventana) for 8 minutes. An antibody denaturation step was performed with CC2 at 100 °C for 20 min. Fourthly, sections were incubated with anti-CCR6 for 120 min at 37 °C followed by universal HQ kit (#760-275, Ventana) and detection with Cy5 (#760-238, Ventana) for 8 min. An antibody denaturation step was performed with CC2 at 100 °C for 20 min. Lastly, incubation with anti-CD8 was performed for 60 min at 37 °C followed by omnimap anti-rabbit HRP (#760-4311, Ventana) and detection with FAM (#760-243, Ventana). Finally, slides were washed in phosphate-buffered saline and mounted with Vectashield containing 4',6-diamidino-2-phenylindole (Vector laboratories, Peterborough, UK). Analysis of the multiplex staining was performed using Qupath the open software platform for bioimage analysis (version 0.3.0). In short, sections were annotated by simple tissue detection after which cells were identified by the default cell detection command using dapi to identify nuclei. Using simple thresholding for all channels all cells were classified and annotated. These measurements were used for further analysis.

### Principal component analysis and statistical evaluation

Principal component analysis (PCA) was performed using R and RStudio, and the packages FactoMineR and Factoextra (254, 262).

Statistical evaluations of T cell subsets, cytokine production, activation markers and PCA dimension coordinates were by Mann-Whitney U tests. Paired diagnosis and 1-year follow-up data were

analyzed using a Wilcoxon matched-pairs signed rank test. Correlation coefficients were calculated using the nonparametric Spearman correlation. All statistical tests were two-sided; p-values <0.05 were considered statistically significant. Statistical analyses were performed using GraphPad Prism v8 (Graph Pad Software).

## RESULTS

### Increased proportions of circulating CCR6<sup>+</sup>CD4<sup>+</sup> T cells in treatment-naive CTEPH patients

We characterized peripheral blood T cells in a cohort of 41 treatment-naive CTEPH patients at diagnosis and 17 HCs (Table 1). Five subpopulations were separately analyzed: CD45RA<sup>+</sup> CD4<sup>+</sup> T cells (FoxP3<sup>-</sup>; mainly naive T cells, but also CD45RA<sup>+</sup> TEMRA cells, which are thought to be antigen-experienced T cells re-expressing CD45RA), CD45RA<sup>-</sup> CD4<sup>+</sup> T cells (FoxP3<sup>-</sup>CXCR5<sup>-</sup>; memory T cells), FoxP3<sup>+</sup> CD4<sup>+</sup> T cells (Tregs and activated T cells), CD45RA<sup>-</sup> CD8<sup>+</sup> T cells and CD45RA<sup>+</sup> CD8<sup>+</sup> T cells (see Figure 1 and Supplementary Figure 1 for gating strategy). The proportions of these five T cell subpopulations did not differ between CTEPH patients and HCs (data not shown).

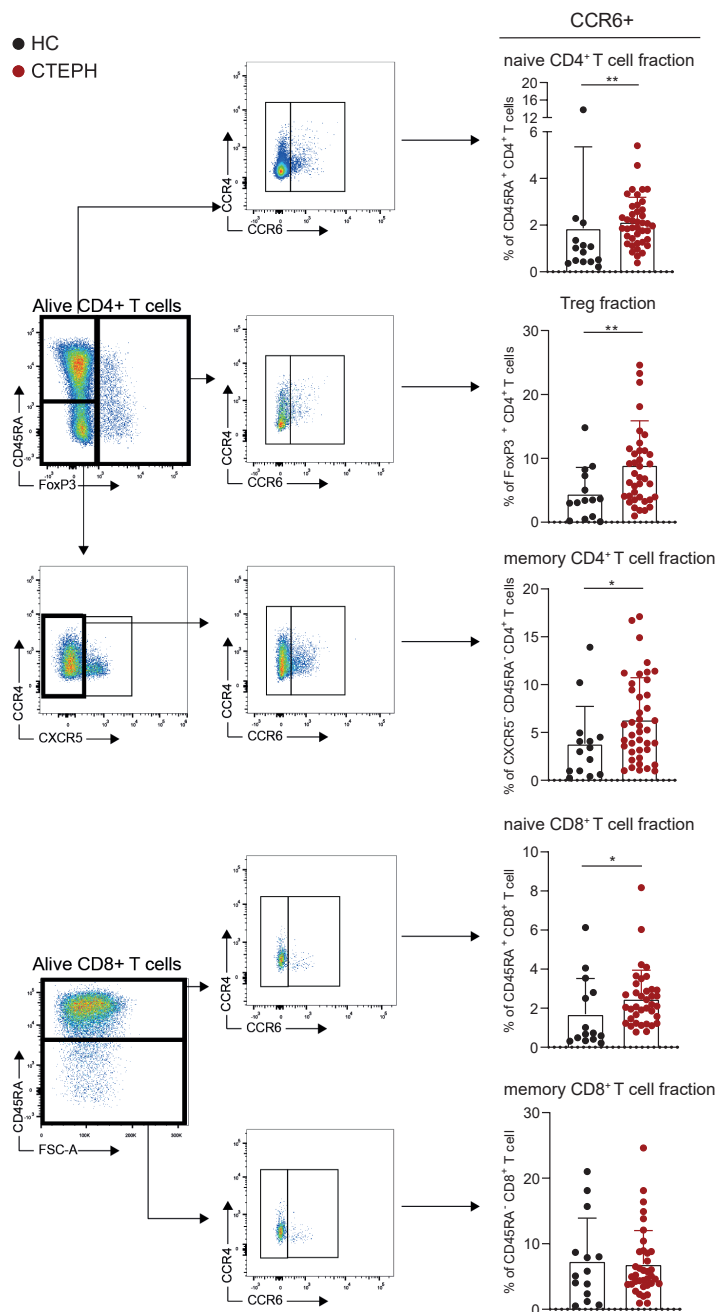


**Figure 1. Frequencies of CCR6<sup>+</sup> T cells are higher in patients with chronic thromboembolic pulmonary hypertension (CTEPH) than in healthy controls (HCs) at diagnosis.** Gating strategy for peripheral blood CCR6<sup>+</sup> T cell subsets (*left*) and percentages of circulating CCR6<sup>+</sup> T cells (*right*) of the indicated T cell subsets for HCs and CTEPH patients at diagnosis determined by flow cytometry. Results are presented as mean + standard deviation. Mann-Whitney U test was used for statistical analysis, \*  $p < 0.05$ , \*\*  $p < 0.01$ . Symbols represent values of individual patients or HCs.

We used the expression of surface chemokine receptors to distinguish distinct CD45RA<sup>-</sup> CD4<sup>+</sup> memory T cell subsets, including Th1 (CCR6<sup>-</sup>CXCR3<sup>+</sup>CCR4<sup>-</sup>), Th2 (CCR6<sup>-</sup>CXCR3<sup>+</sup>CCR4<sup>+</sup>), Th17 (CCR6<sup>+</sup>) and follicular T helper cells (Tfh; CXCR5<sup>+</sup>). Whereas the frequencies of Th1, Th2 and Tfh cells did not differ between CTEPH patients and HCs (data not shown), we observed an increase in Th17 cells within the memory CD4<sup>+</sup> T cells (Figure 1). A sub-analysis of CCR6<sup>+</sup> CD4<sup>+</sup> T cells, identifying CXCR3<sup>-</sup>CCR4<sup>+</sup> Th17, CXCR3<sup>+</sup>CCR4<sup>-</sup> Th17.1, CXCR3<sup>+</sup>CCR4<sup>+</sup> double positive (DP) and CXCR3<sup>-</sup>CCR4<sup>-</sup> double negative (DN) cells, showed a particularly strong increase in the proportions of CXCR3<sup>-</sup>CCR4<sup>-</sup> DN T cells in CTEPH patients compared to HCs (Supplementary Figure 2A, 2B). Although DN Th17 cells are less studied than the classic Th17 and Th17.1 cells, evidence was provided that these cells have pathogenic features in rheumatoid arthritis (263) and display a stable Th17-lineage commitment, even under Th1 polarization conditions (264). They have the capacity to produce IL-17, but little IFN $\gamma$  and co-express the transcription factors TBX21 and ROR $\gamma$ t, which are associated with the Th1 and Th17 subset, respectively. In this context, we confirmed intracellular expression of the key transcription factor ROR $\gamma$ t in the total CCR6<sup>+</sup> CD4<sup>+</sup> T cell population (Supplementary Figure 2C).

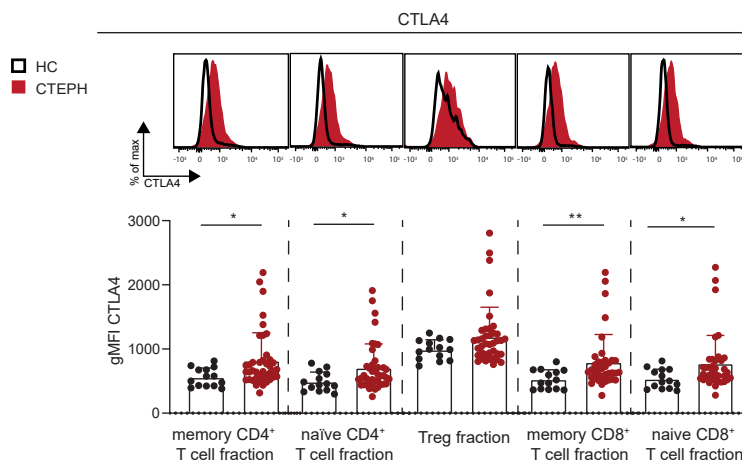
Significantly more CCR6<sup>+</sup> T cells were also present in the fractions of naive CD4<sup>+</sup> and CD8<sup>+</sup> T cells, as well as Tregs (Figure 1). This was not the case for CCR6<sup>+</sup> memory CD8<sup>+</sup> T cells, which would reflect IL-17-producing Tc17 cells (265, 266).

In conclusion, circulating T cells in CTEPH patients show an aberrant phenotype, characterized by increased proportions of CCR6<sup>+</sup> cells in naive and memory CD4<sup>+</sup> T cells, naive CD8<sup>+</sup> T cells and Tregs.

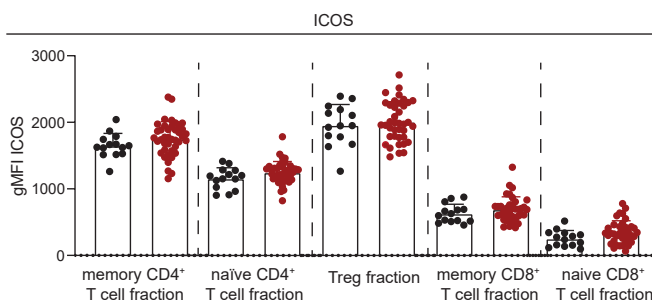
### **Increased CTLA4 expression in CD4<sup>+</sup> and CD8<sup>+</sup> T cells from CTEPH patients**

The activation status of a T cell is reflected by the expression of activation and inhibitory markers, such as T cell co-stimulator (ICOS), programmed cell death 1 (PD1) and cytotoxic T lymphocyte antigen 4 (CTLA4) (267). Their expression was examined in the five T cell subpopulations, as gated in Figure 1. CTLA4 was significantly increased in all T cell fractions from CTEPH patients compared to HCs, except for Tregs in which only a slight trend was observed (Figure 2A). PD1 and ICOS expression were unchanged (Figure 2B, 2C and Supplementary Figure 3A, 3B). No significant correlations between the three different markers were found (shown for memory CD4<sup>+</sup> T cell fractions in Supplementary Figure 3C).

A)



B)



C)

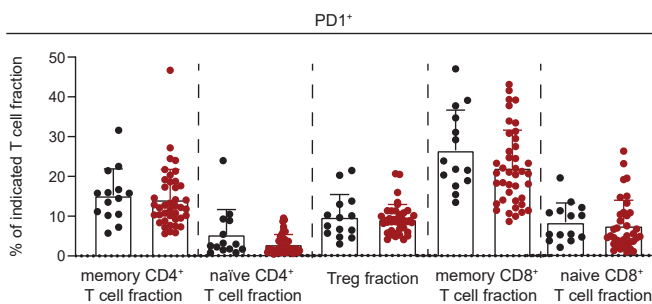


**Figure 2. Increased CTLA4 expression in T cell subsets in CTEPH patients.** (A) Flow cytometry analysis of intracellular CTLA4 expression in the indicated T cells subsets, shown as histogram overlays (*top*) and quantification (*bottom*). (B) Quantification of surface ICOS expression on the indicated T cell subsets. (C) Proportions of PD1<sup>+</sup> cells in the indicated T cell subsets. Results are presented as mean + standard deviation, Mann-Whitney U test was used for statistical analysis, \*  $p < 0.05$ , \*\*  $p < 0.01$ . gMFI = geometric mean fluorescence intensity. Symbols represent values of individual patients or HCs. In summary, these data indicate that both naïve and memory CD4<sup>+</sup> and CD8<sup>+</sup> T cells of CTEPH patients have increased expression of CTLA4.

### Multivariate analysis for T cell subset and activation marker profile separates treatment-naive CTEPH patients from HCs

Subsequently, we used PCA to investigate if a specific T cell profile could separate treatment-naive CTEPH patients from HCs. We observed a non-random distribution that was not due to gender or age (Figure 3A and data not shown). The T cell profile was able to significantly separate patients from HCs in dimension 3 (Dim3) (Figure 3B), to which CCR6 and PD1 contributed most (Figure 3C). Although CTLA4 expression was significantly different between patients and HCs in most T cell populations, these differences did not significantly separate the two groups in Dim1 (Figure 3B, 3C).

Taken together, quantification of CCR6 and PD1 expression creates a T cell profile that separates CTEPH patients from HCs in a multivariate analysis.

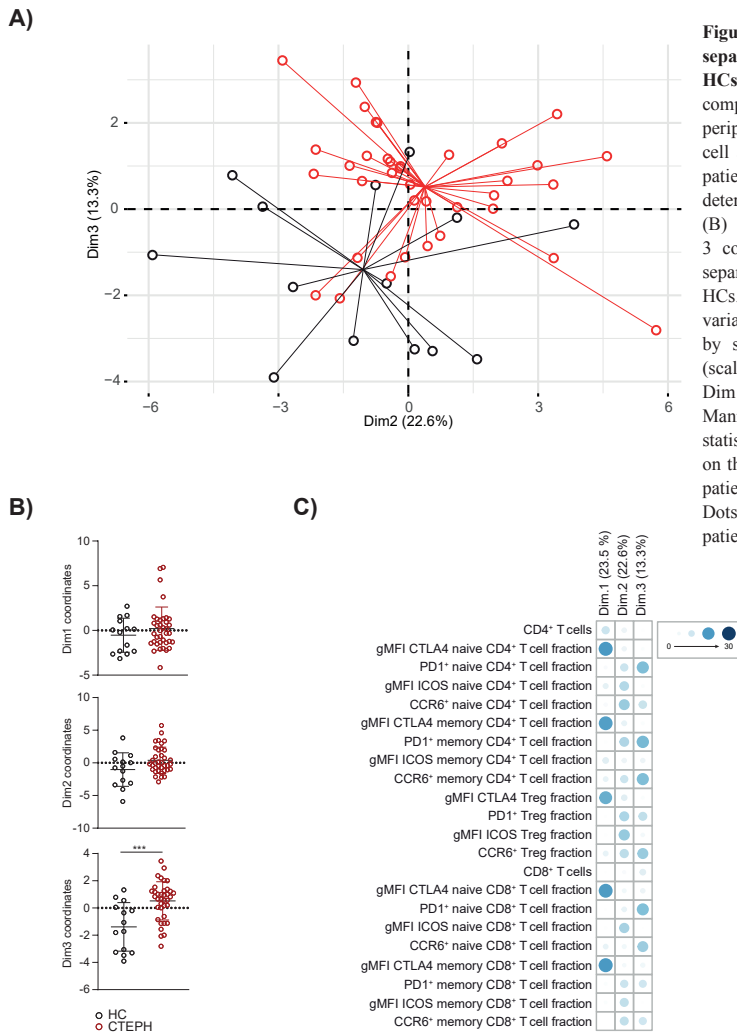


**Figure 3. Multivariate analysis separates CTEPH patients from HCs at diagnosis.** (A) Principal component analysis (PCA) of peripheral T cell subsets and T cell activation markers of CTEPH patients at diagnosis and HCs determined by flow cytometry (B) Dimension (Dim.) 1, 2 and 3 coordinate values showing the separation between patients and HCs. (C) Contribution of the variables in percentages indicated by symbols in blue color range (scale indicates proportions) of Dim1, Dim2 and Dim3 of the PCA. Mann-Whitney U test was used for statistical analysis of coordinates on the dimension between CTEPH patients and HCs, \*\*\* p< 0.001. Dots represent values of individual patients or HCs.

## Reduced cytokine-producing capacity of T cells from CTEPH patients

Next, we determined the cytokine-producing capacity of T cells in a subgroup of 38 CTEPH patients (gating strategy as in Figure 1, except that Tregs were now identified by CD127<sup>-</sup>CD25<sup>+</sup> expression; Figure 4A). We observed that the CD45RA<sup>-</sup> memory CD4<sup>+</sup> T cell fractions of CTEPH patients were less capable of producing TNF $\alpha$ , IFN $\gamma$ , granulocyte-macrophage colony-stimulating factor (GM-CSF) and IL-4 compared with HCs, but intracellular IL-6, IL-10 and IL-17 did not differ between patients and HCs (Figure 4B). A correlation matrix of the proportions of cytokine-expressing CD45RA<sup>-</sup>CD4<sup>+</sup> T cells in HCs indicated a strong coordination between all cytokines analyzed except IL-6, but this was partly lost in CTEPH patients (Figure 4C, examples shown in Supplementary Figure 4). The finding of mainly positive correlations across individual cytokines indicated that both CTEPH patients and HCs did not show skewing toward distinct Th subsets (because this would then have been visible in the matrices as negative correlations). Nevertheless, the significant positive correlation between the proportions of IL-17<sup>+</sup>, IFN $\gamma$ <sup>+</sup> and IL-4<sup>+</sup> T cells in HCs was weaker in CTEPH patients. This observation suggested that in CTEPH patients the decrease of IFN $\gamma$ <sup>+</sup> or IL-4<sup>+</sup> CD4<sup>+</sup> T cells was not associated with a concomitant decrease or increase in IL-17-producing CD4<sup>+</sup> T cells.

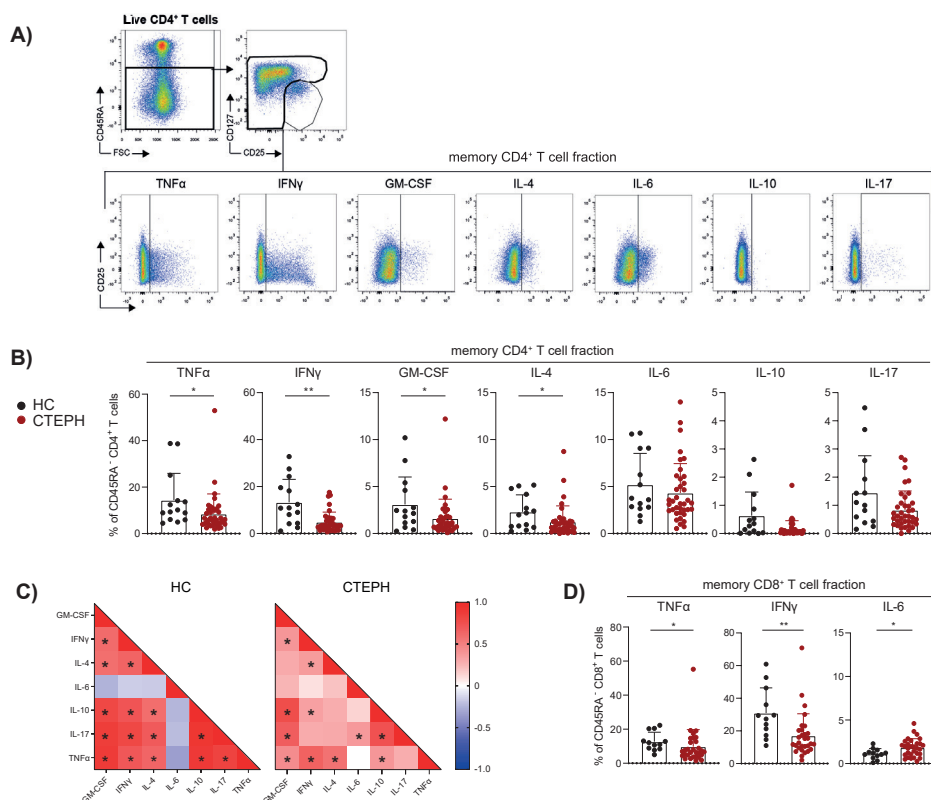


**Figure 4.** CD4<sup>+</sup> and CD8<sup>+</sup> T cells of CTEPH patients display reduced cytokine-producing capacity at diagnosis. (A) Flow cytometric gating strategy of cytokine production by circulating non-Treg CD45RA<sup>-</sup> memory CD4<sup>+</sup> T cells. (B-C) Quantification of the proportions of CD45RA<sup>-</sup> CD4<sup>+</sup> memory T cells expressing the indicated cytokines in HCs and CTEPH patients for CD4 memory

cells (B) and the associated correlation matrixes for cytokine-positive cells (C). Quantification of the proportions of CD45RA<sup>+</sup> CD8<sup>+</sup> T cells expressing the indicated cytokines in CTEPH patients and HCs. Results are presented as mean + standard deviation, Mann-Whitney U test was used for statistical analysis, \* p < 0.05, \*\* p < 0.01. Correlation coefficient was calculated using nonparametric Spearman correlation. Dots represent values of individual patients or HCs.

CD45RA<sup>+</sup> memory CD8<sup>+</sup> T cells from CTEPH patients showed reduced cytokine production, reaching significance for TNF $\alpha$  and IFN $\gamma$ , while their IL-6 production was increased (Figure 4D; Supplementary Figure 5A, 5B). No differences were found in cytokine-producing capacity of CD45RA<sup>+</sup> naive CD8<sup>+</sup> T cells between HCs and CTEPH patients, nor in the cytokine correlation matrix (data not shown). In summary, CD45RA<sup>+</sup>CD4<sup>+</sup> and CD45RA<sup>+</sup>CD8<sup>+</sup> T cells of CTEPH patients are less capable of producing cytokines, whereby correlations between the different cytokines produced by CD4<sup>+</sup> T cells are weaker than in HCs.

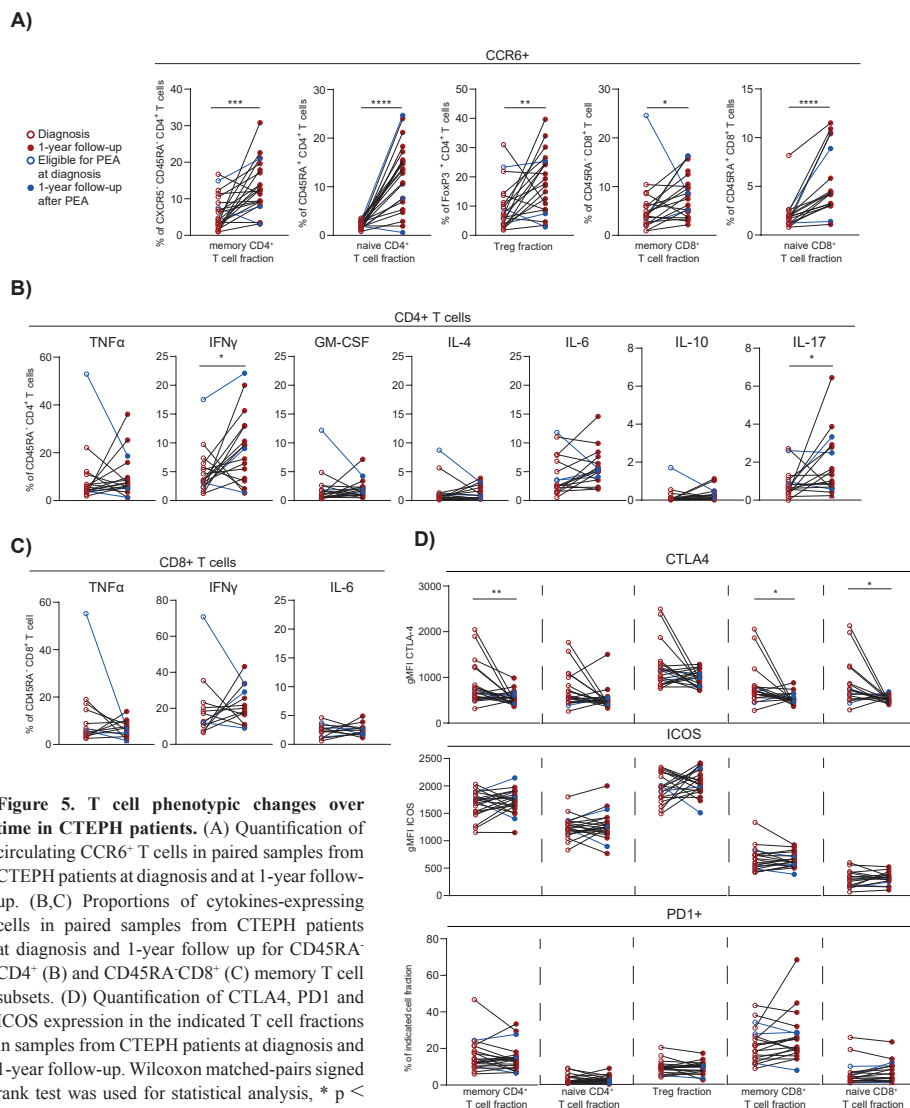


**Figure 5. T cell phenotypic changes over time in CTEPH patients.** (A) Quantification of circulating CCR6<sup>+</sup> T cells in paired samples from CTEPH patients at diagnosis and at 1-year follow-up. (B,C) Proportions of cytokines-expressing cells in paired samples from CTEPH patients at diagnosis and 1-year follow up for CD45RA<sup>+</sup>CD4<sup>+</sup> (B) and CD45RA<sup>+</sup>CD8<sup>+</sup> (C) memory T cell subsets. (D) Quantification of CTLA4, PD1 and ICOS expression in the indicated T cell fractions in samples from CTEPH patients at diagnosis and 1-year follow-up. Wilcoxon matched-pairs signed rank test was used for statistical analysis, \* p < 0.05, \*\* p < 0.01, \*\*\* p < 0.001, \*\*\*\* p < 0.0001. gMFI = geometric mean fluorescence intensity.

Closed and open circles represent values of individual patients at diagnosis or 1-year follow-up, respectively, either not eligible for PEA (red) or eligible for PEA (blue). Paired samples are connected by a line.

## **T cell cytokine profile separates CTEPH patients from HCs and separates CTEPH patients with central and peripheral lesions**

Furthermore, we used PCA to investigate whether besides the T cell subset and activation marker characteristics, cytokine profiles could separate CTEPH patients from HCs (Supplementary Figure 6A). Indeed, cytokine T cell profiles separated patients from HCs in Dim1 to which all cytokines produced by CD4<sup>+</sup> and CD8<sup>+</sup> T cells contributed except IL-6 (Supplementary Figure 6A). A comprehensive PCA analysis that included expression of chemokine receptors, activation markers and cytokine production, showed that HCs were mainly separated from CTEPH patients by cytokine profiles (Supplementary Figure 6B). Given the differences in prognosis and treatment of CTEPH patients with central and peripheral lesions (22), we performed a sub-analysis comparing these two patient groups. We excluded patients with mid lesions eligible for BPA but not for PEA. We found that T cell subset and activation marker profiles did not separate patients with central (n=15) and peripheral (n=9) lesions at diagnosis (Supplementary Figure 7A). However, T cell cytokine profiles (determined in a smaller group of patients; central lesion (n=11) and peripheral lesion (n=6)) did separate the two patient groups in Dim2, largely based on IL-6 production by CD4<sup>+</sup> and CD8<sup>+</sup> T cells and GM-CSF expression by CD8<sup>+</sup> T cells (Supplementary Figure 7B, 7C). We did not find significant correlations between cytokine producing abilities of CD4<sup>+</sup> or CD8<sup>+</sup> T cells and clinical parameters of disease course, such as patient 1-year survival (data not shown).

In conclusion, all T cell cytokines analyzed, except IL-6, constitute a T cell profile that separates CTEPH patients from HCs. In addition, CTEPH patients with central and peripheral lesions could be separated based on IL-6 and GM-CSF production by T cells.

## **Changes in T cell phenotype in CTEPH patients at 1-year follow-up**

Next, we evaluated the T cell profiles of CTEPH patients over time. For this sub-study, we focused on a group of 22 patients of whom we had paired samples at diagnosis and at 1-year follow-up. The increase in CCR6<sup>+</sup> cells in the three CD4<sup>+</sup> T cell fractions analyzed (Figure 1) was significantly more pronounced at 1-year follow-up, especially in the CD45RA<sup>+</sup>CD4<sup>+</sup> (naive) T cells (Figure 5A). An increase was also observed in the CD8<sup>+</sup> T cell fractions.

Cytokine expression remained stable over time for both CD4<sup>+</sup> and CD8<sup>+</sup> T cell populations, except for IFN $\gamma$  and IL-17 in CD4<sup>+</sup> T cells, which were increased at 1-year follow-up (Figure 5B, 5C). CTLA4 expression significantly decreased over time in CD45RA<sup>-</sup>CD4<sup>+</sup> (memory) T cells and in CD8<sup>+</sup> T cells. In contrast, PD1 and ICOS expression were similar for all T cell fractions at the two time points (Figure 5D). Within the follow-up group of 22 patients, three patients underwent a PEA before 1-year follow-up (Figure 5; depicted in blue). The T cell profile of these patients at 1-year follow-up were within the range of the 19 patients who did not undergo a PEA.

These results indicate that at 1-year follow-up, CTEPH patients present with substantial changes in the expression of CCR6, cytokines and activation markers in CD4<sup>+</sup> and CD8<sup>+</sup> T cells, compared to baseline.

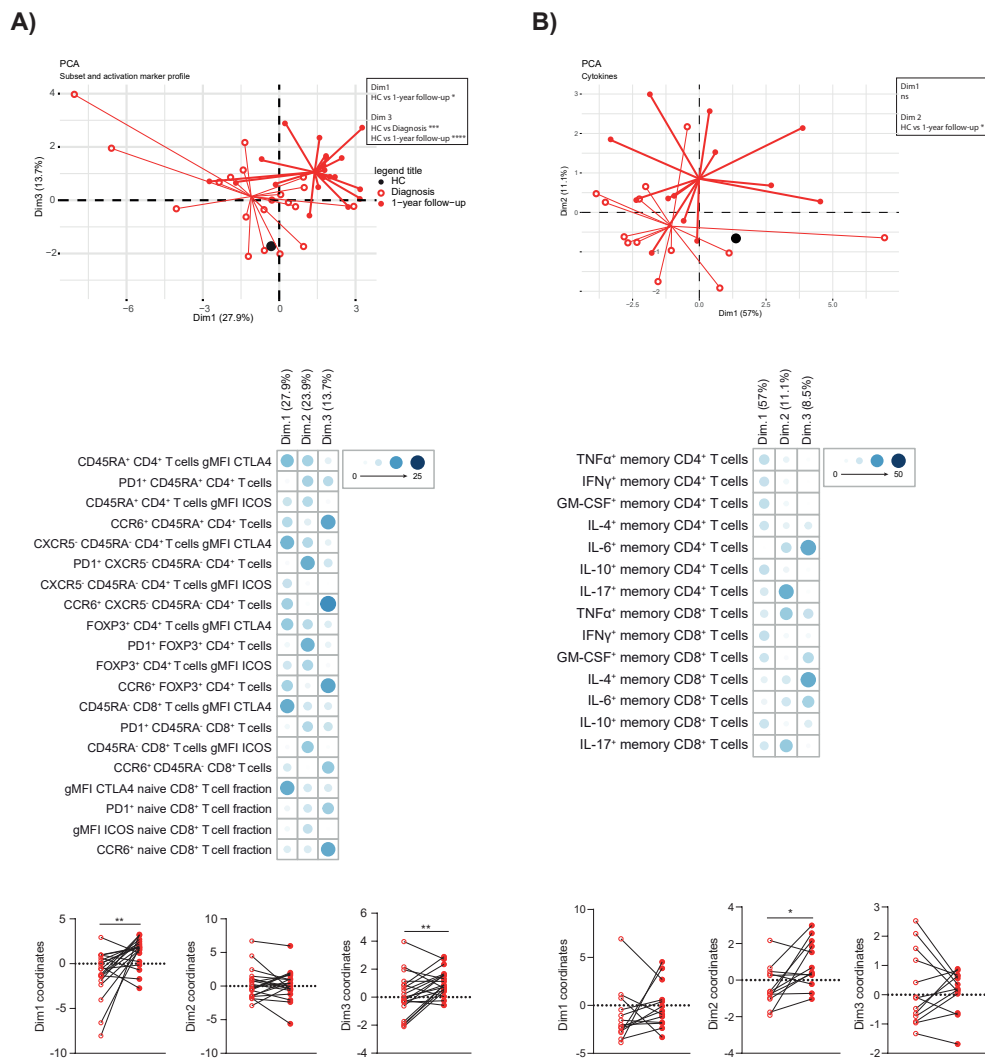


**Figure 6. Multivariate analysis separates CTEPH patients at diagnosis and at 1-year follow-up.** (A,B) Principal component analysis (PCA) of circulating T cell subsets and activation markers (A) or circulating T cell cytokine-producing capacity (B) of CTEPH patients and HCs by flow cytometry at diagnosis and 1-year follow-up. Lines connect the coordinates of individual patient samples to the mean coordinates of the indicated group. Mean coordinates of HCs are depicted by black dots (top). Contribution of the variables in percentages indicated by the blue color range for Dim1, Dim2 and Dim3 of the PCA (middle) and the dimension coordinate values showing the separation between samples of CTEPH patients at diagnosis (open circles) and at 1-year follow-up (closed circles)(bottom). Paired samples are connected by a line. Wilcoxon matched-pairs signed rank test was used for statistical analysis, \*\* p < 0.01.

### **Integration of T cell profile changes of CTEPH patients over time**

Since the T cell profile changed substantially over time, we determined whether PCA would separate CTEPH patients at diagnosis from patients at 1-year follow-up. Indeed, significant differences were observed in Dim1 and Dim3, to which CTLA4 expression and the proportions of CCR6<sup>+</sup> T cells contributed most, respectively (Figure 6A). Likewise, patients at diagnosis and at 1-year follow-up were separated in a PCA based on T cell cytokine profiles, particularly by IL-17 in CD4<sup>+</sup> and CD8<sup>+</sup> T cells and TNF $\alpha$  in CD8<sup>+</sup> T cells in Dim2 (Figure 6B). In these two PCAs the average positions of patient clusters over time did not move towards the position of HCs (Figure 6A, 6B).

Individual PCA analyses of patients with central and with peripheral lesions did not separate patients at diagnosis and at 1-year follow-up, using T cell subsets and activation marker profiles or cytokine expression, likely due to low sample sizes (Supplementary Figure 8A, 8B; data not shown)

Overall, integration of T cell profiles by PCA clearly separated patients at diagnosis from patients at 1-year follow-up.

### **Correlation between phenotype of circulating T cells and inflammatory mediators in plasma from CTEPH patients**

Next, we examined the relationship between the phenotype of circulating T cells and the concentrations of various inflammatory mediators in plasma at diagnosis determined previously (254). Various significant correlations were observed, including a positive correlation between Th17 cells (gated as CCR6<sup>+</sup>CXCR5<sup>+</sup>CD45RA<sup>-</sup>CD4<sup>+</sup> T cells) and CXCL9 (a ligand for CXCR3) (Supplementary Figure 9) of which the plasma levels correlated with patient survival (254). This positive correlation would be consistent with the recent finding that

CXCL9 promoted T17 differentiation in a murine model of liver disease (268). In addition, plasma levels of the anti-inflammatory cytokine IL-10 showed a negative correlation with proportions of intracellular GM-CSF<sup>+</sup>, IL-4<sup>+</sup> and IL-17<sup>+</sup> CD4<sup>+</sup> T cells (Supplementary Figure 9), in line with the capacity of IL-10 to suppress T cell proliferative and cytokine responses (269).

Therefore, the aberrant phenotype of circulating T cells of CTEPH patients at diagnosis displayed correlations with plasma levels of cytokines and chemokines.

### **Vascular lesions of CTEPH patients contain CCR6<sup>+</sup> CD3<sup>+</sup> T cells**

Additionally, we determined the presence of CCR6<sup>+</sup> T cells in paraffin-embedded vascular lesions of 25 CTEPH patients using multiplex immunofluorescence. Vascular lesions of 19 CTEPH patients contained one or more CD3<sup>+</sup> T cell clusters, the majority of which contained CCR6<sup>+</sup> T cells (Figure 7A, Supplementary Figure 10A). T cell clusters were mostly located in organized thrombi and surrounding neo-vasculature, as determined by H&E staining. In the vascular lesions of the remaining 6 CTEPH patients CCR6<sup>+</sup> T cells were present but were more randomly spread in the lesion (Figure 7A). The staining further included CD4, CD8 and FoxP3, enabling the determination of different T cell subpopulations (Figure 7B). Using Qupath quantification, we found that the majority of the CD3<sup>+</sup> T cells were double negative (CD4<sup>-</sup>CD8<sup>-</sup>) T cells, followed by CD4<sup>+</sup> T cells (Figure 7C and Supplementary Figure 10B). CCR6 expression was found on up to 60% of all T cells present, a substantial fraction of which were CD4<sup>+</sup> (Figure 7D).

These findings demonstrate the presence of CCR6<sup>+</sup>CD4<sup>+</sup> T cells in vascular lesions of CTEPH patients, both in T cell clusters and randomly distributed, supporting a role for CCR6<sup>+</sup> T cells in pathology.

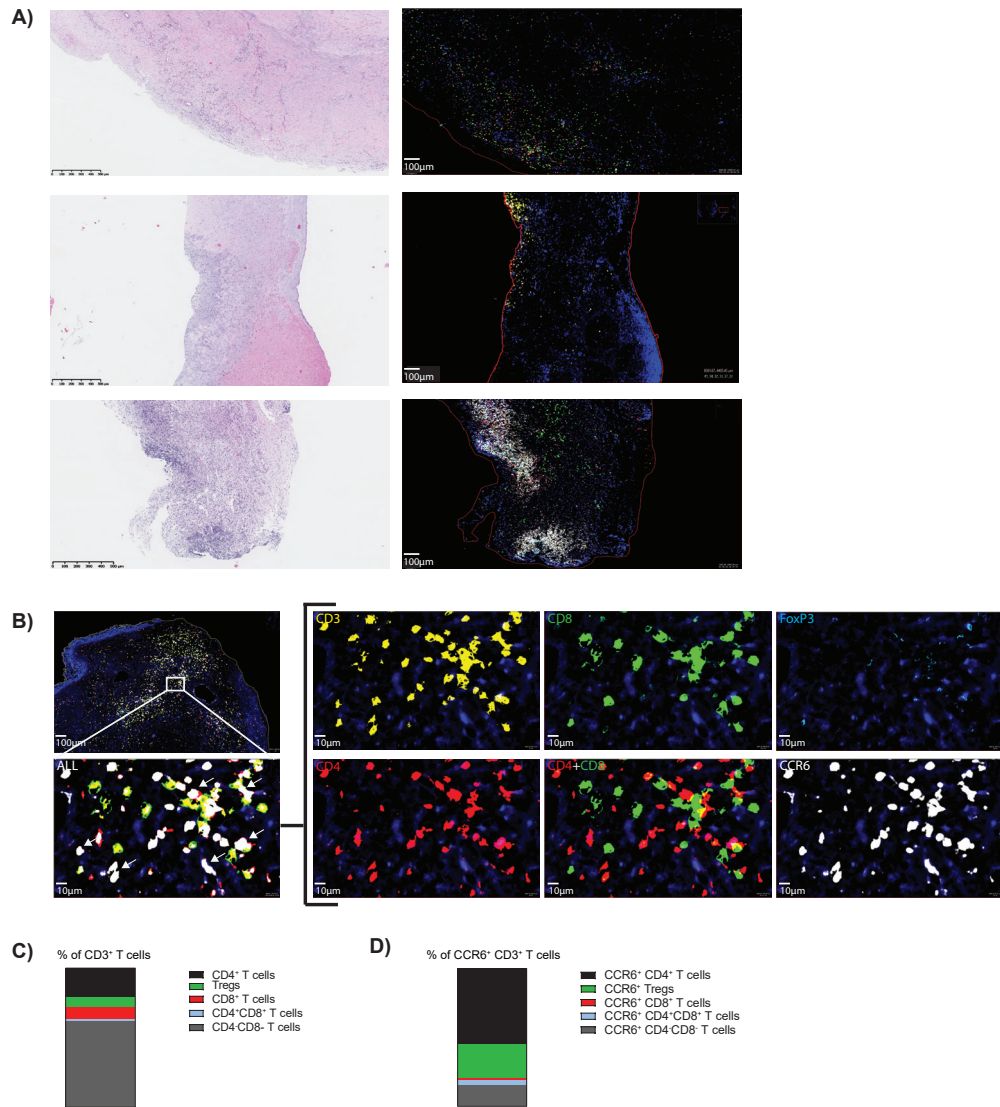


**Figure 7. Vascular lesions of CTEPH patients contain CCR6<sup>+</sup> CD3<sup>+</sup> T cells.** (A) Hematoxylin and eosin (H&E) staining (*left*) and 5-plex immunofluorescent staining of CD3 (yellow), CD4 (red), CD8 (green), FoxP3 (aqua), CCR6 (white) and Dapi (blue) (*right*) in three representative vascular lesions of CTEPH patients. (B) Magnification of the indicated area for immunofluorescent multiplex staining of CD4<sup>+</sup> T cells (CD3+CD4+), CD8<sup>+</sup> T cells (CD3+CD8+) and Tregs (CD3+CD4+FoxP3+) and their CCR6 expression. White arrows (*bottom, left*) indicate examples of CCR6<sup>+</sup> CD3<sup>+</sup> T cells. Scale in overview is 100 µm and in high magnifications 10 µm. (C) Quantification of the proportions of the indicated T cell subpopulations from total CD3<sup>+</sup> T cells. (D) Quantification of the proportions CCR6<sup>+</sup> cells within the indicated T cell subpopulations. Quantifications were by manual thresholding using Qupath in vasculature lesions of 25 CTEPH patients.

## DISCUSSION

Although it is known that T cells are present in thrombotic lesions in the pulmonary vasculature, a detailed characterization of the T cell compartment in CTEPH patients was still lacking. We used flow cytometry to characterize circulating T cells in a well-defined treatment-naïve CTEPH cohort and found that these cells have an abnormal phenotype, compared with HCs. In CTEPH patients we observed (1) that the compartments of naïve CD4<sup>+</sup> and CD8<sup>+</sup> T cells, memory CD4<sup>+</sup> T cells and Tregs contained increased proportions of CCR6<sup>+</sup> cells; (2) that CD4<sup>+</sup> and CD8<sup>+</sup> T cells displayed reduced production of various cytokines, including TNF $\alpha$  and IFN $\gamma$ ; and (3) that in CD4<sup>+</sup> and CD8<sup>+</sup> T cells CTLA4 expression was increased. At 1-year follow-up, we found further increased proportions of CCR6<sup>+</sup> T cells, reduced CTLA4 expression by CD8<sup>+</sup> T cells and memory CD4<sup>+</sup> T cells and increased IFN $\gamma$  and IL-17 production by CD4<sup>+</sup> T cells, compared with baseline values. Finally, we identified CCR6<sup>+</sup> T cells in PEA tissue. They were found to be predominantly CD4<sup>+</sup> T cells and were located in clusters as well as randomly spread over vascular lesions.

The proportions of circulating Th1 and Th2 cells did not differ between CTEPH patients and HCs. In contrast, within the memory CD4<sup>+</sup> T cell population the proportions of CCR6<sup>+</sup> cells were increased, pointing to enhanced T17 cell differentiation. Within the CCR6<sup>+</sup> T cell fraction especially the CXCR3-CCR4<sup>-</sup> DN Th17 cell population was increased in CTEPH patients, compared to HCs. These DN cells reflect a stable Th17-committed cell population that is likely to have pathogenic capacities in autoimmunity (263, 264). Also within the CD45RA<sup>+</sup> FoxP3<sup>-</sup> CD4<sup>+</sup> T cell population, which mainly consists of naïve CD4<sup>+</sup> T cells, the proportions of CCR6<sup>+</sup> cells were significantly increased in CTEPH patients. However, the CD45RA<sup>+</sup> FoxP3<sup>-</sup> CD4<sup>+</sup> T cell population includes next to truly naïve CD4<sup>+</sup> T cells a small population of antigen-experienced effector memory cells re-expressing CD45RA, known as TEMRA cells. Because we observed that in healthy individuals the CCR6<sup>+</sup> CD45RA<sup>+</sup> FoxP3<sup>-</sup> CD4<sup>+</sup> T cell population contained both truly naïve and TEMRA cells (DvU and IMB, unpublished results) it would be interesting to characterize this CCR6<sup>+</sup>CD45RA<sup>+</sup> population in more detail in CTEPH patients and HCs.

Th17 cells are associated with a wide array of inflammatory conditions, including autoimmune diseases, with a strong correlation between CCR6 expression and disease severity (270). Interestingly, Th17-linked systemic autoimmune diseases including systemic sclerosis and systemic lupus erythematosus, are associated with PAH (271). Moreover, CD4<sup>+</sup> T cells from idiopathic (I)PAH patients express higher levels of IL-17 and in circulating white blood cells the *IL17* gene is hypomethylated, supporting a role of Th17 cells in PAH pathology (195). Polarization of Th17 cells is promoted by IL-6 in combination with IL-1 $\beta$  and TGF $\beta$ , indicating an important role for IL-6 in PH. Indeed, IL-6 levels are increased in serum of IPAH patients and transgenic mouse models show that IL-6 overexpression induces PH and, conversely, IL-6 deficiency protects against hypoxia-induced PH (94, 117, 120). In plasma of CTEPH patients, IL-6 was also found to be increased (32). CCR6 expression enables Th17 cells to migrate towards inflamed tissues in response to its ligand CCL20. Accordingly, we found CCR6<sup>+</sup> T cells in clusters as well as randomly spread in PEA tissue. These T cell clusters were more often located in organized thrombi than in newly formed thrombi. It is conceivable that immune cell clusters contribute to increased clotting, leading to the progression of the lesion. The T cells surrounded neo-vasculature, suggesting that part of the increased circulating CCR6<sup>+</sup> T cells migrate towards the pulmonary arteries via this neo-vasculature into the organized thrombi. Further experiments are required to test this hypothesis. Lung CCL20 mRNA levels were found to be increased

in IPAH patients, compared with controls (33) and increased CCL20 expression was associated with accumulation of CCR6<sup>+</sup> and IL-17<sup>+</sup> CD4<sup>+</sup> T cells (94, 117). In this regard, it would be informative to determine CCL20 expression in thrombotic lesions of CTEPH patients. The striking parallels between PAH and CTEPH would support a role of Th17 cells in the etiology of both diseases, even though they are different disease entities. It remains however unknown which mechanisms contribute to the increase in CCR6<sup>+</sup> Th17-lineage-associated CD4<sup>+</sup> and CD8<sup>+</sup> T cells in CTEPH. One of these may involve CXCL9, which has the capacity to promote Th17 differentiation (268), because we found a positive correlation between plasma levels of CXCL9 and peripheral blood Th17 cell frequencies.

Another intriguing parallel may be drawn with atherosclerosis, a chronic inflammatory arterial disease with plaque build-up in vascular lesions (272). In atherosclerosis patients, serum IL-17 and circulating Th17 cells were increased and infiltrates of IL-17-producing cells were found in atherosclerotic plaques (273). Moreover, in mouse models Th17 cells play a causative role in atherosclerosis development (274). This resemblance is striking, given the difference in embryonic origin of the pulmonary and systemic arteries affected in atherosclerosis (275).

At 1-year follow-up we observed increased production of IFN $\gamma$  and IL-17 by CD4<sup>+</sup> T cells and a significant further increase of the proportions of CCR6<sup>+</sup> T cells. Since circulating Th1 cells were unaltered, it is attractive to speculate that the increased IFN $\gamma$  production was linked to CCR6<sup>+</sup> IFN $\gamma$ /IL-17 double-producing Th17.1 cells (237, 266). It remains unknown if the T cell profile changes seen at 1-year follow-up were a consequence of disease progression, medication, recovery after treatment or a combination of these. Although specific PAH and CTEPH medication, such as endothelin receptor antagonists, can affect inflammatory processes (276, 277), it is unknown whether this medication affects Th17 cell differentiation or function.

Because increased CTLA4 expression can be linked to T cell exhaustion and limited DC-T cell interaction (267), it is conceivable that increased CTLA4 expression by CD4<sup>+</sup> T cells contributes to the reduced cytokine-producing capacity of CD4<sup>+</sup> T cells in CTEPH patients. Conversely, the decrease in CTLA4 expression at 1-year follow-up may explain the increased cytokine-producing capacity at 1-year follow-up.

Our study did not provide evidence for defects in FoxP3<sup>+</sup> Tregs in CTEPH patients, except that frequencies of CCR6<sup>+</sup> Tregs were increased, allowing them to migrate towards inflamed tissues. Indeed, we found CCR6<sup>+</sup> Tregs in vascular lesions of CTEPH patients. The aberrant CD8<sup>+</sup> T cell phenotype seen in CTEPH patients, akin to changes in CCR6, CTLA4 and cytokine expression found in CD4<sup>+</sup> T cells, suggests that CD8<sup>+</sup> T cells are involved in the pathogenesis of CTEPH as well. This would parallel reported findings indicating a pathogenic role of IL-17-producing CD8<sup>+</sup> T cells in several autoimmune and lung diseases (258).

Our multivariate analysis based on the cytokine-producing capacity of T cells significantly separated CTEPH patients with central lesions from patients with peripheral lesions. Nevertheless, one of the limitations of our study may be that in our cohort a relatively low proportion of patients had central lesions and was therefore technically eligible for a PEA (~39%, versus ~64% in reported cohorts (240)). This makes it difficult to draw firm conclusions regarding the effects of surgery. BPA is a rather new treatment modality and few patients in our cohort underwent a BPA within 1-year follow-up. Finally, besides differences in IL-6 and GM-CSF production we did not find differences in the T cell profiles of patients with central versus peripheral lesions. This may be due to the relatively small number of patients in these subgroups.

Taken together, we found a significant increase in circulating Th17-associated CCR6<sup>+</sup> T cells in CTEPH patients. Moreover, in vascular lesions CCR6<sup>+</sup> T cells were found randomly spread as well as in T cell clusters. This specific CCR6<sup>+</sup> profile of T cells would indicate a role of these cells in disease pathophysiology. This knowledge may help to explore avenues for the development of novel treatment strategies.

#### **Conflict of Interest**

All authors declare no conflict of interest. The funders had no role in the design of the study, data collection, analyses, writing of the manuscript or in the decision to publish the results.

#### **Author Contributions**

DvU, MK, RWH and KAB conceived the project and designed the experiments. DvU, TK, JACvH, TPPvdB, MV, IMB, KAL, JHvdT generated data or tools for the project. AEB, PB, JHvdT, KAB included material or patients for our study. DvU, TK, RWH and KAB wrote the manuscript. All authors read, provided valuable feedback and approved the final manuscript.

#### **Funding**

This research was funded by the Dutch Heart Foundation under grant number 2016T052 (DvU/MK), and partially supported by an unrestricted grant from Ferrer pharmaceuticals (grant number not applicable), Actelion Pharmaceuticals (grant number not applicable), and the Pulmonary Hypertension Patients Association (grant number not applicable) (TK).

#### **Acknowledgments**

We would like to thank Menno van Nimwegen, Leon van den Toorn, Prewesh Chandoesing and Odilia Corneth for their valuable contribution.

#### **Data Availability Statement**

The data presented in this study are available in this article or upon reasonable request.

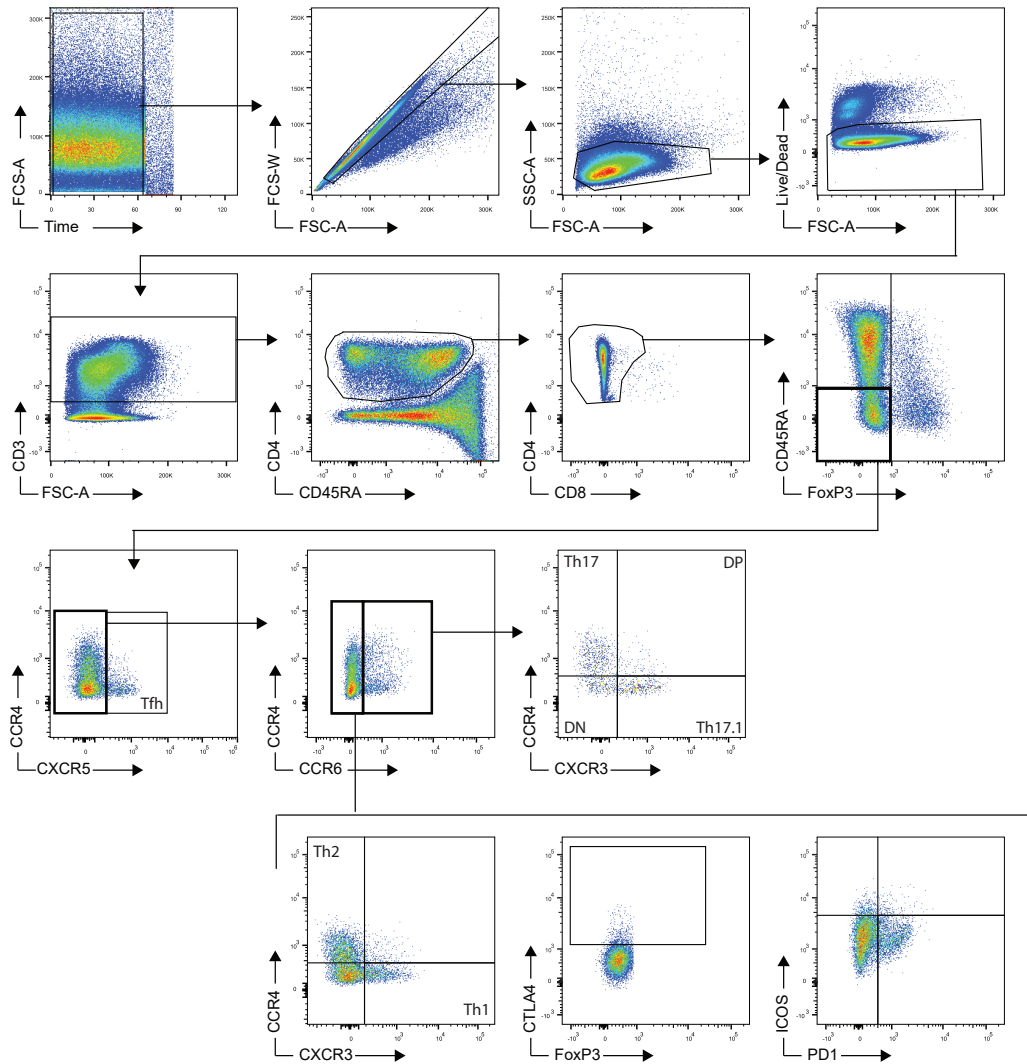
**SUPPLEMENTARY MATERIAL****Supplementary Table 1.** Monoclonal antibodies used for flow cytometry.

<b>Antibody</b>	<b>Conjugate</b>	<b>Clone</b>	<b>Company</b>
CD4	FITC	Okt4	Biologend
CD45RA	BV650	HI100	BD
CD3	Biotin	UCHT	eBioscience
CD8	AF700	SK1	Biologend
CD25	Pe-Cy7	M-A251	BD
CD127	BV421	A019D5	Biologend
Streptavidin	BV605	-	BD
IL-10	PCP	JES3-9D7	Biologend
IL-4	APC-Cy7	MP4-25D2	Biologend
IL-6	PE	MQ2-13A5	eBioscience
IFN $\gamma$	BV711	B27	BD
IL-17a	BV786	N49-653	BD
TNF $\alpha$	APC	6401.111	BD
GM-CSF	PE TxR	BVD2-21C11	BD
CCR4	FITC	-	R&D
CD45RA	PE TxR	MEM-56	Life technology
CD4	PercPcy5.5	RPA-T4	Invitrogen
CXCR5	Pe-Cy7	MU5UBEE	eBioscience
ICOS	BV650	C3984A	Biologend
CXCR3	BV711	1C6/CXCR3	BD
PD1	BV786	EH12.1	BD
CCR6	APC	11A9	BD
CD3	APC-Cy7	UCHT1	Invitrogen
FoxP3	PE	236A/E7	Invitrogen
CTLA4	BV421	BNI3	BD

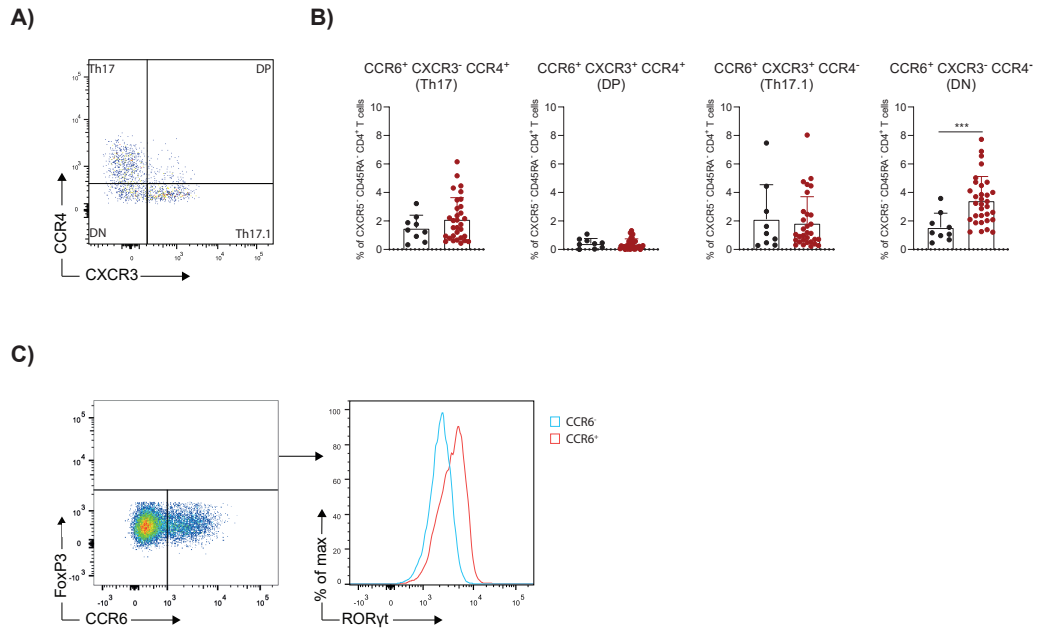
**Supplementary Table 2.** Antibodies used for multiplex immunofluorescence.

<b>Antibody</b>	<b>Clone</b>	<b>Company</b>	<b>Cat number</b>	<b>Concentration</b>
CD3	2GV6	Ventana	790-4341	0.4 ug/ml
CD4	SP35	Ventana	790-4423	2.5 ug/ml
CD8	SP57	Ventana	790-4460	0.35 ug/ml
FOXP3	236A/E7	eBioscience	14-4777-82	1/100
CCR6	polyclonal	Atlas Antibodies	HPA014488	1/50

**SUPPLEMENTARY FIGURES**

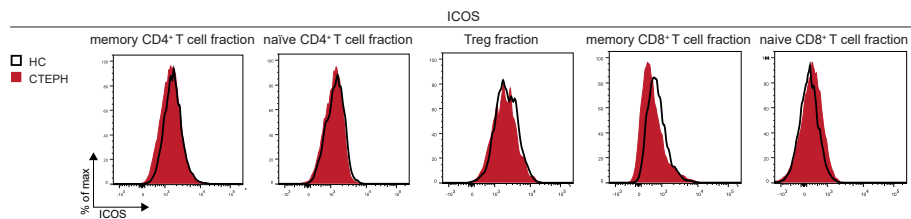


**Supplementary Figure 1. Gating strategy for peripheral T cell populations.** Flow cytometric gating strategy of chemokines and activation markers of peripheral blood mononuclear cells

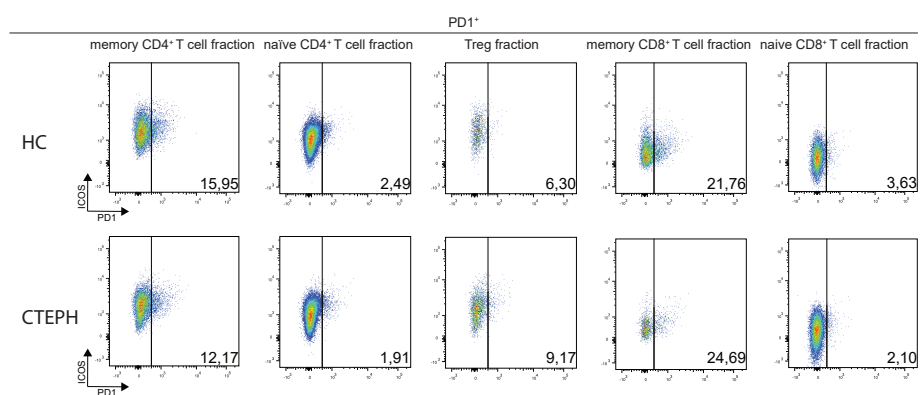


**Supplementary Figure 2. Proportion of DN CCR6<sup>+</sup> T cells are significantly increased in CTEPH patients at diagnosis.** (A) Flow cytometric gating strategy of CXCR3-CCR4<sup>+</sup> Th17, CXCR3<sup>+</sup>CCR4<sup>-</sup> Th17.1, CXCR3<sup>+</sup>CCR4<sup>+</sup> and CXCR3-CCR4<sup>-</sup> cells within CCR6<sup>+</sup> memory CD4<sup>+</sup> T cells. (B) Quantification of Th17, double positive (DP), Th17.1 and double negative (DN) CCR6<sup>+</sup> CD45RA<sup>-</sup> FOXP3<sup>-</sup> CD4<sup>+</sup> T cells. (C) Quantification of RORγt within CCR6<sup>-</sup> and CCR6<sup>+</sup> CD45RA<sup>-</sup> FOXP3<sup>-</sup> CD4<sup>+</sup> T cells. Results are presented as mean + standard deviation, Mann-Whitney U test was used for statistical analysis. Symbols represent values of individual patients or HCs.\*\*\*= p<0.001.

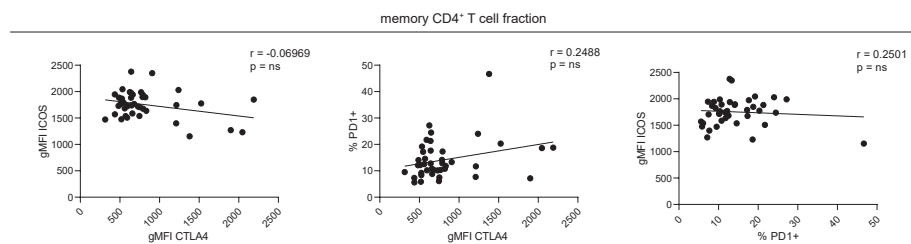
A)



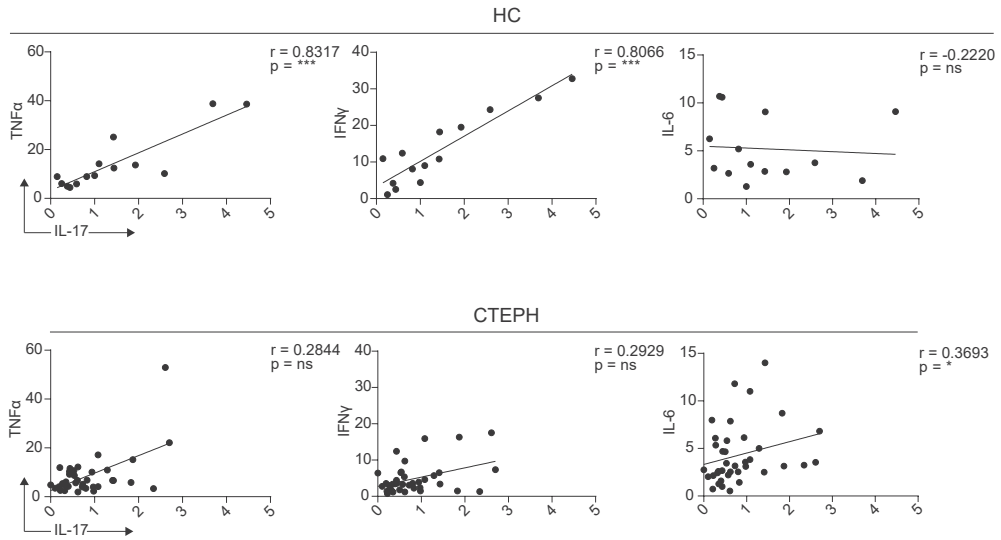
B)



C)

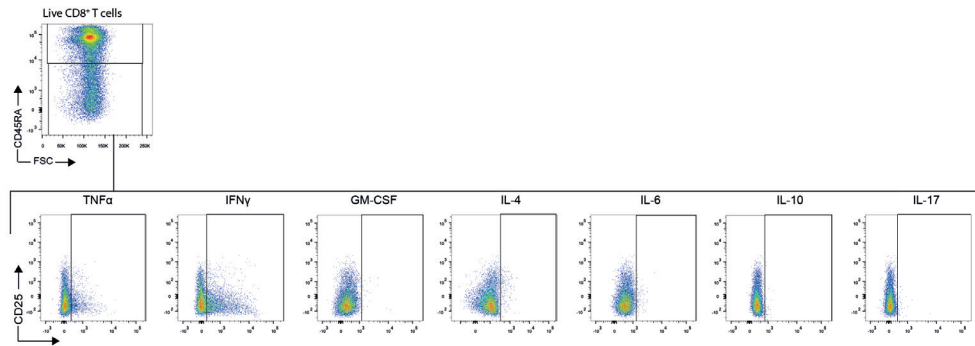


**Supplementary Figure 3. Analysis of activation markers on CD4<sup>+</sup> and CD8<sup>+</sup> T cell fractions in CTEPH patients at diagnosis.** (A) Flow cytometry analysis of ICOS shown as histogram overlays. (B) Flow cytometry analysis of ICOS and PD1 expression for the indicated T cell fractions, percentages of PD1<sup>+</sup> cells is given. (C) Correlation between CTLA4, PD1 and ICOS on CXCR5<sup>+</sup>CD45RA<sup>-</sup> CD4<sup>+</sup> memory T cells. Correlation coefficients were calculated using nonparametric Spearman correlation, \* $p < 0.05$ , \*\* $p < 0.01$ , \*\*\* $p < 0.001$ . gMFI = geometric mean fluorescence intensity. Symbols represent values of individual patients or HCs.

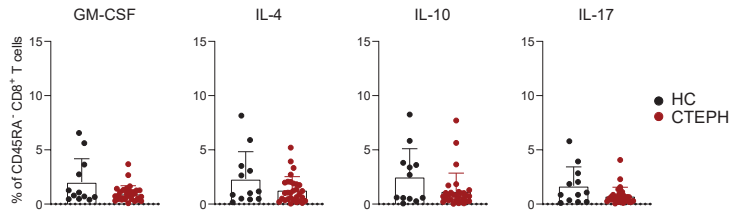


**Supplementary Figure 4. IL-17 expression is correlated with TNF $\alpha$  and IFN $\gamma$  expression in memory CD4<sup>+</sup> T cells in HCs but not in CTEPH patients at diagnosis.** Correlation of IL-17<sup>+</sup> CD45RA<sup>-</sup> CD4<sup>+</sup> memory T cells with TNF $\alpha$ <sup>+</sup>, IFN $\gamma$ <sup>+</sup> and IL-6<sup>+</sup> CD45RA<sup>-</sup> CD4<sup>+</sup> T cells in HC and CTEPH patients. Correlation coefficients were calculated using nonparametric Spearman correlation, \*p<0.05, \*\*p<0.01, \*\*\* p< 0.001. Symbols represent values of individual patients or HCs.

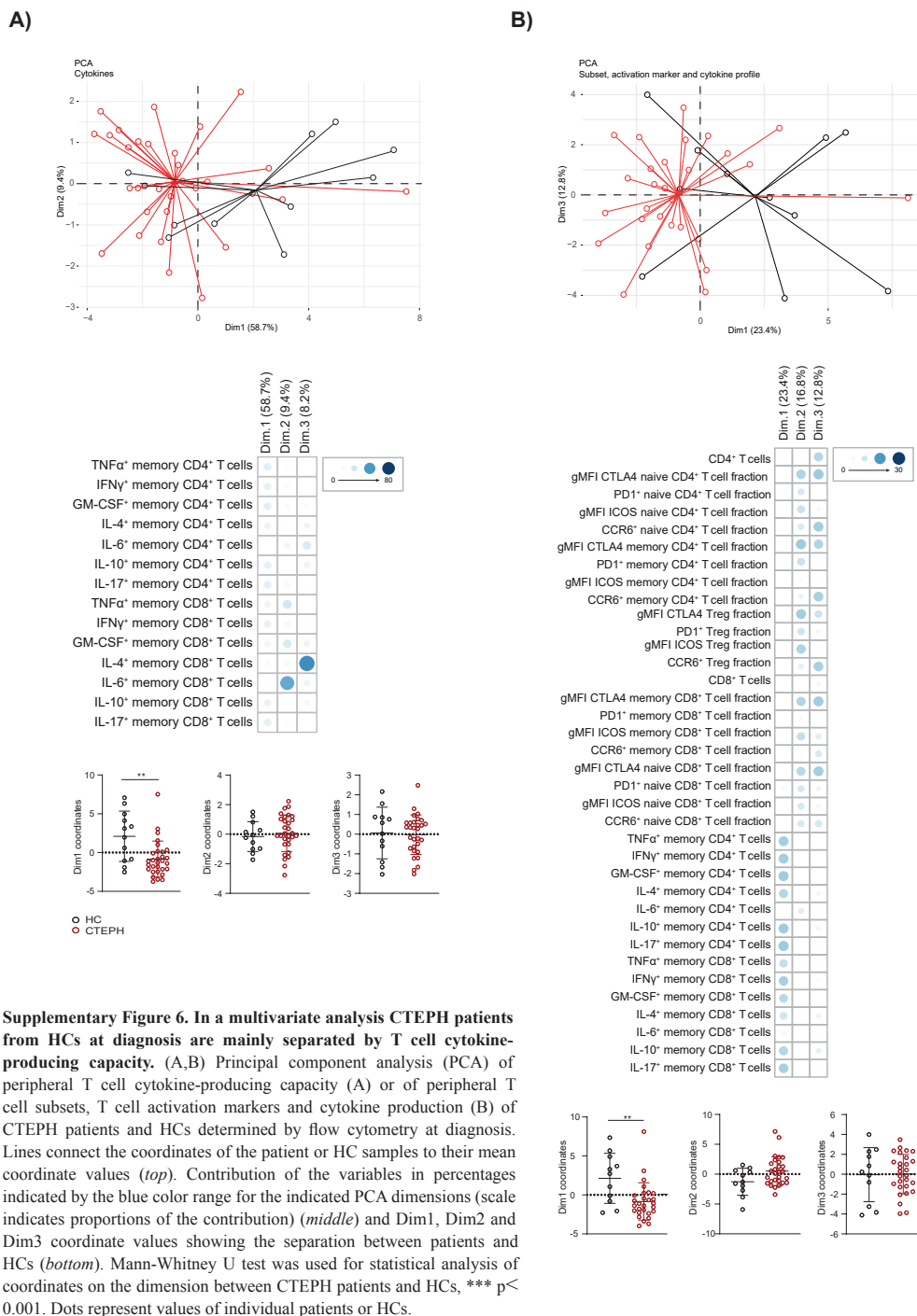
**A)**

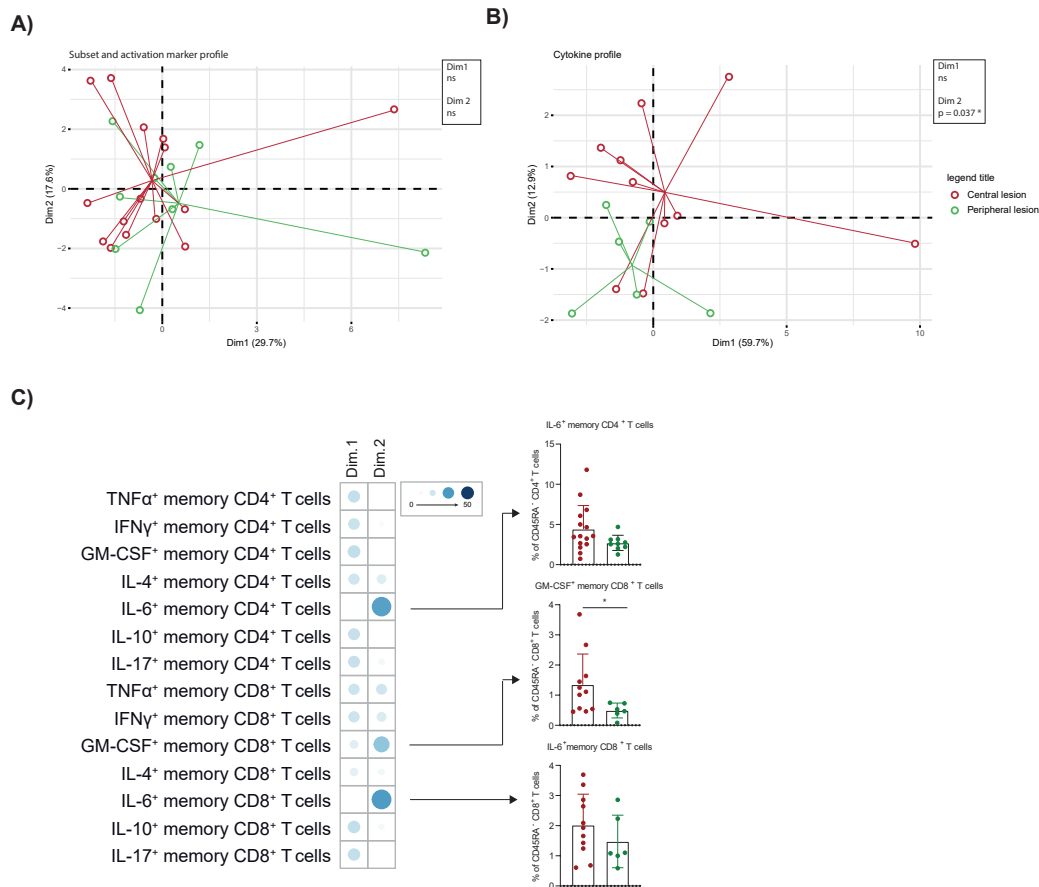


**B)**



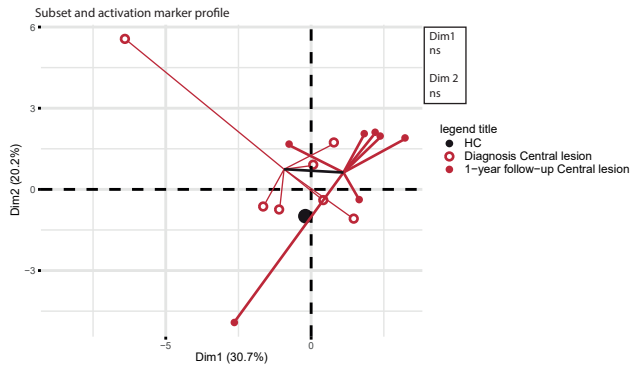
**Supplementary Figure 5. Proportion of GM-CSF<sup>+</sup>, IL-4<sup>+</sup>, IL-10<sup>+</sup> and IL-17<sup>+</sup> CD45RA<sup>-</sup> CD8<sup>+</sup> T cells do not differ between CTEPH patients and HCs at diagnosis.** (A) Flow cytometric gating strategy of cytokine production by circulating CD45RA<sup>-</sup> memory CD8<sup>+</sup> T cells. (B) Quantification of cytokines GM-CSF, IL-4, IL-10 and IL-17 in CD45RA<sup>-</sup> CD8<sup>+</sup> T cells. Results are presented as mean + standard deviation, Mann-Whitney U test was used for statistical analysis. Symbols represent values of individual patients or HCs.



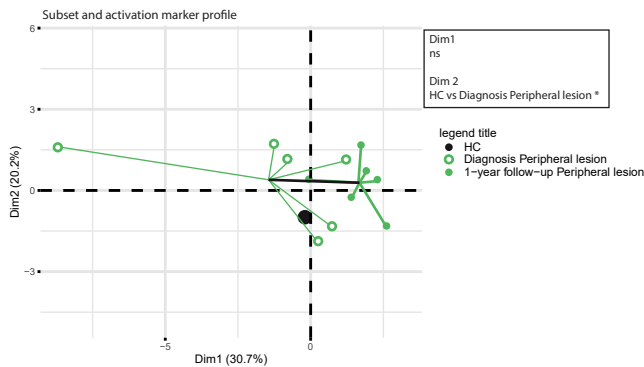


**Supplementary Figure 7. IL-6 and GM-CSF production by T cells separates CTEPH patients with central lesions from CTEPH patients with peripheral lesions at diagnosis in multivariate sub-analysis.** (A,B) Principal component analysis (PCA) of peripheral T cell subsets and T cell activation markers (A) or T cell cytokine-producing capacity (B) of CTEPH patients with central or peripheral lesions at diagnosis. Lines connect the coordinates of the patient samples to their mean coordinate values. (C) Contribution of the variables in percentages indicated by the blue color range for Dim1, Dim2 and Dim3 of the PCA (scale indicates proportions of the contribution). On the right-side flow cytometry analysis of IL-6<sup>+</sup> CD4<sup>+</sup> and CD8<sup>+</sup> T cells and GM-CSF<sup>+</sup> CD8<sup>+</sup> T cells. Results are presented as mean + standard deviation, Mann-Whitney U test was used for statistical analysis between CTEPH patients and HCs, \*\*p<0.01, \*\*\* p< 0.001. Red circles represent individual CTEPH patients with central lesions and green circles represent CTEPH patients with peripheral lesions.

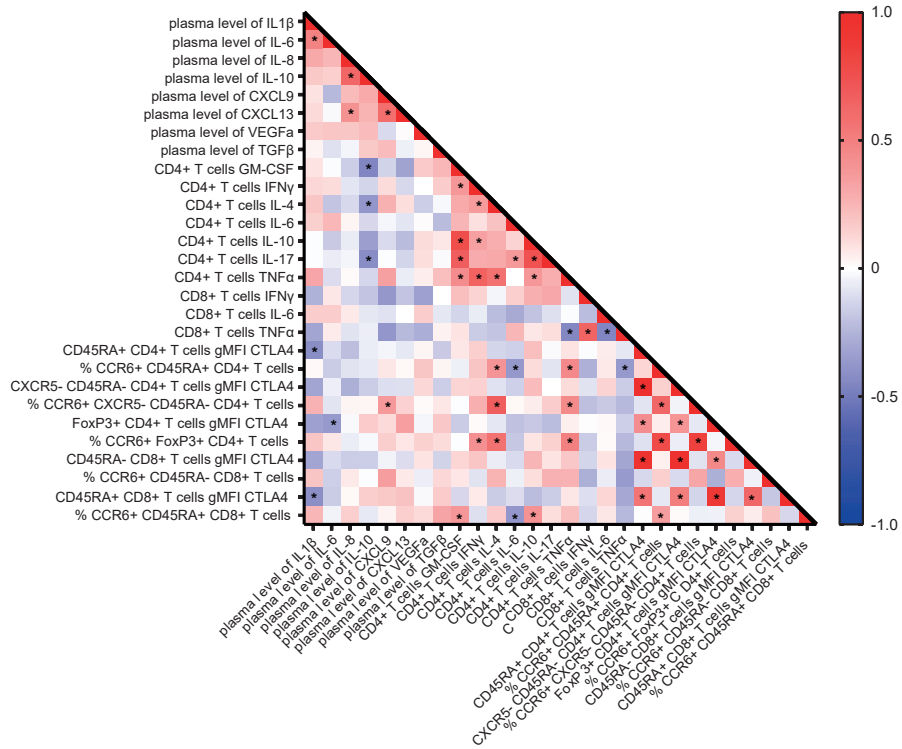
**A)**



**B)**

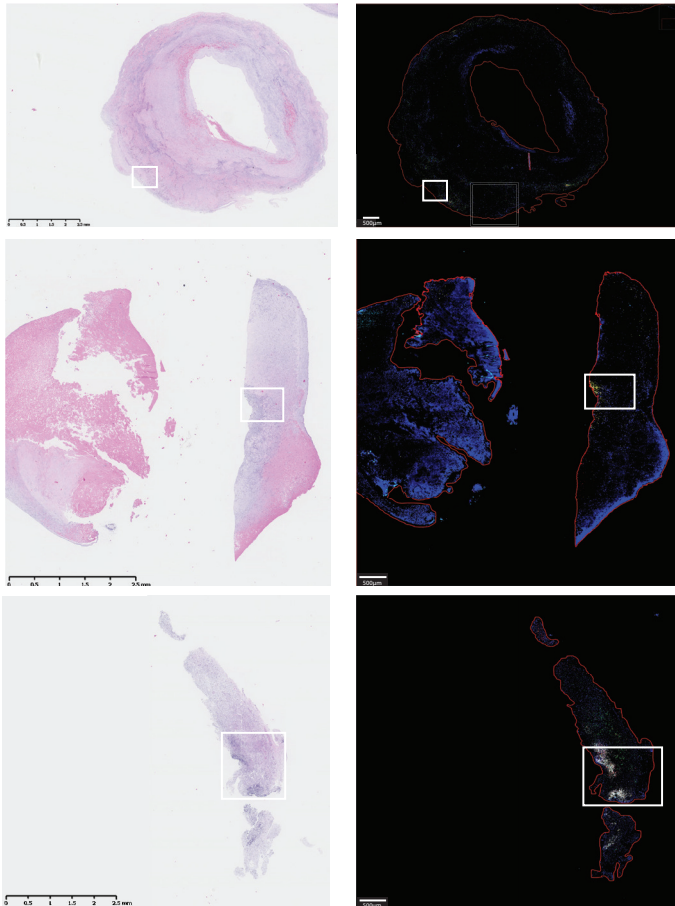


**Supplementary Figure 8. PCA does not distinguish CTEPH patients at diagnosis from patients at 1-year follow-up in a separate analysis of patients with central and peripheral lesions.** (A,B) Principal component analysis (PCA) of peripheral T cell subsets and T cell activation markers of CTEPH patients with central (A) or peripheral lesions (B) at diagnosis or 1-year follow-up and HCs determined by flow cytometry. Lines connect the coordinates of the patient samples to their mean coordinate values. Mann-Whitney U test was used for statistical analysis of coordinates on Dim1 and Dim2 between CTEPH patients and HCs, \*\* $p < 0.01$ , \*\*\* $p < 0.001$ . Open circles represent individual CTEPH patients at diagnosis and closed circles represent individual CTEPH patients at 1-year follow-up. Black symbols indicate mean coordinates of HCs.



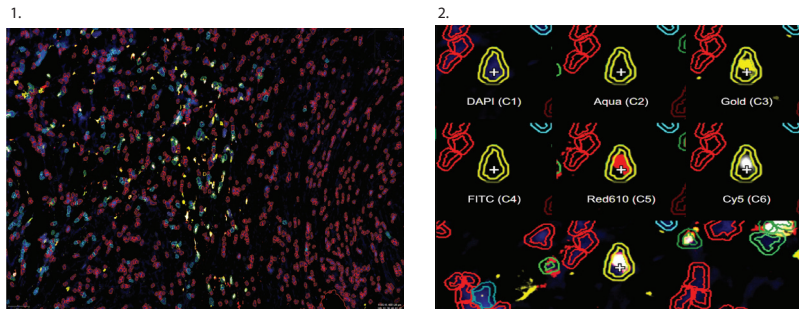
**Supplementary Figure 9. Correlation of phenotype of circulating T cells and plasma levels of inflammatory mediators in CTEPH patients.** Correlation Matrix of plasma levels of the indicated cytokines, chemokines and vascular growth factors and flow cytometry data of CD4<sup>+</sup> and CD8<sup>+</sup> T cells of CTEPH patients. Scale indicates correlation coefficient. Correlation coefficient was calculated using nonparametric Spearman correlation, \*p<0.05.

A)



5

B)



**Supplementary Figure 10. Immunofluorescence multiplex staining to determine CCR6<sup>+</sup> T cells in vascular lesions of CTEPH patients.** (A) Overview of hematoxylin and eosin (H&E) staining (*left*) and 5-multiplex staining (*right*) of selected areas for main Figure 8. (B) Example illustrating the method used to identify cells (*panel 1, left*) and determine marker positivity by manual thresholding (*panel 2, right*) in Qupath.



# CHAPTER 6

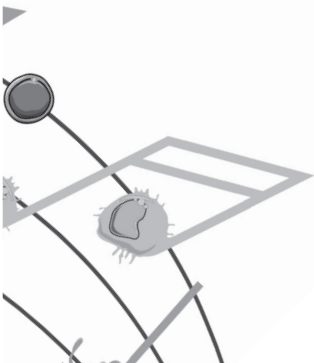
*Peripheral blood T cells of patients with IPAH have a reduced cytokine-producing capacity.*

D. van Uden, **T. Koudstaal**, J.A.C. van Hulst, M. Vink, M. van Nimwegen, L.M. van den Toorn, P.P. Chandoesing, A.E. van den Bosch, M. Kool, R.W. Hendriks\*, K.A. Boomars\*

\*Contributed equally.

Int. J. Mol. Sci. 2022, 23(12), 6508.

6



## ABSTRACT

Pulmonary arterial hypertension (PAH) is rare disease that is categorized as idiopathic (IPAH) when no underlying cause can be identified. Lungs of most patients with IPAH contain increased numbers of T cells and dendritic cells (DCs), suggesting involvement of the immune system in its pathophysiology. However, our knowledge on circulating immune cells in IPAH is rather limited. We used flow cytometry to characterize peripheral blood DCs and T cells in treatment-naive IPAH patients, compared with connective-tissue disease-PAH (CTD-PAH) patients and healthy controls (HCs). At diagnosis, T-helper (Th) cells of IPAH patients were less capable of producing TNF $\alpha$ , IFN $\gamma$ , IL-4 and IL-17 compared to HCs. IPAH patients showed a decreased frequency of Th2 cells and significantly enhanced expression of the CTLA4 checkpoint molecule in naive CD4<sup>+</sup> T cells and both naive and memory CD8<sup>+</sup> T cells. Frequencies and surface marker expression of circulating DCs and monocytes were essentially comparable between IPAH patients and HCs. Principal component analysis (PCA) separated IPAH patients—but not CTD-PAH patients—from HCs, based on T-cell cytokine profiles. At 1-year follow-up, the frequencies of IL-17<sup>+</sup> production by memory CD4<sup>+</sup> T cells were increased in IPAH patients and accompanied by increased proportions of Th17 and Tc17 cells, as well as decreased CTLA4 expression. Treatment-naive IPAH patients displayed a unique T-cell phenotype that was different from CTD-PAH patients and was characterized by reduced cytokine-producing capacity. These findings point to involvement of adaptive immune responses in IPAH, which may have an implication for the development of therapeutic interventions.

## INTRODUCTION

WHO group 1 pulmonary arterial hypertension (PAH) is defined as a condition with a mean pulmonary artery pressure (mPAP) > 20 mmHg, normal left atrium pressure and pulmonary vascular resistance  $\geq 3$  Wood units (1). PAH is a devastating condition with a high burden of disease. Patients with PAH are subdivided into subgroups based on different risk factors or underlying conditions, such as connective tissue disease (CTD). A special subgroup of PAH patients has no known risk factor or underlying disease and is therefore categorized as idiopathic PAH (IPAH).

Currently, accumulating evidence is beginning to reveal an important role for the adaptive immune system in the pathogenesis and progression of PAH (24, 215).

IPAH lung biopsies were shown to contain increased numbers of CD4<sup>+</sup> T-helper (Th) cells, CD8<sup>+</sup> cytotoxic T (Tc) cells and TCR $\gamma\delta$  T cells, which were found in close proximity to blood vessels (34, 55). Likewise, increased peri-arterial Th cells were found in patients with schistosomiasis-associated PAH (90).

Regarding the various currently defined Th subsets (See Supplementary Table S1 for overview), particularly Th17 have been implicated in PAH pathogenesis. Th17 cells are known to play an important role in many inflammatory and autoimmune diseases (91, 237) and were found in pulmonary tertiary lymphoid organs (TLOs) of IPAH patients (33). Furthermore, activated Th cells of PAH patients expressed higher levels of IL-17 (195). Th17 cells are an important source of the pro-inflammatory cytokines IL-17 and IL-22 and differentiate from naive Th cells in the presence of IL-1 $\beta$ , IL-6, and TGF- $\beta$  (93). The finding that both IL-1 $\beta$  and IL-6 are increased in the serum of IPAH patients compared to controls (94) would be in line with a role of Th17 cells in IPAH pathophysiology. Finally, we recently reported increased polarization of circulating follicular T helper (Tfh) cells towards a Th17-associated surface phenotype in IPAH patients (278). A role for Tfh would also be supported by the finding of an increase in IL-21<sup>+</sup> PD-1<sup>+</sup> Tfh cells in TLOs and around pulmonary arteries of IPAH patients (33).

Next to the findings that implicate Th17 and Tfh cells, evidence is accumulating for compromised activity of regulatory T cells (Tregs) in the inflammatory milieu of PAH lungs. Aberrant Treg function is strongly correlated with a predisposition to PAH in patients and frequencies of Tregs were found to be increased in circulation (198, 279, 280). An imbalance in Th17/Tregs cells influenced the prognosis in patients with CTD-PAH, pointing to clinical relevance of the Th17 and Tregs populations (95).

Opposite to lung tissue, in IPAH patients CD8<sup>+</sup> T cells are decreased in circulation and present mostly with an effector memory phenotype (198, 281).

Various recent findings support the involvement of B cells in IPAH. First, circulating plasma blasts are increased in IPAH patients (100). Second, autoantibodies are present in approximately 40% of the IPAH patients (101). These autoantibodies, recognizing endothelial cell surface antigens (102), are thought to be produced by plasma cells located within TLOs in IPAH lungs (33, 100). Third, we recently reported increased B cell receptor (BCR) signalling in circulating B cells in IPAH patients (278). Moreover, we found that pulmonary injury in combination with enhanced B cell activation is sufficient to induce PH symptoms in mice (278).

Consistent with the involvement of adaptive immune responses in IPAH, also dendritic cells (DCs), which are critical for T cell activation, have been implicated in its pathology. In the lungs of IPAH patients, the numbers of conventional DCs (cDCs) and plasmacytoid DCs (pDCs) are increased, whereby pDCs were localised predominantly in the alveolar space in proximity to vessels (55). In

peripheral blood of IPAH patients, cDC numbers were decreased (282). Together with the increase in pulmonary cDCs, this suggests enhanced migration into the lungs. In our mouse studies, specific activation of cDCs resulted in the development of PH symptoms, whereby cDCs were specifically localized in the lungs and right ventricle of the heart (213, 261).

However, despite the evidence for their involvement in PAH pathogenesis, the characterization of circulating T cells and DCs in IPAH patients is limited, the effects of PAH-specific therapy on T cells have also not been investigated. Therefore, we aim to characterize the circulating T cell and DC compartment in patients with IPAH in detail. We investigate the cytokine-producing capacity, activation marker expression and subset distribution of both CD4<sup>+</sup> and CD8<sup>+</sup> T cells in treatment-naive IPAH patients and after one year of PAH-specific treatment. Next to healthy individuals, we analyse patients with CTD-PAH, who show clear involvement of the adaptive immune system, given the increase in Th17 cells (95) and the presence of autoantibodies (283). Thus, we have the opportunity to identify possible overlapping pathophysiological features of the two PAH diseases.

## RESULTS

### **T Cells from Treatment-Naive IPAH Patients Show Reduced Cytokine-Producing Capacity**

We investigated peripheral blood T cells in 15 treatment-naive IPAH and 24 CTD-PAH patients (Table 1), as well as 17 HCs. Cytokine production was analysed in CD45RA<sup>-</sup> memory CD4<sup>+</sup> and CD8<sup>+</sup> T cell fractions, containing the T cells most prone to produce cytokines. Hereby, CD127<sup>low</sup>CD25<sup>high</sup> CD4<sup>+</sup> Tregs were excluded and analysed separately (see Figure 1A for the gating strategy and cytokine production of CD4 cells).

**Table 1.** Baseline demographic and patient characteristics.

	PAH—BASELINE			PAH—1Y FOLLOW-UP		
	IPAH ( <i>n</i> = 15)	CTD-PAH ( <i>n</i> = 24)	<i>p</i> Value	IPAH ( <i>n</i> = 11)	CTD-PAH ( <i>n</i> = 12)	<i>p</i> Value
<b>Baseline clinical characteristics</b>						
Gender, female (%)	13 (87%)	20 (83%)		10 (91%)	11 (92%)	
Age, y	55.6 ± 16.7	64.6 ± 11.2	0.15	60.8 ± 14.8	65.3 ± 12.2	0.59
BMI, kg/m <sup>2</sup>	28.4 ± 7.4	27.6 ± 5.4	0.86	29.1 ± 8.4	28.6 ± 6.1	0.96
NYHA class 3–4, <i>n</i> (%)	11 (73%)	14 (58%)		8 (73%)	7 (58%)	
6MWT, m	332 ± 126	299 ± 138	0.70	298 ± 121	334 ± 131	0.40
NT-pro BNP, pmol/L	242 ± 272	541 ± 1056	0.83	281 ± 308	301 ± 502	0.57
<b>Underlying CTD</b>						
SSc, <i>n</i> (%)		20/24 (83%)				
SLE, <i>n</i> (%)		4/24 (17%)				
<b>Baseline right heart catheterization</b>						
mPAP, mmHg	55.5 ± 15.2	44.0 ± 13.0	0.02	51.1 ± 12.7	41.5 ± 12.2	0.08
mRAP, mmHg	12.4 ± 6.3	9.5 ± 5.2	0.16	11.3 ± 6.5	8.3 ± 5.0	0.22
Capillary wedge pressure, mmHg	9.5 ± 4.8	13.5 ± 7.8	0.11	9.8 ± 5.3	13.6 ± 10	0.44
PVR, wood units	10.2 ± 3.1	6.2 ± 3.4	0.002	9.2 ± 3.0	5.7 ± 3.4	0.01
<b>PH-Medication</b>						
At baseline, <i>n</i> (%)	0/15 (0%)	0/24 (0%)				
At 1-year follow-up						
No PH-medication				0/11 (0%)	0/12 (0%)	
Mono therapy (ERA), <i>n</i> (%)				1/11 (9%) <sup>1</sup>		
Mono therapy (PDE5), <i>n</i> (%)					1/12 (18%) <sup>2</sup>	
Duo therapy (PDE5 + ERA), <i>n</i> (%)				6/11 (55%)	9/12 (73%)	
Triple therapy (PDE5 + ERA + PRC), <i>n</i> (%)				4/11 (36%)	2/12 (9%)	
<b>Immunomodulatory drugs</b>						
At baseline, <i>n</i> (%)	0/15 (0%)	3/24 (13%)				
At 1-year follow-up, <i>n</i> (%)				0/11 (0%)	3/12 (25%)	

<sup>1</sup>: This IPAH patient was on ERA monotherapy, due to severe side effects on PDE5 therapy. <sup>2</sup>: This CTD-PAH patient was on PDE5 monotherapy due to severe side effects on ERA therapy. Data given as 'mean, ± SD', unless otherwise indicated. Abbreviations: BMI, body mass index; PAH, pulmonary arterial hypertension; IPAH, idiopathic pulmonary arterial hypertension; CTD, connective tissue disease; 6MWT, 6-min walk test; NT-pro BNP, The N-terminal prohormone of brain natriuretic peptide; SSc, systemic sclerosis; SLE, systemic lupus erythematosus; mPAP, mean pulmonary arterial pressure; mRAP, mean right atrium pressure; PVR, pulmonary vascular resistance, endothelin receptor antagonist; ERA, Phosphodiesterase 5 inhibitor ; PDE5, prostacyclin; PRC.

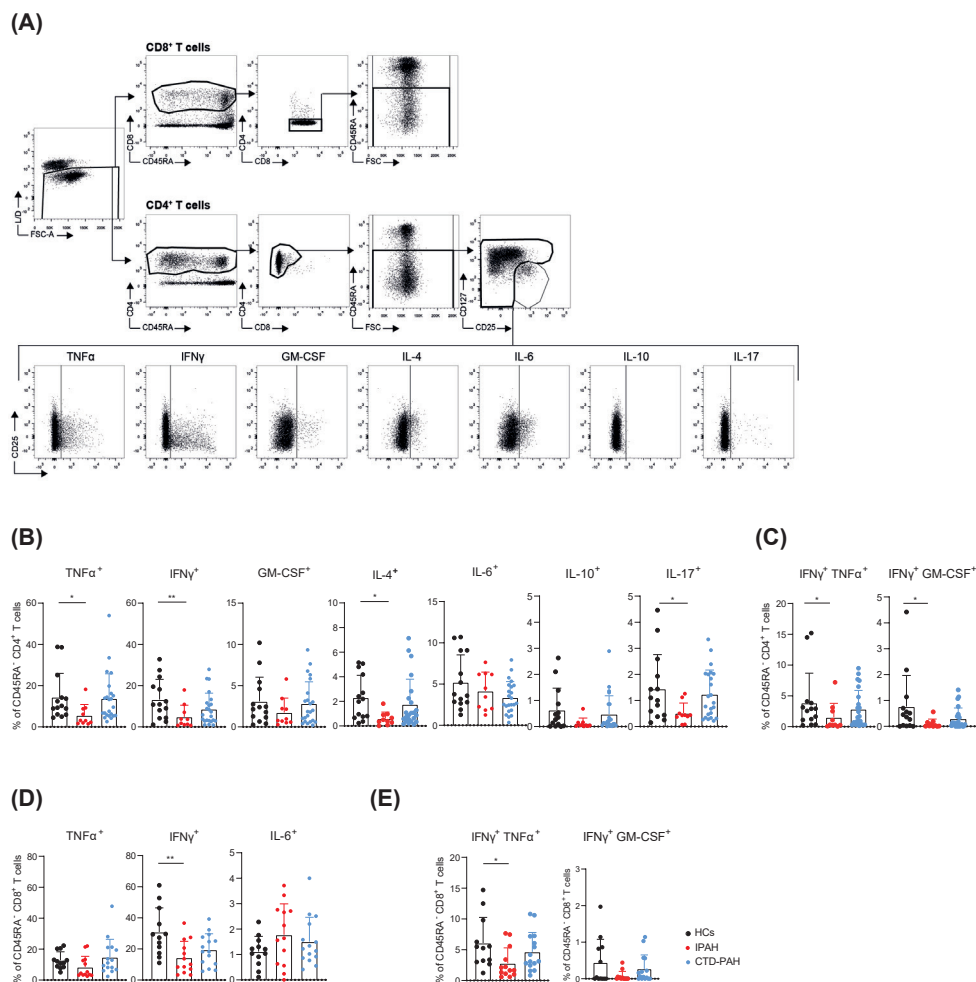


**Figure 1.** Circulating T cells of treatment-naive IPAH patients show reduced cytokine-producing capacity. (A) Flow cytometric gating strategy of cytokine production by circulating non-Treg CD45RA<sup>-</sup> memory CD4<sup>+</sup> T cells. (B,C) Quantification of the proportions of CD45RA<sup>-</sup> CD4<sup>+</sup> memory T cells producing the indicated cytokines in HCs, IPAH and CTD-PAH patients (B), with a subsequent quantification of the proportions of double-producers (C). (D,E) Quantification of the proportions of the cytokine-producing CD45RA<sup>-</sup> CD8<sup>+</sup> memory T cells in the indicated patients and HC groups (D), with a subsequent quantification of the proportions of double producers (E). (A–E) Samples with <500 events in parent gate were excluded from the analysis. Results are presented as mean + standard deviation; symbols represent value of individual patients or HCs. Mann–Whitney U test was used for statistical analysis, \*  $p < 0.05$ , \*\*  $p < 0.01$ .

We observed that the memory CD4<sup>+</sup> T cell fractions of IPAH patients had a significantly reduced cytokine-producing capacity for TNF $\alpha$ , IFN $\gamma$ , IL-4 and IL-17, compared to HCs (Figure 1B). In addition, proportions of IFN $\gamma$ /TNF $\alpha$  and IFN $\gamma$ /GM-CSF double-producing CD45RA<sup>-</sup> CD4<sup>+</sup> T cells were reduced in IPAH patients, compared to HCs (Figure 1C). Likewise, frequencies of IFN $\gamma$  single-producing and double-producing memory CD8<sup>+</sup> T cells were lower in IPAH patients than in HCs (Figure 1D). In contrast, the cytokine-producing capacity of memory CD4<sup>+</sup> and CD8<sup>+</sup> T cells of CTD-PAH patients

was not different from HCs (Figure 1B–E). Three of the CTD-PAH patients had immunomodulatory therapy, but their values for cytokine production were within the range of the other CTD-PAH patients analysed. The cytokines GM-CSF, IL-4, IL-10 and IL-17, which were produced by CD8<sup>+</sup> T cells in lower amounts, did not significantly differ across the three groups analysed (Supplementary Figure S1).

Memory CD4<sup>+</sup> and CD8<sup>+</sup> T cells cannot only be divided into subsets on the basis of their cytokine production but also by specific chemokine receptor expression profiles. Using these profiles, we determined the T cell subset distribution in the two PAH patient groups and healthy controls and found that IPAH patients had reduced frequencies of Th2 cells (Supplementary Figure S2). Even though the Th1, Th17, and Tc1-associated cytokines IFN $\gamma$  and TNF $\alpha$  were reduced, the proportions of Th1 and Th17 or Tc1 and Tc17 cells did not differ between IPAH and HCs (Supplementary Figure S2). By contrast, CTD-PAH patients displayed an increase in Th17 cells and a decrease in Th2 cells, whereas CXCR5<sup>+</sup> (follicular) Tc, Tc17 and Tc1 fractions were reduced (Supplementary Figure S2). The proportion of Tregs did not differ between HCs and PAH patients (data not shown).

In conclusion, memory CD4<sup>+</sup> and CD8<sup>+</sup> T cells of IPAH patients were less capable of producing cytokines compared to HCs, whereas no differences were found in the cytokine-producing capacity of T cells of CTD-PAH patients.

### **T Cells from PAH Patients Show Increased CTLA4 Expression, Correlating with Cytokine-Producing Capacity**

The reduced cytokine-producing capacity of T cells observed in IPAH patients might reflect an altered activation status and effector function of these cells. Therefore, we determined the expression of various surface markers on CD4<sup>+</sup> and CD8<sup>+</sup> T cells. Expression of the co-inhibitory receptor cytotoxic T lymphocyte antigen 4 (CTLA4) was significantly increased on naive CD4<sup>+</sup> T cells and naive and memory CD8<sup>+</sup> T cells in IPAH patients (Figure 2). For CTD-PAH patients, CTLA4 expression was increased in all CD4<sup>+</sup> and CD8<sup>+</sup> T cell fractions. Tregs, known to express high levels of CTLA4, showed similar expression across the three groups analysed. Expression of the activation marker T cell co-stimulator (ICOS) and the co-inhibitory receptor programmed cell death 1 (PD-1) expression did not differ between IPAH patients and HCs for both CD4<sup>+</sup> and CD8<sup>+</sup> T cells (Supplementary Figure S3).

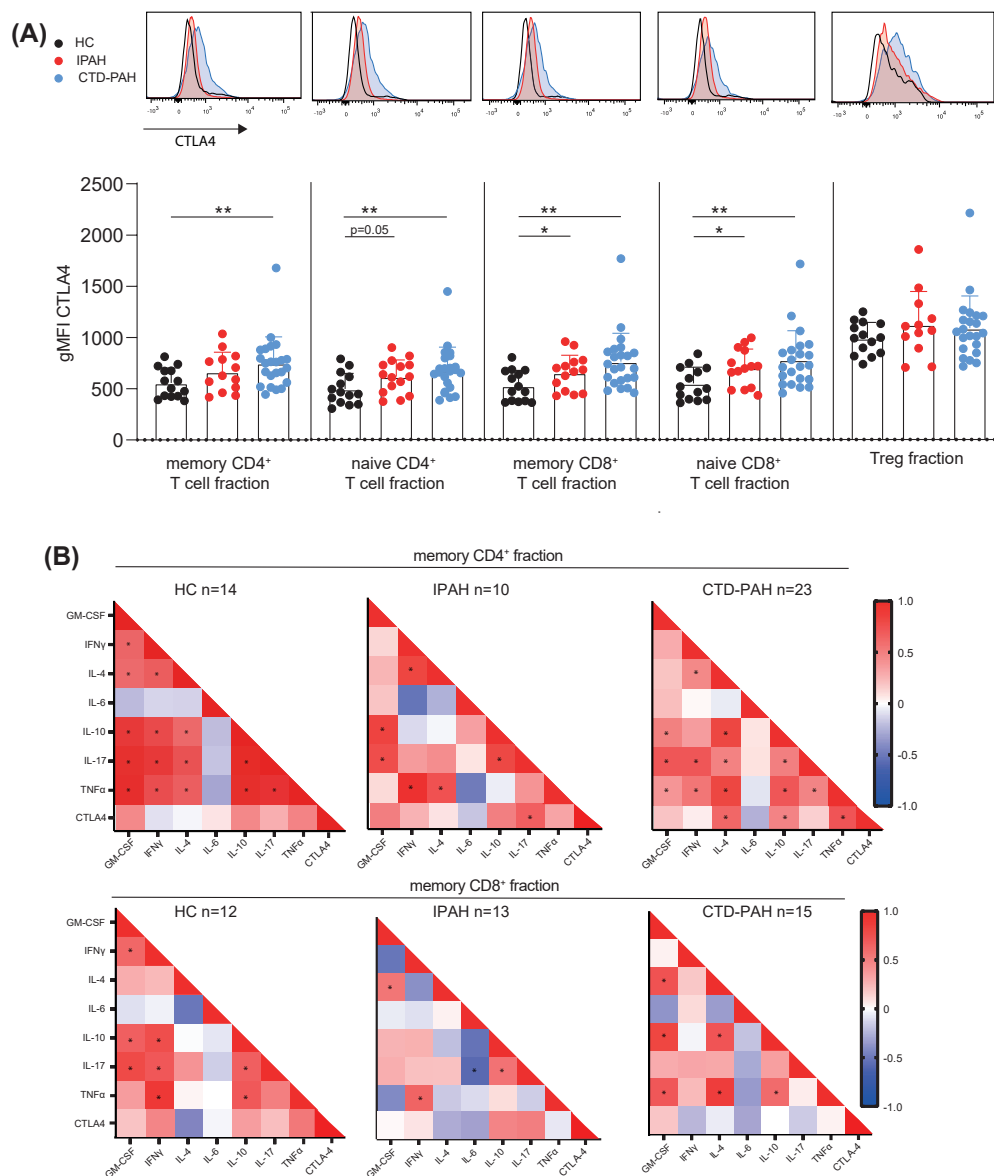


**Figure 2.** T cells of PAH patients show increased CTLA4 expression. **(A)** Quantification of intracellular CTLA4 expression, as determined by flow cytometry, in the indicated CD4<sup>+</sup> and CD8<sup>+</sup> T cells fractions of HCs, IPAH and CTD-PAH patients, shown as histogram overlays (**top**) and quantification (**bottom**). Samples with <500 events in parent gate were excluded (HC  $n = 14$ , IPAH  $n = 12$ –15 and CTD-PAH  $n = 22$ –23). **(B)** Associated correlation matrixes for cytokine-positive CD4<sup>+</sup> and CD8<sup>+</sup> T cells in HCs and patients with IPAH and CTD-PAH. Numbers of patients included are indicated above the correlation matrixes. Correlation coefficient was calculated using nonparametric Spearman correlation. Results are presented as mean + standard deviation and symbols represent values of individual patients or HCs. Mann–Whitney U test was used for statistical analysis, \*  $p < 0.05$ , \*\*  $p < 0.01$ . gMFI = geometric mean fluorescence intensity.

Correlation matrices of the proportions of cytokine-expressing memory CD4<sup>+</sup> T cells and CTLA4 showed a significant correlation with IL-17<sup>+</sup> CD4<sup>+</sup> T cells for IPAH patients and IL-4, IL-10 and TNF $\alpha$  for CTD-PAH patients (Figure 2B). In HCs, the expression levels of CTLA4 did not significantly correlate with the proportions of any of the cytokine-expressing memory CD4<sup>+</sup> T cells in HCs. However, in HCs we found strong and significant correlations between the individual cytokines, except for IL-6, which demonstrated a weak, non-significant negative correlation with all other cytokines measured (Figure 2B). For IPAH patients, the analyses yielded a similar matrix of correlations between individual cytokines, although the observed correlations were more moderate, possibly due to a lower number of individuals included ( $n = 10$ , compared to  $n = 14$  for HCs) (Figure 2B). The correlation matrix for CTD-PAH patients did not essentially differ from the matrix for HCs.

Memory CD8<sup>+</sup> T cells of HCs also showed strong correlations, except for IL-4 and IL-6 (Figure 2B). In memory CD8<sup>+</sup> T cells of IPAH patients, we observed fewer positive and more negative correlations, of which the correlation between IL-6 and IL-17 reached significance. Correlations between IL-17 and other cytokines lost significance in CTD-PAH patients. CTLA4 expression levels on CD8<sup>+</sup> T cells were not significantly correlated with the proportions of positive cells for any of the cytokines in patients or HCs (Figure 2B).

Given that DCs are the main cell type that activate T cells and thereby induce expression of CTLA4 and ICOS, we next characterized DC subsets as well as monocytes, the precursors of inflammatory DCs, in peripheral blood. To this end, we investigated the myeloid compartment in a subgroup of PAH patients at diagnosis (12 IPAH and 17 CTD-PAH patients; see Supplementary Table S2 for patient details and Supplementary Figure S4A for gating strategy). The proportions of monocytes, cDCs, pDCs and AXL<sup>+</sup> Siglec6<sup>+</sup> (AS) DCs [27] did not differ significantly between IPAH patients and HCs (Supplementary Figure S4B–G). In addition, the activation status of DCs and monocytes, as indicated by the expression of CD86, CD80, HLA-DR and CD11c, was not altered, except for HLA-DR expression on classical monocytes which was moderately increased (Supplementary Figure S4H). In CTD-PAH patients, the size of the population of intermediate monocytes was slightly increased (Supplementary Figure S4C). The expression of the activation markers was increased to some extent on monocyte subsets in CTD-PAH patients, but DC subsets displayed a normal activation marker expression, as in IPAH patients (Supplementary Figure S4H).

In summary, except for naive CD4<sup>+</sup> T cells in IPAH patients, the expression of CTLA4 was significantly increased in circulating naive and memory CD4<sup>+</sup> and CD8<sup>+</sup> T cells from both patient groups, compared with HCs. ICOS expression on CD4<sup>+</sup> and CD8<sup>+</sup> T cells was not affected, suggesting that their activation status remained unchanged. The cytokine correlation matrices revealed that in memory CD4<sup>+</sup> T cells from PAH patients, CTLA4 expression correlated with cytokine production capacity, in particular with IL-17<sup>+</sup> Th cells in IPAH. Furthermore, for both CD4<sup>+</sup> and for CD8<sup>+</sup> T cells, the correlations between cytokine expression were weaker in IPAH patients than in those in both HCs and CTD-PAH patients. Analysis of peripheral blood DCs and monocytes did not provide evidence for altered DC activation.

### Principal Component Analysis of T Cell Cytokine Production Separates IPAH Patients from HCs

Next, we investigated whether a multivariate analysis would be able to separate PAH patients and HCs, based on the observed phenotypic differences in the T cell compartments. To this end, we performed

a PCA using the obtained data of cytokine production, chemokine-receptor based Th subset distribution and activation marker expression (Figure 3A). IPAH patients were separated from HCs in the first dimension (Dim1; 31.3%), dominated by intracellular cytokine expression mainly in CD4<sup>+</sup> T cells, and in Dim2 (15.9%), dominated by Th and Tc subset sizes and CTLA4 expression. CTD-PAH patients were separated in Dim2 only. Interestingly, a PCA solely based on frequencies of cytokine-producing cells could also separate IPAH patients from HCs but not CTD-PAH patients from HCs (Figure 3B). Hereby, the Th1- and Th17-associated cytokines contributed most to Dim1 (58%).

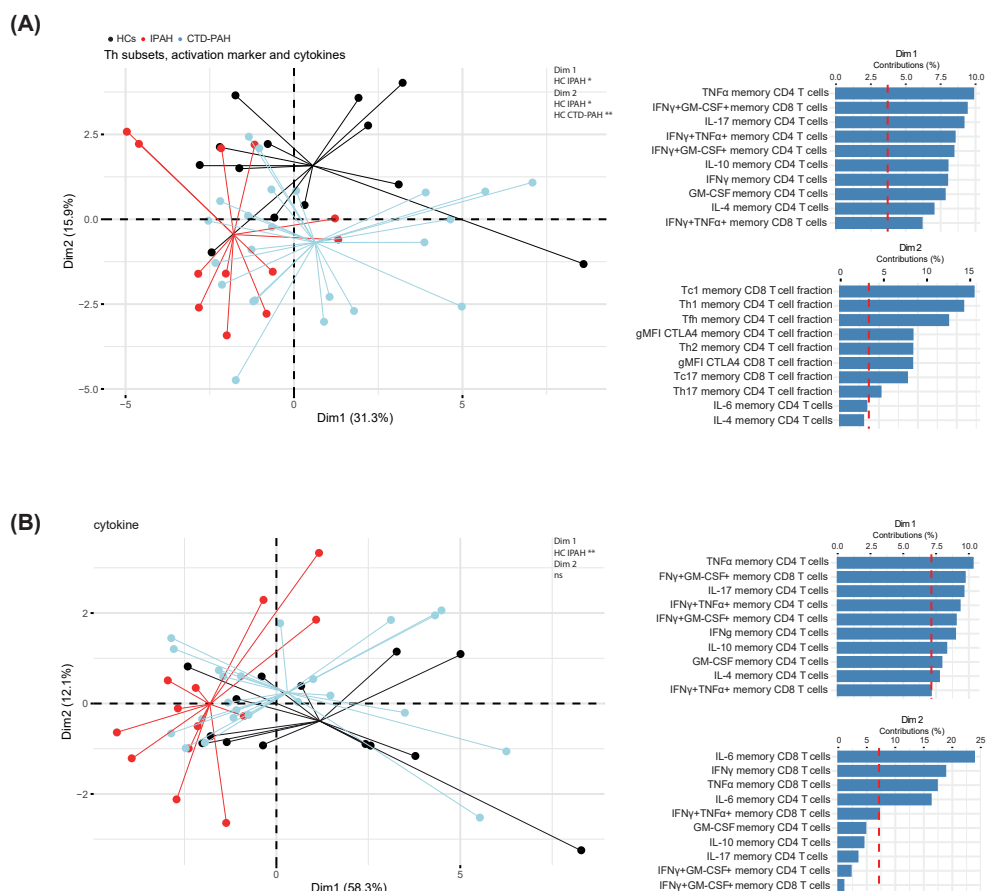


**Figure 3.** Multivariate analysis separates treatment-naive PAH patients from HCs, mainly by T cell cytokine production. **(A)** Principal component analysis (PCA) of HCs ( $n = 13$ ), IPAH ( $n = 12$ ) and CTD-PAH ( $n = 23$ ) patients of whom all variables (peripheral T cell subsets, activation markers and cytokine production) could be determined by flow cytometry (left), with the contributions of the top 10 variables in percentages of Dim1 and Dim2 (right). **(B)** PCA of T cell cytokines only of HCs ( $n = 14$ ), IPAH ( $n = 13$ ) and CTD-PAH ( $n = 23$ ) patients determined by flow cytometry and contributions of the top 10 variables in percentages of Dim1 and Dim2. Symbols represent values of individual patients or HCs, whereby lines connect these values to the mean Dim1 and Dim2 coordinates. Mann-Whitney U test was used for statistical analysis of coordinates on the dimension between PAH patients and HCs, \*  $p < 0.05$ , \*\*  $p < 0.01$ .

Taken together, these findings confirm that CD4<sup>+</sup> and CD8<sup>+</sup> T cells from treatment-naive IPAH patients have unique cytokine expression profiles that are significantly different from HCs.

### T Cell Cytokine and CTLA4 Expression Profiles in IPAH Patients Significantly Change over Time

To determine the dynamics of the T cell cytokine and CTLA4 expression profiles in PAH patients, we analysed subgroups of 11 IPAH patients and 12 CTD-PAH patients of whom paired samples at diagnosis and 1-year follow-up were available for analysis. Whereas intracellular IL-17 in memory CD4<sup>+</sup> T cells of IPAH patients increased over time, the other cytokines analysed remained stable (Figure 4A). The cytokine-producing capacity of memory CD8<sup>+</sup> T cells of IPAH patients (Figure 4B and data not shown) and of memory CD4<sup>+</sup> and CD8<sup>+</sup> T cells of CTD-PAH patients (Figure 4A,B and data not shown) was unaltered over time.

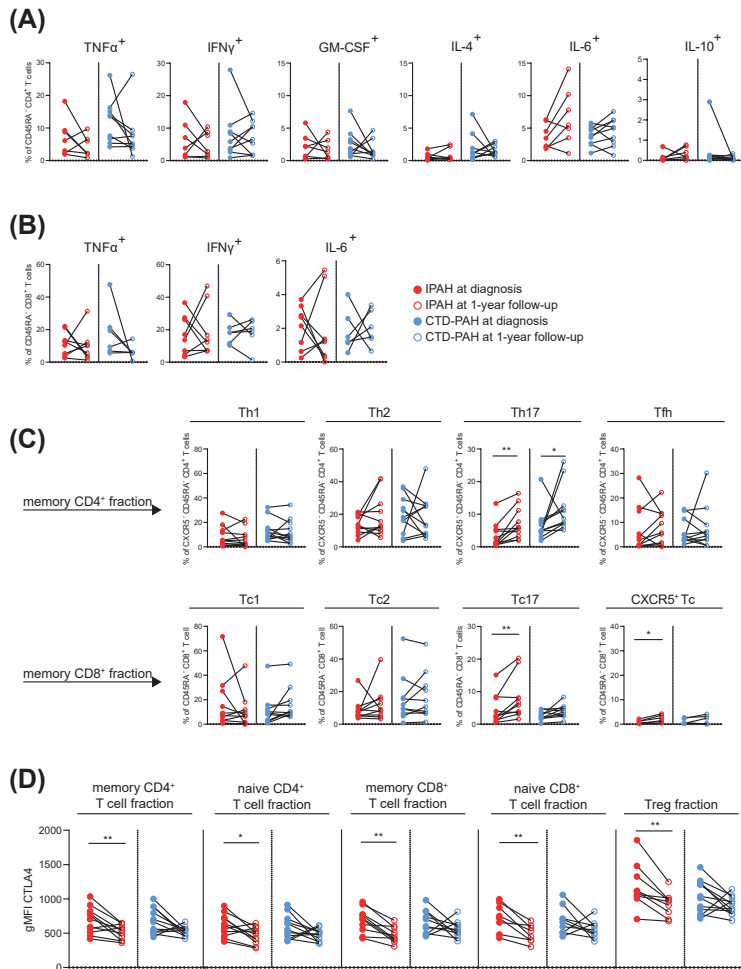


**Figure 4.** T cell profile changes over time in PAH patients. (A,B) Quantification of the proportions of CD45RA<sup>+</sup> CD4<sup>+</sup> memory T cells (A) and CD45RA<sup>+</sup> CD8<sup>+</sup> memory T cells (B) producing the indicated cytokines in paired samples from IPAH and CTD-PAH patients at diagnosis and at 1-year follow-up. (C) Proportions of peripheral blood CD4<sup>+</sup> and CD8<sup>+</sup> T cell subsets, based on chemokine receptor expression, in paired samples from PAH patients at diagnosis and 1-year follow-up. (D) Quantification of CTLA4 expression in the indicated T cell fractions in samples from IPAH and CTD-PAH patients at diagnosis and 1-year follow-up. Closed and open circles represent values of individual patients at diagnosis and 1-year follow-up, respectively. Paired samples are connected by a line. Wilcoxon matched-pairs signed-rank test was used for statistical analysis. \* *p* < 0.05, \*\* *p* < 0.01. gMFI = geometric mean fluorescence intensity.

The proportions of Th17 cells increased over time in both patient groups (Figure 4C). For IPAH patients, this rise of Th17 cells paralleled the observed increased frequency of IL-17<sup>+</sup> CD4<sup>+</sup> T cells over time. At 1-year follow-up, frequencies of CXCR5<sup>+</sup> Tc or Tc17 cells were increased in IPAH patients but not in CTD-PAH patients.

The expression of CTLA4 decreased over time for all T cell populations in both patient groups, which only reached significance in IPAH patients (Figure 4D). Inferred from the values of the geometric mean fluorescence intensities, the CTLA4 expression at 1-year follow-up returned to the levels seen in HCs (compare Figures 4D and 2A). ICOS expression on memory CD4<sup>+</sup> T cells was significantly increased at 1-year follow-up in both patient groups (Supplementary Figure S5A). PD-1 expression remained stable in the memory CD4<sup>+</sup> T cell fractions but decreased in memory CD8<sup>+</sup> T cells, reaching significance for the CTD-PAH patient group only (Supplementary Figure S5B).

To obtain more comprehensive insight, we performed a PCA and found that IPAH patients at diagnosis and at 1-year follow-up were separated in Dim2 (21.5%) and Dim3 (9.5%), to which Th and Tc subsets, IFN $\gamma$ <sup>+</sup> T cells and CTLA4 contributed most (Figure 5A). Hereby, the IPAH patients at 1-year follow-up moved towards the profile seen in HCs in Dim2 but away from HCs in Dim3. Dim 1 (33.3%) did not separate IPAH patients at baseline and at 1-year follow-up. (Supplementary Figure S6A). Furthermore, our T cell parameters did not separate CTD-PAH patients at diagnosis from patients at 1-year follow-up (Dim2 and Dim3: Figure 5B; Dim1 and Dim3: Supplementary Figure S6B).

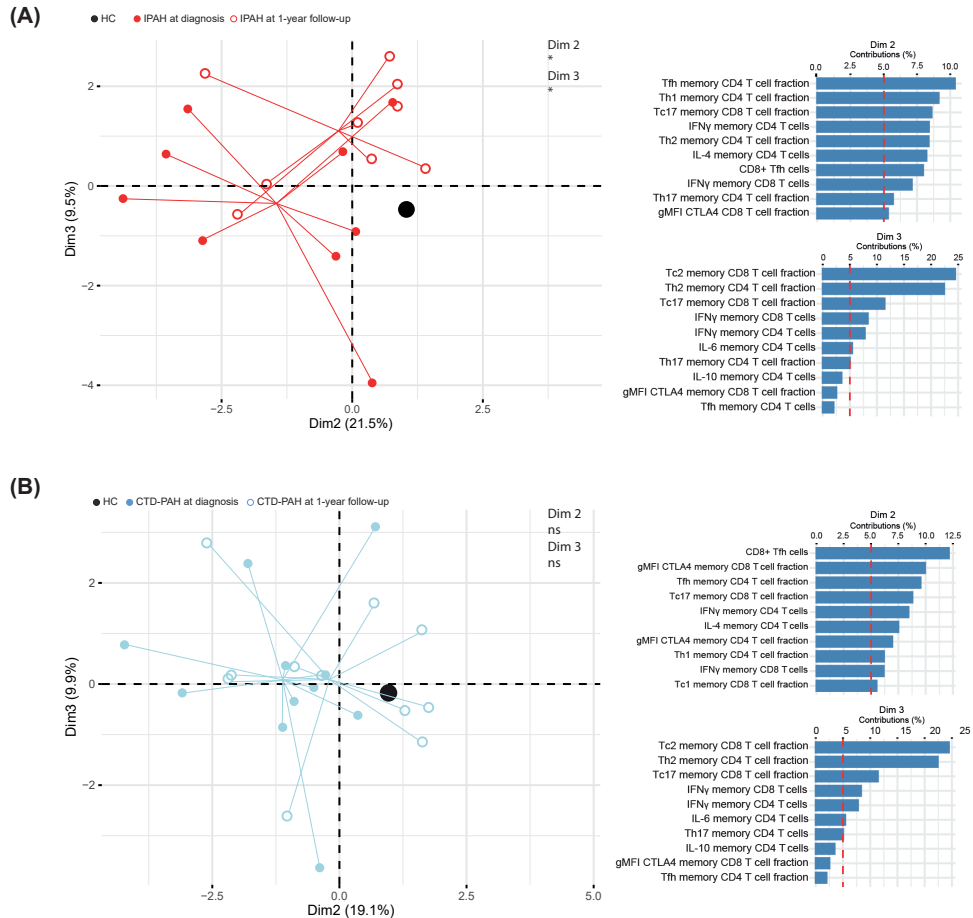


**Figure 5.** Multivariate analysis separates IPAH patients but not CTD-PAH patients at diagnosis and 1-year follow-up. **(A,B)** Principal component analysis (PCA) of IPAH patients ( $n = 9$ ) **(A)** and CTD-PAH patients ( $n = 11$ ) of whom all variables (peripheral T cell subsets, activation markers and cytokine production) could be determined by flow cytometry at 1-year follow-up **(left)**, with the contributions of the top 10 variables in percentages of Dim2 and Dim3 **(right)**. Symbols represent values of individual patients or HCs, whereby lines connect these values to the mean Dim2 and Dim3 coordinates. Mean coordinates of HCs are indicated in black. Wilcoxon matched-pairs signed-rank test was used for statistical analysis, \*  $p < 0.05$ .

In summary, in IPAH patients the proportions of IL-17 $^+$  CD4 $^+$  T cells, Th17 and Tc17 increased at 1-year follow-up, compared to baseline. In both CD4 $^+$  T and CD8 $^+$  T cells, CTLA4 expression decreased, which was accompanied by increased ICOS expression for CD4 $^+$  T cells. Taken together, these dynamic changes suggest an increase in the activation status of T cells over time, with similar trends in IPAH and CTD-PAH patients. However, only in IPAH patients the T cell phenotype at diagnosis and at 1-year follow-up were separated in a PCA.

## DISCUSSION

The finding that the lungs of most patients with IPAH contain increased numbers of T cells and DCs suggested the involvement of the immune system in its pathophysiology (34, 55, 86, 215) and prompted us to investigate these immune cells in peripheral blood. Using flow cytometry, we characterized circulating CD4<sup>+</sup> and CD8<sup>+</sup> T cells, DCs and monocytes in a well-defined cohort of treatment-naïve IPAH patients, whereby results were compared to HCs and CTD-PAH patients.

Our analyses revealed that in IPAH patients, at diagnosis both the CD4<sup>+</sup> and CD8<sup>+</sup> T-cell compartment in peripheral blood contained reduced proportions of cytokine-producing cells and increased expression of the CTLA4 checkpoint molecule. We found a significant decrease for TNF $\alpha$ , IFN $\gamma$ , IL-4 and IL-17 in CD4<sup>+</sup> T cells and for IFN $\gamma$  in CD8<sup>+</sup> T cells, which separated IPAH patients from HCs in a PCA. After 1 year of PAH-specific therapy, proportions of IL-17<sup>+</sup> CD4<sup>+</sup> T cells, Th17 and Te17 cells were increased, whereas CTLA4 expression on both CD4<sup>+</sup> and CD8<sup>+</sup> T cells was concomitantly decreased in IPAH patients. Our analyses showed that the phenotype of T cells in IPAH was different from CTD-PAH, in which cytokine expression was similar to HCs and did not change during 1-year follow-up. At baseline, CTD-PAH CD4<sup>+</sup> and CD8<sup>+</sup> T cells showed increased CTLA4 expression to levels that appeared even higher than those in T cells from IPAH patients.

The finding that the peripheral blood CD4<sup>+</sup> and CD8<sup>+</sup> T cell compartment of IPAH patients contained reduced numbers of cytokine-producing cells was striking. This concerned Th1-, Th2- and Th17-associated cytokines, and therefore we did not find evidence for a shift in Th subset ratios. The underlying mechanisms remain unknown but may involve T cell exhaustion, which is linked to increased CTLA4 expression (267). However, this would not be supported by our finding that CTLA4 expression essentially showed positive correlations with proportions of cytokine-expressing cells. Moreover, in CTD-PAH patients, CTLA4 expression was also increased on CD4<sup>+</sup> and CD8<sup>+</sup> T cells, but their cytokine production was unchanged. Alternatively, the reduced cytokine production capacity could be due to other inhibitory signals.

Expression of PD-1, another co-inhibitory molecule associated with T cell exhaustion, and the activation marker ICOS on T cells remained unaltered in IPAH patients. Nevertheless, the specific increase in anti-inflammatory IL-10 in plasma or serum of IPAH patients (but not CTD-PAH patients) may well contribute to the observed differences in cytokine profiles (94, 254). It is also conceivable that cytokine-producing cells may have migrated into inflamed tissue, particularly because CD3<sup>+</sup> T cells were found to be increased in lungs of IPAH patients (55). Finally, it cannot be excluded that individuals with relatively low proportions of cytokine-producing cells in their circulation have an increased susceptibility to develop IPAH. In this context, the phenomenon may be related to findings in patients with chronic obstructive pulmonary disease (COPD). In the peripheral blood of these patients, significantly increased proportions of IFN- $\gamma$ <sup>+</sup> and TNF- $\alpha$ <sup>+</sup> CD8<sup>+</sup> T cells were only found in less severe disease cases but not in more advanced GOLD stage IV patients (284). COPD patients with severely reduced diffusing capacity also had lower proportions of IL-17<sup>+</sup> CD4<sup>+</sup> T cells in their circulation.

In our analyses, the strong signals induced by PMA and ionomycin *in vitro* bypass the TCR-mediated signals supported by co-stimulatory signals dependent on the CD28/CTLA4 balance. Therefore, further experiments are required to determine the effect of increased CTLA4 expression on T cell activation and cytokine production in T cells from IPAH patients following TCR stimulation and co-stimulation in an interaction with antigen presenting cells. Hereby, it is of note that genetic variation in HLA-DPA1/DPB1 is associated with PAH (285), suggesting that interactions of CD4<sup>+</sup> T cells with

HLA class II-expressing cells, including monocytes, DCs or alveolar epithelial cells, may contribute to PAH development.

Because both IPAH and CTD-PAH are multifactorial diseases thought to develop by a multi-hit principle (286), it is attractive to speculate that the observed increased CTLA4 expression on T cells of both IPAH and CTD-PAH patients reflects one of the things that is common to the two diseases. In this context, it is of note that cytokine signatures, including TNF $\alpha$ , differentiate systemic sclerosis (SSc) patients at high versus low risk for PAH. However, it remains unclear whether immune changes contribute to the initiation of PAH symptoms in CTD or are a consequence of PAH. Another common factor might be Th17 cells, which have been implicated in various systemic auto-immune diseases, including SSc (287), as well as IPAH (195). In addition, Tc17 cells or Tfh cells with a Th17-like chemokine receptor signature, which were increased in a heterogeneous group of IPAH patients (278), may contribute. Our finding that treatment-naive IPAH patients did not show increased frequencies of Th17 cells, whereas IL-17 production and Th17 cell frequencies increased at 1-year follow-up, would suggest that the Th17 phenotype develops during the disease. It remains unknown whether the increase in Th17 cells over time, as well as the increase in cytokine production in general, was a result of disease progression or PAH-specific medication. The former would be supported by the reported correlation between the frequencies of Th17 cells and disease severity in various diseases, including CTD-PAH (95) and psoriasis (288). Overall, the groups of IPAH and CTD-PAH patients did not substantially differ in the specific PAH therapy they received. The increased cytokine production that we observed at 1-year follow-up in IPAH patients was not present in CTD-PAH patients, suggesting that this increase may be due to disease progression or disease-specific response to therapy, rather than a direct immunomodulatory effect of the PAH specific medication. However, effects of PAH-specific medication cannot be excluded, because these drugs have some immunomodulatory effects (289). This may also explain the heterogeneity seen within the IPAH and CTD-PAH patient groups, whereby some patients show increased cytokine production capacity and others show decreased cytokine production capacity at follow-up. Particularly, because patients received either mono, duo or triple therapy with different classes of medication, perhaps exerting different effects on immune cells. A limitation of our study is the number of IPAH patients investigated. Because IPAH is a heterogeneous disease, it is very well possible that the immune profiles of subgroups of IPAH patients show a higher or a lower level of resemblance with CTD-PAH patients. Analysis of a larger group of treatment-naive IPAH patients could identify immune profile-based IPAH subgroups.

In IPAH patients, we did not observe major defects in peripheral blood myeloid cells, including DC subsets and monocytes. Yet, we previously showed spontaneous PH development in mice with a targeted deletion of the *Tnfrsf3* gene in cDCs, resulting in aberrant DC activation (213, 261). Moreover, in human IPAH lung tissue we found co-localization of DCs and CD8<sup>+</sup> T cells (261) and pDCs were more abundant in lung biopsies of IPAH patients (55). Taken together, these studies provide evidence for a local involvement of DCs, which may exert a pathogenic role by initiation or maintenance of T cell activation, by maintaining lymphoid structures in the lung (178) and/or by initiating remodelling of pulmonary vessels (86). The presence and activation status of DCs or monocytes in peripheral blood may not necessarily resemble their equivalents in the lung (209).

In conclusion, we found a significantly reduced cytokine-producing capacity of T cells of IPAH patients but not in CTD-PAH patients. The identified differences between IPAH patients and CTD-PAH patients in T cell subsets, their activation status and cytokine production capacity indicate different immune involvement across the two PAH subgroups. Although clinical trials treating PAH patients with

immunomodulatory medication have been negative or inconclusive so far (290), our study illustrates the importance of a detailed understanding of the different immune phenotypes in the PAH subgroups for future interventional studies.

## MATERIALS AND METHODS

### Subjects and Study Design

Thirty-nine PAH (15 IPAH and 24 CTD-PAH) patients were diagnosed according to the ERS/ECSC guidelines (Table 1) (2). T cell activation, cytokine production and Th subset division was measured. In a subgroup of 29 patients (12 IPAH and 17 CTD-PAH), monocytes and DCs were analysed in addition (Supplementary Table S2). Similar to prior work from our group (233, 254), exclusion criteria were: incomplete diagnostic work-up and therefore no confirmed PH diagnosis, not treatment-naïve for PH therapy and age < 18 years or not capable of understanding or signing informed consent. Additionally, 17 HCs (41% female, mean age  $55.3 \pm 12.5$ ) for T cell characterization and 12 HCs (42% female, mean age  $50 \pm 12.4$ ) for myeloid characterization, were included. Exclusion criteria for HCs were: autoimmune disease, active infectious disease, use of immunomodulatory drugs and history of cardiopulmonary disease. The study protocol was approved by the Erasmus MC medical ethical committee (MEC-2011-392). Written informed consent was given by all patients and controls. The study was performed conforming to the principles outlined in the declaration of Helsinki.

### Clinical Data Collection, Follow-Up and Definition of Endpoints

Hemodynamic and clinical data at diagnosis were collected during inpatient cardiopulmonary screening visits (233, 254). Data were collected and stored in PAHTool (version 4.3.5947.29411, Inovoltus), an online electronic case report form. Patients were treated according to the ERS/ESC guidelines (2) and prospectively followed up by half-yearly scheduled visits to the outpatient clinic.

### Flow Cytometry

Peripheral blood mononuclear cells (PBMCs) were isolated—using ficoll density separation—from peripheral venous blood samples of PAH patients (taken directly after right heart catheterization) and HCs, using standard procedures. Cell counts were determined by manually counting using trypan blue and a Bürker Türk counting chamber. PBMCs were suspended in freezing medium containing 80% FCS and 20% DMSO and stored in cryogenic storage vials at  $-80^{\circ}\text{C}$  until further use. Flow cytometry procedures have been described previously (291) and antibodies used for intra- and extracellular staining are given in Supplementary Table S3. In brief, for the determination of T cell subsets, PBMC fractions were directly stained for the chemokine receptors and extracellular markers CCR4—FITC, CD45RA—PE TxR, CD4—PercP-Cy5.5, CXCR5—Pe-Cy7, ICOS—BV650, CXCR3—BV711, PD1—BV786, CCR6—APC, CD3—APC-Cy7, CD8—AF700 for 60 min at  $4^{\circ}\text{C}$  in phosphate-buffered saline (PBS) supplemented with 5mM EDTA and 1% BSA (MACS buffer). After fixation with paraformaldehyde (2% for 10 min at  $4^{\circ}\text{C}$ ) and permeabilization step with saponin (0.5% for 30 min at room temperature), cells were intracellularly stained for FoxP3—PE and CTLA4—BV421. For DC/monocyte staining, PBMC fractions were stained for extracellular markers CD16—FITC, PD-L1—PE-

CF594, CD56—Pe-Cy7, AXL—APC, CD3—AF700, CD19—AF700, CD20—AF700, CD86—Biotin, CD80—BV421, CD11c—BV605, CD123—BV650, HLA-DR—BV711, CD14—BV785 in MACS buffer for 30 min at 4 °C, after which cells were incubated with streptavidin—APC-Cy7 for 10 min at 4 °C. Subsequently, cells were stained after a fixation and permeabilization step for IRF4—PE and IRF8—Percp-Cy5.5 for 60 min at 4 °C. For the measurement of cytokines, PBMCs were incubated for 4 h at 37 °C in RPMI Medium 1640 + GlutaMAX-I (Gibco) supplemented with 5% fetal bovine serum (Gibco), 10 ng/mL phorbol 12-myrystate 13-acetate (Sigma-Aldrich), 250 ng/mL ionomycin (Sigma-Aldrich) and Golgistop (BD Bioscience), after which cells were stained for extracellular markers CD4—FITC, CD45RA—BV650, CD3—biotin, CD8—AF700, CD25—Pe-Cy7, CD127—BV421 and intracellular markers IL-10—PercP-Cy5.5, IL-4—PAC-Cy7, IL-6—PE, IFN $\gamma$ —BV711, IL-17—BV786, TNF $\alpha$ —APC, GM-CSF—PE-TxR as previously described (260). Non-specific labelling was prevented in all stainings by blocking Fc receptors using human TruStain FcX (Biolegend) and dead cells were excluded with Fixable Viability Dye Live/Dead eF506 (eBioscience) and forward and side scatter values. Data were acquired using a FACSymphony A5 flow cytometer (Beckton Dickinson) and analysed using FlowJo version 10 (Tree Star Inc software).

## Principal Component Analysis and Statistical Evaluation

Principal component analysis (PCA) was performed using R and RStudio, and the packages FactoMineR and Factoextra, and this has been described previously (254, 262). Statistical evaluations of flow cytometry data and PCA dimension coordinates for differences between HCs and either IPAH patients or CTD-PAH patients were performed by Mann–Whitney U tests. Paired diagnosis and 1-year follow-up data were analysed by the Wilcoxon matched-pairs signed-rank test. Correlation coefficients were calculated using the nonparametric Spearman correlation. All statistical tests were two-sided; *p*-values < 0.05 were considered statistically significant. Statistical analyses were performed using GraphPad Prism v8 (Graph Pad Software).

### Author Contributions

D.v.U., M.K., R.W.H. and K.A.B. conceived the project and designed the experiments. D.v.U., T.K., J.A.C.v.H., M.V. and M.v.N. generated data or tools for the project. A.E.v.d.B., L.M.v.d.T., P.P.C. and K.A.B. included material or patients for our study. D.v.U., T.K., R.W.H. and K.A.B. wrote the manuscript. All authors read, provided valuable feedback and approved the final manuscript. All authors have read and agreed to the published version of the manuscript.

### Funding

This research was funded by the Dutch Heart Foundation under grant number 2016T052 (DvU/MK) and partially supported by an unrestricted grant from Ferrer pharmaceuticals, Actelion Pharmaceuticals and the Pulmonary Hypertension Patients Association (TK).

### Institutional Review Board Statement

The study was conducted in accordance with the Declaration of Helsinki and approved by the Erasmus MC medical ethical committee (MEC-2011-392).

**Informed Consent Statement**

Informed consent was obtained from all subjects involved in the study.

**Data Availability Statement**

The data presented in this study are available in this article or upon reasonable request.

**Acknowledgments**

We would like to thank Ingrid M. Bergen for her valuable contribution to this manuscript and we would like to thank all the patients that participated in the study.

**Conflicts of Interest**

The authors declare no conflict of interest. The funders had no role in the design of the study; in the collection, analyses, or interpretation of data; in the writing of the manuscript; or in the decision to publish the results.

## SUPPLEMENTARY MATERIAL

**Table S1.** Characteristics of CD4<sup>+</sup> Th subsets.

	CD4 <sup>+</sup> T cell subsets				
	Th1	Th2	Th17	Tfh	Treg
Cytokines driving differentiation	IL-12, IFN $\gamma$	IL-4	IL-6, IL-23, IL-21, TGF $\beta$	IL-21, IL-6, IL-27, IL-12	IL-2, TGF $\beta$
Major function	Protection against intracellular pathogens	Protection against helminth infection	Protection against extracellular pathogens	Support to B cells in lymphocyte follicles	Maintaining immune tolerance
Pathological conditions	Autoimmunity	Allergy	Autoimmunity	Autoimmunity	Lymphoproliferative disease and autoimmunity
Key transcription factors	T-bet	GATA3	ROR $\gamma$ t	BCL6	FoxP3
Key surface molecule	CXCR3	CCR4	CCR6	CXCR5	CTLA4
Effector cytokines	IFN $\gamma$	IL-4, IL-5, IL-13	IL-17, IL-22	IL-21, IL-10	IL-10, TGF $\beta$

Abbreviations: Th, T-helper; IL, interleukin; IFN $\gamma$ , interferon  $\gamma$ ; TGF $\beta$ , transforming growth factor  $\beta$ ; CTLA4, cytotoxic T lymphocyte antigen 4. References used: (93, 237, 256, 292).

6

**Table S2.** Baseline demographic and patient characteristics.

DC staining (baseline)	PAH - BASELINE		
	IPAH (n=12)	CTD-PAH (n=17)	p Value
<b>Baseline clinical characteristics</b>			
Gender, female (%)	11 (92%)	13 (76%)	
Age, y	57.2 $\pm$ 18.3	65.8 $\pm$ 11.2	0.37
BMI, kg/m <sup>2</sup>	26.5 $\pm$ 4.7	26.1 $\pm$ 5.4	0.71
NYHA class 3-4, n (%)	9 (75%)	11 (65%)	
6MWT, m	354 $\pm$ 109	300 $\pm$ 133	0.40
NT-pro BNP, pmol/L	236 $\pm$ 301	650 $\pm$ 1213	0.61
<b>Underlying CTD</b>			
SSc, n (%)		14/17 (82%)	
SLE, n (%)		3/17 (18%)	
<b>Baseline right heart catheterization</b>			
mPAP, mmHg	55.8 $\pm$ 16.5	41.7 $\pm$ 13.0	<b>0.008</b>
mRAP, mmHg	11.6 $\pm$ 6.0	9.4 $\pm$ 5.8	0.21
Capillary wedge pressure, mmHg	9.0 $\pm$ 5.3	11.3 $\pm$ 5.9	0.31
PVR, wood units	9.7 $\pm$ 3.0	6.6 $\pm$ 3.6	0.02
<b>Immunomodulatory drugs</b>			
At baseline, n (%)	0/12 (0%)	1/17 (6%)	

Data given as 'mean,  $\pm$ SD', unless otherwise indicated. **Abbreviations:** BMI, body mass index; PAH, pulmonary arterial hypertension; IPAH, idiopathic pulmonary arterial hypertension; CTD, connective tissue disease; 6MWT, 6-minute walk test; NT-pro BNP, The N-terminal prohormone of brain natriuretic peptide; SSc, systemic sclerosis; SLE, systemic lupus erythematosus; mPAP, mean pulmonary arterial pressure; mRAP, mean right atrium pressure; PVR, pulmonary vascular resistance.

**Table S3.** Monoclonal antibodies used for flow cytometry.

<b>Antibody</b>	<b>Conjugate</b>	<b>Clone</b>	<b>Company</b>
CD4	FITC	Okt4	Biologend
CD45RA	BV650	HI100	BD
CD3	Biotin	UCHT	eBioscience
CD8	AF700	SK1	Biologend
CD25	Pe-Cy7	M-A251	BD
CD127	BV421	A019D5	Biologend
Streptavidin	BV605	-	BD
IL-10	PCP	JES3-9D7	Biologend
IL-4	APC-Cy7	MP4-25D2	Biologend
IL-6	PE	MQ2-13A5	eBioscience
IFN $\gamma$	BV711	B27	BD
IL-17a	BV786	N49-653	BD
TNF $\alpha$	APC	6401.111	BD
GM-CSF	PE TxR	BVD2-21C11	BD
CCR4	FITC	-	R&D
CD45RA	PE TxR	MEM-56	Life technology
CD4	PercPcy5.5	RPA-T4	Invitrogen
CXCR5	Pe-Cy7	MU5UBEE	eBioscience
ICOS	BV650	C3984A	Biologend
CXCR3	BV711	1C6/CXCR3	BD
PD-1	BV786	EH12.1	BD
CCR6	APC	11A9	BD
CD3	APC-Cy7	UCHT1	Invitrogen
FoxP3	PE	236A/E7	Invitrogen
CTLA4	BV421	BNI3	BD
CD16	FITC	3G8	BD
PD-L1	PE-CF594	M1H1	BD
CD56	Pe-Cy7	B159	BD
AXL	APC	FAB154A	R&D system
CD3	AF700	UCHT1	eBioscience
CD19	AF700	HIB19	eBioscience
CD20	AF700	2H7	BD
CD86	Biotin	FUN-1	BD
CD80	BV421	L307.4	BD
CD11c	BV605	3.9	Biologend
CD123	BV650	7G3	BD
HLA-DR	BV711	G46-6	BD
CD14	BV785	M5E2	BD
Streptavidin	APC-Cy7	-	eBioscience
IRF4	PE	3E4	eBioscience
IRF8	PercPcy5.5	V3GYWCH	eBioscience

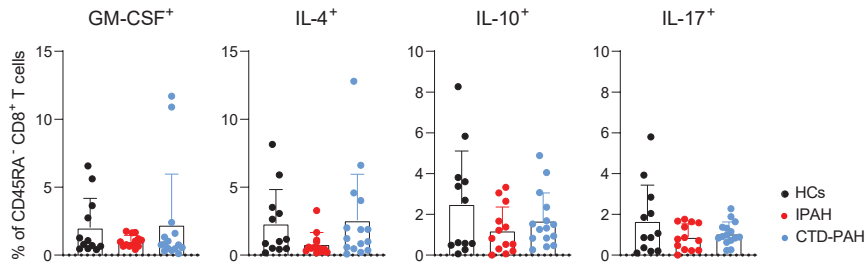


**Figure S1.** GM-CSF<sup>+</sup>, IL-4<sup>+</sup>, IL-10<sup>+</sup> and IL-17<sup>+</sup> memory CD8<sup>+</sup> T cells in IPAH and CTD-PAH patients do not differ from HCs. Quantification of the indicated cytokines in CD45RA<sup>-</sup> CD8<sup>+</sup> T cells. Results are presented as mean + standard deviation, Mann-Whitney U test was used for statistical analysis. Symbols represent values of individual patients or HCs.

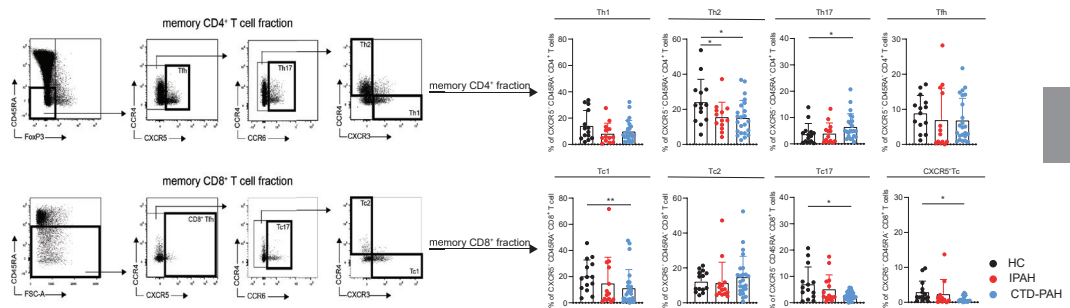


**Figure S2.** Frequency of Th2 cells is higher in PAH patients than in HCs. Gating strategy for peripheral blood Th subsets based on chemokine receptor expression (*left*) and percentages of circulating Th cells (*right*) of the indicated T cell subsets for HCs, IPAH and CTD-PAH patients at diagnosis, as determined by flow cytometry. Symbols represent values of individual patients or HCs. Results are presented as mean + standard deviation, Mann-Whitney U test was used for statistical analysis, \* p<0.05, \*\* p<0.01.

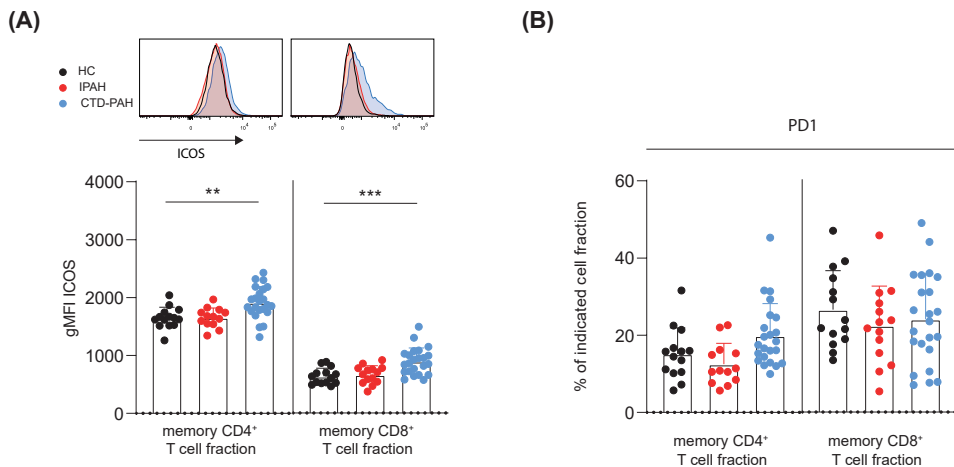


**Figure S3.** Increased ICOS expression on T cells of CTD-PAH patients. (A) Histogram overlays (*top*) and quantification (*bottom*) of ICOS expression, as determined by flow cytometry in HCs, IPAH and CTD-PAH patients. (B) Quantification of PD-1<sup>+</sup> memory CD4<sup>+</sup> and memory CD8<sup>+</sup> T cells. Samples with <500 events in parent gate were excluded (HC n= 14, IPAH n=12-15 and CTD-PAH n=22-23). Results are presented as mean + standard deviation; symbols represent values of individual patients or HCs. Mann-Whitney U test was used for statistical analysis, \*\* p<0.01, \*\*\* p<0.001. gMFI = geometric mean fluorescence intensity.

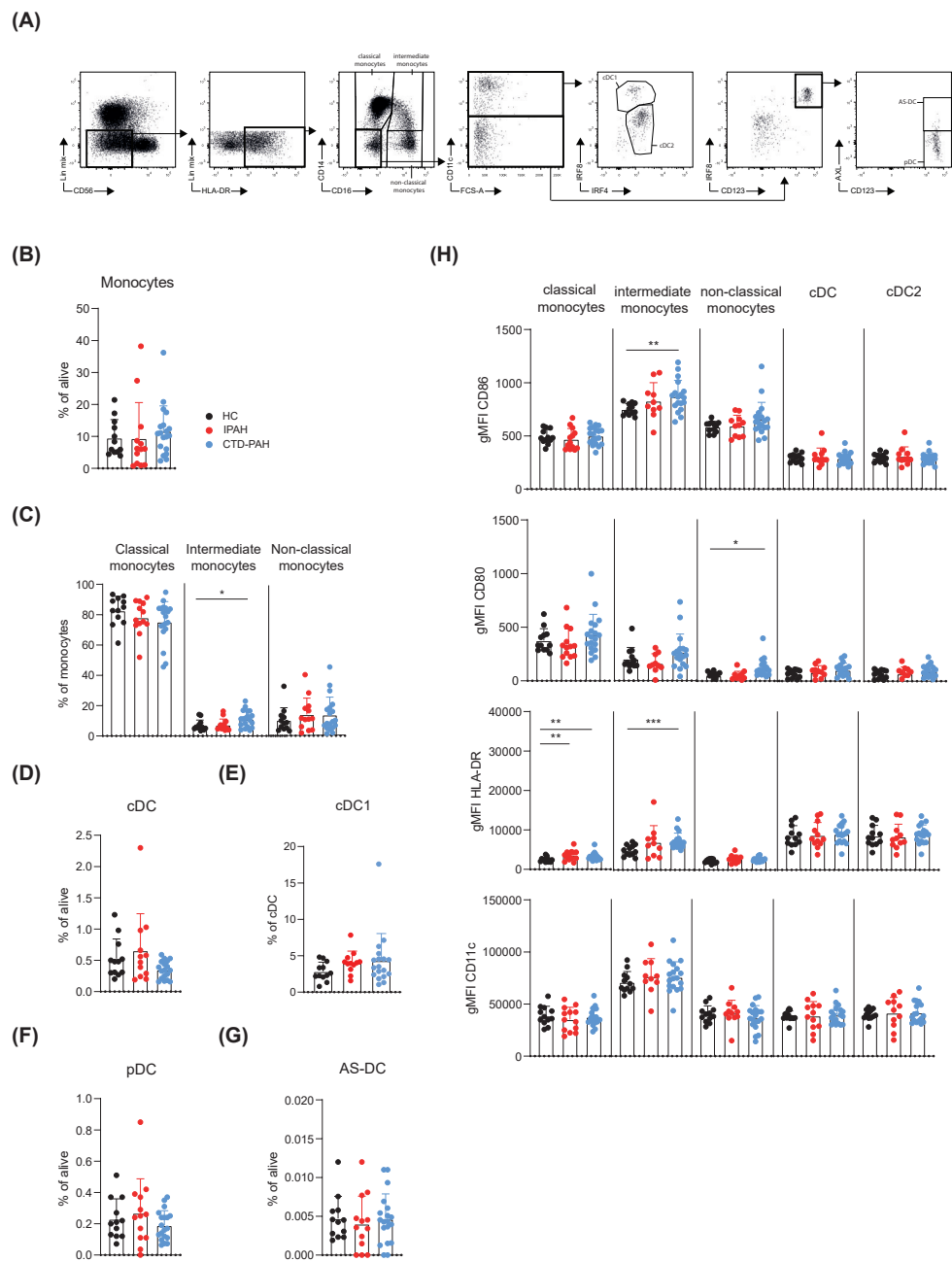


**Figure S4.** Limited differences in peripheral blood monocytes and dendritic cells between IPAH or CTD-PAH patients and HCs. (A) Flow cytometric gating strategy of monocyte and dendritic cell (DC) subsets. (B-G) Quantification of proportions of monocytes (B), monocyte subsets (C), conventional DCs (cDCs) (D), type 1 cDCs (cDC1) (E), plasmacytoid DCs (pDCs) (F) and AXL<sup>+</sup> Siglec<sup>+</sup> DCs (AS-DCs) (G). (H) Expression of the indicated activation markers on monocyte and DC subsets. Results are presented as mean + standard deviation; symbols represent values of individual patients or HCs. Mann-Whitney U test was used for statistical analysis, \*  $p < 0.05$ , \*\*  $p < 0.01$ , \*\*\*  $p < 0.001$ . gMFI = geometric mean fluorescence intensity.

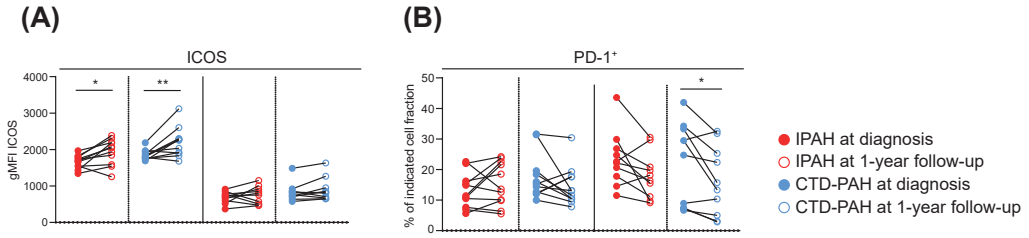


**Figure S5.** PD-1 and CTLA4 expression in PAH patients changes over time. (A-B) Quantification of ICOS expression (A) and PD-1 (B) in the indicated T cell fractions in samples from IPAH and CTD-PAH patients at diagnosis and 1-year follow-up, as determined by flow cytometry. Closed and open circles represent values of individual patients at diagnosis or 1-year follow-up, respectively. Paired samples are connected by lines. Wilcoxon matched-pairs signed rank test was used for statistical analysis, \*  $p < 0.05$ , \*\*  $p < 0.01$ . gMFI = geometric mean fluorescence intensity.

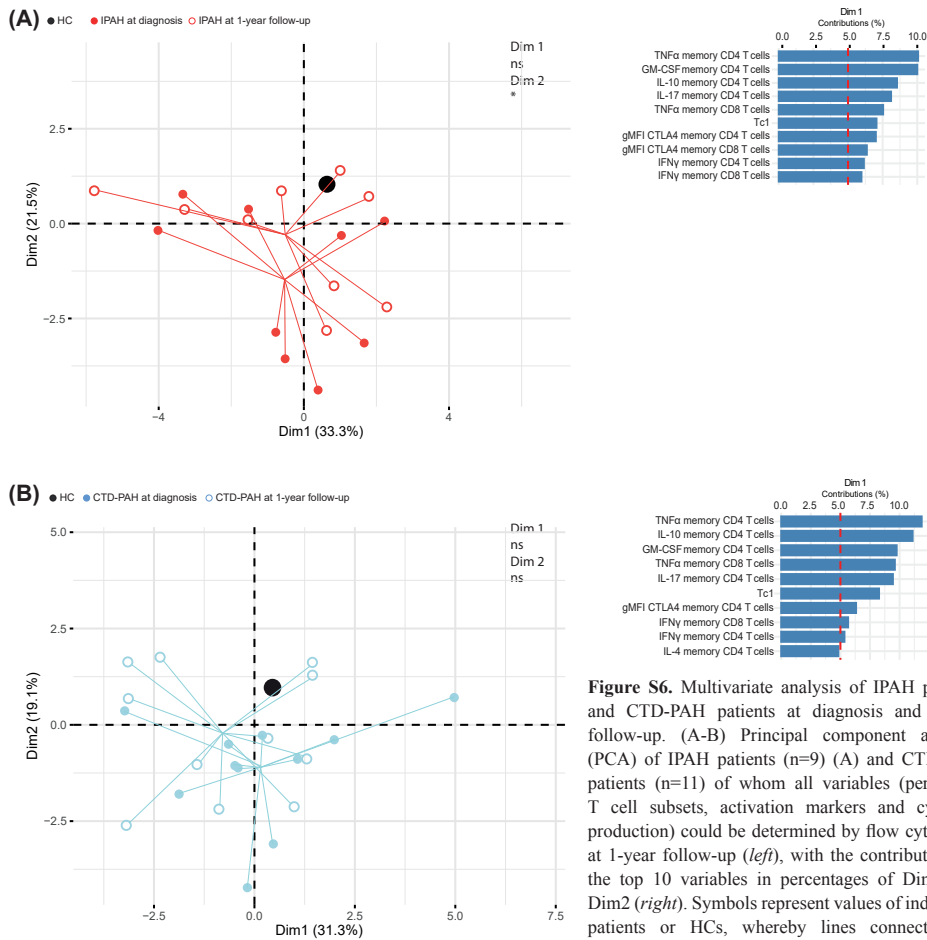


**Figure S6.** Multivariate analysis of IPAH patients and CTD-PAH patients at diagnosis and 1-year follow-up. (A-B) Principal component analysis (PCA) of IPAH patients ( $n=9$ ) (A) and CTD-PAH patients ( $n=11$ ) of whom all variables (peripheral T cell subsets, activation markers and cytokine production) could be determined by flow cytometry at 1-year follow-up (*left*), with the contributions of the top 10 variables in percentages of Dim1 and Dim2 (*right*). Symbols represent values of individual patients or HCs, whereby lines connect these values to the mean Dim1 and Dim2 coordinates. Mean coordinates of HCs are indicated in black. Wilcoxon matched-pairs signed rank test was used for statistical analysis. \*  $p < 0.05$ .



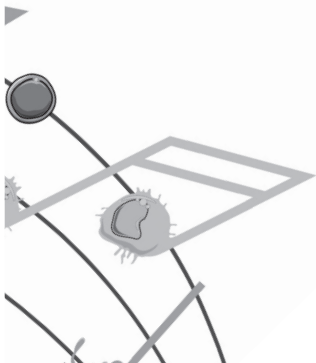
# CHAPTER 7

*The effects of a 10-week outpatient pulmonary rehabilitation programme on exercise performance, muscle strength, soluble biomarkers and quality of life in patients with pulmonary hypertension.*

**T. Koudstaal\***, M. Wapenaar\*, D. van Ranst, R. Beesems, L.M. van den Toorn, A.E. van den Bosch, P.P. Chandoesing, K.A. Boomars

\*Contributed equally.

J Cardiopulm Rehabil Prev. 2019 Oct 4.



## ABSTRACT

### Purpose

Pulmonary arterial hypertension (PAH) is characterized by right ventricular failure, leading to exertional dyspnea, skeletal muscle weakness, and poor quality of life (QOL). Apart from treatment with PAH-specific drugs, guidelines recommend pulmonary rehabilitation (PR). Clinical PR programs have shown improvement in functional capacity and QOL. However, little is known about the effectiveness of an outpatient PR program. The aim of our study was to assess effectiveness of a multidisciplinary outpatient PR program.

### Methods

Patients with PAH or chronic thromboembolic pulmonary hypertension (CTEPH), who were in a stable condition on optimized drug therapy, followed a 10-wk outpatient program in a rehabilitation center. The PR program was designed to improve exercise capacity and health status by means of low load cycling, walking, and muscle training twice a week combined with psychological counseling. QOL was measured by the Cambridge Pulmonary Hypertension Outcome Review (CAMPHOR) questionnaire.

### Results

Twenty-one patients (13 women) with PAH ( $n = 16$ ) or CTEPH ( $n = 5$ ) completed the study. All patients were in New York Heart Association (NYHA) functional class III, and their mean age was  $45 \pm 16$  yr. After PR, the mean cycling endurance time increased by 4.4 min ( $P < .001$ ), 6-min walk distance by 12.2 m ( $P < .05$ ), and maximum inspiratory pressure by 5.8 cm H<sub>2</sub>O ( $P = .01$ ). Skeletal muscle function increased significantly. The CAMPHOR questionnaire demonstrated significant decrease in symptoms and improvement in QOL. Soluble biomarkers did not show any change before and after PR.

### Conclusions

Outpatient PR could be an effective instrument to improve exercise capacity and health status in patients with PAH or CTEPH.

## INTRODUCTION

Pulmonary arterial hypertension (PAH) is a rare and incurable condition of the pulmonary vasculature, characterized by increased pulmonary vascular resistance and elevated pulmonary arterial pressure leading to progressive right ventricular failure. Despite improvement in specific medical treatment of PAH over the last years, patients with PAH still suffer from significant dyspnea, fatigue and skeletal muscle weakness, resulting in exercise limitation/intolerance and poor QoL (17). Exercise intolerance is a key feature in PAH for which the underlying hemodynamic impairment is primarily responsible (13). Several studies however demonstrated that beside hemodynamic impairment and ventilatory - perfusion mismatches, respiratory and skeletal muscle dysfunction plays an important role in exercise limitation in PAH patients (293-298) and therefore is an important determinant for exercise limitation (299-302).

Since muscle impairment limits PAH patients in their daily life activities, it has a strong negative influence on QoL (294, 303, 304). Improvement of muscle dysfunction and exercise intolerance are therefore recognized to be important goals in the treatment of PAH patients. Exercise programmes have been shown to improve muscle function by increasing type I fibre surfaces (296, 305). Moreover, previous studies have shown both a shift from type IIX to type IIA fibres and a total increase in type II fibre numbers. Furthermore, exercise programmes have been demonstrated to improve muscle capillarization (296, 305), muscle strength and exercise capacity in PH patients (295, 306, 307). This not only results in a higher physical activity level, but also in improvement of health-related QoL measured by the 36- Item Short Form Survey (SF-36) (308-310).

Historically, patients with PAH were recommended to restrain from physical activity, including pulmonary rehabilitation (PR) because of poor prognosis and risk of sudden cardiac death. In 2006, Mereles et al. were the first to demonstrate in a small randomized controlled trial that exercise training is safe and has beneficial effects on functional capacity and QoL (308).

Little is known so far about the effect of exercise training on right ventricle (RV) function. Most studies did not show a significant effect, while some showed a minor decrease in systolic RV pressure measured by echocardiography (308, 310-312). The underlying mechanism has not yet been elucidated, although in a rat model it was shown that exercise training may lead to less pronounced pulmonary vascular remodelling, and only high intensive training lowered RV systolic pressure and RV hypertrophy (313, 314). Biomarkers such as N-terminal pro B-type natriuretic peptide (NT-pro BNP) and high sensitive troponin-T (HsTnT), are recognised as markers for RV function and are negatively associated with outcomes in patients with PH (17). We therefore investigated these markers in our patient group before and after PR programme as a marker of RV function.

In recent years, evidence of the beneficial effects of PR is increasing (14-16). The European Respiratory Society (ERS) and the European Society of Cardiology (ESC) Guidelines for the diagnosis and treatment of PH recommend supervised rehabilitation programmes in expert centres for PAH patients in stable condition on optimized PH specific drug therapy (17). However, most programmes so far have been carried out in a hospital setting or were at least started in a hospital setting. Unfortunately, programmes in a hospital setting are not always feasible for patients.

We know PAH as a disease that has great impact on the QoL of these patients (315). This has also been shown by a QoL questionnaire specifically designed for patients with PAH, the Cambridge Pulmonary Hypertension Outcome Review (CAMPHOR) (316, 317). We therefore decided to offer

a PR programme with a multidisciplinary approach including: educational sessions, psychological counselling, advice by an occupational therapist, dietary advice, and group sessions with fellow patients.

Since knowledge about the safety and effectiveness of a PR programme in an exclusively outpatient setting is still lacking, our goal was to develop an achievable multidisciplinary outpatient PR programme.

We considered withholding PAH patients from a PR program at this stage not to be ethical. This study has therefore specifically been designed as a prospective cohort study.

The aim of our study was to assess the effectiveness of such an outpatient PR programme on exercise capacity, muscle strength, soluble biomarkers and QoL.

## **METHODS**

### **Study design**

This prospective cohort study was conducted from January 2016 until December 2017 as a collaboration between the Erasmus University Medical Centre (Rotterdam, The Netherlands) and the Revant rehabilitation centre (Breda, The Netherlands). Patients underwent an assessment at the rehabilitation centre before entering the programme. They followed an outpatient PR programme for ten weeks consisting of two sessions per week. Immediately after the PR programme an assessment was performed to evaluate the effectiveness of the programme.

### **Study procedure**

All patients were diagnosed according to the ERS/ESC guidelines(17). Patients in World Health Organisation (WHO) group I and WHO group IV were eligible for the study. Patients had to be in a clinically stable condition under optimized PH drug therapy for at least three months before entering the study. No changes in PH specific medication were made during the PR programme. Patients were excluded if they had participated in a rehabilitation programme previously, if they were not able to give informed consent, or if they were <18 years of age. This protocol was approved by the medical ethical committee, Erasmus MC Rotterdam, the Netherlands (protocol MEC-2011-392). All participating patients signed an informed consent form before commencing the programme.

### **Outcome measures**

Patients were evaluated at baseline and week 10, immediately after the PR programme. Primary outcome measures were changes at week 10 compared to baseline in exercise capacity, determined by cycling endurance time (CET), and change in QoL as measured by CAMPHOR.

Our PR programme was designed to focus on both muscle strength and endurance for cycling and walking. Therefore, we chose the measured cycling endurance time (minutes) as primary endpoint to investigate the effect of PR on endurance and exercise capacity. The CET was measured by a sub-maximal constant work rate exercise test at a constant load 75% of the baseline peak workload.

The CAMPHOR is a self-administered PH-specific health status questionnaire with three scales to assess symptoms, activity and quality of life. It also contains three symptom-subcales for energy,

The effects of a 10-week outpatient pulmonary rehabilitation programme on exercise performance, muscle strength, soluble biomarkers and quality of life in patients with pulmonary hypertension

breathlessness and mood. Scores for symptoms and QoL range from 0-25, higher scores indicating worse QoL. Activity scores range from 0-30, higher scores indicating more physical limitations. Prior research validated the CAMPHOR questionnaire and the correlation between 6MWD and NYHA classification (317). The CAMPHOR questionnaire was taken at baseline and after 10 weeks of PR.

Secondary outcome measures were changes at week 10 compared to baseline in 6MWD, respiratory muscle strength (maximal inspiratory mouth pressure (MIP)) and skeletal muscle strength (Quadriceps Force (QF) and Biceps Force (BF)). The 6-minute walking test (6MWT) was carried out according European Respiratory Society (ERS)/American Thoracic Society (ATS) technical standards (318). The MIP was measured during a forced inspiratory effort from residual volume, using a respiratory pressure meter (MicroRPM) (319). QF and BF were assessed using a handheld dynamometer (MicroFET2) respectively during maximal isometric knee extension and elbow flexion (320). The maximal peak cycling workload was measured during a maximal incremental symptom-limited cardiopulmonary exercise test (CPET) carried out in semi-supine position. The test was performed according to American Thoracic Society guidelines (321), with 3 minutes of rest, 3 minutes of unloaded cycling, followed by a progressive increase of the workload (5-25 Watt/minute). Ventilation ( $\dot{V}_E$ ), oxygen-uptake ( $\dot{V}O_2$ ) and carbon dioxide output ( $\dot{V}CO_2$ ) were measured breath-by-breath using a Jaeger CPX metabolic cart. Ventilatory efficiency was derived from the measured  $\dot{V}_E$  and  $\dot{V}CO_2$  ( $\dot{V}_E/\dot{V}_{CO_2}$ ).

## Pulmonary rehabilitation programme

The 10-week PR programme with two group training sessions per week was especially developed for PH patients. The programme included endurance training (walking and cycling), lower- and upper limb strength training, individualized psychological counselling, dietary advice, advice by an occupational therapist, educational group sessions and interaction sessions with fellow patients. Once a week the group would go outdoors during a physical training session to train activities in a real-life setting, e.g. going to a supermarket or walking. Supplementary table 1 shows the duration of the different activities of both weekly training sessions. During educational sessions, information was provided by various members of the multidisciplinary team on pathophysiological changes in PH, the importance of dietary advice on the intake of proteins and vitamins, acceptance and coping of the disease and on how to manage energy distribution (breathing techniques etc.). Specific PH questions from the patients were collected and answered by the PH specialized pulmonologist and PH specialized nurse.

To individualize the training programme and determine the training intensity at the start, patients performed exercise tolerance tests during the 2-3 days of baseline assessments. A symptom-limited maximal incremental CPET was performed to assess the maximal workload ( $W_{max}$ ) and two 6MWTs to evaluate distance walked and speed.

### The training programme contained the following components:

*Bicycle occupational training* by a stepwise schedule. Step 1 and 2 started with exercise-rest interval training at 40% of the maximal workload achieved during the incremental CPET at baseline ( $W_{max}$ ). Step 3 till 10 comprised continuous cycling for 15-20 minutes at 40% to 80% of  $W_{max}$ . The training intensity progressed to the next step if perceived exertion during exercise remained  $< 5$  at the Borg dyspnea scale, if fatigue did not last  $> 24$

hours after the previous training session and if existing physical complaints did not increase. *Walking training* on a treadmill according to a protocol with the same stepwise approach as mentioned above. Step 1 to 3 comprised an interval training at 60%-75% of the speed achieved during the 6MWT at baseline. Step 4 to 10 comprised continuous walking during 10-15 minutes at 60-75% to 75-100% of the baseline 6MWT-speed.

*Resistance training* consisted of training leg-, arm and abdominal muscles on weight training equipment (Technogym). During the baseline assessment, the one repetition maximum (1RM) training weight that could correctly be moved with appropriate breathing was determined for each exercise. During subsequent sessions, the training was intensified by gradually increasing repetitions of movements as well as weight/load to respectively improve muscle strength and endurance according to ATS/ERS statement on pulmonary rehabilitation(14).

### **Outdoor session:**

Once weekly the training sessions included a 60-minute outdoor group activity, such as walking or cycling. Physiotherapists supervised all training sessions and, if needed, educated the patients in perceiving their physical limits and optimal breathing technique. Symptoms, heartrate and oxygen saturation (SpO<sub>2</sub>) to exercise, were closely monitored following specific PH rehabilitation guidelines(14, 17)

### **Biomarkers:**

Blood samples were collected on the first and on the last day of the pulmonary rehabilitation program. Biomarker assessment was performed including C-reactive protein (CRP), cystatin C, haemoglobin, red cell distribution width (RDW), NT-pro BNP, HsTnT, iron and uric acid. Biomarkers were measured in peripheral blood samples, within <1 hour after venous puncture at the clinical chemistry department at the Erasmus MC, Rotterdam, The Netherlands.

### **Statistics**

Values are reported as mean (standard deviation) unless otherwise indicated. Changes in exercise capacity, muscle strength and QoL from baseline to 10 weeks were assessed using paired t-test or Wilcoxon signed rank test.

P-values <0.05 were considered statistically significant. All statistical analyses were performed using Prism (GraphPad Software, La Jolla, CA, USA) or SPSS version 24.

## **RESULTS**

In this study, 21 patients were included with either PAH (N=16) or inoperable chronic thromboembolic pulmonary hypertension (CTEPH), (n=5). The demographics of the study group, which consisted of 8 men and 13 women, are provided in Table 1.

The effects of a 10-week outpatient pulmonary rehabilitation programme on exercise performance, muscle strength, soluble biomarkers and quality of life in patients with pulmonary hypertension

**Table 1. Demographic and patient characteristics.**

<b>Characteristic</b>	<b>Pulmonary Hypertension Patients (n=21)</b>
Gender, female	13 (61.9%)
Age, y	45.1, ±15.5
Height, cm	166.7, ±9.4
Weight, kg	79.9, ±23
BMI, kg/m <sup>2</sup>	28.5, ±7.1
<b>WHO functional class</b>	
III	21 (100%)
<b>Cause of pulmonary hypertension, n (%)</b>	
CTEPH	5 (23.9%)
PAH	16 (76.1%)
IPAH (n, % of PAH)	7 (33.3%)
CHD (n, % of PAH)	5 (23.8%)
SLE/SSc (n, % of PAH)	3 (14.3%)
PVOD (n, % of PAH)	1 (4.8%)
<b>PH-specific drugs, n (%)</b>	
PDE5 inhibitor	18 (85.7%)
ERA	19 (90.4%)
Prostacyclins	4 (19.0%)
Selexipag	4 (19.0%)
<b>Drug combination therapy, n (%)</b>	
Monotherapy	3 (14.3%)
Dual therapy	10 (47.6%)
Triple therapy	7 (33.3%)
<b>Echocardiography (&lt;6 months prior to PR)</b>	
RV pressure, mmHg	55.8, ±22.9
RA pressure, mmHg	5.4, ±3.3
RVSP, mmHg	61.2, ±23.4
6MWT, m	465.2, ±97.7
6MWT, %predicted*	84.0 (73-79)
6MWT Borg fatigue score (end of test)	4.4, ±2.3
6MWT Borg dyspnea score (end of test)	5.4, ±2.8
<b>CPET</b>	
Peak Workload, W	70.8, ±37.9
Peak V'O <sub>2</sub> , %pred	55.3, ±18.3
Peak V'O <sub>2</sub> , ml/kg/min	13.7, ±3.4
RER	1.13, ±0.13
V'E <sub>max</sub> , L/min	50.2, ±16.1
HR <sub>max</sub> , %pred	73.1, ±12.6
Peak V'E/V'CO <sub>2</sub>	43.1, ±10.8

Data given as 'mean, ±SD', unless otherwise indicated. \*Median (interquartile range IQR).

**Abbreviations:** BMI, body mass index; CTEPH, chronic thromboembolic pulmonary hypertension; PAH, pulmonary arterial hypertension; IPAH, idiopathic pulmonary arterial hypertension; CHD, congenital heart disease;

SLE/SSc, systemic lupus erythematosus or systemic sclerosis associated PH patient; PVOD, pulmonary veno-occlusive disease; 6MWT, 6-minute walk test; CPET, cardiopulmonary exercise test; PDE-5, phosphodiesterase-5 inhibitor; ERA, endothelin receptor antagonist; RV, right ventricle; RA, right atrium; RVSP, right ventricular systolic pressure.

All study subjects tolerated the exercise testing and training well. No adverse events, defined as an increase in symptoms, progression of PH, or need for hospital admission, took place during the programme. There was no withdrawal or loss to follow up of patients during the PR programme.

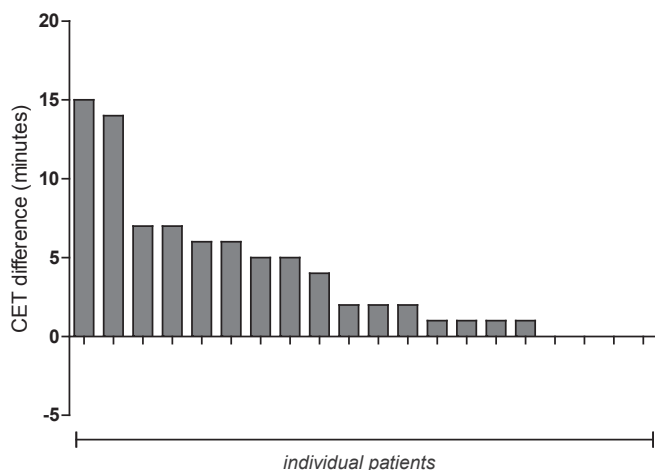


**Figure 1.** Change in CET (cycling endurance time) for individual patients at baseline and after a 10-wk outpatient pulmonary rehabilitation program.

Mean CET increased significantly by 4.4 minutes (+92%) after 10 weeks of PR (Figure 1; table 2). Comparing results of the CAMPHOR questionnaire before and after PR, our study group showed an improvement of scores for symptoms ( $p=0.004$ ) and QoL (Figure 2).

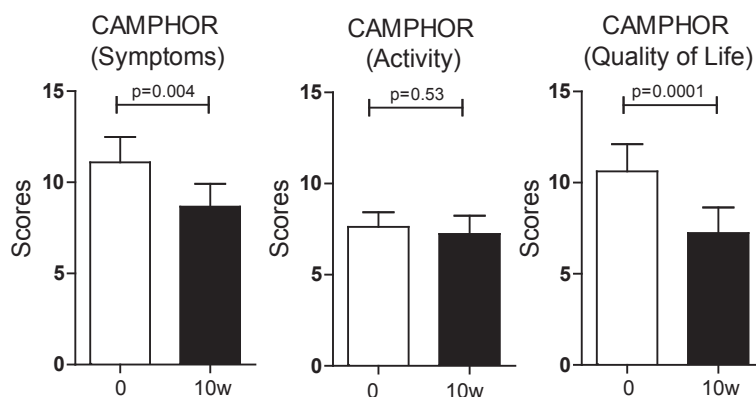


**Figure 2.** Health-related quality-of-life scores (CAMPHOR, Cambridge Pulmonary Hypertension Outcome Review) at baseline (white bars) and after a 10-wk outpatient pulmonary rehabilitation program (black bars). Values are mean  $\pm$  standard error of mean.

The effects of a 10-week outpatient pulmonary rehabilitation programme on exercise performance, muscle strength, soluble biomarkers and quality of life in patients with pulmonary hypertension

## SECONDARY ENDPOINTS

After 10 weeks of PR, 6MWD was increased by 3% (12.2 ±20.4m; Table 2).

After PR therapy, mean muscle function of the dominant quadriceps side increased by 78 newtons (N) (+23%). In the non-dominant quadriceps, mean muscle function increased by 62N (+18%) after PR (Figure 3A). Similarly, biceps dominant muscle function increased by 11N (+6%) after PR. In the non-dominant biceps, muscle function increased by 16N (+9%) after PR (Figure 3B). Changes in percentage of predicted values of the muscle function tests are shown in Figure 3A/B. After 10 weeks of PR, MIP was increased significantly compared to baseline (Table 2).

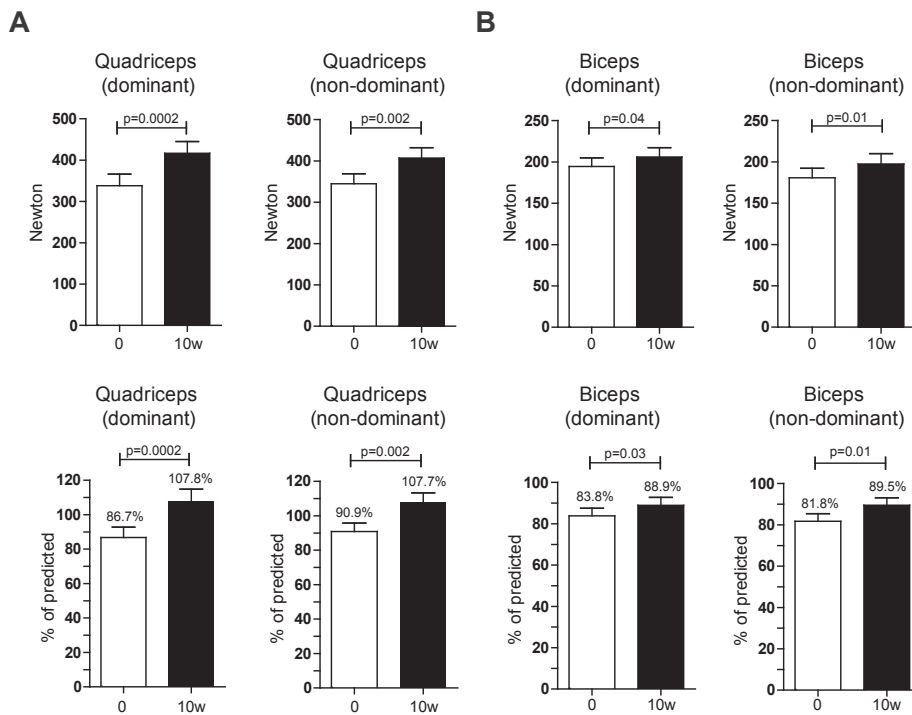


**Figure 3.** Skeletal muscle function of quadriceps (A) and biceps (B) (dominant and nondominant) at baseline (white bars) and after a 10-wk outpatient pulmonary rehabilitation program (black bars). Values are shown as mean percentage of predicted } standard error of mean.

Soluble biomarker levels were measured in all study subjects at baseline and after the PR programme. However, no significant changes were seen in the soluble biomarker profiles. (Table 2).

**Table 2. Test results at baseline and after a 10-week outpatient pulmonary rehabilitation programmed.**

Characteristic	Baseline (n=21)	Post-rehabilitation therapy (n=21)	P Value
CET (min)	4.8 (±2.1)	9.2 (±5.5)	<0.001
6MWT (m)	465.2 (±97)	477.4 (±92)	0.01
6MWT Borg fatigue score	4.4 (±2.3)	4.8 (±2.0)	0.38
6MWT Borg dyspnea score	5.4 (±2.8)	5.3 (±2.1)	0.89
MIP (cm H <sub>2</sub> O)	97.6 (±17.5)	103.40 (±20.1)	0.01
MIP (% of predicted)	102.95 (±17.9)	109.45 (±22.3)	0.01
<b>Soluble biomarkers:</b>	<b>Baseline (n=21)</b>	<b>Post-rehabilitation therapy (n=21)</b>	<b>P Value</b>
Hemoglobin (mmol/L)	8.07 (±1.29)	7.90 (±1.31)	0.06
RDW (%)	15.21 (±2.9)	14.92 (±2.2)	0.36
Uric acid (mmol/L)	0.32 (±0.10)	0.32 (±0.11)	0.78
Iron (micromol/L)	15.21 (±2.85)	14.92 (±2.23)	0.36
Cystatin C (mg/L)	1.18 (±0.50)	1.17 (±0.34)	0.98
CRP (mg/L)	6.13 (±7.25)	5.21 (±6.74)	0.43
Hs-TnT (ng/L)	11.22 (±9.53)	12.11 (±11.00)	0.46
NT-pro BNP (pmol/L)	86.83 (±173.8)	88.72 (±155.4)	0.87

Data given as 'mean, ±SD'. 6MWT Borg score values were end of test scores.

**Abbreviations:** 6MWT, 6-minute walk test; MIP, maximal inspiratory pressure; RDW, red cell distribution width; CRP, C-reactive protein; Hs-TnT, High sensitive troponin-T; NT-pro BNP, N-terminal pro B-type natriuretic peptide.

## DISCUSSION

In this study we demonstrated that our multidisciplinary outpatient PR programme is safe for PH patients, since no adverse events occurred during the 10-week training period. Moreover, there was a positive effect on primary outcome parameters, including exercise capacity and endurance measured by CET, as well as QoL in two out of three scales measured by the CAMPHOR questionnaire. Additionally, all secondary outcome measures were also improved, including 6MWD, respiratory muscle strength and skeletal muscle strength.

While several studies have shown effectiveness of PR in an inpatient setting (308, 309, 322), our study also shows beneficial effects for PR in an exclusively outpatient setting. The most beneficial effect was found in functional endurance measured by bicycle endurance (increase in CET of 4.8 minutes or 288 seconds). This result can be considered as a clinical meaningful effect since in a study by Laviolette et al. (323) in patients with COPD, a difference of 100-200 seconds in the CET was regarded as a clinical significant result. A significant, however small increase in 6MWD was demonstrated as well. This relatively limited effect compared to the larger effect shown in other rehabilitation studies (308, 312), could be due to a 'ceiling' effect in the 6MWT as shown by Frost et al.(324). The mean 6MWD at baseline in our cohort was 465m. Since all other outcome parameters (cycling endurance time, skeletal muscle function, quality of life) changed significantly with a larger improvement and considering the findings by Frost et al, we assume that a ceiling effect in the 6MWT is a more logical explanation of our data than different exercise volumes.

The effects of a 10-week outpatient pulmonary rehabilitation programme on exercise performance, muscle strength, soluble biomarkers and quality of life in patients with pulmonary hypertension

Since assessment of daily activity may be more clinically meaningful to a patient than the 6MWD (325), accelerometry may be an even better indicator of physical activity in daily life (326). Therefore, accelerometry could be considered for all PR programs as an instrument for quantifying physical activity. Consistent with other PR programmes (309, 311, 322), we observed no changes in soluble biomarkers levels before and after the PR programme. A small decrease in RV systolic pressure has been seen in just a few, but not all studies. More studies investigating the effects of exercise training on pulmonary vascular remodelling, RV function and RV remodelling are needed, as well as studies assessing possible underlying mechanisms.

QoL, as measured by the CAMPHOR questionnaire, also improved significantly in our study group for the categories 'symptoms' and 'quality of life'. The 'activity' category however did not show a significant change. Individual patient evaluations on the other hand showed an increased capacity for activity. This observed difference by the CAMPHOR questionnaire might be due to a lack of discriminative power in a relatively small patient group.

In a PR study by Chan and colleagues, the 'functioning' category from the CAMPHOR questionnaire did not show a significant improvement either. This study group however, was even smaller (327).

At the end of this PR programme, all patients received a personalized training programme to continue physical training under supervision of a first line physiotherapist to enhance the duration of the beneficial effect. Future studies are needed to evaluate the duration and clinical implications of our PR programme.

Our study however also has several limitations. Firstly, the study group consisted of PAH patients WHO class 1 with different underlying causes and WHO class 4, CTEPH patients. Analysis of the data of solely the PAH/WHO I group showed similar results. The study unfortunately lacks power to draw conclusions for specific PAH sub-groups. Secondly, only NYHA class III patients were included, which was not our initial intention. However, NYHA class III patients are undoubtedly clinically impaired in their functioning in daily life, more so than NYHA class I and II patients. They might therefore be more motivated to participate in an extensive PR programme. Moreover, NYHA class III patients are still able to participate in an intensive outpatient PR programme, which might not be possible in the case of NYHA class IV patients. This possible explanation was also shown by Hayton et al in a study where COPD patients showed decreased PR attendance when either their disease was too mild or the COPD too severe to benefit from PR (328). Lastly, in a paper by Spruit and colleagues training three times a week was regarded to be even more effective (14). However, our aim was to maximize training efficiency and to minimize the impact of the PR programme on daily life activities of the participating PH patients.

## Conclusion

This study demonstrates that a 10-week multidisciplinary PR programme has considerable beneficial effects on functional capacity, functional endurance, skeletal muscle function and health related QoL. While many studies have shown effectiveness for inpatient rehabilitation programmes for PH patients, our study demonstrated that an exclusively outpatient PR programme for PH patients is effective and safe. Long term durability of these improvements and implications must be further evaluated in future studies.

**Acknowledgements**

The authors would like to thank the staff of the Revant rehabilitation centre for the excellent collaboration. We would also like to thank our specialised PH and research nurses at the Erasmus University Medical Centre for their contribution to this study.

The effects of a 10-week outpatient pulmonary rehabilitation programme on exercise performance, muscle strength, soluble biomarkers and quality of life in patients with pulmonary hypertension

## SUPPLEMENTARY MATERIAL

**Supplementary table 1. Daily group training session schedule.**

Group training - Session 1		Group training - Session 2	
45 minutes	Treadmill walking Cycling Fitness training	45 minutes	Treadmill walking Cycling Fitness training
15 minutes	Rest	15 minutes	Rest
60 minutes	Outdoor walking or cycling	60 minutes	PH specific education on health
15 minutes	Rest		
45 minutes	Treadmill walking Cycling Fitness training	45 minutes	Treadmill walking Cycling Fitness training
15 minutes	Rest	15 minutes	Rest

**Supplementary table 2. Patient characteristics, RHC values at diagnosis.**

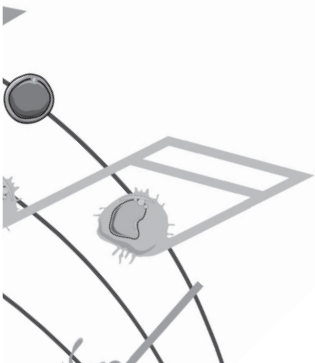
Characteristic	Pulmonary Hypertension Patients (n=21)
Right heart catheterization (at diagnosis)	
Mean pulmonary artery pressure, mmHg	46.0, $\pm$ 15.6
Right atrial pressure, mmHg	8.4, $\pm$ 4.4
Pulmonary capillary wedge pressure, mm Hg	8.7, $\pm$ 4.3

Data given as 'mean,  $\pm$ SD'.



# CHAPTER 8

*General discussion*



## GENERAL DISCUSSION

Pulmonary hypertension is a devastating disease with poor survival, despite PH-specific drug treatment options. Novel insights are required to gain knowledge into critical pathways that reflect possible therapeutic targets and new treatment options for patients. The aims of this thesis were to; **(I)** further unravel the immunological imbalance in pulmonary arterial hypertension (PAH) and chronic thromboembolic pulmonary hypertension (CTEPH) pathogenesis, **(II)** to find novel biomarkers and therapeutic targets for PAH and CTEPH, and **(III)** to improve non-drug treatment options in PAH and CTEPH. In this discussion, research aims and obtained results are placed in perspective of current knowledge and outstanding questions for future research are postulated.

### Main findings in this thesis.

In **chapter 2 and 3**, we described our findings concerning the importance of DC activation in PH pathogenesis in the *Tnfaip3*<sup>DNGRI-KO</sup> mouse model. In this model, we showed that constitutive activation of the NF- $\kappa$ B pathway specifically in conventional DCs (cDCs) in mice, resulted in the development of a PH phenotype with increased right ventricular (RV) systolic pressure (RVSP), RV hypertrophy and pulmonary vascular remodeling. In the *Tnfaip3*<sup>DNGRI-KO</sup> model, we found increased numbers and activation of proliferating CD8<sup>+</sup>T cells in the lungs. Strikingly, we also observed co-localization of DCs and CD8<sup>+</sup>T cells adjacent to the pulmonary vasculature in human IPAH lung samples.

We observed elevated plasma levels of various cytokines in three PAH subgroups and CTEPH patients (**chapter 4**). Strikingly, CXCL9 plasma levels were increased in CTEPH patients, and correlated with survival data. Particularly, when inflammatory mediators were combined with clinical parameters in multivariate analyses, PAH and CTEPH patients clustered into WHO classification-independent subgroups that correlated with patient survival.

Phenotypic analysis of peripheral blood T cells of CTEPH patients revealed increased frequencies of CCR6<sup>+</sup> CD4<sup>+</sup>T-cells, a significantly reduced cytokine production capacity and increased expression of the immune checkpoint protein CTLA4 for both CD4<sup>+</sup> and CD8<sup>+</sup>T cells, compared to healthy controls (**chapter 5**). At 1-year follow-up, proportions of CCR6<sup>+</sup>CD4<sup>+</sup>T cells were further increased, and the IFN $\gamma$  and IL-17 production capacity of CD4<sup>+</sup>T cells was restored. Furthermore, CCR6<sup>+</sup>T-cells were present in vascular lesions in pulmonary endarterectomy material from CTEPH patients.

At the time of diagnosis, T cells of IPAH patients were less capable of producing the cytokines TNF $\alpha$ , IFN $\gamma$ , IL-4 and IL-17 compared to HCs (**chapter 6**). In contrast, the cytokine-capacity of T cells from patients with connective tissue disease PAH (CTD-PAH) did not differ from HCs. T cells of both PAH subgroups had a high CTLA4 expression, which was only accompanied in CTD-PAH patients by increased ICOS expression. Multivariate analysis indicated a specific T cell cytokine profile that separated IPAH patients from HCs. Remarkably, such a profile was not found for CTD-PAH. At 1-year follow-up in IPAH and CTD-PAH patients displayed an increase in the proportions of Th17 and Tc17 cells. Hereby, only the T cell fractions of IPAH patients had decreased CTLA4 expression.

Lastly, a common clinical feature of PAH patients is deterioration of physical condition and diminished quality of life, which naturally needs improvement. In **chapter 7**, we described that a 10-week multidisciplinary pulmonary rehabilitation (PR) programme has considerable beneficial effects on functional capacity, functional endurance, skeletal muscle function and health related QoL. Lastly, we found no changes between clinical biomarkers (**chapter 7**) and in inflammatory biomarkers (Koudstaal

T *et al*, unpublished data) after our 10-week PR programme.

*In summary, our findings demonstrate:*

1. *That aberrant activation of DCs in mice is sufficient to induce an experimental PH phenotype.*
2. *That peripheral blood Tcells in treatment-naïve PAH and CTEPH patients show significant alterations in cytokine production, chemokine expression and activation status.*
3. *That the changes found in peripheral T-cell phenotype are different between PAH subgroups and CTEPH.*
4. *That alterations in T-cell cytokine production, T-helper subsets numbers and activation status change over time, most likely due to PH-specific drug therapy or progression of disease.*
5. *That PAH and CTEPH patients display increased levels of inflammatory mediators in peripheral blood, specifically the chemokine CXCL9, which correlates to survival outcome in CTEPH patients.*
6. *That a correlation exists between inflammatory alterations found in the peripheral blood compartment and locally in the lung, such as increased CCR6<sup>+</sup> T-cell numbers.*
7. *That a fully outpatient pulmonary rehabilitation program is safe and beneficial for functional endurance and quality of life in PAH and CTEPH patients.*

Taken together, we conclude that our findings provide substantial evidence for a pivotal role of the immune system in the pathogenesis of both PAH and CTEPH (**Figure 1**).

## UNRAVELING THE IMMUNOLOGICAL IMBALANCE IN PAH AND CTEPH.

As described in **chapter 1**, accumulating evidence is showing a pathophysiological role for the immune system in the development of PAH and CTEPH (24, 215). Histological studies have shown increased perivascular presence of various immune cells such as T-cells, B-cells and dendritic cells in lungs of idiopathic PAH (IPAH) patients and in pulmonary endarterectomy material (PEA) in CTEPH patients (215). Several studies provided evidence for the pathophysiological involvement of both immune cells in the innate and the adaptive immune system (24, 215). In **chapter 2, 3, 5 and 6**, we further elucidated the possible pathophysiological role for dendritic cells (DCs) and T-cells in PH (**Figure 1**).

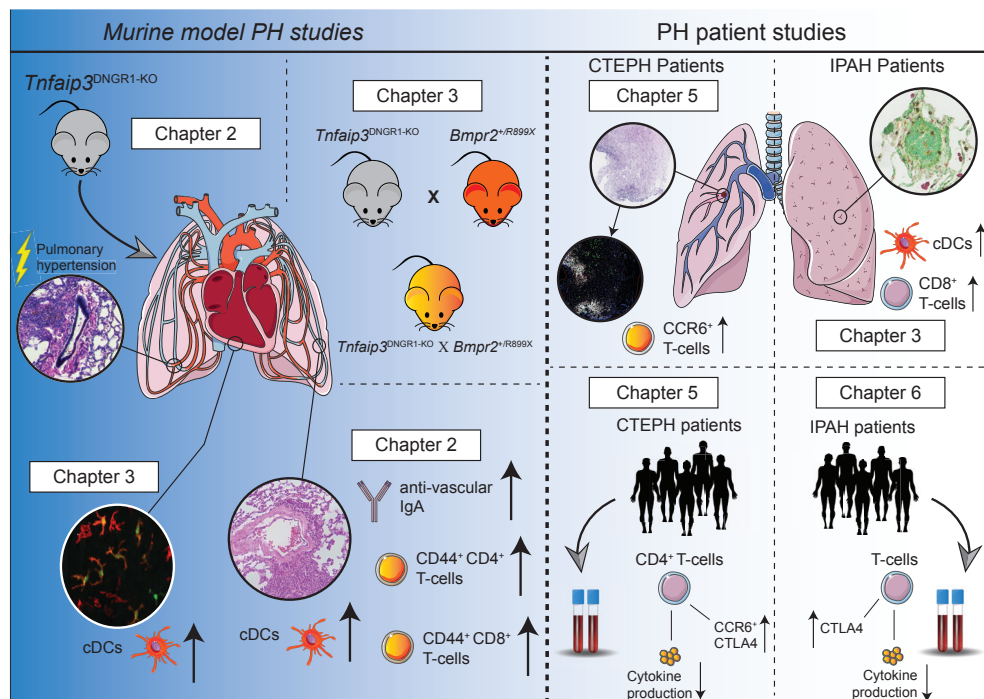


**Figure 1.** Murine and PH patient studies discussed in this thesis. cDCs; conventional dendritic cells, IPAH; idiopathic pulmonary arterial hypertension.

## Dendritic cells in PAH; innocent bystanders or dangerous orchestrators of autoimmunity?

The increased presence of DCs in idiopathic PAH (IPAH) lungs, as shown in 2007 by Perros et al (87), is particularly important, as DCs are known orchestrators of adaptive immunity. Following this interesting finding, subsequent studies showed that these DCs have an immature (DC-SIGN<sup>+</sup>) phenotype (87). Furthermore, the frequencies of conventional DCs (cDCs) and plasmacytoid DCs (pDCs) are augmented in total lung cell suspensions of IPAH patients compared to controls (55). In contrast, in peripheral blood, cDC numbers are decreased in IPAH patients (89), suggesting possible migration to the lungs. Although these studies demonstrate increased presence of DCs in the lungs, it remained unknown whether defects in DC subsets contribute to the pathogenesis of PAH.

In **chapter 2**, we investigated *Tnfaip3*<sup>DN<sup>GR1-KO</sup></sup> mice, with a Clec9a/DNGR1-Cre-mediated deletion of the *Tnfaip3* gene specifically in the type 1 cDC (cDC1) subset. The *Tnfaip3* gene encodes the ubiquitin-binding protein A20, which is a negative regulator of NF-κB, critically involved in DC activation. We demonstrated that these mice developed PH with vascular remodeling, increased right ventricular systolic pressure (RVSP) and right ventricular hypertrophy (RVH). Upon evaluation of known PH-inducing factors in *Tnfaip3*<sup>DN<sup>GR1-KO</sup></sup> mice, we concluded that the experimental PH phenotype was not likely to be induced by obstructive airway pathology or hypoxia. Furthermore, in previous work performed by our group (169), inflammatory auto-immune hepatic injury was found in *Tnfaip3*<sup>DN<sup>GR1-KO</sup></sup> mice. Considering that no signs of porto-pulmonary hypertension (PoPH) were observed, PoPH seems

unlikely to be the causal factor for the experimental PH phenotype in *Tnfaip3*<sup>DNGRI-KO</sup> mice. Neither did we find any signs of LV involvement or signs of LV failure resembling WHO PH group 2. Overall, the experimental PH phenotype in *Tnfaip3*<sup>DNGRI-KO</sup> mice shows resemblances with pulmonary arterial hypertension. WHO PH group II and WHO PH group III seem less likely as an underlying cause.

By crossing our *Tnfaip3*<sup>DNGRI</sup> mouse with ROSA-YFP mice, we evaluated the specificity for cDC1 targeting by the DNGRI-cre. In line with previous reports from our own group (169) and as demonstrated by Schraml *et al* (172), we found ~90% specific targeting of pulmonary cDC1s in *Tnfaip3*<sup>DNGRI-ROSA-WT</sup> mice by the DNGRI promotor-driven cre recombinase, which unexpectedly declined to ~50% in *Tnfaip3*<sup>DNGRI-ROSA-KO</sup> mice. Rather than a reduced DNGRI-cre driven excision specificity in cDC1s in *Tnfaip3*<sup>DNGRI-KO</sup> mice, it is more likely that this is due to a disturbance in cDC1 homeostasis after deletion of A20/*Tnfaip3*. Similar to increased liver DC frequencies in *Tnfaip3*<sup>DNGRI-KO</sup> mice (169), we found increased proportions of pulmonary cDC1s, cDC2s, and mo-DCs. This could partly be due to reduced sensitivity to apoptosis signals, caused by increased sensitivity to CD40L and RANKL pro-survival signals and upregulation of anti-apoptotic proteins Bcl-2 and Bcl-x as previously demonstrated by Kool *et al* in A20 deficient DCs (85). In recent years, many novel cDC1-specific Cre transgenic mouse models have been made available such as the XCR1-Cre or Karma-Cre (329), with superior cDC1 targeting specificity in comparison to the DNGRI-cre. These novel models remain specific for cDC1s even during disturbance of homeostasis, for example during viral infections (329). Considering the possible non-cDC1-specific effects, due to partial targeting of cDC2s and MO-DCs by the DNGRI-cre, utilization of these new models could give a more specific understanding of the pathological role of cDC1s in IPAH. To this end, it will be required to repeat part of the experiments in a more cDC1-specific model.

Furthermore, we demonstrated that specifically cDCs harbored an altered activation status as shown by enhanced MHCI, CD40 and PDL1 expression, which was regulated by both cell-intrinsic and cell-extrinsic effects. The increase in PDL1 is likely caused by cell-extrinsic factors, for which IFN $\gamma$  is a likely candidate as the proportion of IFN $\gamma$ -producing T cells is elevated in *Tnfaip3*<sup>DNGRI-KO</sup> mice. Possibly, this increased expression of PDL1 reflects a feedback mechanism for limiting excess immunopathology, induced by the increased production of IFN $\gamma$  or IL-12 (171). Unexpectedly, we found a decrease in the DC activation marker CD86, specifically in cDC1s. It is therefore conceivable that the homeostasis-disturbing deletion of regulatory enzyme A20/*Tnfaip3* cDC1s induces a more tolerogenic DC phenotype (330). Indeed, a similar phenomenon of decreased CD86 expression in pulmonary cDC1s was demonstrated by Vroman *et al*, in mice harboring a Cd207 (Langerin)-mediated excision of A20/*Tnfaip3* (171). Nevertheless, the phenotype that is seen in mice with a DNGRI-Cre or CD207-Cre-mediated deletion of A20 in DCs appears to be best explained by a more activated status of these cells.

In **chapter 2** and **chapter 3**, we described that A20 deficient DCs showed a perivascular localization in the lungs, and in the right ventricle of the heart in *Tnfaip3*<sup>DNGRI-KO</sup> mice. Remaining questions are how the aberrant activation of DCs result in PH development, what are the mechanisms involved and what is the sequence of events? Considering that increased accumulation of DCs in the lung and RV occurs prior to PH development, it is indicative that DC influx is not merely a consequence of increased pulmonary arterial pressure. Interestingly, increased myocardial inflammation has also been demonstrated in the hearts of systemic sclerosis associated (SSc-)PAH and IPAH patients, compared to controls (218). In SSc-PAH patients, immune cells were predominantly increased in the RV, but DCs were not specifically analyzed (218). A known complication of systemic lupus erythematosus (SLE) is

acute lupus myocarditis, a condition which can co-exist with SLE-PAH, as has been demonstrated in a recent case report (331). However, in SLE-associated PAH, it is most likely that the PAH phenotype is induced by narrowing of vessels due to vasculitis. Another cause of PAH in SLE patients is likely to be a hypercoagulable state induced by antiphospholipid antibodies with resultant in situ pulmonary arteriolar thrombosis, and increased vasoreactivity from decreased formation of endothelial prostacyclin (332, 333). Recent research has associated SLE development with changes in the DC compartment, including altered DC subset frequency and localization, overactivation of myeloid DCs and plasmacytoid DCs, as well as functional defects in DCs (334). The influx of myocardial DCs we demonstrated in **chapter 3**, might therefore resemble this type of SLE myocarditis, although we did not study the presence of thrombotic or vasculitis factors in the myocardium of *Tnfaip3*<sup>DNGRI-KO</sup> mice. Therefore, future studies should further elaborate on the etiology of the myocardial influx of DCs in *Tnfaip3*<sup>DNGRI-KO</sup> mice.

The PH phenotype in *Tnfaip3*<sup>DNGRI-KO</sup> mice was variable in severity, which could be due to variability of the *Tnfaip3/A20* gene deletion efficiency across different DC subsets and cell-extrinsic effects of the targeted deletion. This finding prompted us to consider the necessity of a second hit for PH development. While most other established PH rodent models require a second trigger such as monocrotaline (335), sugen (192) and/or hypoxia (336), no second hit was required for the development of PH in *Tnfaip3*<sup>DNGRI-KO</sup> mice. Steiner *et al* showed a comparable degree of spontaneous mild development of PH in IL-6 transgenic mice, with dramatically increased PH severity after exposure to hypoxic conditions (117). In **chapter 3**, we questioned whether additional inflammatory triggers such as TLR3, TLR4 and TLR9 stimulation would lead to an exacerbated PH phenotype, possibly already present in *Tnfaip3*<sup>DNGRI-KO</sup> mice at a younger age. However, in our studies, we found that none of these secondary triggers led to an additional increase of RV pressures. These findings show that the alterations in the A20-deficient DCs are already sufficient to induce increased pressures over time and cannot be further enhanced by TLR triggering. Possibly, a bacterial or viral infection is a more potent manner for PH induction, since infections with viruses such as HIV, human herpes virus 8 and hepatitis B and C have been described to be associated with PAH development (210). Host defense to bacteria is also thought to contribute to disease by autoantigen-related molecular mimicry (211). As described in **chapter 1**, accumulating reports have shown an important role for the bone morphogenetic protein receptor type 2 (*BMPR2*) gene, causing loss-of-function or reduced receptor signaling (reviewed in (200)). *BMPR2*, which belongs to the transforming growth factor- $\beta$  (TGF $\beta$ ) receptor family, is expressed by various cell types including vascular pulmonary endothelial cells and pulmonary artery smooth muscle cells (PASMCs) and is crucial in vascular homeostasis. In previous pre-clinical studies, *BMPR2* activation has shown to prevent and attenuate PAH phenotypes induced in several rodent models (141-143). Interestingly, in a recent report by Kurakala *et al* evidence was provided that restoration of the BMP signaling through Nur77 agonist (6-mercaptopurine) treatment could prevent and reverse PH progression in the sugen/hypoxia rat PAH model (337). However, although a recent clinical trial of 6-mercaptopurine treatment in 15 PAH patients showed a decrease in PVR, Botros *et al* reported an unfavorable risk/benefit ratio due to a higher frequency and severity of side-effects (338). Treatment strategies for targeting this pathway should aim for improvements in dosing schemes or usage of other thiopurine analogs. In **chapter 3**, we evaluated reduced *Bmpr2* signaling as an additional trigger. However, crossing the *Bmpr2*<sup>+/*RS99X*</sup> mice to our inflammatory *Tnfaip3*<sup>DNGRI-KO</sup> mouse model did not result in an enhanced PH phenotype. This might be related to the mild PH phenotype seen in *Bmpr2*<sup>+/*RS99X*</sup> mice (143). A previous study showed increased susceptibility of pulmonary microvascular endothelial cells responses to inflammatory mediators under the influence

of *BMP2* (339). However, upon evaluation of the *Bmpr2*<sup>+/R899X</sup> mice, we did not find any differences in DC, T-cell and B-cell numbers in the lungs with wildtype mice. This could imply that the *Bmpr2*<sup>+/R899X</sup> mouse model is less likely to be immune driven in its pathogenesis of experimental PH. In summary, we investigated various secondary triggers (TLR triggering, crossing with *Bmpr2*<sup>+/R899X</sup> mice) in our *Tnfaip3*<sup>DNGRI-KO</sup> mouse model, but none of these led to an exaggerated phenotype.

#### Outstanding questions:

1. What is the molecular mechanism by which *Tnfaip3* mutation in cDC1s results in PH?
2. Do cDC1s in *Tnfaip3*<sup>DNGRI-KO</sup> mice have a more tolerogenic phenotype or an increased activation status?
3. Would an additional trigger such as hypoxia induce a more severe PH phenotype in *Tnfaip3*<sup>DNGRI-KO</sup> mice?
4. Does the increased presence of DCs in *Tnfaip3*<sup>DNGRI-KO</sup> mice and IPAH patient lungs reflect an increase in tissue-resident DCs or is there increased migration of DCs to the lungs?
5. What is the DC-subset distribution and their location in the lungs of IPAH patients?

### T-cells in PAH and CTEPH; executors of autoimmunity or damage-controllers?

Apart from increased DCs in the lungs of *Tnfaip3*<sup>DNGRI-KO</sup> mice, these lungs also showed more T cells than WT mice, mostly observed around vessels and co-localizing with DCs (see **chapter 3**). These DCs and T cells might initiate and contribute to vascular remodeling, one of the major hallmarks of PAH histology. In WT and *Tnfaip3*<sup>DNGRI-KO</sup> mice only a minor fraction of the T cells in the lung appeared to be CD8<sup>+</sup> T cells. In IPAH lungs CD8<sup>+</sup> T cells and DCs were abundantly present and thus it will be interesting to characterize these pulmonary T-cells in more detail and to identify their specificity and recognized antigens. The level of *Tnfaip3* expression in DCs has been shown to control T cell differentiation, as *Tnfaip3*-deficient DCs promote Th17-cell differentiation through increased expression of IL-1 $\beta$ , IL-6 and IL-23 (85, 96). In **chapter 2**, we described an increase in Th17 cells in *Tnfaip3*<sup>DNGRI-KO</sup> mice. In addition to these findings, increased proportions of IFN $\gamma$ -producing Th1 cells and IL-10-producing Th-cells were observed in *Tnfaip3*<sup>DNGRI-KO</sup> mice. These findings may support involvement of both Th17 cells and Th1 cells in IPAH and PAH pathology (195, 196). Furthermore, our studies in **chapter 2** showed a higher number of CD8<sup>+</sup> T cells, increased proliferative capacity, and elevated proportion of IFN $\gamma$  and IL-10-producing cells in lungs of *Tnfaip3*<sup>DNGRI-KO</sup> mice compared to control mice.

Interestingly, increased numbers of CD4<sup>+</sup>, CD8<sup>+</sup> and  $\gamma\delta$  T cells were found in close proximity to pulmonary arteries of IPAH lung biopsies, using flow cytometry (55). These CD4<sup>+</sup> and CD8<sup>+</sup> T cells were present in the adventitial space around the pulmonary vessels in IPAH patients (34). Moreover, in thrombotic material of CTEPH patient an increased presence of intramural T cells was demonstrated (36). These findings indicate that through direct and indirect effects, T cells may play a pathophysiological role in vascular remodeling in PAH and CTEPH.

In **chapter 5** and **chapter 6**, T-cell subsets, T-cell cytokine production capacity and T-cell activation status in peripheral blood from CTEPH and PAH patients was described. In CTEPH patients (**chapter 5**), we observed (1) that the compartments of naive CD4<sup>+</sup> and CD8<sup>+</sup> T cells, memory CD4<sup>+</sup> T cells and Tregs contained increased proportions of CCR6<sup>+</sup> cells; (2) that CD4<sup>+</sup> and CD8<sup>+</sup> T cells displayed reduced production of various cytokines, including TNF $\alpha$  and IFN $\gamma$ ; and (3) that in CD4<sup>+</sup> and CD8<sup>+</sup> T cells CTLA4 expression was increased. At 1-year follow-up, we found further increased proportions of CCR6<sup>+</sup> T cells, reduced CTLA4 expression by CD8<sup>+</sup> T cells and memory CD4<sup>+</sup> T cells and increased IFN $\gamma$  and IL-17 production by CD4<sup>+</sup> T cells, compared with baseline values. Finally, we identified CCR6<sup>+</sup> T cells in PEA tissue. These cells were demonstrated to be predominantly CD4<sup>+</sup> T cells and they were located in clusters as well as randomly spread over vascular lesions.

Th17 cells are associated with a wide array of inflammatory conditions, including autoimmune diseases, and a strong correlation between CCR6 expression and disease severity has been noticed (270). Interestingly, Th17-linked systemic autoimmune diseases including systemic sclerosis and systemic lupus erythematosus, are also known to be associated with PAH (271). Moreover, CD4<sup>+</sup> T cells from IPAH patients express higher levels of IL-17 and in circulating white blood cells the *IL17* gene is hypomethylated, supporting a role of Th17 cells in PAH pathology (195). Th17 cells might be involved in PAH pathogenesis through production of pro-inflammatory cytokines such as IL-17, IL-21 and IL22, which may be linked to an auto-reactive specific (340) and contribute to remodeling of pulmonary vasculature (see below, **Figure 2**). This inflammation-driven vascular remodeling could then in turn be responsible for the increased right ventricular systolic pressures.

Polarization of Th17 cells is promoted by IL-6 in combination with IL-1 $\beta$  and TGF $\beta$ , indicating an important role for IL-6 in PH. Indeed, IL-6 levels are shown to be increased in serum of IPAH patients and transgenic mouse models show that IL-6 overexpression induces PH and, conversely, IL-6 deficiency protects against hypoxia-induced PH (94, 117, 120). In plasma of CTEPH patients, IL-6 was also found to be increased (32). In **chapter 4**, we described a similar increase in IL-6 in a subgroup of IPAH and CTEPH patients. However, IL-6 levels of the entire IPAH and CTEPH group were not significantly different from healthy controls.

Lung CCL20 mRNA levels were described to be increased in IPAH patients, compared with controls (33) and increased CCL20 expression was associated with accumulation of CCR6<sup>+</sup> and IL-17<sup>+</sup> CD4<sup>+</sup> T cells [39, 40]. In this regard, it would be informative to determine CCL20 expression in thrombotic lesions of CTEPH patients. The striking parallels between PAH and CTEPH would support a role of Th17 cells in the etiology of both diseases, even though they are different disease entities. Another intriguing parallel may be drawn with atherosclerosis, a chronic inflammatory arterial disease with plaque build-up in vascular lesions (272). In atherosclerosis patients, serum IL-17 and circulating Th17 cells were found to be increased and infiltrates of IL-17-producing cells have been found in atherosclerotic plaques (273). Moreover, in mouse models Th17 cells play a causative role in atherosclerosis development (274). This resemblance is striking, given the difference in embryonic origin of the pulmonary and systemic arteries affected in atherosclerosis (275).

Similar to CTEPH patients, in IPAH patients (**chapter 6**) both CD4<sup>+</sup> and CD8<sup>+</sup> T cytokine-producing capacity was reduced; (2) T cells of IPAH patients showed a higher surface expression of CTLA4 and (3) multivariate analysis separated IPAH patients from HCs by a specific IPAH T cell profile based on cytokines. It is known that both in IPAH and in CTD-PAH patients, plasma and serum cytokine levels are increased, which may lead to a high pro-inflammatory cytokine milieu (94, 254).

In addition, results of these studies, showed that the T cell cytokine profiles found were not identical across the PAH subgroups and that the profile of the increased circulating cytokines found also differed between IPAH and CTD-PAH patients. Furthermore, plasma levels of IL-10 and TGF- $\beta$  were only increased in treatment-naïve IPAH patients, and not in treatment-naïve CTD-PAH patients (254). The increase in the anti-inflammatory cytokine IL-10 in IPAH patients at diagnosis, which was not seen in CTD-PAH patients, might explain the different behavior in cytokine production by T cells in either IPAH or CTD-PAH.

A possible explanation for the decrease in the proportions of intracellular cytokine-positive T cells in the circulation might be that these T cells have migrated to target organs, since Marsh and colleagues showed that CD3<sup>+</sup> T cells were increased in lungs of IPAH patients (55). In IPAH, only a decrease in the size of the Th2 population was found, which might explain the decrease in IL-4 production by the full memory CD4<sup>+</sup> T cell population. Other T cell subsets, for example Th1 and Th17 cells, the major producers of IFN $\gamma$  or IL-17, respectively, were not decreased in number in the circulation of these patients. A different picture was seen in CTD-PAH patients: cytokine-production by T cells was not altered, but a decrease was demonstrated in the size of the Th2 population. Taken together, these findings suggest that migration and homing of cytokine-producing T cells to the lung might not be the main reason for the lower cytokine-producing capacity of T cells in IPAH patients.

Reduced cytokine expression in circulating T cells of IPAH patients might be explained by exhaustion or a strong inhibitory effect linked to CTLA. In our analyses, the strong signals induced by PMA and ionomycin *in vitro* bypass the TCR-mediated signals supported by co-stimulatory signals dependent on the CD28/CTLA4 balance. Therefore, further experiments are required to determine the effect of increased CTLA4 expression on T cell activation and cytokine production in T cells from IPAH patients.

In conclusion, treatment-naïve IPAH patients displayed a unique T cell phenotype that was different from CTD-PAH patients and was characterized by a reduced cytokine-producing capacity. These findings point to involvement of adaptive immune responses in IPAH. This may have implications for development of therapeutic interventions, since we feel that immunomodulatory treatment may be considered.

#### Outstanding questions:

1. Do (a part of the increased) circulating CCR6<sup>+</sup> T cells migrate towards the pulmonary arteries via neo-vasculature into the organized thrombi in CTEPH patients?
2. Are T-cells in IPAH and CTEPH lower in cytokine-producing capacity due to an exhaustion phenotype?
3. Are the T-cell profile changes seen at 1-year follow-up a consequence of disease progression, medication, recovery after treatment or a combination of these factors?
4. Are there differences in pathogenesis and PH development in peripheral vs central thrombotic lesions CTEPH patients?

## IMPROVING DRUG TREATMENT OPTIONS IN PAH AND CTEPH.

### Expanding the horizon for PH-drug therapy: novel biomarkers and therapeutic targets in PAH and CTEPH

Despite novel therapies, pulmonary hypertension remains a disease with poor survival and a high burden of disease. One of the complicating factors is that patients commonly present at an advanced stage of PH. As shown by Brown *et al*, 21.1% of the PAH patients in the REVEAL registry reported symptoms for longer than 2 years before recognition and diagnosis of their disease (341). Therefore, there is an increasing need for earlier detection of the disease. Furthermore, there is a growing call for biomarkers to determine disease severity and as predictors of prognosis. Inflammatory cytokines may be useful for prediction of disease progression and prognosis in patients suffering from PAH and CTEPH. In 2009, Soon *et al* showed for the first time that elevated inflammatory cytokines in peripheral blood of PAH patients correlates with survival (94). Following this report, many other studies have shown increased inflammatory cytokines in PAH and CTEPH patients peripheral blood samples (see for overview: **chapter 1, table 2**). In an unsupervised analysis of blood cytokine profiles of PAH patients, different immune phenotypes were distinguished with different clinical risk profiles, independent of WHO PH subgroups (122).

Throughout these important studies, several lines of evidence support a prominent role for IL-6, as (I) serum IL-6 concentrations correlate with survival (94), (II) IL-6-overexpressing transgenic mice spontaneously develop a PH phenotype (117), and (III) IL-6 receptor (IL-6R) expression and signaling is crucial for PAH development and progression (129). In **chapter 4**, we described increased levels of IL-6 in most of the CTD-PAH patients at baseline, as well as in a subgroup of IPAH patients. In contrast to earlier cross-sectional studies in IPAH patients (94), we did not find a correlation of IL-6 with survival in any of our PAH subgroups or CTEPH patients. We did not find a correlation between changes over time for IL-6 and survival either. Furthermore, in our multivariate analyses IL-6 did not display a major role in the distinction between survival of PAH patients. These differences could be due to sample size, different patient subtypes, usage of different assays and different time sampling point in the course of the disease. In **chapter 2**, we also described a higher mRNA expression of IL-6, both in lungs and hearts in our *Tnfaip3*<sup>DNGRI-KO</sup> mouse model. Our data showed that neutralization of IL-6 in *Tnfaip3*<sup>DNGRI-KO</sup> mice ameliorated the experimental PH phenotype, providing evidence that IL-6 is a major contributor to PH development in these mice. Considering the marginal effects of IL-6 blockade on the inflammatory compartment in *Tnfaip3*<sup>DNGRI-KO</sup> mice, other effectual pathways of IL-6 blockade might be responsible for this effect. Possibly, anti-IL-6 treatment of KO mice may attenuate the pulmonary vascular remodeling through a different mode of action, including through reduction of PA-SMC survival (129). IL-6 is known to have profound direct effects on the vasculature as well (342), and it is known to be involved in the process of arteriosclerosis (343). These potent effects of anti-IL-6 treatment were also demonstrated by Tamura *et al* in other various established rodent models for PH (129). However, preliminary results from a recent phase II clinical trial with anti-IL-6 therapy (Tocilizumab) in PAH patients showed no changes in WHO functional class, 6-minute walking test (6MWT), NT-proBNP and quality of life for the majority of PAH patients (130). Although, in a small subgroup of CTD-associated PAH and in hereditary (H)PAH/IPAH patients a decrease in PVR >15% was seen (130). Possibly, this mild effect in IPAH patients could be due to the heterogeneous nature of

IPAH patients, considering that approximately 40% of the IPAH patients have auto-antibodies (101). These studies reflect the challenges of the translation of pre-clinical compounds into clinical trials in PH research. As described in **chapter 1** (supplementary table 1), many anti-inflammatory compounds have been tested in established rodent models for PH, and have shown complete reversal or prevention of PH. While many exiting clinical trials are underway, so far very few have led to significant therapeutic effects in PAH. Future research should therefore more closely focus on the complex underlying pathophysiological inflammatory pathways in PAH and CTEPH, for better determination and more precise targeting of therapy. Regarding targeting IL-6, it will be beneficial to identify direct and indirect effects of IL-6 in PAH and CTEPH. Possibly, more precise phenotyping of patients earlier in the disease process can be beneficial for a tailor-made precision treatment strategy.

In **chapter 4**, we also described significantly increased plasma levels of IL-10, TGF $\beta$ , and CXCL9 in IPAH patients, of IL-6, CXCL9 and CXCL13 in CTD-PAH patients, and of CXCL9 in CTEPH patients at diagnosis. The increased TGF $\beta$  is particularly interesting, considering a recent phase II clinical trial showing beneficial effects in PAH patients for Sotatercept, a novel ligand trap for members of the TGF $\beta$  superfamily (344). Our analyses revealed lower levels of several circulating cytokines in our IPAH patients at diagnosis compared to previous reports of cross-sectional data (94, 108). This might be indicative for existing heterogeneity between patients, different pathophysiological changes over time during disease progression or therapeutic effects due to PAH-specific therapy.

In CTEPH patients, high levels of CXCL9 and IL-8 at baseline correlated with decreased survival. CXCL9 is a known regulator of immune cell migration, differentiation and activation and is required for optimal Th1 cell differentiation and IFN $\gamma$  production by T cells *in vivo* (231). The receptor for CXCL9 is CXCR3, which is a marker for Th1 cells and IFN $\gamma$ -producing Th17 cells, also known as Th17.1 cells (237). Previous research showed that PAH patients display Th17 cell immune polarization (195). Possibly, CXCL9 is upregulated by endovascular triggers in CTEPH, for the recruitment of cytotoxic lymphocytes, natural killer cells and macrophages. Moreover, CXCL9 is known to be involved in activation of immune cells in response to IFN $\gamma$ . CXCL9 may prove to be a biomarker reflecting pathological involvement of the immune system in CTEPH patients. In future studies, it would be interesting to evaluate whether CXCR3 expression is increased in T-cells in peripheral blood samples, lungs and in experimental PH rodent models. However, it remains to be clarified which cells are the main producers of CXCL9. From the tumor-immunology field, we know that cDC1s within the tumor microenvironment are the main producers of CXCL9, leading to recruitment of CD8 $^{+}$  effector T cells (345). Future research should investigate whether cDC1s are major producers of CXCL9 in CTEPH patients.

In **chapter 4**, a key finding in our multivariate analyses was that combined profiling, using both inflammatory and clinical parameters, provided the most significant distinction for patient survival. Interestingly, in this sub-analysis of the three PAH patient groups, clinical data alone did not provide a significant distinction in survival. Rather, levels of cytokines and particularly of the chemokines CXCL9 and CXCL13 appeared to be major determining factors in survival. Previously, it has been shown that CXCL9 and several CC-family chemokines important for chemotaxis of myeloid cells play a central role in distinguishing clusters of PAH immune phenotypes with different clinical risks (122). Overall, unsupervised clustering of our cytokine data revealed clustering of PH patients based on inflammatory mediators and clinical parameters, but did not separate the different WHO-1 subgroups. Importantly, these multivariate analyses separated patients with <3 years and >3 years survival, in particular when inflammatory mediators were combined with clinical parameters. In future research, novel techniques

such as high-dimensional multi-color FACS (Cytof), RNA-Seq and serum protein arrays should be utilized to compose a comprehensive immunomics overview and a better understanding of the intricate network of inflammation and immunity. Furthermore, this should include extensive integration of data combining DCs, T-cells, NK cells, innate lymphoid cells (ILCs), monocytes and chemo/cytokines. Hopefully, this will lead to better prediction of disease development and precision medicine.

### The right tool for the right targets: evaluating rodent models for compound testing in PH

Over the past decades, many potent rodent models have been evaluated for the presence of different PH phenotypes (346) and for the possibilities of compound testing either to study if development of PH could be prevented, or to investigate amelioration of the disease. Recently, apart from well-known models such as the monocrotaline rat model and the sugen/hypoxia rodent model (346), many new rodent models have been developed to study PH. One of the major problems in finding a potent rodent model for PAH is the challenge to generate a model that closely mimics the human PAH disease development and its resistance to treatment. While many current rodent models are responsive to various (anti-inflammatory) treatments, unfortunately translational studies often show only limited effects in PAH patients. These translational challenges might be due to differences in rodent vs human biology or could be due to the complex nature of inflammation and immunity in human PH as well. In **chapter 2** and **chapter 3**, we described various mouse models for immune-mediated development of PH.

In our studies, we evaluated the *Tnfaip3*<sup>DNGRI-KO</sup> mouse model, the *Bmpr2*<sup>+/*R899X*</sup> mouse model, a genetic crossing between these 2 models, and lastly, the *Ccr7*<sup>-/-</sup> model. In these studies, we found a dominant immune-driven PH phenotype in the *Tnfaip3*<sup>DNGRI-KO</sup> mouse model, with no exacerbating effect of genetic crosses with the *Bmpr2*<sup>+/*R899X*</sup> mouse model (**chapter 3**). These mouse models and some previously studies models, such as the IL-6 transgenic model (117), mice develop PH spontaneously. In contrast, most established rodent models for PH require a second hit, such as the monocrotaline, hypoxia or Sugén mouse model(346). Considering the current difficulties in the translation of results of pre-clinical studies to comparable beneficial treatment effects in clinical trials, the question arises what the “perfect” rodent model would be to study PH development and progression. The necessity for a second hit to induce pulmonary hypertension in clinical PAH remains unexplained. Therefore, the choice for rodent models with or without a secondary trigger is still undecided. However, current triggers such as monocrotaline might be less preferable considering the toxic damage to the lungs. Introducing a trigger that is less dependent on direct cellular damage might be preferable to investigate possible immune-mediated PH development. Another method of inducing PH is hypoxia, which also could be a less preferable way of PH induction, considering that the high altitude-induced hypoxic PH in humans is completely reversible upon return to sea-level. This is in contrast to human PAH, which has a persistent and progressive nature of pulmonary vascular remodeling and right ventricular failure.

In another mouse model for PH, the *Ccr7*<sup>-/-</sup> model, mice develop PH at a young age without a secondary trigger (347). In our studies in the *Ccr7*<sup>-/-</sup> model, we were also able to demonstrate increased RVSP and RV hypertrophy at 11-week-old mice. However, we found that this PH phenotype diminished over time, and spontaneously reverted to wildtype level at older age. Although we also demonstrated increased perivascular inflammation in the lung, we found no evidence of increased activation of the immune compartment (DCs, T-cells and B-cells) in our flow cytometry analysis of lungs, mediastinal lymph nodes and bronchiolar alveolar lavage samples (unpublished data T. Koudstaal *et al*). Moreover,

the previously reported immune cell infiltration in the lung decreased over time as well, without specific treatment. This makes the *Ccr7*<sup>-/-</sup> model less preferable as a model for PAH, considering that PAH is a persistent and progressive disease. Therefore, characteristics of a “perfect” rodent model for PH would be: (I) histological resemblance to PAH with pulmonary vascular plexiform lesion formation, (II) therapeutic resistance to vascular remodeling resolution and PH amelioration, (III) spontaneous and persistent PH development, without a lung damaging inducement of PH, (IV) involvement of the immune system, which could be causal or a bystander effect. In the future, novel technologies such as organoids and lung-on-a-chip could provide improved and more specific methods for pulmonary hypertension research.

## IMPROVING NON-DRUG TREATMENT OPTIONS IN PAH AND CTEPH.

While the standard treatment for PAH and inoperable CTEPH patient consists of PH-specific drug treatment, non-drug treatment options can be additionally beneficial. In recent years, evidence for beneficial effects of pulmonary rehabilitation (PR) therapy is increasing (14-16, 348). The European Respiratory Society (ERS) and the European Society of Cardiology (ESC) guidelines for the diagnosis and treatment of PH recommend supervised PR programs in expert centers for PAH patients in stable condition on optimized PH specific drug therapy (17). However, knowledge about the safety and effectiveness of a PR program in an exclusively outpatient setting is still lacking.

While these guidelines give various recommendations for PH-specific drug treatment and PR therapy, very few recommendations and knowledge are provided on nutrition. Moreover, there are currently no data available concerning the influence of nutritional status on prognostic indicators as defined by the ESC/ERS (5). However, nutritional status, including the occurrence of micronutrient deficiencies is likely to be relevant to both the overall physiological status and the exercise capacity of the patient. It is known that micronutrient deficiencies, such as those of magnesium, vitamin D and iron are linked to inflammatory processes, which may contribute to exercise intolerance. The main iron transporter of the intestine (ferroportin) is inhibited by hepcidin, resulting in decreased intestinal absorption of iron (349). Inflammatory cytokines, such as interleukin 1-beta (IL-1 $\beta$ ) and IL-6, stimulate hepcidin transcription via different mechanisms, leading to excessive hepcidin production. Increased levels of circulating IL-6 may activate sIL6R and membrane-bound IL6R in hepatocytes, increasing hepatic IL-6 signaling, leading to STAT3 activation and IL-6-dependent BMP signaling, further increasing hepcidin levels (350). Both IL-6 and STAT3 have recently emerged as main regulators of the differentiation and function of Th17 cells, via a positive feedback loop enhancing expression and/or activation of IL-6 itself, IL-17 and STAT3 (351). In **chapter 7** and in recently published data from our group (349), we provide additional insights in the possibilities for outpatient rehabilitation therapy and nutritional deficiencies in PH patients.

### Outpatient rehabilitation therapy: towards individual tailor-made rehabilitation therapy in PAH and CTEPH

Despite improvements in specific medical treatment of PAH over the last years, PH patients suffer from significant dyspnea, fatigue and skeletal muscle weakness, resulting in exercise limitation/

intolerance and poor QoL (17). Exercise intolerance is a key feature in PAH for which the underlying hemodynamic impairment is primarily responsible (13). Improvement of muscle dysfunction and exercise intolerance are therefore recognized to be important goals in the treatment of PAH patients (348). Historically, patients with PAH were recommended to restrain from physical activity, including PR because of poor prognosis and risk of sudden cardiac death. However, most programs so far have been carried out in a hospital setting or were at least started in a hospital setting.

In **chapter 7**, we demonstrated that a multidisciplinary completely outpatient PR program is beneficial and safe for PH patients. Major findings were significant increases in exercise capacity and endurance, and improved quality of life. Similar beneficial results for PR therapy were recently demonstrated in a very recent large randomized controlled trial (RCT) by Grünig et al (352). Although this study started with a standardized in-hospital rehabilitation period prior to outpatient therapy in contrast to our program which was solely out-patient. The results of our study are particularly relevant, considering that there is a large group of PH patients, who are “too well” to combine an intensive inpatient PR therapy with their daily life activities. Our results show that a completely outpatient PR therapy could be an attractive option for NYHA II and III patients. Indeed, Hayton et al demonstrated decreased PR attendance in COPD patients when either their disease was too mild or the COPD too severe to benefit from PR (328).

However, there are still several factors unknown for outpatient PR programs. Below, an overview of outstanding questions is depicted for possible future studies.

#### **Outstanding questions:**

1. What is the duration of the beneficial effects in completely outpatient PR therapy with or without prolonged training therapy?
2. Are the beneficial effects in completely outpatient setting significantly different when compared to a non-PR therapy cohort in an RCT?
3. What is the optimal training program for outpatient strategy in terms of combination of exercise training, PH education and mental wellbeing awareness?
4. What is the optimal continuation strategy after outpatient PR for maintaining the beneficial effects?

#### **Nutrition in PAH patients: food for thought in the non-drug treatment possibilities in PAH**

Nutritional status in patients with PAH and CTEPH is an understudied field, although accumulating evidence is showing that nutritional status and micronutrient deficiencies are likely to beneficially influence quality of life of these patients via their potential effects on inflammatory status, skeletal muscle functions and other (patho-) physiological processes (353-355).

In collaboration with colleagues from the University of Wageningen, we demonstrated that deficiencies in iron and vitamin D are highly prevalent in patients with PAH and CTEPH both at diagnosis and after 1,5 years of conventional treatment (349). Previously, Ruiters *et al* reported that intravenous iron therapy in IPAH patients improved exercise endurance capacity, but not the 6MWT (356). Interestingly, the iron deficit has been suggested to be related to IL-6 levels, because IL-6 levels

correlated with iron levels in idiopathic PAH patients, but not in CTEPH patients (357). Inflammatory cytokines such as IL-1 $\beta$  and IL-6 stimulate hepcidin transcription via different mechanisms, leading to excessive hepcidin production. Interleukin 1-beta might even provide the onset signal, as it induces the transcription of IL-6 (358). Data from our studies show that this iron deficiency is already present at onset of diagnosis and negatively correlated with 6MWT. It is currently unknown whether in PAH patients low iron levels can be treated by supplementation with the normal recommended daily dose or that a subgroup of patients might need intravenously supplementation. Future studies are needed to further investigate this.

## CONCLUDING REMARKS

Overall, PH is a complex and heterogeneous disease with poor prognosis, despite medical advances in PH-specific drug therapies. There is mounting evidence for involvement of the immune system in the pathophysiology of PAH and CTEPH. In this thesis, we described additional evidence for the involvement of DCs in the development of PH, and alterations in the T cell subsets in patients with CTEPH and PAH. The combined results are illustrated in a proposed model for PH development in **Figure 2**. While future studies are needed to further determine the specific role for different immune cells in the development of PH, many promising immunomodulatory drug treatment trials are currently underway. This thesis has given novel understanding of DC and T-cell mediated immunity in pulmonary hypertension, potentially leading to new therapeutic strategies in the future. To further unravel the role of the immune system in the development of different forms of PH, potent rodent models for immune-mediated PH are required for pre-clinical research. In **chapter 2 and 3**, of this thesis, new insights have been provided in possibilities for immune-driven PH rodent models, without requirement for an additional trigger.

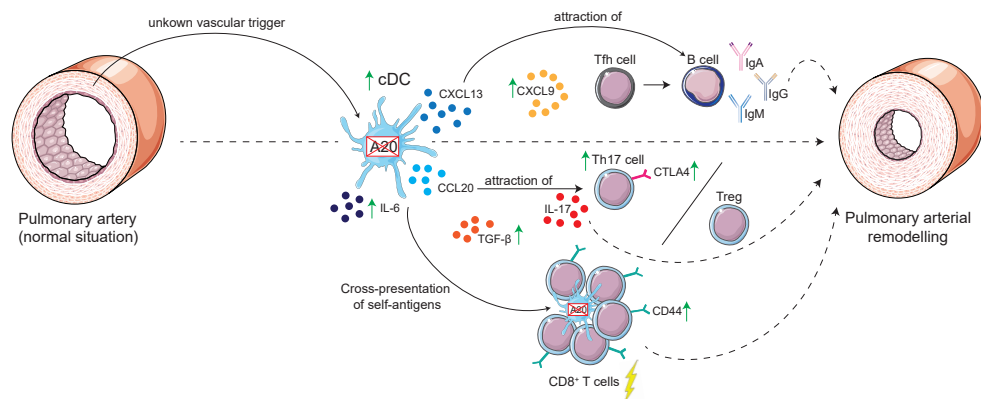


**Figure 2.** Proposed model for DC and T cell driven immunopathology in pulmonary hypertension development.

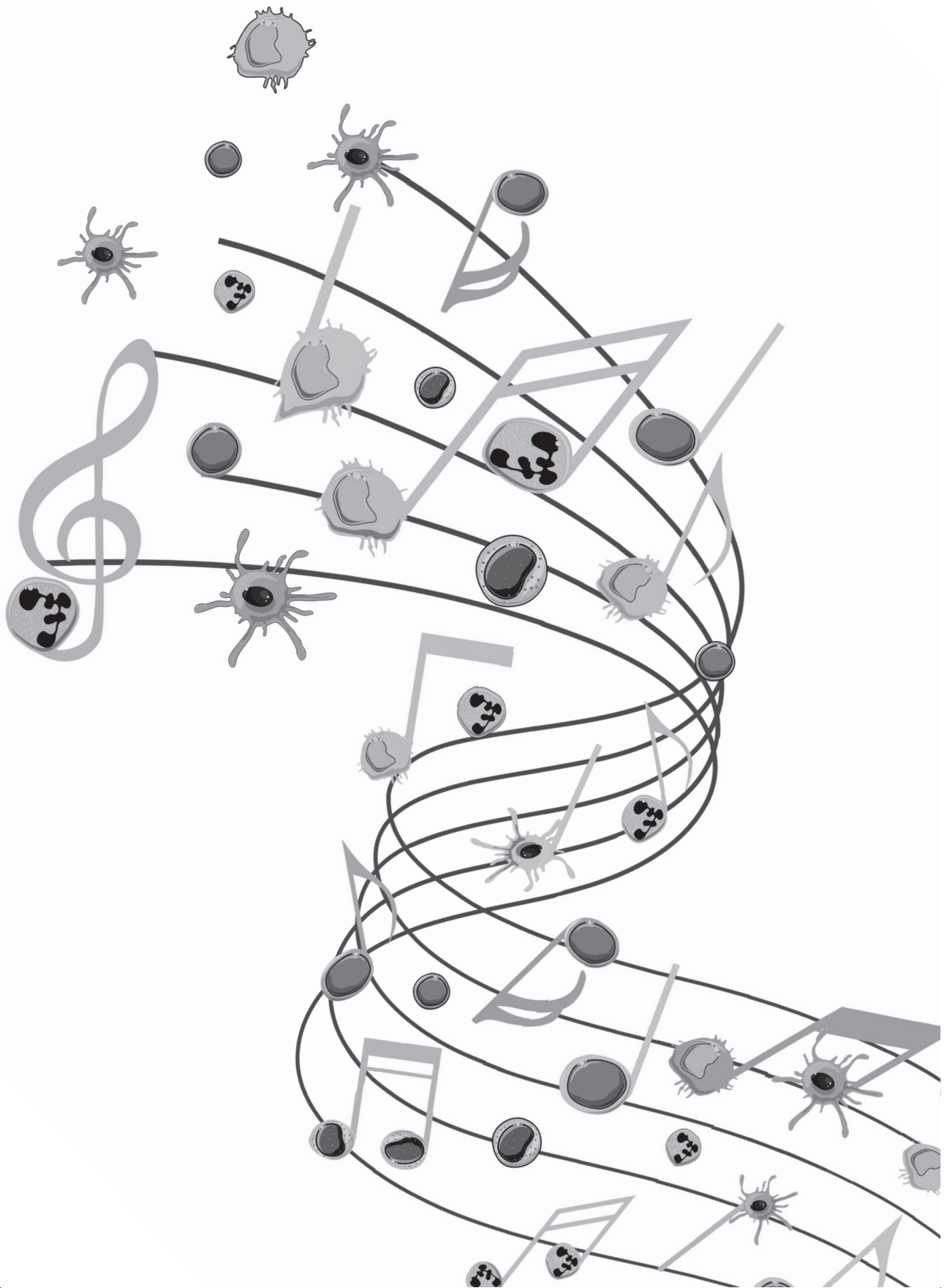
After an unknown vascular trigger, cDCs have an enhanced cytokine production (e.g. IL-6) which can lead to pulmonary artery remodeling directly or indirectly by production of CXCL13 and CCL20. Furthermore, CXCL13 leads to migration of B cells towards the lungs. B cells will produce pathogenic antibodies after interaction with follicular T helper (T<sub>fh</sub>) cells, leading to remodeling of PAs. CCL20 attracts T cells such as Tregs and Th17 cells leading to an increase in Th17 cells in the lung resulting in a Th17/Treg disbalance and by IL-17 production contributes to PA remodeling. cDC1s are very capable in presenting auto-apoptotic antigens to CD8<sup>+</sup> T cells, and by doing so, increasing CD44 expression and activating these CD8<sup>+</sup> T cells leading to pulmonary artery remodeling. Whereas in our mouse model aberrant activation of DCs is induced by A20/Tnfr1 deletion, in patients very different mechanisms, e.g. involving enhanced TLR or IL-1R signaling, could result in a similar or overlapping abnormalities in DCs. Adapted from van Uden et al, 2019 (86).

A major challenge in PH care is the growing requirement for tools to determine disease severity and prediction of prognosis. In **chapter 4**, we demonstrated prognosis-predicting value for inflammatory cytokine assessment in PAH and CTEPH patients. In combination with other important circulating cytokine assessments in PAH and CTEPH, this study could pave the way for integration of immune status assessment in the determination of disease severity, prognosis and therapeutic evaluation in current clinical care.

Another very important part of PH clinical care, are the non-drug treatment options such as rehabilitation therapy and nutrition status optimization. In **chapter 7**, we showed significant beneficial effects for a completely outpatient pulmonary rehabilitation program. Potentially, the findings in this thesis might lead to more accessible forms of PR for patients who are struggling to combine rehabilitation therapy with their daily life activities.

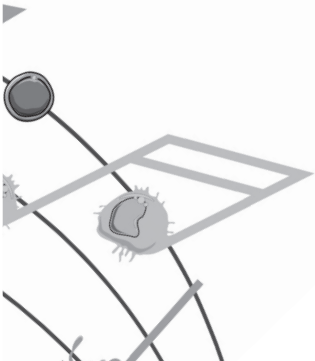
Taken together, PH is a complex devastating disease with a dangerous imbalance in the immune system in a subgroup of patients. PH is most likely a multi-factorial disease, including pathological involvement of other non-immune factors such as VEGF, EGF/EGFR, and GWAS genes such as SOX17. Ideally, immune factors from previous research and from this thesis, should be integrated with these non-immune factors, to achieve an intricate holistic view of the multi-factorial pathogenesis in PH. It is expected that this will lead to novel potential (immunomodulatory) strategies and improved identification of different immune-driven subgroups of PH.





# REFERENCE LIST

# R



## REFERENCES

1. Simonneau G, Montani D, Celermajer DS, Denton CP, Gatzoulis MA, Krowka M, et al. Haemodynamic definitions and updated clinical classification of pulmonary hypertension. *Eur Respir J*. 2019;53(1).
2. Galie N, Humbert M, Vachiery JL, Gibbs S, Lang I, Torbicki A, et al. 2015 ESC/ERS Guidelines for the diagnosis and treatment of pulmonary hypertension: The Joint Task Force for the Diagnosis and Treatment of Pulmonary Hypertension of the European Society of Cardiology (ESC) and the European Respiratory Society (ERS): Endorsed by: Association for European Paediatric and Congenital Cardiology (AEPC), International Society for Heart and Lung Transplantation (ISHLT). *Eur Respir J*. 2015;46(4):903-75.
3. Wijeratne DT, Lajkosz K, Brogly SB, Lougheed MD, Jiang L, Housin A, et al. Increasing Incidence and Prevalence of World Health Organization Groups 1 to 4 Pulmonary Hypertension: A Population-Based Cohort Study in Ontario, Canada. *Circ Cardiovasc Qual Outcomes*. 2018;11(2):e003973.
4. Peacock AJ, Murphy NF, McMurray JJ, Caballero L, Stewart S. An epidemiological study of pulmonary arterial hypertension. *Eur Respir J*. 2007;30(1):104-9.
5. Frost AE, Badesch DB, Barst RJ, Benza RL, Elliott CG, Farber HW, et al. The changing picture of patients with pulmonary arterial hypertension in the United States: how REVEAL differs from historic and non-US Contemporary Registries. *Chest*. 2011;139(1):128-37.
6. Escribano-Subias P, Blanco I, Lopez-Meseguer M, Lopez-Guarch CJ, Roman A, Morales P, et al. Survival in pulmonary hypertension in Spain: insights from the Spanish registry. *Eur Respir J*. 2012;40(3):596-603.
7. Ling Y, Johnson MK, Kiely DG, Condliffe R, Elliot CA, Gibbs JS, et al. Changing demographics, epidemiology, and survival of incident pulmonary arterial hypertension: results from the pulmonary hypertension registry of the United Kingdom and Ireland. *Am J Respir Crit Care Med*. 2012;186(8):790-6.
8. Jansa P, Jarkovsky J, Al-Hiti H, Popelova J, Ambroz D, Zatocil T, et al. Epidemiology and long-term survival of pulmonary arterial hypertension in the Czech Republic: a retrospective analysis of a nationwide registry. *BMC Pulm Med*. 2014;14:45.
9. Humbert M, Sitbon O, Chaouat A, Bertocchi M, Habib G, Gressin V, et al. Pulmonary arterial hypertension in France: results from a national registry. *Am J Respir Crit Care Med*. 2006;173(9):1023-30.
10. Hassoun PM. Pulmonary Arterial Hypertension. *N Engl J Med*. 2021;385(25):2361-76.
11. Southgate L, Machado RD, Graf S, Morrell NW. Molecular genetic framework underlying pulmonary arterial hypertension. *Nat Rev Cardiol*. 2019.
12. Garg L, Akbar G, Agrawal S, Agarwal M, Khaddour L, Handa R, et al. Drug-induced pulmonary arterial hypertension: a review. *Heart Fail Rev*. 2017;22(3):289-97.
13. Sun XG, Hansen JE, Oudiz RJ, Wasserman K. Exercise pathophysiology in patients with primary pulmonary hypertension. *Circulation*. 2001;104(4):429-35.
14. Spruit MA, Singh SJ, Garvey C, ZuWallack R, Nici L, Rochester C, et al. An official American Thoracic Society/ European Respiratory Society statement: key concepts and advances in pulmonary rehabilitation. *Am J Respir Crit Care Med*. 2013;188(8):e13-64.
15. Leggio M, Fusco A, Armeni M, D'Emidio S, Severi P, Calvaruso S, et al. Pulmonary hypertension and exercise training: a synopsis on the more recent evidences. *Ann Med*. 2018:1-8.
16. Dalla Vecchia LA, Bussotti M. Exercise training in pulmonary arterial hypertension. *Journal of Thoracic Disease*. 2018;10(1):508-21.
17. Galie N, Humbert M, Vachiery JL, Gibbs S, Lang I, Torbicki A, et al. 2015 ESC/ERS Guidelines for the diagnosis and treatment of pulmonary hypertension: The Joint Task Force for the Diagnosis and Treatment of Pulmonary Hypertension of the European Society of Cardiology (ESC) and the European Respiratory Society (ERS): Endorsed by: Association for European Paediatric and Congenital Cardiology (AEPC), International Society for Heart and Lung Transplantation (ISHLT). *Eur Heart J*. 2016;37(1):67-119.
18. Budhiraja R, Tuder RM, Hassoun PM. Endothelial dysfunction in pulmonary hypertension. *Circulation*. 2004;109(2):159-65.
19. Humbert M, Sitbon O, Simonneau G. Treatment of pulmonary arterial hypertension. *N Engl J Med*. 2004;351(14):1425-36.

20. Benza RL, Miller DP, Barst RJ, Badesch DB, Frost AE, McGoon MD. An evaluation of long-term survival from time of diagnosis in pulmonary arterial hypertension from the REVEAL Registry. *Chest*. 2012;142(2):448-56.
21. Radegran G, Kjellstrom B, Ekmechag B, Larsen F, Rundqvist B, Blomquist SB, et al. Characteristics and survival of adult Swedish PAH and CTEPH patients 2000-2014. *Scand Cardiovasc J*. 2016;50(4):243-50.
22. Quadery SR, Swift AJ, Billings CG, Thompson AAR, Elliot CA, Hurdman J, et al. The impact of patient choice on survival in chronic thromboembolic pulmonary hypertension. *Eur Respir J*. 2018;52(3).
23. Boucly A, Weatherald J, Savale L, Jais X, Cottin V, Prevot G, et al. Risk assessment, prognosis and guideline implementation in pulmonary arterial hypertension. *Eur Respir J*. 2017;50(2).
24. Rabinovitch M, Guignabert C, Humbert M, Nicolls MR. Inflammation and immunity in the pathogenesis of pulmonary arterial hypertension. *Circ Res*. 2014;115(1):165-75.
25. Matthews DT, Hemnes AR. Current concepts in the pathogenesis of chronic thromboembolic pulmonary hypertension. *Pulm Circ*. 2016;6(2):145-54.
26. Bonderman D, Jakowitsch J, Adlbrecht C, Schemper M, Kyrle PA, Schonauer V, et al. Medical conditions increasing the risk of chronic thromboembolic pulmonary hypertension. *Thromb Haemost*. 2005;93(3):512-6.
27. Tuder RM. Pulmonary vascular remodeling in pulmonary hypertension. *Cell Tissue Res*. 2017;367(3):643-9.
28. Chazova I, Loyd JE, Zhdanov VS, Newman JH, Belenkov Y, Meyrick B. Pulmonary artery adventitial changes and venous involvement in primary pulmonary hypertension. *Am J Pathol*. 1995;146(2):389-97.
29. Jonigk D, Golpon H, Bockmeyer CL, Maegel L, Hoepfer MM, Gottlieb J, et al. Plexiform lesions in pulmonary arterial hypertension composition, architecture, and microenvironment. *Am J Pathol*. 2011;179(1):167-79.
30. Wagenvoort CA. Pathology of pulmonary thromboembolism. *Chest*. 1995;107(1 Suppl):10S-7S.
31. Lang IM, Dorfmueller P, Vonk Noordegraaf A. The Pathobiology of Chronic Thromboembolic Pulmonary Hypertension. *Ann Am Thorac Soc*. 2016;13 Suppl 3:S215-21.
32. Zabini D, Heinemann A, Foris V, Nagaraj C, Nierlich P, Balint Z, et al. Comprehensive analysis of inflammatory markers in chronic thromboembolic pulmonary hypertension patients. *Eur Respir J*. 2014;44(4):951-62.
33. Perros F, Dorfmueller P, Montani D, Hammad H, Waelput W, Girerd B, et al. Pulmonary lymphoid neogenesis in idiopathic pulmonary arterial hypertension. *Am J Respir Crit Care Med*. 2012;185(3):311-21.
34. Savai R, Pullamsetti SS, Kolbe J, Bieniek E, Voswinckel R, Fink L, et al. Immune and inflammatory cell involvement in the pathology of idiopathic pulmonary arterial hypertension. *Am J Respir Crit Care Med*. 2012;186(9):897-908.
35. Stacher E, Graham BB, Hunt JM, Gandjeva A, Groshong SD, McLaughlin VV, et al. Modern age pathology of pulmonary arterial hypertension. *Am J Respir Crit Care Med*. 2012;186(3):261-72.
36. Quarck R, Wynants M, Verbeke E, Meyns B, Delcroix M. Contribution of inflammation and impaired angiogenesis to the pathobiology of chronic thromboembolic pulmonary hypertension. *Eur Respir J*. 2015;46(2):431-43.
37. El Kasmi KC, Pugliese SC, Riddle SR, Poth JM, Anderson AL, Frid MG, et al. Adventitial fibroblasts induce a distinct proinflammatory/profibrotic macrophage phenotype in pulmonary hypertension. *J Immunol*. 2014;193(2):597-609.
38. Tuder RM, Groves B, Badesch DB, Voelkel NF. Exuberant endothelial cell growth and elements of inflammation are present in plexiform lesions of pulmonary hypertension. *Am J Pathol*. 1994;144(2):275-85.
39. Tan SY, Krasnow MA. Developmental origin of lung macrophage diversity. *Development*. 2016;143(8):1318-27.
40. Cohen M, Giladi A, Gorki AD, Solodkin DG, Zada M, Hladik A, et al. Lung Single-Cell Signaling Interaction Map Reveals Basophil Role in Macrophage Imprinting. *Cell*. 2018;175(4):1031-44 e18.
41. Travaglini KJ, Nabhan AN, Penland L, Sinha R, Gillich A, Sit RV, et al. A molecular cell atlas of the human lung from single cell RNA sequencing. *bioRxiv*. 2019:742320.
42. Pugliese SC, Kumar S, Janssen WJ, Graham BB, Frid MG, Riddle SR, et al. A Time- and Compartment-Specific Activation of Lung Macrophages in Hypoxic Pulmonary Hypertension. *J Immunol*. 2017;198(12):4802-12.
43. Franke-Ullmann G, Pfortner C, Walter P, Steinmuller C, Lohmann-Matthes ML, Kobzik L. Characterization of murine lung interstitial macrophages in comparison with alveolar macrophages in vitro. *J Immunol*. 1996;157(7):3097-104.
44. Bedoret D, Wallemaq H, Marichal T, Desmet C, Quesada Calvo F, Henry E, et al. Lung interstitial macrophages alter dendritic cell functions to prevent airway allergy in mice. *J Clin Invest*. 2009;119(12):3723-38.

## Reference list

45. Laskin DL, Weinberger B, Laskin JD. Functional heterogeneity in liver and lung macrophages. *J Leukoc Biol.* 2001;70(2):163-70.
46. Florentin J, Coppin E, Vasamsetti SB, Zhao J, Tai YY, Tang Y, et al. Inflammatory Macrophage Expansion in Pulmonary Hypertension Depends upon Mobilization of Blood-Borne Monocytes. *J Immunol.* 2018;200(10):3612-25.
47. Sanchez O, Marcos E, Perros F, Fadel E, Tu L, Humbert M, et al. Role of endothelium-derived CC chemokine ligand 2 in idiopathic pulmonary arterial hypertension. *Am J Respir Crit Care Med.* 2007;176(10):1041-7.
48. Abid S, Marcos E, Parpaleix A, Amsellem V, Breau M, Houssaini A, et al. CCR2/CCR5-mediated macrophage-smooth muscle cell crosstalk in pulmonary hypertension. *Eur Respir J.* 2019;54(4).
49. Kumar R, Mickael C, Kassa B, Sanders L, Hernandez-Saavedra D, Koyanagi DE, et al. Interstitial Macrophage-Derived Thrombospondin-1 Contributes to Hypoxia-Induced Pulmonary Hypertension. *Cardiovasc Res.* 2019.
50. Vergadi E, Chang MS, Lee C, Liang OD, Liu X, Fernandez-Gonzalez A, et al. Early macrophage recruitment and alternative activation are critical for the later development of hypoxia-induced pulmonary hypertension. *Circulation.* 2011;123(18):1986-95.
51. Frid MG, Brunetti JA, Burke DL, Carpenter TC, Davie NJ, Reeves JT, et al. Hypoxia-induced pulmonary vascular remodeling requires recruitment of circulating mesenchymal precursors of a monocyte/macrophage lineage. *Am J Pathol.* 2006;168(2):659-69.
52. Tian W, Jiang X, Tamosiuniene R, Sung YK, Qian J, Dhillon G, et al. Blocking macrophage leukotriene b4 prevents endothelial injury and reverses pulmonary hypertension. *Sci Transl Med.* 2013;5(200):200ra117.
53. Tuder RM, Chacon M, Alger L, Wang J, Taraseviciene-Stewart L, Kasahara Y, et al. Expression of angiogenesis-related molecules in plexiform lesions in severe pulmonary hypertension: evidence for a process of disordered angiogenesis. *J Pathol.* 2001;195(3):367-74.
54. Kojima H, Tokunou T, Takahara Y, Sunagawa K, Hirooka Y, Ichiki T, et al. Hypoxia-inducible factor-1 alpha deletion in myeloid lineage attenuates hypoxia-induced pulmonary hypertension. *Physiol Rep.* 2019;7(7):e14025.
55. Marsh LM, Jandl K, Grunig G, Foris V, Bashir M, Ghanim B, et al. The inflammatory cell landscape in the lungs of patients with idiopathic pulmonary arterial hypertension. *Eur Respir J.* 2018;51(1).
56. Lin Q, Fan C, Skinner JT, Hunter EN, Macdonald AA, Illei PB, et al. RELMalpha Licenses Macrophages for Damage-Associated Molecular Pattern Activation to Instigate Pulmonary Vascular Remodeling. *J Immunol.* 2019;203(11):2862-71.
57. Florentin J, Dutta P. Origin and production of inflammatory perivascular macrophages in pulmonary hypertension. *Cytokine.* 2017;100:11-5.
58. Pullamsetti SS, Savai R. Macrophage Regulation during Vascular Remodeling: Implications for Pulmonary Hypertension Therapy. *Am J Respir Cell Mol Biol.* 2017;56(5):556-8.
59. Ozpelit E, Akdeniz B, Ozpelit ME, Tas S, Bozkurt S, Tertemiz KC, et al. Prognostic value of neutrophil-to-lymphocyte ratio in pulmonary arterial hypertension. *J Int Med Res.* 2015;43(5):661-71.
60. Harbaum L, Baaske KM, Simon M, Oqueka T, Sinning C, Glatzel A, et al. Exploratory analysis of the neutrophil to lymphocyte ratio in patients with pulmonary arterial hypertension. *BMC Pulm Med.* 2017;17(1):72.
61. Yanartas M, Kalkan ME, Arslan A, Tas SG, Koksall C, Bekiroglu N, et al. Neutrophil/Lymphocyte Ratio Can Predict Postoperative Mortality in Patients with Chronic Thromboembolic Pulmonary Hypertension. *Ann Thorac Cardiovasc Surg.* 2015;21(3):229-35.
62. Schultze AE, Wagner JG, White SM, Roth RA. Early indications of monocrotaline pyrrole-induced lung injury in rats. *Toxicol Appl Pharmacol.* 1991;109(1):41-50.
63. Klinke A, Berghausen E, Friedrichs K, Molz S, Lau D, Remane L, et al. Myeloperoxidase aggravates pulmonary arterial hypertension by activation of vascular Rho-kinase. *JCI Insight.* 2018;3(11).
64. Theoharides TC. Mast cells and pancreatic cancer. *N Engl J Med.* 2008;358(17):1860-1.
65. Coussens LM, Raymond WW, Bergers G, Laig-Webster M, Behrendtsen O, Werb Z, et al. Inflammatory mast cells up-regulate angiogenesis during squamous epithelial carcinogenesis. *Genes Dev.* 1999;13(11):1382-97.
66. Mitani Y, Ueda M, Maruyama K, Shimpo H, Kojima A, Matsumura M, et al. Mast cell chymase in pulmonary hypertension. *Thorax.* 1999;54(1):88-90.
67. Heath D, Yacoub M. Lung mast cells in plexogenic pulmonary arteriopathy. *J Clin Pathol.* 1991;44(12):1003-6.
68. Gilfillan AM, Rivera J. The tyrosine kinase network regulating mast cell activation. *Immunol Rev.* 2009;228(1):149-69.

69. Hoffmann J, Yin J, Kukucka M, Yin N, Saarikko I, Sterner-Kock A, et al. Mast cells promote lung vascular remodelling in pulmonary hypertension. *Eur Respir J*. 2011;37(6):1400-10.
70. Bartelds B, van Loon RLE, Mohaupt S, Wijnberg H, Dickinson MG, Boersma B, et al. Mast cell inhibition improves pulmonary vascular remodeling in pulmonary hypertension. *Chest*. 2012;141(3):651-60.
71. Dahal BK, Kosanovic D, Kaulen C, Cornitescu T, Savai R, Hoffmann J, et al. Involvement of mast cells in monocrotaline-induced pulmonary hypertension in rats. *Respir Res*. 2011;12:60.
72. Banasova A, Maxova H, Hampl V, Vizek M, Povysilova V, Novotna J, et al. Prevention of mast cell degranulation by disodium cromoglycate attenuates the development of hypoxic pulmonary hypertension in rats exposed to chronic hypoxia. *Respiration*. 2008;76(1):102-7.
73. Farha S, Sharp J, Asosingh K, Park M, Comhair SA, Tang WH, et al. Mast cell number, phenotype, and function in human pulmonary arterial hypertension. *Pulm Circ*. 2012;2(2):220-8.
74. Hamada H, Terai M, Kimura H, Hirano K, Oana S, Niimi H. Increased expression of mast cell chymase in the lungs of patients with congenital heart disease associated with early pulmonary vascular disease. *Am J Respir Crit Care Med*. 1999;160(4):1303-8.
75. Doggrel SA, Wanstall JC. Vascular chymase: pathophysiological role and therapeutic potential of inhibition. *Cardiovasc Res*. 2004;61(4):653-62.
76. Kosanovic D, Luitel H, Dahal BK, Cornitescu T, Janssen W, Danser AH, et al. Chymase: a multifunctional player in pulmonary hypertension associated with lung fibrosis. *Eur Respir J*. 2015;46(4):1084-94.
77. Riley DJ, Thakker-Varia S, Wilson FJ, Poiani GJ, Tozzi CA. Role of proteolysis and apoptosis in regression of pulmonary vascular remodeling. *Physiol Res*. 2000;49(5):577-85.
78. Xu J, Wang J, Shao C, Zeng X, Sun L, Kong H, et al. New dynamic viewing of mast cells in pulmonary arterial hypertension (PAH): contributors or outsiders to cardiovascular remodeling. *J Thorac Dis*. 2018;10(5):3016-26.
79. Ormiston ML, Chang C, Long LL, Soon E, Jones D, Machado R, et al. Impaired natural killer cell phenotype and function in idiopathic and heritable pulmonary arterial hypertension. *Circulation*. 2012;126(9):1099-109.
80. Ratsep MT, Moore SD, Jaffri S, Mitchell M, Brady HJM, Mandelboim O, et al. Spontaneous pulmonary hypertension in genetic mouse models of natural killer cell deficiency. *Am J Physiol Lung Cell Mol Physiol*. 2018;315(6):L977-L990.
81. Zhu J, Yamane H, Paul WE. Differentiation of effector CD4 T cell populations (\*). *Annu Rev Immunol*. 2010;28:445-89.
82. Lewis KL, Reizis B. Dendritic cells: arbiters of immunity and immunological tolerance. *Cold Spring Harb Perspect Biol*. 2012;4(8):a007401.
83. Ganguly D, Haak S, Sisirak V, Reizis B. The role of dendritic cells in autoimmunity. *Nat Rev Immunol*. 2013;13(8):566-77.
84. Blanco P, Palucka AK, Pascual V, Banchereau J. Dendritic cells and cytokines in human inflammatory and autoimmune diseases. *Cytokine Growth Factor Rev*. 2008;19(1):41-52.
85. Kool M, van Loo G, Waelpuut W, De Prijck S, Muskens F, Sze M, et al. The ubiquitin-editing protein A20 prevents dendritic cell activation, recognition of apoptotic cells, and systemic autoimmunity. *Immunity*. 2011;35(1):82-96.
86. van Uden D, Boomars K, Kool M. Dendritic Cell Subsets and Effector Function in Idiopathic and Connective Tissue Disease-Associated Pulmonary Arterial Hypertension. *Front Immunol*. 2019;10:11.
87. Perros F, Dorfmueller P, Souza R, Durand-Gasselin I, Mussot S, Mazmanian M, et al. Dendritic cell recruitment in lesions of human and experimental pulmonary hypertension. *Eur Respir J*. 2007;29(3):462-8.
88. Guillemins M, Ginhoux F, Jakubzick C, Naik SH, Onai N, Schraml BU, et al. Dendritic cells, monocytes and macrophages: a unified nomenclature based on ontogeny. *Nat Rev Immunol*. 2014;14(8):571-8.
89. Wang W, Yan H, Zhu W, Cui Y, Chen J, Wang X, et al. Impairment of monocyte-derived dendritic cells in idiopathic pulmonary arterial hypertension. *J Clin Immunol*. 2009;29(6):705-13.
90. Mauad T, Pozzan G, Lancas T, Overbeek MJ, Souza R, Jardim C, et al. Immunopathological aspects of schistosomiasis-associated pulmonary arterial hypertension. *J Infect*. 2014;68(1):90-8.
91. Gaffen SL, Jain R, Garg AV, Cua DJ. The IL-23-IL-17 immune axis: from mechanisms to therapeutic testing. *Nat Rev Immunol*. 2014;14(9):585-600.
92. Hashimoto-Kataoka T, Hosen N, Sonobe T, Arita Y, Yasui T, Masaki T, et al. Interleukin-6/interleukin-21 signaling axis is critical in the pathogenesis of pulmonary arterial hypertension. *Proc Natl Acad Sci U S A*. 2015;112(20):E2677-86.

## Reference list

93. van Hamburg JP, Tas SW. Molecular mechanisms underpinning T helper 17 cell heterogeneity and functions in rheumatoid arthritis. *J Autoimmun.* 2018;87:69-81.
94. Soon E, Holmes AM, Treacy CM, Doughty NJ, Southgate L, Machado RD, et al. Elevated levels of inflammatory cytokines predict survival in idiopathic and familial pulmonary arterial hypertension. *Circulation.* 2010;122(9):920-7.
95. Gaowa S, Zhou W, Yu L, Zhou X, Liao K, Yang K, et al. Effect of Th17 and Treg axis disorder on outcomes of pulmonary arterial hypertension in connective tissue diseases. *Mediators Inflamm.* 2014;2014:247372.
96. Vroman H, Bergen IM, van Hulst JAC, van Nimwegen M, van Uden D, Schuijs MJ, et al. TNF-alpha-induced protein 3 levels in lung dendritic cells instruct TH2 or TH17 cell differentiation in eosinophilic or neutrophilic asthma. *J Allergy Clin Immunol.* 2018;141(5):1620-33 e12.
97. Pitzalis C, Jones GW, Bombardieri M, Jones SA. Ectopic lymphoid-like structures in infection, cancer and autoimmunity. *Nat Rev Immunol.* 2014;14(7):447-62.
98. de Bourcy CFA, Dekker CL, Davis MM, Nicolls MR, Quake SR. Dynamics of the human antibody repertoire after B cell depletion in systemic sclerosis. *Sci Immunol.* 2017;2(15).
99. Ulrich S, Taraseviciene-Stewart L, Huber LC, Speich R, Voelkel N. Peripheral blood B lymphocytes derived from patients with idiopathic pulmonary arterial hypertension express a different RNA pattern compared with healthy controls: a cross sectional study. *Respir Res.* 2008;9:20.
100. Blum LK, Cao RRL, Sweatt AJ, Bill M, Lahey LJ, Hsi AC, et al. Circulating plasmablasts are elevated and produce pathogenic anti-endothelial cell autoantibodies in idiopathic pulmonary arterial hypertension. *Eur J Immunol.* 2018;48(5):874-84.
101. Rich S, Kieras K, Hart K, Groves BM, Stobo JD, Brundage BH. Antinuclear antibodies in primary pulmonary hypertension. *J Am Coll Cardiol.* 1986;8(6):1307-11.
102. Arends SJ, Damoiseaux J, Duijvestijn A, Debrus-Palmans L, Boomars K, Broers B, et al. Prevalence of anti-endothelial cell antibodies in idiopathic pulmonary arterial hypertension. *Eur Respir J.* 2010;35(4):923-5.
103. Dib H, Tamby MC, Bussone G, Regent A, Berezne A, Lafine C, et al. Targets of anti-endothelial cell antibodies in pulmonary hypertension and scleroderma. *Eur Respir J.* 2012;39(6):1405-14.
104. Tamby MC, Chanseaud Y, Humbert M, Fermanian J, Guilpain P, Garcia-de-la-Pena-Lefebvre P, et al. Anti-endothelial cell antibodies in idiopathic and systemic sclerosis associated pulmonary arterial hypertension. *Thorax.* 2005;60(9):765-72.
105. Arends SJ, Damoiseaux JG, Duijvestijn AM, Debrus-Palmans L, Vroomen M, Boomars KA, et al. Immunoglobulin G anti-endothelial cell antibodies: inducers of endothelial cell apoptosis in pulmonary arterial hypertension? *Clin Exp Immunol.* 2013;174(3):433-40.
106. Becker MO, Kill A, Kutsche M, Guenther J, Rose A, Tabeling C, et al. Vascular receptor autoantibodies in pulmonary arterial hypertension associated with systemic sclerosis. *Am J Respir Crit Care Med.* 2014;190(7):808-17.
107. Colvin KL, Cripe PJ, Ivy DD, Stenmark KR, Yeager ME. Bronchus-associated lymphoid tissue in pulmonary hypertension produces pathologic autoantibodies. *Am J Respir Crit Care Med.* 2013;188(9):1126-36.
108. Cracowski JL, Chabot F, Labarere J, Faure P, Degano B, Schwebel C, et al. Proinflammatory cytokine levels are linked to death in pulmonary arterial hypertension. *Eur Respir J.* 2014;43(3):915-7.
109. Saleby J, Bouzina H, Lundgren J, Radegran G. Angiogenic and inflammatory biomarkers in the differentiation of pulmonary hypertension. *Scand Cardiovasc J.* 2017;51(5):261-70.
110. Kimura H, Okada O, Tanabe N, Tanaka Y, Terai M, Takiguchi Y, et al. Plasma monocyte chemoattractant protein-1 and pulmonary vascular resistance in chronic thromboembolic pulmonary hypertension. *Am J Respir Crit Care Med.* 2001;164(2):319-24.
111. Langer F, Schramm R, Bauer M, Tscholl D, Kunihara T, Schafers HJ. Cytokine response to pulmonary thromboendarterectomy. *Chest.* 2004;126(1):135-41.
112. Soon E HA, Barker L, et al. Inflammatory cytokines are elevated in patients with operable chronic thromboembolic pulmonary hypertension and predict outcome post-endarterectomy. *Thorax.* 2010;65.
113. Kylhammar D, Hesselstrand R, Nielsen S, Scheele C, Radegran G. Angiogenic and inflammatory biomarkers for screening and follow-up in patients with pulmonary arterial hypertension. *Scand J Rheumatol.* 2018;47(4):319-24.
114. Low A, George S, Howard L, Bell N, Millar A, Tulloh RMR. Lung Function, Inflammation, and Endothelin-1 in Congenital Heart Disease-Associated Pulmonary Arterial Hypertension. *J Am Heart Assoc.* 2018;7(4).

115. Joshi AA, Davey R, Rao Y, Shen K, Benza RL, Raina A. Association between cytokines and functional, hemodynamic parameters, and clinical outcomes in pulmonary arterial hypertension. *Pulm Circ.* 2018;8(3):2045894018794051.
116. Dorfmueller P, Zarka V, Durand-Gasselini I, Monti G, Balabanian K, Garcia G, et al. Chemokine RANTES in severe pulmonary arterial hypertension. *Am J Respir Crit Care Med.* 2002;165(4):534-9.
117. Steiner MK, Syrkina OL, Kolliputi N, Mark EJ, Hales CA, Waxman AB. Interleukin-6 overexpression induces pulmonary hypertension. *Circ Res.* 2009;104(2):236-44, 28p following 44.
118. Golembeski SM, West J, Tada Y, Fagan KA. Interleukin-6 causes mild pulmonary hypertension and augments hypoxia-induced pulmonary hypertension in mice. *Chest.* 2005;128(6 Suppl):572S-3S.
119. Miyata M, Sakuma F, Yoshimura A, Ishikawa H, Nishimaki T, Kasukawa R. Pulmonary hypertension in rats. 2. Role of interleukin-6. *Int Arch Allergy Immunol.* 1995;108(3):287-91.
120. Savale L, Tu L, Rideau D, Izziki M, Maitre B, Adnot S, et al. Impact of interleukin-6 on hypoxia-induced pulmonary hypertension and lung inflammation in mice. *Respir Res.* 2009;10:6.
121. Matura LA, Ventetuolo CE, Palevsky HI, Lederer DJ, Horn EM, Mathai SC, et al. Interleukin-6 and tumor necrosis factor-alpha are associated with quality of life-related symptoms in pulmonary arterial hypertension. *Ann Am Thorac Soc.* 2015;12(3):370-5.
122. Sweatt AJ, Hedlin HK, Balasubramanian V, Hsi A, Blum LK, Robinson WH, et al. Discovery of Distinct Immune Phenotypes Using Machine Learning in Pulmonary Arterial Hypertension. *Circ Res.* 2019;124(6):904-19.
123. Fujita M, Mason RJ, Cool C, Shannon JM, Hara N, Fagan KA. Pulmonary hypertension in TNF-alpha-overexpressing mice is associated with decreased VEGF gene expression. *J Appl Physiol (1985).* 2002;93(6):2162-70.
124. Price LC, Montani D, Tcherakian C, Dorfmueller P, Souza R, Gambaryan N, et al. Dexamethasone reverses monocrotaline-induced pulmonary arterial hypertension in rats. *Eur Respir J.* 2011;37(4):813-22.
125. Suzuki C, Takahashi M, Morimoto H, Izawa A, Ise H, Hongo M, et al. Mycophenolate mofetil attenuates pulmonary arterial hypertension in rats. *Biochem Biophys Res Commun.* 2006;349(2):781-8.
126. Bonnet S, Rochefort G, Sutendra G, Archer SL, Haromy A, Webster L, et al. The nuclear factor of activated T cells in pulmonary arterial hypertension can be therapeutically targeted. *Proc Natl Acad Sci U S A.* 2007;104(27):11418-23.
127. Jais X, Launay D, Yaici A, Le Pavec J, Tcherakian C, Sitbon O, et al. Immunosuppressive therapy in lupus- and mixed connective tissue disease-associated pulmonary arterial hypertension: a retrospective analysis of twenty-three cases. *Arthritis Rheum.* 2008;58(2):521-31.
128. Voelkel NF, Tuder RM, Bridges J, Arend WP. Interleukin-1 receptor antagonist treatment reduces pulmonary hypertension generated in rats by monocrotaline. *Am J Respir Cell Mol Biol.* 1994;11(6):664-75.
129. Tamura Y, Phan C, Tu L, Le Hiress M, Thuillet R, Jutant EM, et al. Ectopic upregulation of membrane-bound IL6R drives vascular remodeling in pulmonary arterial hypertension. *J Clin Invest.* 2018;128(5):1956-70.
130. Toshner M, Church C, Morrell M, Corris P. A phase II study of tocilizumab in group 1 pulmonary arterial hypertension. Published final results report clinical trials register; <https://www.clinicaltrialsregister.eu/ctr-search/rest/download/result/attachment/2015-002799-26/1/26831>. 2018.
131. Roeleveld DM, Marijnissen RJ, Walgreen B, Helsen MM, van den Bersselaar L, van de Loo FA, et al. Higher efficacy of anti-IL-6/IL-21 combination therapy compared to monotherapy in the induction phase of Th17-driven experimental arthritis. *PLoS One.* 2017;12(2):e0171757.
132. Wang Q, Zuo XR, Wang YY, Xie WP, Wang H, Zhang M. Monocrotaline-induced pulmonary arterial hypertension is attenuated by TNF-alpha antagonists via the suppression of TNF-alpha expression and NF-kappaB pathway in rats. *Vascul Pharmacol.* 2013;58(1-2):71-7.
133. Zhang LL, Lu J, Li MT, Wang Q, Zeng XF. Preventive and remedial application of etanercept attenuate monocrotaline-induced pulmonary arterial hypertension. *Int J Rheum Dis.* 2016;19(2):192-8.
134. Hurst LA, Dunmore BJ, Long L, Crosby A, Al-Lamki R, Deighton J, et al. TNFalpha drives pulmonary arterial hypertension by suppressing the BMP type-II receptor and altering NOTCH signalling. *Nat Commun.* 2017;8:14079.
135. Mutschler D, Wikstrom G, Lind L, Larsson A, Lagrange A, Eriksson M. Etanercept reduces late endotoxin-induced pulmonary hypertension in the pig. *J Interferon Cytokine Res.* 2006;26(9):661-7.
136. Pousada G, Lupo V, Castro-Sanchez S, Alvarez-Satta M, Sanchez-Monteagudo A, Baloiira A, et al. Molecular and functional characterization of the BMPR2 gene in Pulmonary Arterial Hypertension. *Sci Rep.* 2017;7(1):1923.

## Reference list

137. Rol N, Kurakula KB, Happe C, Bogaard HJ, Goumans MJ. TGF-beta and BMPR2 Signaling in PAH: Two Black Sheep in One Family. *Int J Mol Sci.* 2018;19(9).
138. Evans JD, Girerd B, Montani D, Wang XJ, Galie N, Austin ED, et al. BMPR2 mutations and survival in pulmonary arterial hypertension: an individual participant data meta-analysis. *Lancet Respir Med.* 2016;4(2):129-37.
139. Nikolic I, Yung LM, Yang P, Malhotra R, Paskin-Flerlage SD, Dinter T, et al. Bone Morphogenetic Protein 9 Is a Mechanistic Biomarker of Portopulmonary Hypertension. *Am J Respir Crit Care Med.* 2019;199(7):891-902.
140. Sawada H, Saito T, Nickel NP, Alastalo TP, Glotzbach JP, Chan R, et al. Reduced BMPR2 expression induces GM-CSF translation and macrophage recruitment in humans and mice to exacerbate pulmonary hypertension. *J Exp Med.* 2014;211(2):263-80.
141. Hensley MK, Levine A, Gladwin MT, Lai YC. Emerging therapeutics in pulmonary hypertension. *Am J Physiol Lung Cell Mol Physiol.* 2018;314(5):L769-L81.
142. Reynolds AM, Xia W, Holmes MD, Hodge SJ, Danilov S, Curiel DT, et al. Bone morphogenetic protein type 2 receptor gene therapy attenuates hypoxic pulmonary hypertension. *Am J Physiol Lung Cell Mol Physiol.* 2007;292(5):L1182-92.
143. Long L, Ormiston ML, Yang X, Southwood M, Graf S, Machado RD, et al. Selective enhancement of endothelial BMPR-II with BMP9 reverses pulmonary arterial hypertension. *Nat Med.* 2015;21(7):777-85.
144. Morrell NW, Yang X, Upton PD, Jourdan KB, Morgan N, Sheares KK, et al. Altered growth responses of pulmonary artery smooth muscle cells from patients with primary pulmonary hypertension to transforming growth factor-beta(1) and bone morphogenetic proteins. *Circulation.* 2001;104(7):790-5.
145. Long L, Crosby A, Yang X, Southwood M, Upton PD, Kim DK, et al. Altered bone morphogenetic protein and transforming growth factor-beta signaling in rat models of pulmonary hypertension: potential for activin receptor-like kinase-5 inhibition in prevention and progression of disease. *Circulation.* 2009;119(4):566-76.
146. Yung LM, Nikolic I, Paskin-Flerlage SD, Pearsall RS, Kumar R, Yu PB. A Selective Transforming Growth Factor-beta Ligand Trap Attenuates Pulmonary Hypertension. *Am J Respir Crit Care Med.* 2016;194(9):1140-51.
147. Spiekerkoetter E, Tian X, Cai J, Hopper RK, Sudheendra D, Li CG, et al. FK506 activates BMPR2, rescues endothelial dysfunction, and reverses pulmonary hypertension. *J Clin Invest.* 2013;123(8):3600-13.
148. Spiekerkoetter E, Sung YK, Sudheendra D, Scott V, Del Rosario P, Bill M, et al. Randomised placebo-controlled safety and tolerability trial of FK506 (tacrolimus) for pulmonary arterial hypertension. *Eur Respir J.* 2017;50(3).
149. Liu T, Zhang L, Joo D, Sun SC. NF-kappaB signaling in inflammation. *Signal Transduct Target Ther.* 2017;2.
150. Kimura S, Egashira K, Chen L, Nakano K, Iwata E, Miyagawa M, et al. Nanoparticle-mediated delivery of nuclear factor kappaB decoy into lungs ameliorates monocrotaline-induced pulmonary arterial hypertension. *Hypertension.* 2009;53(5):877-83.
151. Huang J, Kaminski PM, Edwards JG, Yeh A, Wolin MS, Frishman WH, et al. Pyrrolidine dithiocarbamate restores endothelial cell membrane integrity and attenuates monocrotaline-induced pulmonary artery hypertension. *Am J Physiol Lung Cell Mol Physiol.* 2008;294(6):L1250-9.
152. Li L, Wei C, Kim IK, Janssen-Heininger Y, Gupta S. Inhibition of nuclear factor-kappaB in the lungs prevents monocrotaline-induced pulmonary hypertension in mice. *Hypertension.* 2014;63(6):1260-9.
153. Farkas D, Alhussaini AA, Kraskauskas D, Kraskauskiene V, Cool CD, Nicolls MR, et al. Nuclear factor kappaB inhibition reduces lung vascular lumen obliteration in severe pulmonary hypertension in rats. *Am J Respir Cell Mol Biol.* 2014;51(3):413-25.
154. Kumar S, Wei C, Thomas CM, Kim IK, Seqqat R, Kumar R, et al. Cardiac-specific genetic inhibition of nuclear factor-kappaB prevents right ventricular hypertrophy induced by monocrotaline. *Am J Physiol Heart Circ Physiol.* 2012;302(8):H1655-66.
155. Price LC, Caramori G, Perros F, Meng C, Gambaryan N, Dorfmueller P, et al. Nuclear factor kappa-B is activated in the pulmonary vessels of patients with end-stage idiopathic pulmonary arterial hypertension. *PLoS One.* 2013;8(10):e75415.
156. Wang YY, Yang YX, Zhe H, He ZX, Zhou SF. Bardoxolone methyl (CDDO-Me) as a therapeutic agent: an update on its pharmacokinetic and pharmacodynamic properties. *Drug Des Devel Ther.* 2014;8:2075-88.
157. Heiss EH, Schachner D, Werner ER, Dirsch VM. Active NF-E2-related factor (Nrf2) contributes to keep endothelial NO synthase (eNOS) in the coupled state: role of reactive oxygen species (ROS), eNOS, and heme oxygenase (HO-1) levels. *J Biol Chem.* 2009;284(46):31579-86.

158. Chan SY, Rubin LJ. Metabolic dysfunction in pulmonary hypertension: from basic science to clinical practice. *Eur Respir Rev.* 2017;26(146).
159. Tebay LE, Robertson H, Durant ST, Vitale SR, Penning TM, Dinkova-Kostova AT, et al. Mechanisms of activation of the transcription factor Nrf2 by redox stressors, nutrient cues, and energy status and the pathways through which it attenuates degenerative disease. *Free Radic Biol Med.* 2015;88(Pt B):108-46.
160. Li W, Khor TO, Xu C, Shen G, Jeong WS, Yu S, et al. Activation of Nrf2-antioxidant signaling attenuates NFkappaB-inflammatory response and elicits apoptosis. *Biochem Pharmacol.* 2008;76(11):1485-9.
161. Grzegorzewska AP, Seta F, Han R, Czajka CA, Makino K, Stawski L, et al. Dimethyl Fumarate ameliorates pulmonary arterial hypertension and lung fibrosis by targeting multiple pathways. *Sci Rep.* 2017;7:41605.
162. Hennigan S, Channick RN, Silverman GJ. Rituximab treatment of pulmonary arterial hypertension associated with systemic lupus erythematosus: a case report. *Lupus.* 2008;17(8):754-6.
163. Zamanian RT, Badesch D, Chung L, Domsic RT, Medsger T, Pinckney A, et al. Safety and Efficacy of B-Cell Depletion with Rituximab for the Treatment of Systemic Sclerosis-associated Pulmonary Arterial Hypertension: A Multicenter, Double-Blind, Randomized, Placebo-controlled Trial. *Am J Respir Crit Care Med.* 2021;204(2):209-21.
164. Samuelsson B, Dahlen SE, Lindgren JA, Rouzer CA, Serhan CN. Leukotrienes and lipoxins: structures, biosynthesis, and biological effects. *Science.* 1987;237(4819):1171-6.
165. Tian W, Jiang X, Sung YK, Qian J, Yuan K, Nicolls MR. Leukotrienes in pulmonary arterial hypertension. *Immunol Res.* 2014;58(2-3):387-93.
166. Das T, Chen Z, Hendriks RW, Kool M. A20/Tumor Necrosis Factor alpha-Induced Protein 3 in Immune Cells Controls Development of Autoinflammation and Autoimmunity: Lessons from Mouse Models. *Front Immunol.* 2018;9:104.
167. Hammer GE, Turer EE, Taylor KE, Fang CJ, Advincola R, Oshima S, et al. Expression of A20 by dendritic cells preserves immune homeostasis and prevents colitis and spondyloarthritis. *Nat Immunol.* 2011;12(12):1184-93.
168. Matmati M, Jacques P, Maelfait J, Verheugen E, Kool M, Sze M, et al. A20 (TNFAIP3) deficiency in myeloid cells triggers erosive polyarthritis resembling rheumatoid arthritis. *Nat Genet.* 2011;43(9):908-12.
169. Das T, Bergen IM, Koudstaal T, van Hulst JAC, van Loo G, Boonstra A, et al. DNGR1-mediated deletion of A20/Tnfaip3 in dendritic cells alters T and B-cell homeostasis and promotes autoimmune liver pathology. *J Autoimmun.* 2019.
170. Ma A, Malynn BA. A20: linking a complex regulator of ubiquitylation to immunity and human disease. *Nat Rev Immunol.* 2012;12(11):774-85.
171. Vroman H, van Uden D, Bergen IM, van Hulst JAC, Lukkes M, van Loo G, et al. Tnfaip3 expression in pulmonary conventional type 1 Langerin-expressing dendritic cells regulates T helper 2-mediated airway inflammation in mice. *Allergy.* 2020.
172. Schraml BU, van Blijswijk J, Zelenay S, Whitney PG, Filby A, Acton SE, et al. Genetic tracing via DNGR-1 expression history defines dendritic cells as a hematopoietic lineage. *Cell.* 2013;154(4):843-58.
173. Peacock AJ, National Pulmonary Hypertension Services of UK, Ireland. Treatment of pulmonary hypertension. *BMJ.* 2003;326(7394):835-6.
174. D'Alonzo GE, Barst RJ, Ayres SM, Bergofsky EH, Brundage BH, Detre KM, et al. Survival in patients with primary pulmonary hypertension. Results from a national prospective registry. *Ann Intern Med.* 1991;115(5):343-9.
175. Hoepfer MM, Oudiz RJ, Peacock A, Tapson VF, Haworth SG, Frost AE, et al. End points and clinical trial designs in pulmonary arterial hypertension: clinical and regulatory perspectives. *Journal of the American College of Cardiology.* 2004;43(12 Suppl S):48S-55S.
176. Huertas A, Perros F, Tu L, Cohen-Kaminsky S, Montani D, Dorfmueller P, et al. Immune dysregulation and endothelial dysfunction in pulmonary arterial hypertension: a complex interplay. *Circulation.* 2014;129(12):1332-40.
177. Humbert M, Guignabert C, Bonnet S, Dorfmueller P, Klinger JR, Nicolls MR, et al. Pathology and pathobiology of pulmonary hypertension: state of the art and research perspectives. *Eur Respir J.* 2019;53(1).
178. GeurtsvanKessel CH, Willart MA, Bergen IM, van Rijt LS, Muskens F, Elewaut D, et al. Dendritic cells are crucial for maintenance of tertiary lymphoid structures in the lung of influenza virus-infected mice. *J Exp Med.* 2009;206(11):2339-49.
179. Nacionales DC, Kelly KM, Lee PY, Zhuang H, Li Y, Weinstein JS, et al. Type I interferon production by tertiary lymphoid tissue developing in response to 2,6,10,14-tetramethyl-pentadecane (pristane). *Am J Pathol.* 2006;168(4):1227-40.

## Reference list

180. Neyt K, Perros F, GeurtsvanKessel CH, Hammad H, Lambrecht BN. Tertiary lymphoid organs in infection and autoimmunity. *Trends Immunol.* 2012;33(6):297-305.
181. Dieude P, Guedj M, Wipff J, Ruiz B, Riemekasten G, Matucci-Cerinic M, et al. Association of the TNFAIP3 rs5029939 variant with systemic sclerosis in the European Caucasian population. *Ann Rheum Dis.* 2010;69(11):1958-64.
182. Vereecke L, Sze M, Mc Guire C, Rogiers B, Chu Y, Schmidt-Supprian M, et al. Enterocyte-specific A20 deficiency sensitizes to tumor necrosis factor-induced toxicity and experimental colitis. *J Exp Med.* 2010;207(7):1513-23.
183. Srinivas S, Watanabe T, Lin CS, William CM, Tanabe Y, Jessell TM, et al. Cre reporter strains produced by targeted insertion of EYFP and ECFP into the ROSA26 locus. *BMC Dev Biol.* 2001;1:4.
184. Mombaerts P, Iacomini J, Johnson RS, Herrup K, Tonegawa S, Papaioannou VE. RAG-1-deficient mice have no mature B and T lymphocytes. *Cell.* 1992;68(5):869-77.
185. de Raaf MA, Herrmann FE, Schaliq I, de Man FS, Vonk-Noordegraaf A, Guignabert C, et al. Tyrosine kinase inhibitor BIBF1000 does not hamper right ventricular pressure adaptation in rats. *Am J Physiol Heart Circ Physiol.* 2016;311(3):H604-12.
186. Hammad H, Kool M, Soullie T, Narumiya S, Trottein F, Hoogsteden HC, et al. Activation of the D prostanoid 1 receptor suppresses asthma by modulation of lung dendritic cell function and induction of regulatory T cells. *J Exp Med.* 2007;204(2):357-67.
187. Pal Singh S, de Bruijn MJW, de Almeida MP, Meijers RWJ, Nitschke L, Langerak AW, et al. Identification of Distinct Unmutated Chronic Lymphocytic Leukemia Subsets in Mice Based on Their T Cell Dependency. *Front Immunol.* 2018;9:1996.
188. Hayashida K, Johnston DR, Goldberger O, Park PW. Syndecan-1 expression in epithelial cells is induced by transforming growth factor beta through a PKA-dependent pathway. *J Biol Chem.* 2006;281(34):24365-74.
189. Redinus K, Baek JH, Yalamanoglu A, Shin HKH, Moldova R, Harral JW, et al. An Hb-mediated circulating macrophage contributing to pulmonary vascular remodeling in sickle cell disease. *JCI Insight.* 2019;4(15).
190. Chan EK, Damoiseaux J, Carballo OG, Conrad K, de Melo Cruvinel W, Francescantonio PL, et al. Report of the First International Consensus on Standardized Nomenclature of Antinuclear Antibody HEp-2 Cell Patterns 2014-2015. *Front Immunol.* 2015;6:412.
191. Parthvi R, Sikachi RR, Agrawal A, Adial A, Vulisha A, Khanijo S, et al. Pulmonary hypertension associated with antiphospholipid antibody: Call for a screening tool? *Intractable Rare Dis Res.* 2017;6(3):163-71.
192. Taraseviciene-Stewart L, Kasahara Y, Alger L, Hirth P, Mc Mahon G, Waltenberger J, et al. Inhibition of the VEGF receptor 2 combined with chronic hypoxia causes cell death-dependent pulmonary endothelial cell proliferation and severe pulmonary hypertension. *FASEB J.* 2001;15(2):427-38.
193. Wang GS, Qian GS, Mao BL, Cai WQ, Chen WZ, Chen Y. [Changes of interleukin-6 and Janus kinases in rats with hypoxic pulmonary hypertension]. *Zhonghua Jie He He Hu Xi Za Zhi.* 2003;26(11):664-7.
194. Kasahara Y, Kimura H, Kurosu K, Sugito K, Mukaida N, Matsushima K, et al. MCAF/MCP-1 protein expression in a rat model for pulmonary hypertension induced by monocrotaline. *Chest.* 1998;114(1 Suppl):67S.
195. Hautefort A, Girerd B, Montani D, Cohen-Kaminsky S, Price L, Lambrecht BN, et al. T-helper 17 cell polarization in pulmonary arterial hypertension. *Chest.* 2015;147(6):1610-20.
196. Ross DJ, Strieter RM, Fishbein MC, Ardehali A, Belperio JA. Type I immune response cytokine-chemokine cascade is associated with pulmonary arterial hypertension. *J Heart Lung Transplant.* 2012;31(8):865-73.
197. Theisen D, Murphy K. The role of cDC1s in vivo: CD8 T cell priming through cross-presentation. *F1000Res.* 2017;6:98.
198. Austin ED, Rock MT, Mosse CA, Vnencak-Jones CL, Yoder SM, Robbins IM, et al. T lymphocyte subset abnormalities in the blood and lung in pulmonary arterial hypertension. *Respir Med.* 2010;104(3):454-62.
199. Heink S, Yogev N, Garbers C, Herwerth M, Aly L, Gasperi C, et al. Trans-presentation of IL-6 by dendritic cells is required for the priming of pathogenic TH17 cells. *Nat Immunol.* 2017;18(1):74-85.
200. Southgate L, Machado RD, Graf S, Morrell NW. Molecular genetic framework underlying pulmonary arterial hypertension. *Nat Rev Cardiol.* 2020;17(2):85-95.
201. Morrell NW, Aldred MA, Chung WK, Elliott CG, Nichols WC, Soubrier F, et al. Genetics and genomics of pulmonary arterial hypertension. *Eur Respir J.* 2019;53(1).

202. Atkinson C, Stewart S, Upton PD, Machado R, Thomson JR, Trembath RC, et al. Primary pulmonary hypertension is associated with reduced pulmonary vascular expression of type II bone morphogenetic protein receptor. *Circulation*. 2002;105(14):1672-8.
203. Machado RD, Southgate L, Eichstaedt CA, Aldred MA, Austin ED, Best DH, et al. Pulmonary Arterial Hypertension: A Current Perspective on Established and Emerging Molecular Genetic Defects. *Hum Mutat*. 2015;36(12):1113-27.
204. Andruska A, Spiekerkoetter E. Consequences of BMPR2 Deficiency in the Pulmonary Vasculature and Beyond: Contributions to Pulmonary Arterial Hypertension. *Int J Mol Sci*. 2018;19(9).
205. Elinoff JM, Mazer AJ, Cai R, Lu M, Graninger G, Harper B, et al. Meta-analysis of blood genome-wide expression profiling studies in pulmonary arterial hypertension. *Am J Physiol Lung Cell Mol Physiol*. 2020;318(1):L98-L111.
206. Xiao G, Zhuang W, Wang T, Lian G, Luo L, Ye C, et al. Transcriptomic analysis identifies Toll-like and Nod-like pathways and necroptosis in pulmonary arterial hypertension. *J Cell Mol Med*. 2020;24(19):11409-21.
207. Zhao E, Xie H, Zhang Y. Identification of Differentially Expressed Genes Associated with Idiopathic Pulmonary Arterial Hypertension by Integrated Bioinformatics Approaches. *J Comput Biol*. 2020.
208. George PM, Badiger R, Shao D, Edwards MR, Wort SJ, Paul-Clark MJ, et al. Viral Toll Like Receptor activation of pulmonary vascular smooth muscle cells results in endothelin-1 generation; relevance to pathogenesis of pulmonary arterial hypertension. *Biochem Biophys Res Commun*. 2012;426(4):486-91.
209. Collin M, Bigley V. Human dendritic cell subsets: an update. *Immunology*. 2018;154(1):3-20.
210. Cool CD, Voelkel NF, Bull T. Viral infection and pulmonary hypertension: is there an association? *Expert Rev Respir Med*. 2011;5(2):207-16.
211. Kubrycht J, Novotna J. Sequence-based prediction of linear autoepitopes involved in pathogenesis of IPAH and the corresponding organism sources of molecular mimicry. *Int J Bioinform Res Appl*. 2014;10(6):587-612.
212. Halle S, Dujardin HC, Bakocevic N, Fleige H, Danzer H, Willenzon S, et al. Induced bronchus-associated lymphoid tissue serves as a general priming site for T cells and is maintained by dendritic cells. *J Exp Med*. 2009;206(12):2593-601.
213. Koudstaal T, van Hulst JAC, Das T, Neys SFH, Merkus D, Bergen IM, et al. DNGR1-Cre-mediated Deletion of Tnfrsf25/A20 in Conventional Dendritic Cells Induces Pulmonary Hypertension in Mice. *Am J Respir Cell Mol Biol*. 2020;63(5):665-80.
214. Sabatel C, Radermecker C, Fievez L, Paulissen G, Chakarov S, Fernandes C, et al. Exposure to Bacterial CpG DNA Protects from Airway Allergic Inflammation by Expanding Regulatory Lung Interstitial Macrophages. *Immunity*. 2017;46(3):457-73.
215. Koudstaal T, Boomars KA, Kool M. Pulmonary Arterial Hypertension and Chronic Thromboembolic Pulmonary Hypertension: An Immunological Perspective. *J Clin Med*. 2020;9(2).
216. Frump A, Prewitt A, de Caestecker MP. BMPR2 mutations and endothelial dysfunction in pulmonary arterial hypertension (2017 Grover Conference Series). *Pulm Circ*. 2018;8(2):2045894018765840.
217. Sun XQ, Abbate A, Bogaard HJ. Role of cardiac inflammation in right ventricular failure. *Cardiovasc Res*. 2017;113(12):1441-52.
218. Overbeek MJ, Mouchaers KT, Niessen HM, Hadi AM, Kupreishvili K, Boonstra A, et al. Characteristics of interstitial fibrosis and inflammatory cell infiltration in right ventricles of systemic sclerosis-associated pulmonary arterial hypertension. *Int J Rheumatol*. 2010;2010.
219. Swirski FK, Nahrendorf M. Cardioimmunology: the immune system in cardiac homeostasis and disease. *Nat Rev Immunol*. 2018;18(12):733-44.
220. Zaman R, Hamidzada H, Epelman S. Exploring cardiac macrophage heterogeneity in the healthy and diseased myocardium. *Curr Opin Immunol*. 2020;68:54-63.
221. Siamwala JH, Zhao A, Barthel H, Pagano FS, Gilbert RJ, Rounds S. Adaptive and innate immune mechanisms in cardiac fibrosis complicating pulmonary arterial hypertension. *Physiol Rep*. 2020;8(15):e14532.
222. Latz E, Xiao TS, Stutz A. Activation and regulation of the inflammasomes. *Nat Rev Immunol*. 2013;13(6):397-411.
223. Duong BH, Onizawa M, Oses-Prieto JA, Advincula R, Burlingame A, Malynn BA, et al. A20 restricts ubiquitination of pro-interleukin-1beta protein complexes and suppresses NLRP3 inflammasome activity. *Immunity*. 2015;42(1):55-67.
224. Vande Walle L, Van Opdenbosch N, Jacques P, Fossoul A, Verheugen E, Vogel P, et al. Negative regulation of the NLRP3 inflammasome by A20 protects against arthritis. *Nature*. 2014;512(7512):69-73.

## Reference list

225. Zhivaki D, Borriello F, Chow OA, Doran B, Fleming I, Theisen DJ, et al. Inflammasomes within Hyperactive Murine Dendritic Cells Stimulate Long-Lived T Cell-Mediated Anti-tumor Immunity. *Cell Rep.* 2020;33(7):108381.
226. Abdi K, Singh NJ, Matzinger P. Lipopolysaccharide-activated dendritic cells: "exhausted" or alert and waiting? *J Immunol.* 2012;188(12):5981-9.
227. Ranchoux B, Harvey LD, Ayon RJ, Babicheva A, Bonnet S, Chan SY, et al. Endothelial dysfunction in pulmonary arterial hypertension: an evolving landscape (2017 Grover Conference Series). *Pulm Circ.* 2018;8(1):2045893217752912.
228. Rhodes CJ, Otero-Nunez P, Wharton J, Swietlik EM, Kariotis S, Harbaum L, et al. Whole-Blood RNA Profiles Associated with Pulmonary Arterial Hypertension and Clinical Outcome. *Am J Respir Crit Care Med.* 2020;202(4):586-94.
229. Simpson CE, Chen JY, Damico RL, Hassoun PM, Martin LJ, Yang J, et al. Cellular sources of interleukin-6 and associations with clinical phenotypes and outcomes in pulmonary arterial hypertension. *Eur Respir J.* 2020;55(4).
230. Tielemans B, Delcroix M, Belge C, Quarck R. TGFbeta and BMPRII signalling pathways in the pathogenesis of pulmonary arterial hypertension. *Drug Discov Today.* 2019;24(3):703-16.
231. Groom JR, Richmond J, Murooka TT, Sorensen EW, Sung JH, Bankert K, et al. CXCR3 chemokine receptor-ligand interactions in the lymph node optimize CD4+ T helper 1 cell differentiation. *Immunity.* 2012;37(6):1091-103.
232. Olsson KM, Olle S, Fuge J, Welte T, Hoepfer MM, Lerch C, et al. CXCL13 in idiopathic pulmonary arterial hypertension and chronic thromboembolic pulmonary hypertension. *Respir Res.* 2016;17:21.
233. Geenen LW, Baggen VJM, Koudstaal T, Boomars KA, Eindhoven JA, Boersma E, et al. The prognostic value of various biomarkers in adults with pulmonary hypertension; a multi-biomarker approach. *Am Heart J.* 2019;208:91-9.
234. Lê S, Josse J, Husson F. FactoMineR: An R Package for Multivariate Analysis. 2008. 2008;25(1):18.
235. Josse J, Husson F. *missMDA: A Package for Handling Missing Values in Multivariate Data Analysis.* 2016. 2016;70(1):31.
236. Kniotek M, Boguska A. Sildenafil Can Affect Innate and Adaptive Immune System in Both Experimental Animals and Patients. *J Immunol Res.* 2017;2017:4541958.
237. Stadhouders R, Lubberts E, Hendriks RW. A cellular and molecular view of T helper 17 cell plasticity in autoimmunity. *J Autoimmun.* 2018;87:1-15.
238. Hernandez-Sanchez J, Harlow L, Church C, Gaine S, Knightbridge E, Bunclark K, et al. Clinical trial protocol for TRANSFORM-UK: A therapeutic open-label study of tocilizumab in the treatment of pulmonary arterial hypertension. *Pulm Circ.* 2018;8(1):2045893217735820.
239. Delcroix M, Torbicki A, Gopalan D, Sitbon O, Klok FA, Lang I, et al. ERS statement on chronic thromboembolic pulmonary hypertension. *Eur Respir J.* 2021;57(6):2002828.
240. Guth S, D'Armini AM, Delcroix M, Nakayama K, Fadel E, Hoole SP, et al. Current strategies for managing chronic thromboembolic pulmonary hypertension: results of the worldwide prospective CTEPH Registry. *ERJ Open Res.* 2021;7(3).
241. Delcroix M, Lang I, Pepke-Zaba J, Jansa P, D'Armini AM, Snijder R, et al. Long-Term Outcome of Patients With Chronic Thromboembolic Pulmonary Hypertension: Results From an International Prospective Registry. *Circulation.* 2016;133(9):859-71.
242. Cannon JE, Su L, Kiely DG, Page K, Toshner M, Swietlik E, et al. Dynamic Risk Stratification of Patient Long-Term Outcome After Pulmonary Endarterectomy: Results From the United Kingdom National Cohort. *Circulation.* 2016;133(18):1761-71.
243. Bochenek ML, Rosinus NS, Lankeit M, Hobohm L, Bremmer F, Schutz E, et al. From thrombosis to fibrosis in chronic thromboembolic pulmonary hypertension. *Thromb Haemost.* 2017;117(4):769-83.
244. Arbustini E, Morbini P, D'Armini AM, Repetto A, Minzioni G, Piovella F, et al. Plaque composition in plexogenic and thromboembolic pulmonary hypertension: the critical role of thrombotic material in pultaceous core formation. *Heart.* 2002;88(2):177-82.
245. Simonneau G, Torbicki A, Dorfmueller P, Kim N. The pathophysiology of chronic thromboembolic pulmonary hypertension. *Eur Respir Rev.* 2017;26(143).
246. Yang M, Deng C, Wu D, Zhong Z, Lv X, Huang Z, et al. The role of mononuclear cell tissue factor and inflammatory cytokines in patients with chronic thromboembolic pulmonary hypertension. *J Thromb Thrombolysis.* 2016;42(1):38-45.
247. Sharma S, Hofbauer TM, Ondracek AS, Chausheva S, Alimohammadi A, Artner T, et al. Neutrophil extracellular traps promote fibrous vascular occlusions in chronic thrombosis. *Blood.* 2021;137(8):1104-16.

248. Aldabbous L, Abdul-Salam V, McKinnon T, Duluc L, Pepke-Zaba J, Southwood M, et al. Neutrophil Extracellular Traps Promote Angiogenesis: Evidence From Vascular Pathology in Pulmonary Hypertension. *Arterioscler Thromb Vasc Biol.* 2016;36(10):2078-87.
249. Humbert M. Pulmonary arterial hypertension and chronic thromboembolic pulmonary hypertension: pathophysiology. *Eur Respir Rev.* 2010;19(115):59-63.
250. Miao R, Dong X, Gong J, Li Y, Guo X, Wang J, et al. Cell landscape atlas for patients with chronic thromboembolic pulmonary hypertension after pulmonary endarterectomy constructed using single-cell RNA sequencing. *Aging (Albany NY).* 2021;13(12):16485-99.
251. Tomaszewski M, Grywalska E, Topyla-Putowska W, Blaszczyk P, Kurzyna M, Rolinski J, et al. High CD200 Expression on T CD4+ and T CD8+ Lymphocytes as a Non-Invasive Marker of Idiopathic Pulmonary Hypertension- Preliminary Study. *J Clin Med.* 2021;10(5).
252. Deshmane SL, Kremlev S, Amini S, Sawaya BE. Monocyte chemoattractant protein-1 (MCP-1): an overview. *J Interferon Cytokine Res.* 2009;29(6):313-26.
253. Yao W, Firth AL, Sacks RS, Ogawa A, Auger WR, Fedullo PF, et al. Identification of putative endothelial progenitor cells (CD34+CD133+Flk-1+) in endarterectomized tissue of patients with chronic thromboembolic pulmonary hypertension. *Am J Physiol Lung Cell Mol Physiol.* 2009;296(6):L870-8.
254. Koudstaal T, van Uden D, van Hulst JAC, Heukels P, Bergen IM, Geenen LW, et al. Plasma markers in pulmonary hypertension subgroups correlate with patient survival. *Respir Res.* 2021;22(1):137.
255. Naito A, Sakao S, Terada J, Iwasawa S, Jujo Sanada T, Suda R, et al. Nocturnal Hypoxemia and High Circulating TNF-alpha Levels in Chronic Thromboembolic Pulmonary Hypertension. *Intern Med.* 2020;59(15):1819-26.
256. Tesmer LA, Lundy SK, Sarkar S, Fox DA. Th17 cells in human disease. *Immunol Rev.* 2008;223:87-113.
257. Kondo T, Takata H, Matsuki F, Takiguchi M. Cutting edge: Phenotypic characterization and differentiation of human CD8+ T cells producing IL-17. *J Immunol.* 2009;182(4):1794-8.
258. Srenathan U, Steel K, Taams LS. IL-17+ CD8+ T cells: Differentiation, phenotype and role in inflammatory disease. *Immunol Lett.* 2016;178:20-6.
259. Heukels P, Corneth OBJ, van Uden D, van Hulst JAC, van den Toorn LM, van den Bosch AE, et al. Loss of immune homeostasis in patients with idiopathic pulmonary arterial hypertension. *Thorax.* 2021.
260. van der Ploeg EK, Golebski K, van Nimwegen M, Fergusson JR, Heesters BA, Martinez-Gonzalez I, et al. Steroid-resistant human inflammatory ILC2s are marked by CD45RO and elevated in type 2 respiratory diseases. *Sci Immunol.* 2021;6(55).
261. van Uden D, Koudstaal T, van Hulst JAC, Bergen IM, Gootjes C, Morrell NW, et al. Central Role of Dendritic Cells in Pulmonary Arterial Hypertension in Human and Mice. *Int J Mol Sci.* 2021;22(4).
262. Le S, Josse J, Husson F. FactoMineR: An R package for multivariate analysis. *Journal of Statistical Software.* 2008;25(1):1-18.
263. Dankers W, den Braanker H, Paulissen SMJ, van Hamburg JP, Davelaar N, Colin EM, et al. The heterogeneous human memory CCR6+ T helper-17 populations differ in T-bet and cytokine expression but all activate synovial fibroblasts in an IFNgamma-independent manner. *Arthritis Res Ther.* 2021;23(1):157.
264. Wacleche VS, Goulet JP, Gosselin A, Monteiro P, Soudeyns H, Fromentin R, et al. New insights into the heterogeneity of Th17 subsets contributing to HIV-1 persistence during antiretroviral therapy. *Retrovirology.* 2016;13(1):59.
265. Kondo T, Takata H, Matsuki F, Takiguchi M. Cutting Edge: Phenotypic Characterization and Differentiation of Human CD8(+) T Cells Producing IL-17. *Journal of Immunology.* 2009;182(4):1794-8.
266. Maggi L, Santarlasci V, Capone M, Rossi MC, Querci V, Mazzoni A, et al. Distinctive features of classic and nonclassic (Th17 derived) human Th1 cells. *Eur J Immunol.* 2012;42(12):3180-8.
267. Chen L, Flies DB. Molecular mechanisms of T cell co-stimulation and co-inhibition. *Nat Rev Immunol.* 2013;13(4):227-42.
268. Li L, Xia Y, Ji X, Wang H, Zhang Z, Lu P, et al. MIG/CXCL9 exacerbates the progression of metabolic-associated fatty liver disease by disrupting Treg/Th17 balance. *Exp Cell Res.* 2021;407(2):112801.
269. Akdis CA, Blaser K. Mechanisms of interleukin-10-mediated immune suppression. *Immunology.* 2001;103(2):131-6.
270. Meitei HT, Jadhav N, Lal G. CCR6-CCL20 axis as a therapeutic target for autoimmune diseases. *Autoimmun Rev.* 2021;20(7):102846.

## Reference list

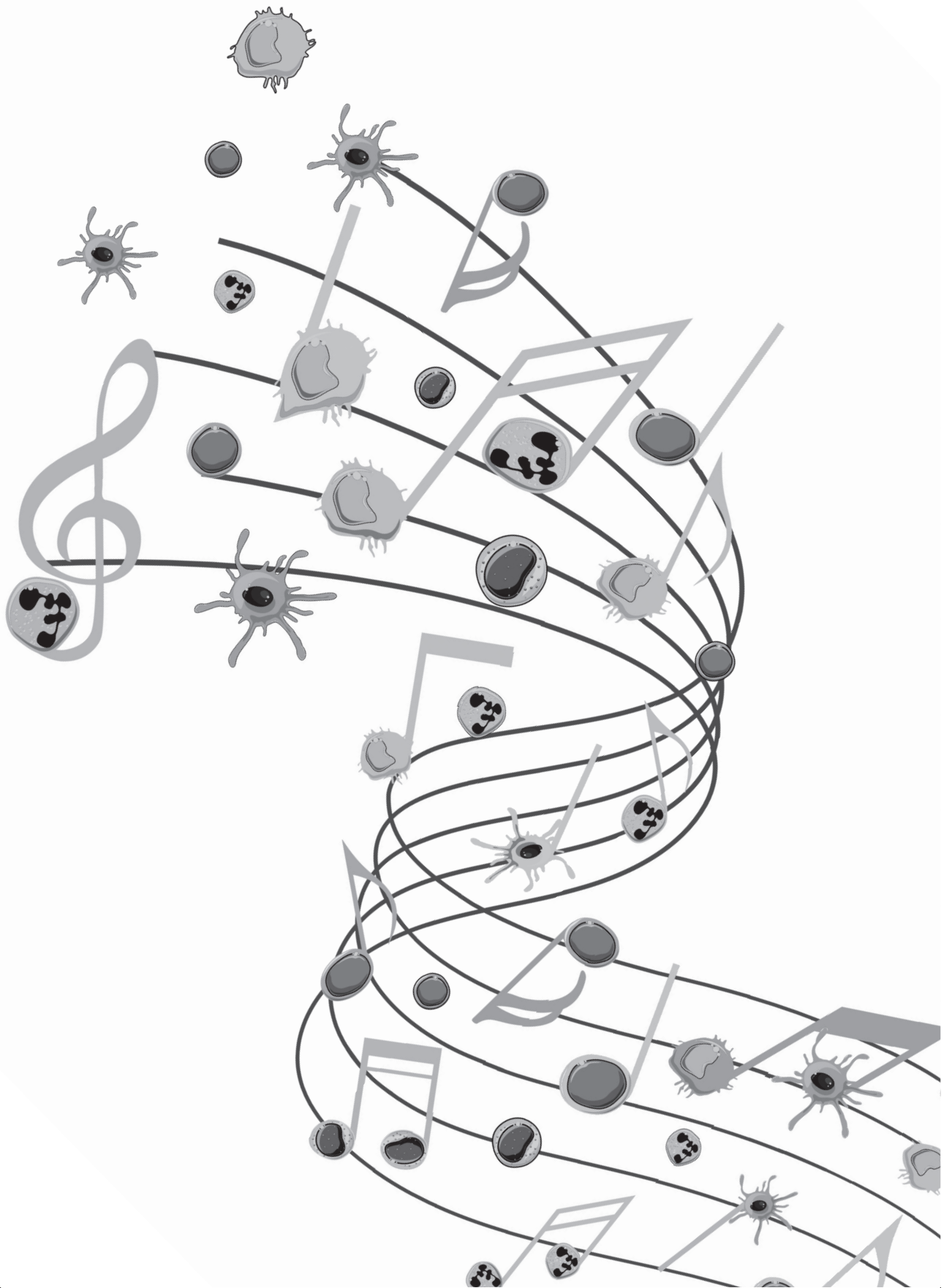
271. Lau EMT, Giannoulitou E, Celermajer DS, Humbert M. Epidemiology and treatment of pulmonary arterial hypertension. *Nat Rev Cardiol*. 2017;14(10):603-14.
272. Roy P, Orecchioni M, Ley K. How the immune system shapes atherosclerosis: roles of innate and adaptive immunity. *Nat Rev Immunol*. 2021.
273. Eid RE, Rao DA, Zhou J, Lo SF, Ranjbaran H, Gallo A, et al. Interleukin-17 and interferon-gamma are produced concomitantly by human coronary artery-infiltrating T cells and act synergistically on vascular smooth muscle cells. *Circulation*. 2009;119(10):1424-32.
274. Gao Q, Jiang Y, Ma T, Zhu F, Gao F, Zhang P, et al. A critical function of Th17 proinflammatory cells in the development of atherosclerotic plaque in mice. *J Immunol*. 2010;185(10):5820-7.
275. Bennett MR, Sinha S, Owens GK. Vascular Smooth Muscle Cells in Atherosclerosis. *Circ Res*. 2016;118(4):692-702.
276. Montani D, Humbert M, Souza R. Letter by Montani et al regarding article, "Elevated levels of inflammatory cytokines predict survival in idiopathic and familial pulmonary arterial hypertension". *Circulation*. 2011;123(21):e614; author reply e5.
277. Muller DN, Mervaala EM, Schmidt F, Park JK, Dechend R, Genersch E, et al. Effect of bosentan on NF-kappaB, inflammation, and tissue factor in angiotensin II-induced end-organ damage. *Hypertension*. 2000;36(2):282-90.
278. Heukels P, Corneth OBJ, van Uden D, van Hulst JAC, van den Toorn LM, van den Bosch AE, et al. Loss of immune homeostasis in patients with idiopathic pulmonary arterial hypertension. *Thorax*. 2021;76(12):1209-18.
279. Tian W, Jiang SY, Jiang X, Tamosiuniene R, Kim D, Guan T, et al. The Role of Regulatory T Cells in Pulmonary Arterial Hypertension. *Front Immunol*. 2021;12:684657.
280. Huertas A, Phan C, Bordenave J, Tu L, Thuillet R, Le Hires M, et al. Regulatory T Cell Dysfunction in Idiopathic, Heritable and Connective Tissue-Associated Pulmonary Arterial Hypertension. *Chest*. 2016;149(6):1482-93.
281. Ulrich S, Nicolls MR, Taraseviciene L, Speich R, Voelkel N. Increased regulatory and decreased CD8+ cytotoxic T cells in the blood of patients with idiopathic pulmonary arterial hypertension. *Respiration*. 2008;75(3):272-80.
282. Wang C, Kang SG, Lee J, Sun Z, Kim CH. The roles of CCR6 in migration of Th17 cells and regulation of effector T-cell balance in the gut. *Mucosal Immunol*. 2009;2(2):173-83.
283. Shu T, Xing Y, Wang J. Autoimmunity in Pulmonary Arterial Hypertension: Evidence for Local Immunoglobulin Production. *Front Cardiovasc Med*. 2021;8:680109.
284. Paats MS, Bergen IM, Hoogsteden HC, van der Eerden MM, Hendriks RW. Systemic CD4+ and CD8+ T-cell cytokine profiles correlate with GOLD stage in stable COPD. *Eur Respir J*. 2012;40(2):330-7.
285. Rhodes CJ, Batai K, Bleda M, Haimel M, Southgate L, Germain M, et al. Genetic determinants of risk in pulmonary arterial hypertension: international genome-wide association studies and meta-analysis. *Lancet Respir Med*. 2019;7(3):227-38.
286. Yang P, Yu PB. In Search of the Second Hit in Pulmonary Arterial Hypertension. *Circ Res*. 2019;124(1):6-8.
287. Kumar R, Theiss AL, Venuprasad K. RORgammat protein modifications and IL-17-mediated inflammation. *Trends Immunol*. 2021;42(11):1037-50.
288. Aguilar-Flores C, Castro-Escamilla O, Ortega-Rocha EM, Maldonado-Garcia C, Jurado-Santa Cruz F, Perez-Montesinos G, et al. Association of Pathogenic Th17 Cells with the Disease Severity and Its Potential Implication for Biological Treatment Selection in Psoriasis Patients. *Mediators Inflamm*. 2020;2020:8065147.
289. Yoo HHB, Marin FL. Treating Inflammation Associated with Pulmonary Hypertension: An Overview of the Literature. *Int J Gen Med*. 2022;15:1075-83.
290. Hu Y, Chi L, Kuebler WM, Goldenberg NM. Perivascular Inflammation in Pulmonary Arterial Hypertension. *Cells*. 2020;9(11).
291. van Uden D, Koudstaal T, van Hulst JAC, van den Bosch TPP, Vink M, Bergen IM, et al. Evidence for a Role of CCR6+ T Cells in Chronic Thromboembolic Pulmonary Hypertension. *Front Immunol*. 2022;13:861450.
292. Rakebrandt N, Littringer K, Joller N. Regulatory T cells: balancing protection versus pathology. *Swiss Med Wkly*. 2016;146:w14343.
293. de Man FS, Handoko ML, Groepenhoff H, van 't Hul AJ, Abbink J, Koppers RJ, et al. Effects of exercise training in patients with idiopathic pulmonary arterial hypertension. *Eur Respir J*. 2009;34(3):669-75.
294. Marra AM, Arcopinto M, Bossone E, Ehlken N, Cittadini A, Grunig E. Pulmonary arterial hypertension-related myopathy: an overview of current data and future perspectives. *Nutr Metab Cardiovasc Dis*. 2015;25(2):131-9.

295. Breda AP, Pereira de Albuquerque AL, Jardim C, Morinaga LK, Suesada MM, Fernandes CJ, et al. Skeletal muscle abnormalities in pulmonary arterial hypertension. *PLoS One*. 2014;9(12):e114101.
296. Batt J, Ahmed SS, Correa J, Bain A, Granton J. Skeletal muscle dysfunction in idiopathic pulmonary arterial hypertension. *Am J Respir Cell Mol Biol*. 2014;50(1):74-86.
297. Malenfant S, Potus F, Fournier F, Breuils-Bonnet S, Pflieger A, Bourassa S, et al. Skeletal muscle proteomic signature and metabolic impairment in pulmonary hypertension. *J Mol Med (Berl)*. 2015;93(5):573-84.
298. Malenfant S, Potus F, Mainguy V, Leblanc E, Malenfant M, Ribeiro F, et al. Impaired Skeletal Muscle Oxygenation and Exercise Tolerance in Pulmonary Hypertension. *Med Sci Sports Exerc*. 2015;47(11):2273-82.
299. Meyer FJ, Lossnitzer D, Kristen AV, Schoene AM, Kubler W, Katus HA, et al. Respiratory muscle dysfunction in idiopathic pulmonary arterial hypertension. *Eur Respir J*. 2005;25(1):125-30.
300. Bauer R, Dehnert C, Schoene P, Filusch A, Bartsch P, Borst MM, et al. Skeletal muscle dysfunction in patients with idiopathic pulmonary arterial hypertension. *Respir Med*. 2007;101(11):2366-9.
301. Mainguy V, Maltais F, Saey D, Gagnon P, Martel S, Simon M, et al. Peripheral muscle dysfunction in idiopathic pulmonary arterial hypertension. *Thorax*. 2010;65(2):113-7.
302. de Man FS, van Hees HW, Handoko ML, Niessen HW, Schalij I, Humbert M, et al. Diaphragm muscle fiber weakness in pulmonary hypertension. *Am J Respir Crit Care Med*. 2011;183(10):1411-8.
303. Mainguy V, Provencher S, Maltais F, Malenfant S, Saey D. Assessment of daily life physical activities in pulmonary arterial hypertension. *PLoS One*. 2011;6(11):e27993.
304. Saglam M, Vardar-Yagli N, Calik-Kutukcu E, Arikan H, Savci S, Inal-Ince D, et al. Functional exercise capacity, physical activity, and respiratory and peripheral muscle strength in pulmonary hypertension according to disease severity. *J Phys Ther Sci*. 2015;27(5):1309-12.
305. Mainguy V, Maltais F, Saey D, Gagnon P, Martel S, Simon M, et al. Effects of a rehabilitation program on skeletal muscle function in idiopathic pulmonary arterial hypertension. *J Cardiopulm Rehabil Prev*. 2010;30(5):319-23.
306. Kabitz HJ, Bremer HC, Schwoerer A, Sonntag F, Waltersbacher S, Walker DJ, et al. The combination of exercise and respiratory training improves respiratory muscle function in pulmonary hypertension. *Lung*. 2014;192(2):321-8.
307. Saglam M, Arikan H, Vardar-Yagli N, Calik-Kutukcu E, Inal-Ince D, Savci S, et al. Inspiratory muscle training in pulmonary arterial hypertension. *J Cardiopulm Rehabil Prev*. 2015;35(3):198-206.
308. Mereles D, Ehlken N, Kreuzer S, Ghofrani S, Hoepfer MM, Halank M, et al. Exercise and respiratory training improve exercise capacity and quality of life in patients with severe chronic pulmonary hypertension. *Circulation*. 2006;114(14):1482-9.
309. Grunig E, Ehlken N, Ghofrani A, Staehler G, Meyer FJ, Juenger J, et al. Effect of exercise and respiratory training on clinical progression and survival in patients with severe chronic pulmonary hypertension. *Respiration*. 2011;81(5):394-401.
310. Inagaki T, Terada J, Tanabe N, Kawata N, Kasai H, Sugiura T, et al. Home-based pulmonary rehabilitation in patients with inoperable or residual chronic thromboembolic pulmonary hypertension: a preliminary study. *Respir Investig*. 2014;52(6):357-64.
311. Fox BD, Kassirer M, Weiss I, Raviv Y, Peled N, Shritit D, et al. Ambulatory rehabilitation improves exercise capacity in patients with pulmonary hypertension. *J Card Fail*. 2011;17(3):196-200.
312. Grunig E, Lichtblau M, Ehlken N, Ghofrani HA, Reichenberger F, Staehler G, et al. Safety and efficacy of exercise training in various forms of pulmonary hypertension. *Eur Respir J*. 2012;40(1):84-92.
313. Brown MB, Neves E, Long G, Graber J, Gladish B, Wiseman A, et al. High-intensity interval training, but not continuous training, reverses right ventricular hypertrophy and dysfunction in a rat model of pulmonary hypertension. *Am J Physiol Regul Integr Comp Physiol*. 2017;312(2):R197-R210.
314. Colombo R, Siqueira R, Conzatti A, Fernandes TR, Tavares AM, Araujo AS, et al. Aerobic Exercise Promotes a Decrease in Right Ventricle Apoptotic Proteins in Experimental Cor Pulmonale. *J Cardiovasc Pharmacol*. 2015;66(3):246-53.
315. Delcroix M, Howard L. Pulmonary arterial hypertension: the burden of disease and impact on quality of life. *Eur Respir Rev*. 2015;24(138):621-9.
316. McKenna SP, Doughty N, Meads DM, Doward LC, Pepke-Zaba J. The Cambridge Pulmonary Hypertension Outcome Review (CAMPHOR): a measure of health-related quality of life and quality of life for patients with pulmonary hypertension. *Qual Life Res*. 2006;15(1):103-15.

## Reference list

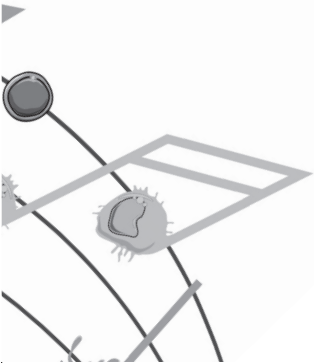
317. Wapenaar M, Twiss J, Wagenaar M, Seijkens P, van den Toorn L, Stepanous J, et al. Adaptation and validation of the Cambridge Pulmonary Hypertension Outcome Review (CAMPHOR) for the Netherlands. *Neth Heart J*. 2016;24(6):417-24.
318. Holland AE, Spruit MA, Troosters T, Puhan MA, Pepin V, Saey D, et al. An official European Respiratory Society/American Thoracic Society technical standard: field walking tests in chronic respiratory disease. *Eur Respir J*. 2014;44(6):1428-46.
319. Dimitriadis Z, Kapreli E, Konstantinidou I, Oldham J, Strimpakos N. Test/retest reliability of maximum mouth pressure measurements with the MicroRPM in healthy volunteers. *Respir Care*. 2011;56(6):776-82.
320. Mentiplay BF, Perraton LG, Bower KJ, Adair B, Pua YH, Williams GP, et al. Assessment of Lower Limb Muscle Strength and Power Using Hand-Held and Fixed Dynamometry: A Reliability and Validity Study. *PLoS One*. 2015;10(10):e0140822.
321. American Thoracic S, American College of Chest P. ATS/ACCP Statement on cardiopulmonary exercise testing. *Am J Respir Crit Care Med*. 2003;167(2):211-77.
322. Nagel C, Prange F, Guth S, Herb J, Ehlken N, Fischer C, et al. Exercise training improves exercise capacity and quality of life in patients with inoperable or residual chronic thromboembolic pulmonary hypertension. *PLoS One*. 2012;7(7):e41603.
323. Laviolette L, Bourbeau J, Bernard S, Lacasse Y, Pepin V, Breton MJ, et al. Assessing the impact of pulmonary rehabilitation on functional status in COPD. *Thorax*. 2008;63(2):115-21.
324. Frost AE, Langleben D, Oudiz R, Hill N, Horn E, McLaughlin V, et al. The 6-min walk test (6MW) as an efficacy endpoint in pulmonary arterial hypertension clinical trials: demonstration of a ceiling effect. *Vascul Pharmacol*. 2005;43(1):36-9.
325. Matura LA, Shou H, Fritz JS, Smith KA, Vaidya A, Pinder D, et al. Physical Activity and Symptoms in Pulmonary Arterial Hypertension. *Chest*. 2016;150(1):46-56.
326. Pugh ME, Buchowski MS, Robbins IM, Newman JH, Hemnes AR. Physical activity limitation as measured by accelerometry in pulmonary arterial hypertension. *Chest*. 2012;142(6):1391-8.
327. Chan L, Chin LMK, Kennedy M, Woolstenhulme JG, Nathan SD, Weinstein AA, et al. Benefits of intensive treadmill exercise training on cardiorespiratory function and quality of life in patients with pulmonary hypertension. *Chest*. 2013;143(2):333-43.
328. Hayton C, Clark A, Olive S, Browne P, Galey P, Knights E, et al. Barriers to pulmonary rehabilitation: characteristics that predict patient attendance and adherence. *Respir Med*. 2013;107(3):401-7.
329. Mattiuz R, Wohn C, Ghilas S, Ambrosini M, Alexandre YO, Sanchez C, et al. Novel Cre-Expressing Mouse Strains Permitting to Selectively Track and Edit Type 1 Conventional Dendritic Cells Facilitate Disentangling Their Complexity in vivo. *Front Immunol*. 2018;9:2805.
330. Lee JH, Park CS, Jang S, Kim JW, Kim SH, Song S, et al. Tolerogenic dendritic cells are efficiently generated using minocycline and dexamethasone. *Sci Rep*. 2017;7(1):15087.
331. Ando T, Yamasaki Y, Takakuwa Y, Iida H, Asari Y, Suzuki K, et al. Concurrent onset of acute lupus myocarditis, pulmonary arterial hypertension and digital gangrene in a lupus patient: a possible role of vasculitis to the rare disorders. *Mod Rheumatol Case Rep*. 2020;4(1):21-7.
332. Cheng TO. Pulmonary hypertension in systemic lupus erythematosus. *Mayo Clin Proc*. 1999;74(8):845.
333. Winslow TM, Ossipov MA, Fazio GP, Simonson JS, Redberg RF, Schiller NB. Five-year follow-up study of the prevalence and progression of pulmonary hypertension in systemic lupus erythematosus. *Am Heart J*. 1995;129(3):510-5.
334. Klarquist J, Zhou Z, Shen N, Janssen EM. Dendritic Cells in Systemic Lupus Erythematosus: From Pathogenic Players to Therapeutic Tools. *Mediators Inflamm*. 2016;2016:5045248.
335. Kay JM, Harris P, Heath D. Pulmonary hypertension produced in rats by ingestion of *Crotalaria spectabilis* seeds. *Thorax*. 1967;22(2):176-9.
336. Millatt LJ, Whitley GS, Li D, Leiper JM, Siragy HM, Carey RM, et al. Evidence for dysregulation of dimethylarginine dimethylaminohydrolase I in chronic hypoxia-induced pulmonary hypertension. *Circulation*. 2003;108(12):1493-8.
337. Kurakula K, Sun XQ, Happe C, da Silva Goncalves Bos D, Szulcek R, Schalij I, et al. Prevention of progression of pulmonary hypertension by the Nur77 agonist 6-mercaptopurine: role of BMP signalling. *Eur Respir J*. 2019;54(3).

338. Botros L, Szulcek R, Jansen SMA, Kurakula K, Goumans MTH, van Kuilenburg ABP, et al. The Effects of Mercaptopurine on Pulmonary Vascular Resistance and BMPR2 Expression in Pulmonary Arterial Hypertension. *Am J Respir Crit Care Med.* 2020;202(2):296-9.
339. Vengethasamy L, Hautefort A, Tielemans B, Belge C, Perros F, Verleden S, et al. BMPRII influences the response of pulmonary microvascular endothelial cells to inflammatory mediators. *Pflugers Arch.* 2016;468(11-12):1969-83.
340. Zambrano-Zaragoza JF, Romo-Martinez EJ, Duran-Avelar Mde J, Garcia-Magallanes N, Vibanco-Perez N. Th17 cells in autoimmune and infectious diseases. *Int J Inflam.* 2014;2014:651503.
341. Brown LM, Chen H, Halpern S, Taichman D, McGoan MD, Farber HW, et al. Delay in recognition of pulmonary arterial hypertension: factors identified from the REVEAL Registry. *Chest.* 2011;140(1):19-26.
342. Villar-Fincheira P, Sanhueza-Olivares F, Norambuena-Soto I, Cancino-Arenas N, Hernandez-Vargas F, Troncoso R, et al. Role of Interleukin-6 in Vascular Health and Disease. *Front Mol Biosci.* 2021;8:641734.
343. Hartman J, Frishman WH. Inflammation and atherosclerosis: a review of the role of interleukin-6 in the development of atherosclerosis and the potential for targeted drug therapy. *Cardiol Rev.* 2014;22(3):147-51.
344. Humbert M, McLaughlin V, Gibbs JSR, Gomberg-Maitland M, Hoeper MM, Preston IR, et al. Sotatercept for the Treatment of Pulmonary Arterial Hypertension. *N Engl J Med.* 2021;384(13):1204-15.
345. Bottcher JP, Reis e Sousa C. The Role of Type 1 Conventional Dendritic Cells in Cancer Immunity. *Trends Cancer.* 2018;4(11):784-92.
346. Stenmark KR, Meyrick B, Galie N, Mooi WJ, McMurtry IF. Animal models of pulmonary arterial hypertension: the hope for etiological discovery and pharmacological cure. *Am J Physiol Lung Cell Mol Physiol.* 2009;297(6):L1013-32.
347. Larsen KO, Yndestad A, Sjaastad I, Loberg EM, Goverud IL, Halvorsen B, et al. Lack of CCR7 induces pulmonary hypertension involving perivascular leukocyte infiltration and inflammation. *Am J Physiol Lung Cell Mol Physiol.* 2011;301(1):L50-9.
348. Grunig E, Eichstaedt C, Barbera JA, Benjamin N, Blanco I, Bossone E, et al. ERS statement on exercise training and rehabilitation in patients with severe chronic pulmonary hypertension. *Eur Respir J.* 2019;53(2).
349. Vinke P, Koudstaal T, Muskens F, van den Bosch A, Balvers M, Poland M, et al. Prevalence of Micronutrient Deficiencies and Relationship with Clinical and Patient-Related Outcomes in Pulmonary Hypertension Types I and IV. *Nutrients.* 2021;13(11).
350. Quatreteniers M, Mendes-Ferreira P, Santos-Ribeiro D, Nakhleh MK, Ghigna MR, Cohen-Kaminsky S, et al. Iron Deficiency in Pulmonary Arterial Hypertension: A Deep Dive into the Mechanisms. *Cells.* 2021;10(2).
351. Camporeale A, Poli V. IL-6, IL-17 and STAT3: a holy trinity in auto-immunity? *Front Biosci (Landmark Ed).* 2012;17:2306-26.
352. Grunig E, MacKenzie A, Peacock AJ, Eichstaedt CA, Benjamin N, Nechwatal R, et al. Standardized exercise training is feasible, safe, and effective in pulmonary arterial and chronic thromboembolic pulmonary hypertension: results from a large European multicentre randomized controlled trial. *Eur Heart J.* 2021;42(23):2284-95.
353. Vinke P, Jansen SM, Witkamp RF, van Norren K. Increasing quality of life in pulmonary arterial hypertension: is there a role for nutrition? *Heart Fail Rev.* 2018;23(5):711-22.
354. Semen KO, Bast A. Towards improved pharmacotherapy in pulmonary arterial hypertension. Can diet play a role? *Clin Nutr ESPEN.* 2019;30:159-69.
355. Nobs SP, Zmora N, Elinav E. Nutrition Regulates Innate Immunity in Health and Disease. *Annu Rev Nutr.* 2020;40:189-219.
356. Ruitter G, Manders E, Happe CM, Schaliij I, Groepenhoff H, Howard LS, et al. Intravenous iron therapy in patients with idiopathic pulmonary arterial hypertension and iron deficiency. *Pulm Circ.* 2015;5(3):466-72.
357. Soon E, Treacy CM, Toshner MR, MacKenzie-Ross R, Manglam V, Busbridge M, et al. Unexplained iron deficiency in idiopathic and heritable pulmonary arterial hypertension. *Thorax.* 2011;66(4):326-32.
358. Kanamori Y, Murakami M, Sugiyama M, Hashimoto O, Matsui T, Funaba M. Interleukin-1beta (IL-1beta) transcriptionally activates hepcidin by inducing CCAAT enhancer-binding protein delta (C/EBPdelta) expression in hepatocytes. *J Biol Chem.* 2017;292(24):10275-87.



ENGLISH  
SUMMARY

S



Pulmonary hypertension (PH) is a debilitating disease characterized by structural remodeling of the arterial vasculature of the lung leading to increased vascular resistance and increased pulmonary arterial pressures, right ventricular (RV) hypertrophy, heart failure and ultimately, death. Based on the underlying causes of PH, the WHO classification system divides PH patients into 5 groups: (1) Pulmonary Arterial Hypertension (PAH), (2) PH due to left heart disease, (3) PH due to lung disease, (4) Chronic Thromboembolic PH (CTEPH), and (5) PH with unclear and/or multifactorial mechanisms.

In pulmonary arterial hypertension (PAH) patients, vascular endothelial cell proliferation along with concurrent formation of new blood vessels (neoangiogenesis), when exuberant, results in the formation of glomeruloid structures in pulmonary arterioles known as the plexiform lesions. These plexiform lesions are typically defined as dynamic networks of vascular channels formed by uncontrolled proliferation of endothelial cells. Both PAH and CTEPH histology displays extensive accumulation of immune cells. IPAH patient lungs and lung biopsy material from CTEPH patients shows compelling evidence for activation of the innate immune system. This includes pathological involvement of macrophages, mast cells (MCs) and neutrophils by production of inflammatory cytokines, recruitment of other immune cells and local inflammation and damage. Lungs of IPAH patients demonstrate increased numbers of dendritic cells (DCs), acting as a bridge between innate and the adaptive immune system by presentation of antigens to T cells. DCs contribute to increased production of cytokines and chemokines, attracting other inflammatory cells to the site of inflammation. Dysregulated Th17 immunity is another phenomenon in PAH patients, creating a pro-inflammatory auto-immune environment. Moreover, IPAH patients display an increase of circulating autoantibodies specifically targeting endothelial cell surface antigens. Extensive biomarker research reveals that many inflammatory and immune markers correlate with hemodynamics and/or prognosis of PAH and CTEPH patients.

Currently, there is still much unknown about the pathological involvement of the immune system in PAH and CTEPH etiology. Novel insights are required, to gain knowledge into novel pathways for therapeutic targets and new treatment options for researchers and clinicians. Therefore, the aims of this thesis were to; **(I)** further unravel the immunological imbalance in pulmonary arterial hypertension (PAH) and chronic thromboembolic pulmonary hypertension (CTEPH) pathogenesis, **(II)** to find novel biomarkers and therapeutic targets for PAH and CTEPH, and **(III)** to improve non-drug treatment options in PAH and CTEPH.

## Unraveling the immunological imbalance in PAH and CTEPH pathogenesis

Firstly, in **chapter 1**, we review the accumulating evidence indicating a critical involvement of the immune system in PAH and CTEPH pathogenesis, leading to decreased survival and high burden of disease. However, there are still many questions unanswered as to how and through which immune cells this occurs.

Considering that conventional dendritic cells (cDCs), a subtype of DCs, are increased in the lungs of IPAH, our aim in **chapter 2** was to investigate whether constitutive activation of cDCs would result in PH development in mice. To this end, we utilized the *Tnfaip3*<sup>DNGR1-KO</sup> mouse model, in which a negative regulator of DC activation (A20/Tnfaip3) was specifically knocked out, thus leading to uncontrolled activation of DCs. In these studies, we found that *Tnfaip3*<sup>DNGR1-KO</sup> mice develop an experimental PH phenotype characterized by increased right ventricular (RV) systolic pressure (RVSP), thickening of the RV due to increased RVSP (RV hypertrophy (RVH)), perivascular accumulation of immune cells (lymphocytic infiltration), and vascular remodeling. Expression of IL-1 $\beta$ , IL-6 and IL-10

were enhanced in the lungs of *Tnfaip3*<sup>DNGRI-KO</sup> mice. All signs of PH were ameliorated in *Tnfaip3*<sup>DNGRI-KO</sup> mice by anti-IL-6 antibody treatment. These results indicate that activation of the NF- $\kappa$ B pathway in DCs, through deletion of *A20/Tnfaip3*, leads to experimental PH with accompanied pulmonary inflammation in an IL-6-dependent fashion.

The exact mechanism by which the *Tnfaip3*<sup>DNGRI-KO</sup> mice described in **chapter 2** develop PH symptoms and the importance of the altered activation status of DCs or other immune cells in this model, is largely unknown. In **chapter 3**, we investigated the immunological landscape of the heart in *Tnfaip3*<sup>DNGRI-KO</sup> mice more closely. We also addressed the question whether additional immune activation would have effects on PH development by exposing the airways of *Tnfaip3*<sup>DNGRI-KO</sup> mice to TLR-ligands *in vivo*. Furthermore, our aim in chapter 3 was to determine whether a vascular trigger would result in enhancement of the PH phenotype. To this end, we crossed *Tnfaip3*<sup>DNGRI-KO</sup> mice with mice that harbor a mutation in the *Bmpr2* gene, which is associated with a susceptibility to develop PH. Lastly, we explored the relevance of our findings by determining DC and CD8+ T cell co-localization in human IPAH lung tissue. In our studies, we found various immune cells, including DCs, in the hearts of *Tnfaip3*<sup>DNGRI-KO</sup> mice, particularly in the right ventricle (RV). Secondly, in young *Tnfaip3*<sup>DNGRI-KO</sup> mice innate immune activation through airway exposure to Toll-like receptor ligands *in vivo* did not result in elevated RV pressures, although we did observe RV enlargement. Thirdly, PAH symptoms in *Tnfaip3*<sup>DNGRI-KO</sup> mice were not enhanced by concomitant mutation of *Bmpr2*, which is the most affected gene in PAH patients. Finally, in human IPAH lung tissue we found co-localization of DCs and CD8+ T cells, representing the main cell type activated by cDC1s. Taken together, these findings support a unique role of cDC1s in PAH pathogenesis, independent of general immune activation or a mutation in the *Bmpr2* gene.

## Expanding the horizon for PH-drug therapy: novel biomarkers and therapeutic targets in PAH and CTEPH

In PAH and CTEPH patients, increased levels of inflammatory cytokines and chemokines were observed in previous studies. However, limited data are available on the levels of cytokines or chemokines in treatment-naïve patients, particularly in CTEPH. Furthermore, little is known about possible changes in cytokine and chemokine levels during follow-up or on the correlation of inflammatory marker signatures with prognosis. Therefore, our aim in **chapter 4** was to study circulating inflammatory markers in PAH and CTEPH patients at diagnosis and at 1-year follow-up in relation to clinical outcome parameters. In **chapter 4**, we found significantly increased plasma levels of various cytokines in three PAH subgroups and CTEPH patients. Particularly when inflammatory mediators were combined with clinical parameters, unbiased clustering and multivariate analyses clustered PAH and CTEPH patients into WHO classification-independent subgroups that correlated with patient survival.

## T-cells in PAH and CTEPH; executors of autoimmunity or damage-controllers?

In CTEPH patients, previous studies have shown increased presence of T cells and chemokines in surgical pulmonary endarterectomy (PEA) material. Currently, there is limited data present on the determination and classification of these T cells. Moreover, few data on T-cell activation, cytokine production and Th-subset division are available in treatment-naïve CTEPH patients. Therefore, in **chapter 5**, our aim was to more closely investigate T cell activation, cytokine production and Th-subset

division in CTEPH patients at diagnosis and after 1-year of follow up. In our studies, we found increased numbers of CCR6<sup>+</sup> CD4<sup>+</sup> T-cells in CTEPH patients at diagnosis in the peripheral blood compartment when compared to healthy controls. Furthermore, we demonstrated a significantly reduced production capacity of several inflammatory cytokines and we found that CD4<sup>+</sup> and CD8<sup>+</sup> T cells showed increased expression of the immune checkpoint protein cytotoxic T-lymphocyte-associated protein 4 (CTLA4), a negative regulator of T cell activation. Multivariate analysis separated CTEPH patients from HCs, based on CCR6 and CTLA4 expression. At 1-year follow-up, proportions of CCR6<sup>+</sup>CD4<sup>+</sup> T cells were further increased, and the IFN $\gamma$  and IL-17 production capacity of CD4<sup>+</sup> T cells was restored. Interestingly, we were also able to demonstrate the increased presence of CCR6<sup>+</sup> T-cells in vascular lesions in pulmonary endarterectomy material from CTEPH patients. Taken together, these findings point to a role of Th17 cells, which are known to be also involved in autoimmune diseases such as sarcoidosis, and therefore suggest an autoimmune component in CTEPH.

In PAH patients, numbers of CD4<sup>+</sup> T cells (especially Tregs) and CD8<sup>+</sup> T cells were found to be altered. However, in depth classification and phenotypical characterization of these T cells are still lacking, particularly in treatment-naïve patients. Therefore, in **chapter 6**, our aim was to more closely investigate T-cell activation, cytokine production and Th-subset distribution in PAH patients at diagnosis and after 1-year of PAH-specific treatment. We observed that at diagnosis, T cells of IPAH patients were less capable of producing the cytokines TNF $\alpha$ , IFN $\gamma$ , IL-4 and IL-17 compared to HCs, while the T cell cytokine-capacity of CTD-PAH patients did not differ from HCs. The reduced IL-4 production by CD4<sup>+</sup> T cells in IPAH patients was accompanied by a decrease in Th2 cells. T cells of both PAH subgroups had a high CTLA4 expression which was only accompanied in CTD-PAH patients by increased inducible T-cell costimulatory (ICOS) expression, a marker for T cell activation. multivariate analysis indicated a specific T cell cytokine profile that separates IPAH patients from HCs. Remarkably such a profile was not found for CTD-PAH. At 1-year follow-up IL-17 production by memory CD4<sup>+</sup> T cells was increased in IPAH patients, accompanied by an increase in proportion of Th17/Tc17 cells. This increase in Th17/Tc17 cells was also seen in CTD-PAH patients. After 1-year follow-up only the T cell fractions of IPAH patients had decreased CTLA4 expression. Multivariate analysis for T cell profile at diagnosis and 1-year follow-up separated IPAH patients at diagnosis from IPAH patients at 1-year follow-up. This was not the case for CTD-PAH. These findings point to involvement of adaptive immune responses in IPAH, which may have implication for development of therapeutic interventions.

## **Outpatient rehabilitation therapy: towards individual tailor-made rehabilitation therapy in PAH and CTEPH**

A common clinical feature of PAH patients is deterioration of physical condition and diminished quality of life, which obviously needs improvement. Accumulating evidence is showing beneficial effects of pulmonary rehabilitation (PR) therapy. In current literature, most studies have been performed in an entirely clinical setting. Knowledge about safety and efficacy of a PR program in an exclusively outpatient setting is still lacking. Furthermore, little is known about soluble biomarkers levels and possible changes herein during PR therapy. Our aim in **chapter 7** was to design and study an achievable multidisciplinary outpatient PR program and to evaluate soluble biomarker levels during PR therapy. In this chapter, we demonstrated that a 10-week multidisciplinary pulmonary rehabilitation programme has considerable beneficial effects on functional capacity, functional endurance, skeletal muscle function and health related QoL.

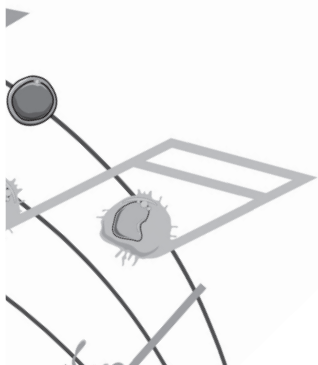
Finally, the findings in this thesis are integrated into a general discussion in **chapter 8**. Taken together, in our studies, we found additional evidence for DC involvement in PH etiology, and alterations in T cell subsets for CTEPH and PAH patients. Future studies are needed to further determine the specific roles of various immune cells in PH development and to integrate these roles into pathogenesis models that also include many non-immune factors. While many promising immunomodulatory drug treatment trials are underway, this thesis has given novel understanding of DC and T-cell mediated immunity in pulmonary hypertension, potentially leading to new future therapeutic strategies. To further unravel the immunological etiology of PH development, potent rodent models for immune-mediated PH are required for pre-clinical research. This thesis has provided new insights in possibilities for immune-driven PH rodent models, without requirement for an additional trigger. Furthermore, we demonstrated prognosis predicting value for inflammatory cytokine assessment in PAH and CTEPH patients. In combination with other important circulating cytokine assessments in PAH and CTEPH, this study could pave the way for integration of immune status assessment in the determination of disease severity, prognosis and therapeutic evaluation in current clinical care. Lastly, we showed significant beneficial effects for a completely outpatient pulmonary rehabilitation program. Potentially, the findings in this thesis might lead to more accessible forms of PR for patients who are struggling to combine rehabilitation therapy with their daily life activities.

Thus, PH is a complex devastating disease with a dangerous imbalance in the immune system in a subgroup of patients. However, PH is most likely a multi-factorial disease, including pathological involvement of other non-immune factors such as vascular and endothelial growth factors. Ideally, immune factors from previous research and from this thesis, should be integrated with these non-immune factors, to achieve an intricate holistic view of the multi-factorial pathogenesis in PH. Hopefully, this will lead to novel potential immunomodulatory strategies and improved identification of different immune-driven subgroups of PH.



# NEDERLANDSE SAMENVATTING

# S



**Pulmonale hypertensie (PH)** is een zeldzame, zeer ernstige ziekte die gekenmerkt wordt door een abnormaal hoge bloeddruk in de longen. Deze hoge druk heeft gevolgen voor de werking van het hart. De rechterkant van het hart (de rechterkamer) moet harder werken om het bloed tegen de hoge druk door de longen te pompen. In eerste instantie past de rechterkamer zich aan doordat het een dikker dikkere spierwand ontwikkelt (hypertrofie). Wanneer dit langer duurt wordt de hartkamer groter (dilatatie). Op den duur kan de rechterkamer echter niet meer tegen de verhoogde drukken “oppompen” en ontstaat er hartfalen. De klachten waarmee patiënten zich bij de huisarts presenteren zijn vaak aspecifiek en lijken op andere longziekten- en hartziekten. Hierdoor ontstaat vaak vertraging in het diagnosticeren van de aandoening. Bij vermoeden van de diagnose PH wordt eerst een echocardiogram van het hart gemaakt. De uiteindelijke diagnose moet worden bevestigd door middel van een rechterhart catheterisatie. Bij dit onderzoek worden de drukken in de longslagader gemeten. Als deze druk boven de 20 mmHg is, spreekt men van PH.

PH wordt vaak veroorzaakt door andere onderliggende aandoeningen, zoals een doorgemaakt hartinfarct of longembolieën. Hierbij maken we onderscheid tussen vijf subgroepen van PH, ingedeeld op basis van de onderliggende oorzaak; (1) pulmonale arteriële hypertensie (PAH), (2) PH door hartziekten, (3) PH door longziekten, (4) chronische trombo-embolische PH (CTEPH; door chronische longembolieën) en (5) PH met een onduidelijke of multifactoriële oorzaak. Pulmonale arteriële hypertensie (groep 1 PH) kenmerkt zich door proliferatie van de endotheelcellen, die de binnenste bekleding van de bloedvaten vormen, waarbij ook nieuwvorming van bloedvaten (neoangiogenesis) ontstaat. Uiteindelijk ontstaan door dit proces zogeheten plexiforme laesies in de longen, die zich kenmerken door een dynamisch netwerk van endotheelcellen, immuuncellen en vasculaire netwerken. Dergelijke plexiforme laesies, die veel immuuncellen bevatten, worden specifiek gevonden in een subgroep van PAH; de idiopathische PAH (waarbij geen duidelijke oorzaak voor de PH te vinden is).

In de longen van IPAH en CTEPH patiënten is er een specifieke toename en activatie te zien van immuuncellen van het aangeboren immuunsysteem, zoals macrofagen, mestcellen en neutrofiële granulocyten. In IPAH longen wordt ook een toename van dendritische cellen (DCs) gezien. Dit zijn belangrijke antigeen presenterende cellen (APCs), die fungeren als een brug tussen het aangeboren en het adaptieve immuunsysteem. Ze kunnen antigenen opnemen en presenteren aan T-cellen, een witte bloedcel van het adaptieve immuunsysteem. DCs kunnen bijdragen aan een afweerreactie door de productie van ontstekingsbevorderende cytokines en chemokines, die ervoor zorgen dat andere immuuncellen zich verplaatsen naar de plek van ontsteking. DCs zijn hiermee enorm belangrijk voor de balans tussen ofwel ontsteking (immuunreactie) tegen een bepaald agens, of tolerantie (geen immuunreactie). Dit proces speelt zich continu af in het menselijk lichaam, waarbij een verstoring van de balans tussen tolerantie en immuniteit kan leiden tot auto-immuniteit, een conditie waarbij een (onnodige) immuunreactie optreedt tegen lichaamseigen materiaal. Bij pulmonale hypertensie is in de afgelopen decennia toenemend bewijs gevonden voor een rol van immuunsysteem bij het ontstaan en onderhouden van pulmonale hypertensie. Zo zijn er auto-antilichamen gevonden bij IPAH patiënten, die specifiek zijn gericht tegen endotheelcellen van de longbloedvaten. Tevens zijn er verhoogde cytokines gevonden in het bloed van IPAH patiënten, waarbij de hoeveelheid van deze cytokines correleert met een slechtere prognose van deze patiënten. Bij CTEPH zijn ook in toenemende mate bewijzen gevonden voor een actieve rol van het immuunsysteem in het ontstaan en het onderhouden van de aandoening. Bij CTEPH wordt gekeken of patiënten in aanmerking komen voor een pulmonale endarterectomie (PEA), een operatie waarbij de chronische longembolieën met een operatie kunnen worden verwijderd. In dit PEA-materiaal zijn een verhoogd aantal immuuncellen gevonden, met daarbij ook toename van cytokines en chemokines.

Ondanks deze aanwijzingen voor een actieve rol van het immuunsysteem in PAH en CTEPH, is er nog veel onduidelijk over de specifieke mechanismen hierachter. Nieuwe inzichten hierin zijn hard nodig, gezien PH een ongeneeslijke ziekte is. De 5-jaars overleving van patiënten met PAH en inoperabel CTEPH is respectievelijk ~58% en 53-69%.

Daarom zijn de doelen van dit proefschrift de volgende; **(I)** het verder ontrafelen van de rol van het immuunsysteem in de pathogenese (ziekteontwikkeling) van PAH en CTEPH, **(II)** het opsporen van biomarkers om beter in staat te zijn de prognose van patiënten te voorspellen, **(III)** Het identificeren van nieuwe therapeutische aangrijpingspunten voor de behandeling van PAH en CTEPH, en **(III)** het optimaliseren van niet-medicamenteuze behandelopties voor PAH en CTEPH patiënten.

### **Ontrafelen van de immunologische onbalans in PAH en CTEPH pathogenese.**

In **hoofdstuk 1** wordt een overzicht gegeven van het toenemende bewijs voor een kritische betrokkenheid van het immuunsysteem in de pathogenese van PAH en CTEPH, leidend tot een verminderde overleving en een hoge ziektelast. Desalniettemin blijven er veel vragen onbeantwoord over welke immuuncellen dit proces op welke manier beïnvloeden.

Eerdere studies hebben laten zien dat conventionele DCs (cDCs), een subtype van DCs, verhoogd aanwezig zijn in de longen van IPAH patiënten. Ons doel in **hoofdstuk 2** was om te onderzoeken of ongeremde activiteit van cDCs leidt tot het ontwikkelen van PH in een muismodel. Hiervoor hebben we het *Tnfaip3*<sup>DNGRI-KO</sup> muismodel gebruikt, waarin de activiteit-remmende factor A20/Tnfaip3 specifiek uitgeschakeld is in DCs, hetgeen leidt tot ongeremde activiteit van deze DCs. We hebben aangetoond dat deze muizen PH ontwikkelden, hetgeen werd gekenmerkt door verhoogde druk in het de rechterkamer, met daarbij rechterkamer hypertrofie. Tevens zagen we accumulatie van immuuncellen in de longen van deze muizen en remodelering van de bloedvaten in de longen. Hiernaast werd ook een verhoogde aanwezigheid van cytokines (IL-1B, IL-6 en IL-10) gevonden in de longen van *Tnfaip3*<sup>DNGRI-KO</sup> muizen. Opvallend hierbij is dat na behandeling met anti-IL-6, het PH beeld geheel normaliseerde. Deze bevindingen tonen aan dat bij ongeremde activiteit van DCs een beeld van immunologisch gedreven PH ontstaat, welke afhankelijk lijkt van IL-6 signalering.

Het exacte mechanisme waardoor het PH fenotype ontstaan in *Tnfaip3*<sup>DNGRI-KO</sup> muizen en het belang van de veranderde immunologische balans in DCs en andere immuuncellen is grotendeels onbekend. In **hoofdstuk 3**, hebben we het immunologische landschap in het hart van de *Tnfaip3*<sup>DNGRI-KO</sup> muis verder onderzocht. Hierin zagen we een toename van verschillende immuuncellen, waaronder DCs, met name in de rechterkamer. We hebben ook kunnen aantonen dat het toevoegen van een extra immunologische stimulans door TLR-liganden niet leidt tot een verergering van de PH. Daarnaast hebben we ook gekeken of het toevoegen van een vasculaire trigger, zoals we die kennen bij een *Bmpr2* gen mutatie, effect heeft op de pathogenese van PH. Voor dit doeleinde hebben we door middel van kruisingen *Tnfaip3*<sup>DNGRI-KO</sup> muizen verkregen met een genetische mutatie in het *Bmpr2* gen. In deze muizen zagen we dat het immunologische PH fenotype met name gedreven werd door het *Tnfaip3*<sup>DNGRI-KO</sup> genotype, waarbij geen toegevoegd nadelig effect gezien werd van de *Bmpr2* mutatie. Als laatste hebben we ook de relevantie van deze resultaten in de humane situatie onderzocht. In longen van IPAH patiënten bleken veel DCs aanwezig, vaak dichtbij CD8 T-cellen (celtype wat met name door cDC1s wordt geactiveerd).

Samengevat laten deze resultaten een unieke en kritieke rol zien voor cDC1s in de pathogenese van PAH, onafhankelijk van vasculaire factoren zoals een *Bmpr2* mutatie.

## **Uitbreiden van de horizon van PH-medicamenteuze therapie: nieuwe biomarkers en doelen voor behandeling in PAH en CTEPH.**

In PAH en CTEPH patiënten is in eerdere studies tijdens de behandeling met PH medicatie een verhoogde aanwezigheid van inflammatoire cytokines en chemokines gevonden. Er de gegevens zijn beperkt en veel vragen onbeantwoord. Bijvoorbeeld: zijn deze inflammatoire cytokines en chemokines al aanwezig aan het begin van de ziekte in patiënten die nog geen specifieke PAH therapie hebben gehad? Correleren de spiegels van deze cytokines en chemokines met de prognose van PAH patiënten? Daarom hebben we in **hoofdstuk 4** in het PAH en CTEPH patiënten cohort in het Erasmus MC gekeken naar inflammatoire cytokines en chemokines bij het stellen van de diagnose (baseline) en na één jaar therapie. Hierbij hebben we significant verhoogde aanwezigheid gevonden van verschillende cytokines in PAH en CTEPH patiënten bij diagnose, waarbij één specifiek chemokine (CXCR9) een voorspellende correlatie liet zien met de overleving van CTEPH patiënten. Interessant genoeg vonden we dat het toevoegen van de spiegels van deze cytokines en chemokines aan de klinische parameters in een ongesuperviseerde clustering analyse, leidde tot een betere voorspellende waarde voor prognose in PAH.

Samengevat vonden we aanwijzingen dat bij het moment van diagnose, voorafgaand aan PH-specifieke therapie, al een verhoging van inflammatoire cytokines aanwezig is. Gezien ook de correlatie met overleving van PH patiënten, kan dit betekenen dat er een actieve rol is van immuuncellen in de inductie van het ziekteproces in PH.

## **T-cellen in PAH en CTEPH; executeurs van auto-immuniteit of schadebeperkers?**

In CTEPH patiënten is in eerder onderzoek een verhoogd aantal T-cellen en chemokines gevonden in PEA materiaal. Tot op heden zijn er echter maar beperkte data beschikbaar over de determinatie en classificatie van deze T-cellen. Verder is er ook weinig bekend over de mate van activatie en cytokine productie van een subgroep van T-cellen, de T helper (Th) cellen. In **hoofdstuk 5** hebben we in het eerder beschreven CTEPH cohort gekeken op het moment van stellen van de diagnose en na 1 jaar follow up naar de T-cel activatie en sub classificatie. Hierin hebben we gevonden dat er een verhoogd aantal CCR6+ T-cellen aanwezig is in CTEPH patiënten in het bloed. Dit kan betekenen dat er betrokkenheid is van Th17 cellen, welke bekend staan om hun actieve rol in de inductie en het onderhouden van auto-immuniteit. Verder hebben we gevonden dat de T-cellen in het bloed een verminderde cytokine productie laten zien en dat er verhoogde expressie is van CTLA4, een remmende factor voor activiteit in T-cellen. Een verklaring voor deze verlaagde activiteit kan zijn dat deze T-cellen uitgeput zijn, of dat de actieve T-cellen niet in het bloed zitten, maar juist in de longen op de plek van het probleem. Op basis van een multivariate analyse hebben we gevonden dat de CTEPH patiënten significant te onderscheiden waren van gezonde controles, op basis van de CCR6 en CTLA4 expressie. Na 1 jaar follow up zagen we een verdere toename van deze CCR6+ T-cellen, en zagen we herstel van cytokine (IFN $\gamma$  en IL-17) productie in CD4+ T-cellen. Op histologisch niveau was deze toename van CCR6+ T-cellen ook te zien in PEA materiaal van CTEPH patiënten.

De resultaten in dit hoofdstuk vormen aanwijzingen voor een actieve rol van Th17 cellen in CTEPH patiënten, die we kennen van het induceren en onderhouden van auto-immuunziekten zoals reumatoïde artritis en van sarcoïdose.

In PAH patiënten werd eerder al aangetoond dat er een verhoogd aantal CD4+ en CD8+ T-cellen aanwezig is in het perifere bloed. Ook bij deze patiënten is het tot op heden nog onduidelijk of er veranderingen zijn in de activatie, cytokine productie en (sub)classificatie van de T-cellen. In **hoofdstuk 6** hebben we gevonden dat, net als bij CTEPH, de T-cellen in het bloed verminderd in staat zijn tot de productie van inflammatoire cytokines in alle subgroepen, behalve bij connective tissue disease (CTD-PAH (PAH door een bindweefselziekte)). De gevonden verminderde productie van IL-4 bij CD4+ T-cellen ging samen met een vermindering in T helper 2 (Th2) cellen. Net als bij CTEPH patiënten, werd bij PAH patiënten een verhoogde expressie van CTLA4 gevonden in het bloed, welke na een jaar opvolging juist verlaagd was. Bij CTD-PAH patiënten ging de verhoogde CTLA4 expressie gepaard met verhoogde ICOS expressie, een marker voor T-cel activatie. In een multivariate analyse werd een significant onderscheid gevonden tussen cytokines in IPAH patiënten en gezonde personen. Dit laat zien dat er bij IPAH patiënten een uniek cytokine profiel is, dat afwijkend is van dat van gezonde controles. In IPAH en CTD-PAH patiënten werd een verhoogde aantal Th17/Th17 cellen gevonden. Verder werd in een multivariate analyse na 1 jaar follow up een significant veranderd immunologisch profiel gevonden tussen IPAH patiënten bij diagnose en na 1 jaar follow up. Samengenomen geven deze resultaten een sterke aanwijzing voor een belangrijke rol voor het adaptieve immuunsysteem in IPAH. Dit kan implicaties hebben voor therapeutische mogelijkheden in de toekomst.

### **Poliklinische revalidatie therapie; toewerken naar individuele patiënt-specifieke therapie in PAH en CTEPH.**

Een veelvoorkomend klinisch kenmerk van PH is verslechtering van de fysieke conditie en een verminderde kwaliteit van leven. Toenemend bewijs laat zien dat er gunstige effecten zijn van longrevalidatie (PR) therapie. Vaak zijn deze studies echter alleen uitgevoerd met patiënten die hiervoor werden opgenomen in een ziekenhuis of revalidatie kliniek, dus in een niet-poliklinische setting. Er is een grote groep PH patiënten die veel klachten ervaart, waarbij PR een goede uitkomst tot verbetering zou kunnen bieden. Inderdaad zien we in **hoofdstuk 7** dat wanneer PAH en CTEPH patiënten deelnemen aan een multidisciplinaire PR in een volledig poliklinische setting, er significante verbetering ontstaat in spierkracht, conditioneel uithoudingsvermogen en kwaliteit van leven. Bij verdere analyse vonden we geen verschillen in klinische en inflammatoire biomarkers tussen begin en einde van de PR bij de verschillende patiënten. Deze resultaten tonen aan dat poliklinische PH patiënten op een veilig manier zouden kunnen deelnemen aan PR met gunstige effecten. De effecten op de langere termijn moeten nog verder onderzocht worden.

Tenslotte zijn al de resultaten van de bovengenoemde hoofdstukken samengevoegd in een algemene discussie in **hoofdstuk 8**. Samengevat hebben we in onze studies gevonden dat er structureel bewijs is voor DC betrokkenheid bij PH pathogenese, met daarbij ook veranderingen in T-cellen bij PAH en CTEPH patiënten.

Verdere studies zijn nodig om te bepalen wat de specifieke rol is van de verschillende immunocellen in het ontstaan en onderhouden van PH, waarbij ook de invloed van non-immuun factoren zal moeten worden geïntegreerd. Er zijn verscheidene veelbelovende klinische trials met nieuwe therapieën onderweg. Daarnaast heeft dit proefschrift nieuwe inzichten gegeven over de rol en interactie van DCs en T cellen in PH, mogelijk leidend tot weer nieuwe therapeutische mogelijkheden. Potente immunologische PH muis/rat modellen zijn nodig om dit preklinische onderzoek verder op weg te helpen. In dit proefschrift

zijn nieuwe inzichten gevonden voor mogelijkheden voor inflammatie gedreven PH muismodellen, zonder de noodzaak voor een aanvullende trigger.

Verder hebben we prognose voorspellende inflammatoire cytokines gevonden in het bloed van PAH en CTEPH patiënten. Deze studie kan bijdragen aan het integreren van immunologische data in de klinische work-up van PH patiënten. Als laatste hebben we aangetoond dat een volledig poliklinisch longrevalidatie veilig is, met verbetering van spierkracht, conditie en kwaliteit van leven bij PAH en CTEPH patiënten.

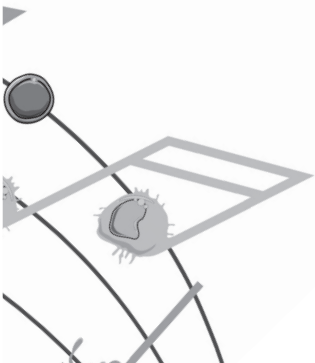
Concluderend, PH is een complexe en vernietigende ziekte met een gevaarlijke onbalans in het immuunsysteem in een subgroep van PH patiënten. PH is waarschijnlijk multifactorieel, met pathologische invloeden van zowel non-immunogene factoren (zoals genetische predispositie en omgevingsfactoren) als immunogene factoren. Idealiter zouden integratie van deze factoren kunnen bijdragen aan een holistische benadering van de multifactoriële pathogenese van PH. Dit zal dan resulteren in nieuwe potente immunomodulatoire therapeutische strategieën en verbeterende en vervroegde herkenning van immuun-gedreven PH.





# LIST OF PUBLICATIONS

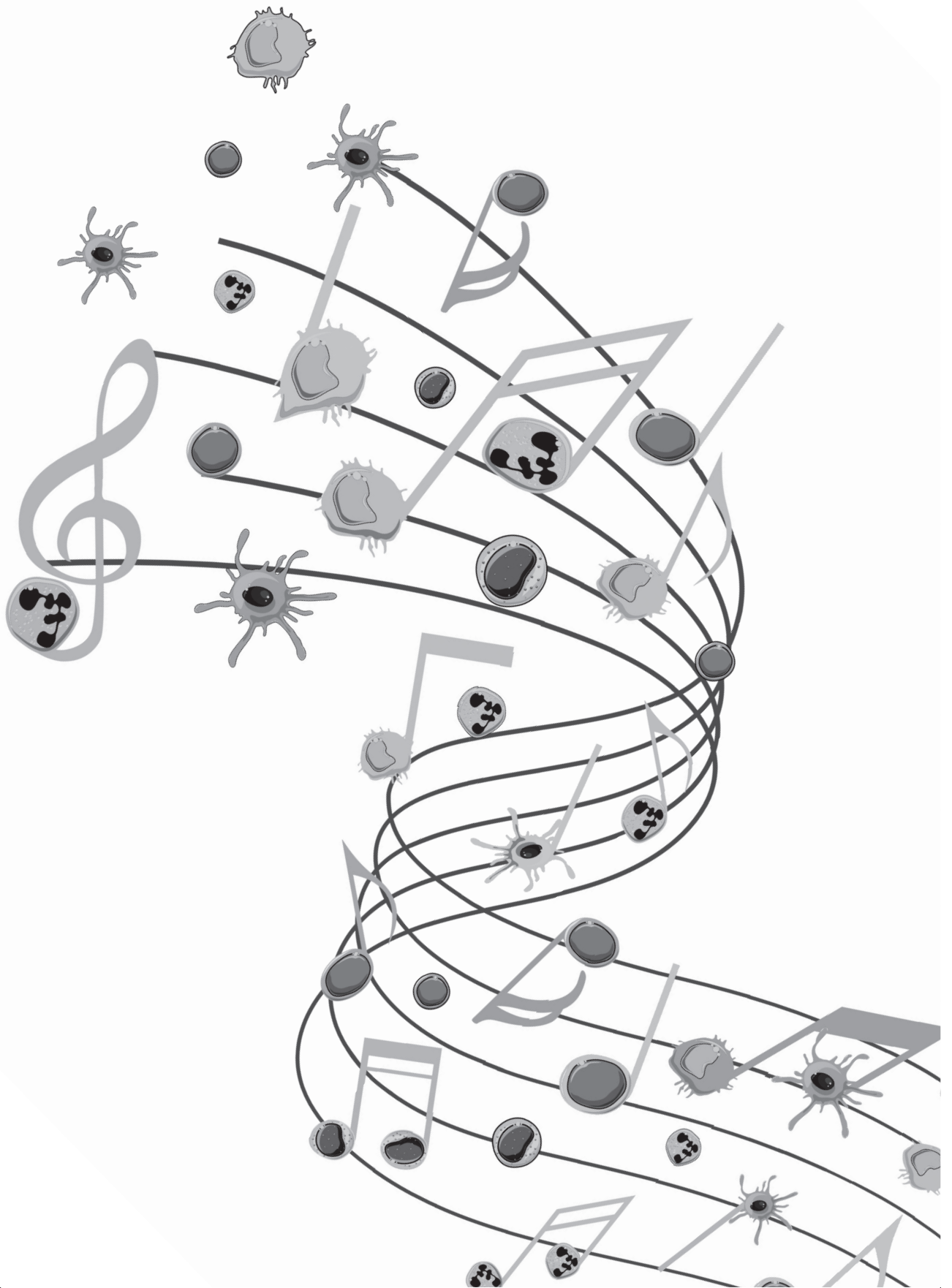
L



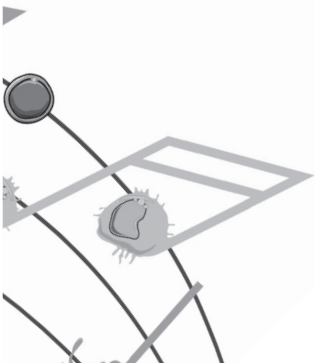
## LIST OF PUBLICATIONS:

1. L.W. Geenen\*, V.J.M. Baggen\*, **T. Koudstaal**, K.A. Boomars, J.A. Eindhoven, E. Boersma, J.W. Roos-Hesselink, A.E. van den Bosch  
*Diagnosis-specific biomarker profiles and the association with clinical outcomes in patients with pulmonary hypertension.*  
\*Contributed equally. **Am Heart J.** 2019 Feb; 208:91-99.
2. T. Das, I.M. Bergen, **T. Koudstaal**, J.A.C. van Hulst, G. van Loo, A. Boonstra, T. Vanwollegem, P.S.C. Leung, M.E. Gershwin, R.W. Hendriks, M. Kool  
*Clec9a-mediated deletion of A20/Tnfrsf3 in dendritic cells alters T and B-cell homeostasis promoting autoimmune liver pathology.* J Autoimmun. 2019 Aug; 102:167-178.
3. L.W. Geenen, V.J.M. Baggen, R.M. Kauling, **T. Koudstaal**, K.A. Boomars, E. Boersma, J.W. Roos-Hesselink, A.E. van den Bosch.  
*Growth Differentiation Factor-15 as candidate predictor for mortality in adults with pulmonary hypertension.* Heart. 2019 Sep 6. pii: heartjnl-2019-315111.
4. L.W. Geenen, V.J.M. Baggen, R.M. Kauling, **T. Koudstaal**, K.A. Boomars, E. Boersma, J.W. Roos-Hesselink, A.E. van den Bosch.  
*The prognostic value of soluble ST2 in adults with pulmonary hypertension.* J Clin Med. 2019 Sep 20;8(10).
5. **T. Koudstaal\***, M. Wapenaar\*, D. van Ranst, R. Beesems, L. van den Toorn, A.E. van den Bosch, P.P. Chandoesing, K.A. Boomars  
*The effects of a 10-week outpatient pulmonary rehabilitation programme on exercise performance, muscle strength, soluble biomarkers and quality of life in patients with pulmonary hypertension.*  
\*Contributed equally. **J Cardiopulm Rehabil Prev.** 2019 Oct 4.
6. **T. Koudstaal**, K.A. Boomars\*, M. Kool\*  
*Pulmonary Arterial Hypertension and Chronic Thromboembolic Pulmonary Hypertension: an immunological perspective.*  
\*Contributed equally. **J Clin Med.** 2020 Feb 19;9(2).
7. **T. Koudstaal**, J.A.C. van Hulst, T. Das, S. Neys, D. Merkus, M.A. de Raaf, I.M. Bergen, H.J. Bogaard, L. Boon, G. van Loo, J.G.J.V. Aerts, K.A. Boomars, M. Kool\*, R.W. Hendriks\*  
*DNGR1-Cre-mediated Deletion of Tnfrsf3/A20 in Conventional Dendritic Cells Induces Pulmonary Hypertension in Mice.* **Am J Respir Cell Mol Biol** 2020 Nov; 63(5):665-680.
8. D. van Uden, **T. Koudstaal**, J.A.C. van Hulst, I.M. Bergen, C. Gootjes, B. Morrel, M. Toshner, J. von der Thusen, T. van den Bosch, M. Ghigna, F. Perros, D. Montani, M. Kool, K.A. Boomars\*, R.W. Hendriks\*  
*Central role of dendritic cells in human and murine pulmonary arterial hypertension.*  
\*Contributed equally. **Int. J. Mol. Sci.** 2021, 22(4), 1756.

9. **T. Koudstaal**, J.A.C. van Hulst, P. Heukels, I.M. Bergen, L.W. Geenen, V.J.M. Baggen, A.E. van den Bosch, L.M. van den Toorn, P.P. Chandoesing, M. Kool, E. Boersma, R.W. Hendriks, K.A. Boomars  
*Plasma markers in pulmonary hypertension subgroups correlate with patient survival.* **Respir Res.** **2021 May 4;22(1):137.**
10. P. Vinke, **T. Koudstaal**, A.E. van den Bosch, F. Muskens, M. Balvers, M. Poland, K. van Norren, K.A. Boomars.  
*Micronutrient deficiencies in idiopathic pulmonary arterial hypertension and chronic thromboembolic pulmonary hypertension.*  
Nutrients. **2021 Nov 1;13(11):3923.**
11. D. van Uden, **T. Koudstaal**, J.A.C. van Hulst, T.P.P. van den Bosch, M. Vink, I.M. Bergen, K. Lila, A.E. van den Bosch, P. Bresser, M. Kool, J.H. von der Thüsen, R.W. Hendriks\*, K.A. Boomars\*  
*Evidence for a role of CCR6<sup>+</sup> T cell in chronic thromboembolic pulmonary hypertension patients.*  
\*Contributed equally. **Front Immunol 2022 Apr 27;13:861450**
12. D. van Uden, **T. Koudstaal**, J.A.C. van Hulst, M. Vink, M. van Nimwegen, L.M. van den Toorn, P.P. Chandoesing, A.E. van den Bosch, M. Kool, R.W. Hendriks\*, K.A. Boomars\*  
*Peripheral blood T-cells of patients with IPAH have a reduced cytokine-producing capacity.*  
\*Contributed equally. **Int. J. Mol. Sci. 2022, 23(12), 6508.**
13. Z. Cai, S. Tian, T Klein, L Tu, L. Geenen, **T. Koudstaal**, A. van den Bosch, Y. de Rijke, I. Reis, E. Boersma, C. van der Ley, M. van Faassen, I. Kema, D. Duncker, K. Boomars, K. Tran-Lundmark, C. Guignabert, D. Merkus  
*Kynurenine metabolites predict survival in pulmonary arterial hypertension: a role for IL-6/IL-6a*  
**Accepted for publication in Scientific Reports.**



# ACKNOWLEDGEMENTS



## DANKWOORD

Het mooie moment is aangebroken: mijn proefschrift is klaar! Het is een cliché maar daarom niet minder waar; wetenschappelijk onderzoek is alleen optimaal uit te oefenen met goede samenwerking in een fijn team. Er zijn heel veel mensen die ik heel graag wil bedanken voor de deelname, steun, samenwerking en de inspiratie.

### Het begeleidingsteam & paranimfen.

**Prof. Dr. R.W. Hendriks:** Beste Rudi, vanaf mijn eerste momenten op het lab longziekten heb ik mij zeer welkom gevoeld en is er altijd ruimte geweest om te groeien in het wetenschappelijk onderzoek. Bij elke data meeting (van kleine tot grote meetings) weet je altijd met prikkelende vragen en scherpe observaties het onderzoek tot een hoger niveau te tillen. Je hebt mij geleerd om scherp en kritisch vanuit goed gefundeerde onderzoeksvragen te denken in het wetenschappelijk onderzoek. Met je humor en aanstekelijke passie voor wetenschappelijk onderzoek heb je gezorgd dat ik altijd met een kritische blik maar met name veel plezier aan mijn promotie onderzoek heb kunnen werken.

**Dr. K.A. Boomars:** Beste Karin, ik zal nooit vergeten hoe ons zeer prettige contact is begonnen. Ik was in 2015 als medisch student enigszins verwaald aan het rondlopen in het oude SVLO longziekten gebouw, op zoek naar Dr. Karin Boomars, met wie ik een afspraak had om het over een oudste coschap longziekten te hebben. Bij onze eerste ontmoeting was het gelijk duidelijk, we delen een passie voor de combinatie van dokter zijn in combinatie met wetenschappelijk onderzoek. Jij hebt me geïntroduceerd in de wondere wereld van pulmonale hypertensie en ik bewonder je gedrevenheid hierin enorm. Niet alleen ga je door het vuur voor je patiënten, maar ook in het wetenschappelijk onderzoek heb je een zeer grote rol gespeeld in (pre-)klinische studies. Je aanstekelijke enthousiasme heeft ervoor gezorgd dat we in voor- en tegenspoed mooie publicaties hebben weten te produceren. Heel veel dank dat je altijd voor mij klaarstond voor overleg, advies en bovenal ook gezelligheid en goede gesprekken tijdens alle congressen die we samen hebben bezocht. Met name het PVRI congres in Lima, Peru zal ik nooit vergeten; Toen we daar samen zaten op de spoedeisende hulp met jou als (vloeiend) Spaans sprekende tolk, aangezien ik na een val van een paard een L3 fractuur had opgelopen..!

**Prof. Dr. J.G.J.V. Aerts:** Beste Joachim, vanaf ons eerste gesprek in jouw nieuwe rol als afdelingshoofd van de longziekten heb je er altijd voor gezorgd dat ik zowel op klinisch als wetenschappelijk vlak heb kunnen groeien. Ik wil je graag hartelijk danken voor je hulp bij het mogelijk maken van het combineren van mijn klinische werkzaamheden als AIOS in combinatie met het wetenschappelijk onderzoek.

**Prof. Dr. C. Guignabert,** merci beaucoup d'avoir accepté de faire partie de mon jury de thèse. Votre éditorial sur notre manuscrit à propos des souris à cellules dendritiques était un plaisir à lire!

**Prof. Dr. I.K.M. Reiss, Dr. B. Bartelds, Prof. Dr. H-J. Bogaard, Prof. Dr. B.N.M. Lambrecht, Prof. Dr. D. Merkus:** Hartelijk dank voor het plaatsnemen in de kleine en grote commissie en het kritisch doornemen van dit proefschrift.

**Dr. M. Kool,** beste Mirjam, inmiddels heb je een nieuwe weg ingeslagen maar in de eerste helft van mijn promotietraject was jij mijn copromotor vanaf het eerste uur. Ik wil je graag hartelijk bedanken

voor alle begeleiding en lessen binnen het onderzoek die je me hebt geleerd en voor het introduceren in de wondere wereld van de dendritische cellen. Onze brainstorm sessies over de dendritische cel muizen en een weg vinden door een moeras van flow cytometrie plotjes heb ik enorm gewaardeerd. Heel veel succes met je nieuwe baan en de allerbeste wensen.

Beste **Jennifer**, met veel weemoed denk ik terug aan mijn eerste maand als arts-onderzoeker, waarin we samen gelijk aan de slag gingen met een hele grote proef van het dendritische cel PH project. Zoals altijd was jij tot in de puntjes voorbereid en hebben we door samen te knallen daar gelijk een mooi succes van gemaakt. Ook hier is het cliché van een arts met twee linkerhanden op het lab weer van toepassing, waarbij jij met je humor, je didactische uitleg en begeleiding ervoor gezorgd hebt dat ik geen (niet te veel) stress heb ervaren tijdens de proeven. Inmiddels heb je naast je werkzaamheden op het lab ook samen met Robert een prachtig gezin met 3 zoons en vind ik het enorm bewonderingswaardig hoe je dat zo goed weet te combineren allemaal, altijd met een glimlach en altijd met optimisme. Ik wil je hartelijk bedanken dat jij mijn paranimf bent, en voor de drijvende kracht die jij bent geweest voor het technische werk achter dit proefschrift maar ook voor de gezellige koffietjes die we gedaan hebben met goede gesprekken over het onderzoek maar vooral ook vaak niet over werk. Dankzij jouw nuchterheid, je humor, je perfecte voorbereiding en technische expertise heb je er altijd voor gezorgd dat ik met enorm veel plezier samen met jou aan onze onderzoeksprojecten heb gewerkt.

**Dr. M. Baas (Sinds kort Dr. i.p.v. Drs.!),** Beste Martijn, recent ben jij met vlag en wimpel gepromoveerd binnen de plastische chirurgie, waarvan ik de grote eer had om jouw paranimf te mogen zijn. Ik vind het dan ook fantastisch dat de rollen inmiddels zijn omgedraaid en ik wil je hartelijk danken dat je mijn paranimf bent. Ik vind het bewonderingswaardig en aanstekelijk om te zien hoe gedreven jij bent binnen je opleiding als plastisch chirurg en je eerdere promotieonderzoek. Dit ook in combinatie met de gezelligheid buiten het ziekenhuis, waarbij we altijd kunnen sparren met elkaar over vervolgstappen, maar ook over onze gedeelde passie van goed eten en drinken. Ik kijk uit naar onze toekomstige afspraken binnen en buiten het ziekenhuis!

## Het lab longziekten

Met heel veel plezier heb ik meerdere jaren op het lab longziekten mogen doorbrengen, waarbij ik altijd met veel plezier heb samengewerkt (of gewoon gezellig koffie gedronken) met PhD-studenten, laboranten en postdocs. In het begin was ik welkom op de PhD kamer met **Tridib, Heleen, Caroline en Peter**. Ik wil jullie enorm bedanken voor het wegwijs maken binnen de wondere wereld van SPSS, matlab, adobe illustrator, prism en allerlei andere programma's welke ik nooit had begrepen zonder jullie hulp! **Tridib**, dank voor de gezelligheid en de experimenten die soms tot 02:30 nachts doorgingen. Met jouw goede playlists hebben we dat altijd met plezier doorstaan! **Heleen**, dank voor je hulp bij het leren analyseren met flowjo en je gezelligheid op de kamer. **Caroline**, dank voor alle tips & tricks over onderzoek en de goede adviezen omtrent eigenaarschap nemen voor je eigen PhD traject. **Peter**, vanaf mijn eerste moment als student bij jouw PhD project heb ik genoten van onze gedeelde (flauwe) humor, maar vooral ook van jouw vermogen om alle ballen van kliniek, onderzoek, een gezin en sporten in de lucht te houden.

Na enkele jaren had ik de grote eer om de PhD kamer te mogen delen met **Jasper, Stefan en Denise**. **Jasper**, dank voor de gezelligheid en heel veel succes met je verdere loopbaan! **Stefan**, vanaf het moment dat je als master student bij "mijn" project startte, is het geen geheim geweest dat ik ongelofelijk

## Acknowledgements

veel bewondering heb voor je kennis, je gedrevenheid en je vermogen om een project naar een hoger niveau te tillen. Samen met Jennifer heb je ervoor gezorgd dat de immunohistochemische kleuringen van de longcoupes er niet alleen prachtig uit zagen, maar dat we die ook hebben weten te kwantificeren met prachtige resultaten. Inmiddels ben je al een lange tijd geen master student meer, maar zelf PhD. Ik weet zeker dat dit een prachtig proefschrift gaat opleveren en ik ben apetrots op wat we samen hebben bereikt binnen het dendritische cel PH project. **Denise**, mijn PH partner in crime! Eerst werkten we meer als solist en los van elkaar, maar later in de samenwerking hebben we aan hele leuke projecten gewerkt. Jij hebt je naast PH onderzoeker ontwikkeld tot een waar expert van de PCA en MFA. Hiermee heb je wat mij betreft aangetoond hoe leergierig en innovatief je bent in het onderzoek, mede ook door een (voor mij zeer ingewikkelde) techniek, meester te maken. Ik ben heel dankbaar voor onze samenwerking en nog heel veel succes met de afronding van je proefschrift.

Tijdens mijn promotieonderzoek heb ik vaak fantastische ondersteuning mogen ervaren van de technische analisten op het lab longziekten. **Jennifer, Menno, Koen, Ingrid en Marjolein** wil ik graag hartelijk danken voor de ondersteuning en hulp bij alle experimenten. Hierin wil ik in het bijzonder **Ingrid** bedanken, waarmee ik alle jaren enorm prettig heb samengewerkt op de verschillende PH projecten. Je Rotterdam-waardige directheid in combinatie met je humor heeft ervoor gezorgd dat de experimenten altijd soepel verliepen, en dat de data van hoge technische kwaliteit was. Ik wil je enorm bedanken voor de zeer prettige samenwerking.

**Floris, Menno en Peter** (*huidige groepsnaam: de bon vivants*), ik kan met recht zeggen dat jullie mijn promotietraject hebben verheven tot een geweldige ervaring door de vriendschap die we over de jaren hebben opgebouwd. Het was een feest om met jullie te kunnen relativeren door flauwe (zeer abstracte) humor, gesprekken over (abstracte) kunst en potjes pokeren op en buiten het lab. Dank voor jullie humor en gezelligheid waarbij ik hoop dat we elkaar nog vele jaren zullen zien!

Uiteraard wil ik alle eerdere PhD studenten, laboranten en postdocs bedanken voor de prettige samenwerking de afgelopen jaren.

Vanuit de hele prettige samenwerking met de afdeling pathologie wil ik ook in het bijzonder **Jan von der Thüsen** en **Thierry van den Bosch** bedanken. Onze huidige samenwerking op het gebied van macrofagen in CTEPH waarvan jullie de prachtige IHC kleuringen hebben verzorgd, waardeer ik enorm.

**Dr. A. van den Bosch, Dr. V. Baggen, Dr. L. Geenen**, hartelijk dank voor de fijne samenwerking tussen de cardiologie en de longziekten bij de Biopulse studie.

Voor het dendritische cel PH project hebben we voor de experimenten ook nauwe samenwerking gehad met de afdeling experimentele cardiologie. In het bijzonder wil ik daar **Prof. Daphne Merkus** en **Liesbeth Eekhout** bedanken voor de prettige samenwerking bij de echocardiografie en de rechterhart katheterisaties.

De collega's van het Revant revalidatie centrum in Breda wil ik hartelijk bedanken voor de mooie samenwerking bij de pulmonale revalidatie studie. **Dr. D van Ranst, Dr. H. Otten, Dr. M. Wapenaar en Ruud Beesems** wil ik daarbij bedanken voor het mogelijk maken van deze studie en de gepubliceerde resultaten daarvan.

Bij de (pre-)klinische studies hebben we ook een samenwerking opgebouwd met onze collega's van het Amsterdam UMC. In het bijzonder wil ik daar **Prof. H-J Bogaard** en **Prof. A. Vonk Noordegraaf** bedanken voor de samenwerking die nu nog steeds gaande is met ons macrofagen in CTEPH project.

Mijn passie voor wetenschap is ooit in 2006 begonnen bij de afdeling neurowetenschappen bij **Prof. Chris de Zeeuw** en **Martijn Schonewille**. Beste Chris en Martijn, ik wil jullie enorm bedanken voor de fantastische tijd die ik op jullie lab heb mogen doorbrengen en het mooie werk wat we hebben verricht.

Zonder sponsoring is onderzoek niet mogelijk. Daarom wil ik heel graag de **pulmonale hypertensie patiëntenvereniging** in het bijzonder bedanken voor de financiële steun die dit onderzoek heeft mogelijk gemaakt. De zeer bijzondere en mooie patiëntendagen die ik heb mogen bijwonen heb ik altijd enorm gewaardeerd. Als laatste van dit onderdeel wil ik alle **pulmonale hypertensie patiënten** bedanken die hebben deelgenomen aan dit onderzoek. Met recht kan ik zeggen het een voorrecht was om dit onderzoek te mogen uitvoeren, om zo hopelijk bij te dragen aan nieuwe perspectieven voor onderzoek en behandeling van pulmonale hypertensie.

## Opleiding tot longarts

Inmiddels ben ik synchroon naast mijn PhD onderzoek sinds 2016 bezig met mijn opleiding tot longarts. Heel graag wil ik **dr. L. van den Toorn** bedanken voor de opleiding tot longarts en de kansen die ik heb gekregen om te mogen groeien binnen mijn klinische en wetenschappelijke carrière. Hiernaast wil ik ook alle **longartsen, AIOS, ANIOS** en **verpleegkundigen** van de afdeling longziekten bedanken voor de altijd zeer prettige samenwerking.

In het bijzonder wil ik graag het klinische pulmonale hypertensie team bestaande uit **Dr. L. van den Toorn, Drs. P. Chandoesing, Dr. K. Boomars, Miriam, Lieke, Jolande** en **Corine** ook bedanken, dankzij jullie inclusies en harde klinische werk hebben de studies uit dit proefschrift kunnen plaatsvinden, dank daarvoor!

## De belangrijkste personen in mijn leven

Mijn vrienden vanaf de middelbare school, met uitbreiding later, wil ik graag enorm bedanken. **Roland, Ard Jan, Hugo, Pim, Niels** en **Jannes**; bedankt voor de humor die we delen. Jullie weten mij altijd (hardop) aan het lachen te krijgen en ik hoop dat we dat blijven doen tot we oud en grijs zijn.

Heren van **jaarclub Blitzkroech**, het is geen geheim dat jullie mij enorm dierbaar zijn. We trekken al sinds 2007 met elkaar op, en nog steeds zijn we enorm actief in onze vriendschappen. Dit proefschrift is mede door jullie tot stand gekomen, door mij te helpen bij het relativeren waardoor ik elke keer weer opnieuw mijn focus kon vinden om aan de slag te gaan. Heel veel dank en ik geniet van elke keer als we elkaar zien of spreken.

Ik mag mij enorm gelukkig prijzen met een fantastische (schoon)familie. **Marie-José** en **Wouter**, inmiddels wonen jullie in het pittoreske Zwijndrecht maar daarvoor hebben we vele uurtjes samen gezellig etend en drinkend doorgebracht op de Straatweg 106 in Rotterdam. Er waren onvergetelijke sinterklaasavonden met ook altijd een prachtig gedicht en kluif voor Joep de hond. En ik heb zo enorm

## Acknowledgements

genoten van de fantastische kookkunsten van Marie-José en de vlijmscherpe humor en actualiteiten analyses met Wouter. Met jullie is relativeren een feest.

Dan de **(smul)spaapjes**, ik zal over onze kerstfeesten hier maar niet al te veel over uitweiden... maar van kerststallen met schapen (die nu in therapie moeten) tot aan café de Mert in Eersel hebben we altijd gelachen en genoten van elkaars gezelschap. **Bas**, je humor, je nuchterheid en gezelligheid zijn een groot voorbeeld en daar hoop ik nog vele jaren van te mogen genieten. **Vincent** en **Rogier**, jullie zijn beiden uniek in jullie levenspad maar jullie delen ook zoveel eigenschappen zoals humor, gezelligheid, en jullie immer aanwezige optimisme.

**Reinier**, je hebt vele titels zoals de diddly dogoe, clubgenoot, Rein.. maar voor mij ben je eigenlijk gewoon één van mijn beste vrienden. Je droge humor, je vlijmscherpe analytisch vermogen, je vermogen tot relativeren, maar vooral het kiezen van je eigen levenspad, onafhankelijk van invloeden van buitenaf, zijn aanstekelijk. Het is een feest om te zien dat je een heerlijke plek in Rotterdam hebt, dat je als een raket promotie aan het maken bent op je werk en dat je geniet van borrels met je vrienden.

**Werner** en **Blendinet**, ook jullie hartelijk dank voor de gezellige etentjes de afgelopen jaren. In het bijzonder wil ik Werner (na onze verbouwing beter bekend als “**de sloopkogel**”) enorm bedanken voor zijn grote aandeel in de werkzaamheden voorafgaand aan de verbouwing van ons nieuwe huis. Ik hoop nog veel van jouw klus-skills te mogen leren!

**Stefan**, **Jolein**, **Hein**, **Loek** en **Abe**; Dank voor jullie onvoorwaardelijke liefde en steun. Stef, vanaf het begin van mijn studententijd heb ik genoten van onze lunch afspraken waarin we samen strategieën uitstippelden voor mijn carrière. Ik heb enorm respect voor jou en Jolein hoe jullie een gezin van drie jongens combineren met jullie baan als medisch specialist. Dit proefschrift is mede aan jullie, mijn dierbare familie, opgedragen.

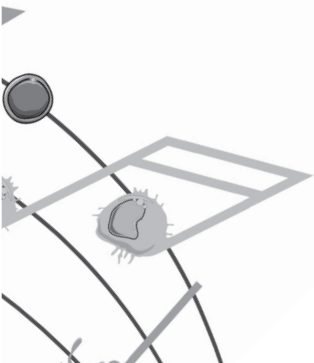
**Martin**, **Charlotte**, **Kate** en **Vivianne**; ook jullie bedankt voor alle liefde en onvoorwaardelijke steun die ik heb mogen ervaren bij jullie. In het bijzonder denk ik gelijk terug aan New York waarbij Kirsten en ik het genot hadden om langs te komen. Jullie hebben samen al zoveel ondernomen, en zijn in New York ook ouders geworden van jullie 2 prachtige dochters. Dit proefschrift is aan jullie opgedragen, voor de muziek die jullie in mijn leven brengen.

**Peter**, **Adrie / Pap** & **mam**; woorden schieten tekort om te beschrijven hoe dankbaar ik ben voor alle liefde, steun, hulp, adviezen en inspiratie die ik van jullie heb mogen ontvangen. Jullie hebben mij altijd gedreven om het beste uit mezelf te halen. Ik ben zo ongelofelijk blij en trots om jullie mijn ouders te mogen noemen, en jullie onvoorwaardelijke liefde voor elkaar is een genot om als kind mee te mogen maken. Jullie hebben er altijd voor gezorgd dat Martin, Stefan en mij niks tekort kwam. Vanaf mijn eerste herinneringen delen wij al een passie voor muziek; van prachtige piano symfonieën gespeeld door Peet, tot meedansen op de Beatles met Aadje. De muziek van dit proefschrift is ook een ode aan jullie, de lieve ouders die mij altijd het zelfvertrouwen hebben gegeven, ook op momenten dat ik dat zelf niet (meer) zag, om te vertrouwen op de muziek in jezelf en om nooit op te geven.

Dan als laatste en daarom het belangrijkste: **Kirsten**, de muziek in mijn leven (ik moest je beloven je niet “*mijn muze*” te noemen, maar over dat je de “*muziek in mijn leven*” bent heb je niks gezegd ;-)). Dit is het jaar dat we 10 jaar een relatie hebben, maar met recht kan ik zeggen dat we het afgelopen jaar samen een enorme groei hebben doorgemaakt. Vanaf het eerste moment tijdens één van onze eerste dates, dat je me geïnteresseerd vroeg naar mijn neurowetenschappen onderzoek, tot aan het afronden van dit proefschrift heb je me altijd gesteund. Je hebt mij kanten van mijzelf laten zien en dingen geleerd die ik nog nooit heb meegemaakt. Ik wil je enorm bedanken voor alle liefde en steun die je mij hebt gegeven. Met jou aan mijn zijde durf ik elke uitdaging (op uitzondering van de Vogelrock in de Efteling) aan! Ik houd enorm veel van je.



ABOUT THE  
AUTHOR



## ABOUT THE AUTHOR

Thomas Koudstaal was born on June 30th 1987 in Hellevoetsluis, The Netherlands. At the age of 3, he and his family moved to Rotterdam. There, he attended primary school at the *van-Veldhuizen school* and graduated from secondary school in 2006 (*Marnix Gymnasium*) with profile; nature and health sciences. The same year he started his study biomedical sciences at the Vrije Universiteit (VU) in Amsterdam.

During this year, he simultaneously started as a research student at the neuroscience laboratory at the Erasmus University in Rotterdam under the supervision of associate Professor M. Schonewille and Professor C. de Zeeuw. Here, his passion for scientific research started to develop and throughout his medical studies which he started in 2007 at the Erasmus University to become a doctor, he continued to participate in research projects at the neuroscience department.

After graduating from medical school in 2015, he started as a resident at the department of internal medicine at the Ikazia Hospital in Rotterdam. In 2016, he started both his PhD research in the pulmonary medicine department (*supervisor: Prof. Dr. R. Hendriks and Dr. K. Boomars*), and his training to become a pulmonologist (*supervisor: Dr. L. van den Toorn*), both at the Erasmus University Medical Center in Rotterdam.

During his PhD research period, he was awarded the *Professor Butrous Foundation young investigator award* at the Pulmonary Vascular Research Institute conference in Lima, Peru in 2020.

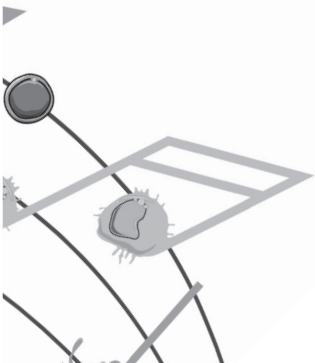
In November 2022, he finished his PhD research and will continue to be involved in pulmonary medicine research at the Erasmus University Medical Center. He will finish his training to become a pulmonologist in October 2023.





# PHD PORTFOLIO

# P



## SUMMARY OF PHD TRAINING AND TEACHING

**Name PhD student:** T. (Thomas) Koudstaal  
**Erasmus MC department:** Pulmonary Medicine  
**Research School:** Molecular Medicine  
**PhD period:** 2015 - 2022  
**Promotor:** Prof. Dr. R.W. Hendriks  
**Co-promotor:** Dr. K.A. Boomars

<b>1. PhD training</b>	<b>Year</b>	<b>Workload (ECTS)</b>
<b>General academy skills and in-depth courses</b>		
-Article 9 animal experiments course	04-2016	4.3
-BROK course	01-2017	2.0
-Research integrity course	04-2017	0.3
-Biomedical English writing course	02-2019	2.0
<b>(Inter)national scientific presentations</b>		
-Poster presentation Molecular Medicine Day Rotterdam	02-2016	0.3
-Poster presentation PH patient symposium Amsterdam	04-2016	0.3
-Oral presentation NRS animal symposium Utrecht	10-2016	0.3
-Moderated poster presentation ERS congress London	09-2016	0.6
-Oral presentation NVALT PH workgroup Utrecht	11-2016	0.1
-Moderated poster presentation PAH symposium Copenhagen	12-2016	0.6
-Oral presentation NVALT longartsen-week Papendal	04-2017	0.3
-Oral presentation ATS congress Washington D.C.	05-2017	0.6
-Poster presentation NVALT najaarscongres Papendal	09-2017	0.3
-Moderated poster presentation PAH symposium Leuven	12-2017	0.6
-Poster presentation PH world symposium Nice	02-2018	0.6
-Poster presentation PH dendritic cell symposium Aachen	06-2018	0.6
-Oral presentation NVALT PH workgroup Utrecht	06-2018	0.1
-Poster presentation ERS congress Paris	09-2018	0.3
-Oral presentation Immunology scientific seminar Rotterdam	12-2018	0.1

-Oral presentation PH patient symposium Utrecht	05-2019	0.3
-Moderated poster presentation ATS congress Dallas	05-2019	0.6
-Oral presentation Immunology symposium Maastricht	10-2019	0.3
-Oral presentation PVRI world symposium Lima	02-2020	0.3
-Oral presentation ERS (digital conference)	09-2021	0.3
<b>(Inter)national scientific conferences and seminars</b>		
-NRS Young investigator meeting Amsterdam (1 day)	11-2015	0.3
-PAH symposium GSK Lund (1.5 days)	12-2015	0.4
-Molecular Medicine Day Rotterdam (1 day)	02-2016	0.3
-PH patient symposium Amsterdam (1 day)	04-2016	0.3
-ERS congress London (5 days)	09-2016	1.5
-NRS animal symposium Utrecht (1 day)	10-2016	0.3
-PAH symposium GSK Copenhagen (1.5 days)	12-2016	0.4
-ATS congress Washington (5 days)	05-2017	1.5
-PAH Masterclass Bologna (3 days)	11-2017	0.9
-PAH symposium GSK Leuven (1.5 days)	12-2018	0.4
-PH world symposium Nice (3 days)	02-2018	0.9
-Dendritic cell world symposium Aachen (4 days)	06-2018	1.2
-ERS congress Paris (5 days)	09-2018	1.5
-PH patient symposium Utrecht (1 day)	05-2019	0.3
-ATS congress Dallas (5 days)	05-2019	1.5
-Immunologie in balans symposium Maastricht (1 day)	10-2019	0.3
-PVRI world symposium Lima (4 days)	02-2020	1.2
-ERS congress, digital due to covid19 pandemic (4 days)	09-2021	1.2

<b>2. Teaching activities</b>	<b>Year</b>	<b>Workload (ECTS)</b>
<b>Lecturing</b>		
-PH education for medical students	10-2017	0.3
<b>Supervising students</b>		
-Supervising I&I research master internship S. Neys, Erasmus University, Rotterdam (9 months)	02-2017	5.0
-Supervising research technician student N. Verboon, research project pulmonary medicine (9 months)	08-2017	3.0
-Supervising medical student T. Janssen, research internship pulmonary medicine (2 months)	10-2018	2.0
<b>3. Awards</b>		
	<b>Year</b>	
-Abstract Scholarship Award, ATS congress, Washington DC, USA	2017	
-Abstract Travel Grant Award, PH world symposium, Nice, France	2018	
-Abstract Scholarship Award, ATS congress, Dallas, USA	2019	
-Abstract Travel Grant Award, PVRI world symposium, Lima, Peru	2020	
-Best Clinical Rapid-fire Award, PVRI world symposium, Lima, Peru	2020	
-Prof. Butrous Young Investigator Award, PVRI world symposium, Lima, Peru	2020	

